MEASUREMENTS OF SECONDARY PLANT METABOLITES, PARTICULARLY ISOPRENE AND MONOTERPENES, IN A TEMPERATE FOREST

by

ANTHONY HYACINTH

A thesis submitted to the University of Birmingham for the degree of

MASTER OF PHILOSOPHY

Department of Environmental Health and Safety

School of Geography, Earth and Environmental Sciences

College of Life and Environmental Sciences

University of Birmingham

October 2019

Abstract

The need to monitor and measure more accurately the biogenic contributions to the atmospheric hydrocarbon budget — especially the contribution from forested landscapes — is becoming more imperative since the biogenic hydrocarbon source to the atmosphere has been identified to be even more significant than the anthropogenic. Isoprene (C_5H_8) is the most abundant biogenic volatile organic compound (BVOC) in temperate and tropical forest ecosystems. It is also very reactive in the atmosphere, with several potential degradation pathways that produce different oxidation products, including ozone and secondary organic aerosol. Other BVOCs are present in lower quantities in temperate forest air, but can be both photochemically and ecologically active, i.e., contribute to the production of atmospheric oxidants and perform signaling functions between individuals of the same or different species. A holistic approach to monitoring isoprene and other secondary metabolites is therefore highly desirable. This thesis reports results from two measurement campaigns that were carried out between August and September of 2015 and 2016 at Mill Haft forest in central England, the site of the Birmingham Institute of Forest Research (BIFoR) research facility. Measurements used a proton transfer reaction time of flight mass spectrometer (PTR-ToF-MS). The measurements were divided into periods 1 and 2 for2015, and periods 1 to 5 for 2016.The measurements formed part of the baseline characterisation of the Mill Haft forest, which is dominated by mature (170 year-old, 25 m tall) English Oak (Quercus robur). Air sampling for P1 (2015) was at a height of about 2 metres, while P2 was at 15 and 30metres and all of 2016 were at 30 metres, close to the top of the canopy.

Results from 2015 suggest that Isoprene, and its oxidation products MVK/MACR, also detected by PTR-ToF-MS, do not always show a diurnal pattern when their mixing ratios are low. The isoprene concentrations in period 2 (2015, at inlet heights of 15m and 30m), are more representative of isoprene concentrations in forested landscapes — i.e., in temperate regions like Mill Haft — than the

concentrations in period 1. The presence of isoprene and its oxidation products; MVK/MACR, was confirmed in the 2016 sample at the canopy height of about 30 metres. The daily mixing ratios and diurnal patterns vary based on prevailing environmental, physical and climatic conditions; but show median and mean values; that agree with results from similar forests in temperate regions. VOC 'fingerprints' (i.e., full mass spectra tentatively assigned) of the forest environment using the PTR-MS is shown to be a fast and reliable method for identifying stable and recurring compounds. Overall, the results show that isoprene, MVK/MACR, and other secondary plant metabolites in these baseline samples have been successfully identified using PTR-MS. A more accurate quantification of identified compounds will require additional methods, such as gas chromatography with mass spectrometry (GC-MS). A better interpretation of observed patterns would be possible if more correlative environmental factors were used in the investigation: e.g., relative humidity; photosynthetic active radiation (PAR); wind speed and direction; and ozone (O_3) and nitrogen oxides (NOx) mixing ratios, where possible.

Acknowledgements

I would like to express profound appreciation to Professor Rob Mackenzie for letting me work with him in BIFoR, and to Professor Francis Pope who together with Rob, have been very kind and patient because they did not see my visual impairment as a handicap. I also express special gratitude to Professor Jon Sadler for his invaluable role in my admission to BIFoR. Thanks go also to Professor Roy Harrison and Dr Zongbo Shi who supported my admission to the faculty. Immense gratitude to Dr Daniel Blenkhorn who was directly instrumental in collecting the data used for this study and was kind enough to spare the time to show me how the PTR-MS works at a time when he needed time to write up his own thesis. I received great benefit from the support and advice of Julie Kendal and the University of Birmingham Disability Unit. Much help came to me through the professional assessments arranged and the reasonable adjustments that were recommended as a part of my support process. I owe you much gratitude for the interventions you brought in to my case at different times. To Dr Jo Southworth; Reasonable Adjustment Coordinator for GEES; goes my sincere gratitude for your advice and support. I also acknowledge the diligent and dedicated efforts of Professor Stuart Harrad, Dr Gregor Leckebusch and, Dr Ian Phillips in all the supervisory board meetings. I will not forget to say many special thanks to Gretchel Coldicott, our PGR. Manager, in the GEES office; who was always willing to give the help and support I needed. To Deanne Brettle our BIFoR Project Administrator and back-bone at Rob's office, I send very dear and heartfelt appreciation. My thanks also go to Dr Kris Hart and all the amazing team of people at the BIFoR FACE facility, Mill Haft, Staffordshire for all their different contributions. I owe much gratitude to Claire Evans; Head of Research Student Administration and her team at the Registry; for the help and support that came to me by the exercise of their diligence, empathy and discretion. I deeply appreciate the efforts of Dr Nicholas Davidson; who at the start of my program, was a senior colleague who invested time and energy to introduce me to the labs and some of the initial processes. Thank you to the University of Birmingham for being courageous enough to make room for people like me who are confronted with many physical challenges. You have indeed kept to your pledge to be 'persuasive, persistent and bold' in turning 'ingenuity into reality and make important things happen' despite all odds. I am truly grateful for all the people I met at the University of Birmingham with their all unique qualities and genuine response to the challenges that confront them in this unique learning environment. To my family, Dr Timi Hyacinth, Hannah Hyacinth and Josiah Hyacinth, I say that am most grateful for your unflinching love, support and persistent determination. I specially appreciate close family friends: Moyo and Mr Akinyemi Akinyoade; Dr Busola and Emmanuel Eshiet; Ozi and Dr Eze Ekeokwu; Chioma and Obinna Okpoechi; Tutu and Mobolawa Akinkoye; Fosola and Diji Oludipo, Ade Bamgboshe, Hornsey Fellowship and Potters Place Church Port Harcourt and other precious ones. To you all, I say a great thank you for your support and contributions to my development. Thanks to all who have helped me in one way or the other. You will have no regrets.

De basileus aion aphthartos aoratos monos sophos theos time kai doxa eis aion aion amen

Table of Contents

List of Figures

List of Tables

Chapter 1

Introduction

1.0 Overview: guide to entire thesis

This thesis is written in seven chapters: Chapter 1, Introduction; Chapter 2, Description of method; Chapter 3, Isoprene and its reaction products in a deciduous temperate forest (August – September 2015); Chapter 4, Isoprene and its reaction products in a deciduous temperate forest (August – September 2016); Chapter 5, Fingerprint of possible Volatile organic compounds in a deciduous temperate forest (August – September 2016); Chapter 6, Overall conclusion; and Chapter 7, Suggestions for further work. Three of the chapters — 3, 4 and 5 — are discussions of results from the data collected at the Mill Haft forest site of the Birmingham Institute of Forests Research (BIFoR); using the Proton transfer reactor mass spectrometer PTR-MS; more specifically the KORE series 1 model of the PTR-ToF-MS (KORE 2014). The Mill Haft site hosts the latest forest Free Air Carbon dioxide Enhancement (FACE) facility in the world (Norby et al., 2015). The facility is designed to investigate the global impact of elevated CO_2 on forested ecosystems within the natural systems (that is 'insitu') (MacKenzie et al 2016, BIFoR FACE 2017). The data used in this research, was collected as part of the initial measurements, in the summer of 2015 and 2016; for baseline studies in the forest. The results in Chapters 3 and 4 are for 2015 and 2016, respectively, and are used to determine the presence of isoprene and its oxidation products; MVK/MACR. Chapter 5 seeks to identify the presence of other biogenic volatile organic compounds (BVOCs) from the 2016 data, through VOC finger-printing, before considering additional and sometimes more complex methods that may be required to establish and confirm presence and quantify compounds of interest. The main part of the analysis was carried out using the Rstudio (2016).

1.1 Overview: guide to Chapter 1

This chapter has two main sections: section 1.2, Why isoprene measurements in forests are important; and section 1.3, Brief Description of the BIFoR FACE Oak Forest. Section 1.2 is made up of 3 subsections: 1.2.1, The typical isoprene time series, 1.2.2, HO radical reactions serve as a major chemical sink and 1.2.3, Shawbury air temperature data used in place of missing Flux tower temperatures (19 - 21 August 2015).

1.2. Why isoprene measurements in forests are important

Isoprene (2-methyl-1,3-butadiene) is the most abundant biogenic volatile organic compound (BVOC) in most forested ecosystems (Guenther et al. 1994, 1995, 2012, Geron et al. 1994), exceeding those from anthropogenic sources (Rasmussen 1970, Lamb et al. 1987, 1993, Guenther et al. 2012), and reacts very fast in the atmosphere (Pressley et al. 2005), to produce a range of other secondary hydrocarbons, especially oxidation products. This makes isoprene an important contributor to the atmospheric hydrocarbon budget. Important emitting sources need to be monitored to update regional atmospheric models, especially in relation to predicting ozone formation. Isoprene, like other hydrocarbons, forms ozone in sunlight, when NOx is within a range of high concentrations (Trainer et al. 1987, Chameides et al. 1988, Thompson 1992). NOx is usually present in polluted urban air and mixes out into rural environments where BVOC emissions can be high. Ozone episodes reduce crop and forest output and create respiratory difficulties (Reich and Amundson 1985, Runeckles and Chevone 1992). Formulation of

mitigation strategies requires a proper inventory of major emission sources in a region, including isoprene (Sharkey et al. 1996).

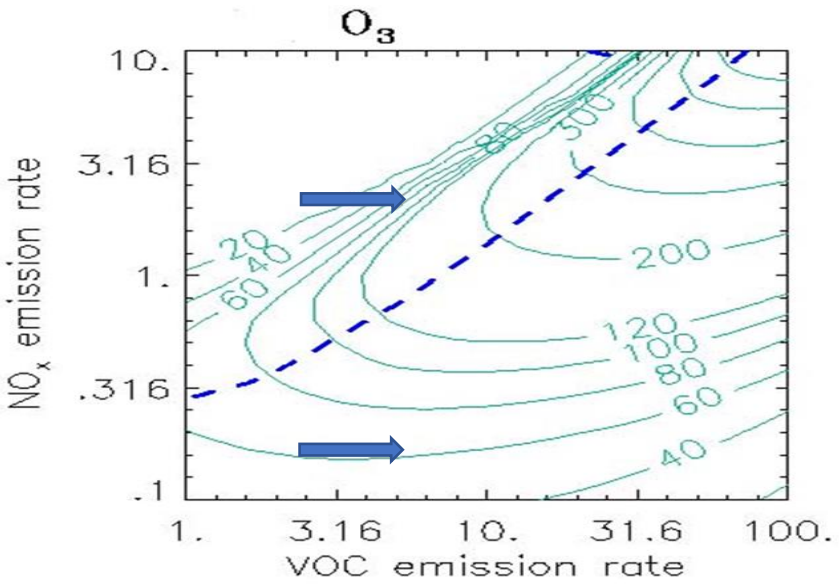

Figure 1.1: Adapted from Sillman and He (2002); The solid green lines are the ozone isopleth plots that reflect atmospheric conditions in the afternoon; A 3day calculation was done at a constant rate of emission for both VOC and NOx during an hour identified for maximum Ozone (O3). The ozone isopleths in ppb are plotted as a function of VOC and NOx average emission rates (10^{12} molecules $cm^{-2}s^{-1}$) in 0-dimensional (i.e., box model) calculations. The solid dotted line that rises upwards from the NOx (y) axis marks the point of cross over from the VOC-limited (top left) to the NOx-limited (bottom right) regime. The blue horizontal arrows show, schematically, the effect of BVOC emissions in VOC-limited conditions (top) and NOx-limited conditions (bottom).

The photochemistry behind the O_3 - VOC – NOx relationship can be complicated when many VOCs are present, and is nonlinear, as can be seen in figure 1.1 (Sillman and He, 2002). Isopleth plots such as Figure 1.1 are used to diagnose peak ozone mixing ratios as a function of NOx and VOC emissions rates. Two atmospheric regimes emerge in the O_3 – VOC – NOx plots: VOC-limited, and NOx-limited. In the VOC-limited regime (sometimes called the VOC-sensitive regime or the NOx-saturated regime), O_3 increases with increasing VOC and decreases with any further increase in NOx. While in the NOx-limited

regime (in which NOx emissions are low, with VOC emissions are high), there is little or no increase to O_3, for any further increase in VOC, but only show relevant increase with increases in NOx. The dotted line shows the point that demarcates the VOC and NOx limited regimes for the local area or region involved.

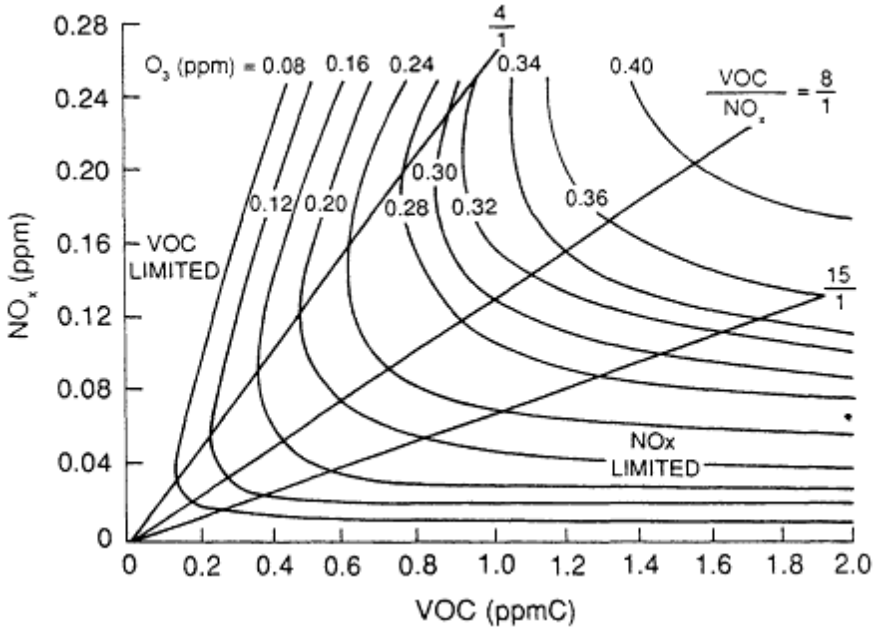

Figure 1.2: Adapted from Dodge, 1977; An example of ozone isopleth lines used to develop control strategies by the United States Environmental Protection Agency (USEPA). Using the Empirical Kinetic Modelling Approach (EKMA), a range of O_3 - VOC - NOx quantitative relationships were derived through combining modelling techniques and smog chamber data. The isopleth diagram in this case is derived from initial NOx mixing ratios in parts per million (y-axis), initial VOC mixing ratios in parts per million of Carbon (ppmC, x-axis), and resulting ozone mixing ratios (ppm). Straight lines show behavior along lines of constant VOC/NOx.

The maximum concentration of O_3 generated over a fixed time interval by an initial mix of VOCs and NOx can also be used to generate isopleths (figure 1.2). Atmospheric models, use photochemical reaction mechanisms and test model output against smog chamber data, to develop control strategies, for ozone reduction. Figure 1.2, is a typical example that show how the USEPA, uses the empirical kinetic modeling (EKMA) in such an approach (Dodge, 1977). The peak ozone concentration set by the National

Ambient Air Quality Standard (NAAQS) is 120 parts per billion (ppb), so the procedure is to measure the maximum ozone concentration of a city and then determine the VOC and NOx reductions required to meet the 120 ppb (NAAQS), using the (EKMA) diagram in figure 1.2. The solid vertical lines showing the various VOC / NOx ratios (4, 8 and 15) give a guide to the various points on the ozone isopleth lines that demarcate regions of the isopleth diagram for which different control strategies are appropriate, that is, different emphases on reducing VOC or NOx emissions. A typical VOC-limited region would be a polluted urban area, while the characteristic NOx-limited region will be downwind of urban and suburban areas.

1.2.1 The typical isoprene time series

Trees emit isoprene in response to light and temperature, and in the absence of water stress (e.g., Guenther et al. 2012). The typical diurnal pattern of response to daytime light and temperature changes, observed for isoprene, especially for measurements taken above the canopy, is shown in figure 1.3. The plot shows a time series of MVK/MACR and isoprene fluxes along with the photosynthetic active radiation (PAR) above the canopy of a forest site in southeast of France, dominated by downy oak, (*Quercus pubescens) (*Kalogridis et. al. 2014). The daily minimum and maximum values correspond with those for the PAR and is consistent with times expected respectively, to have corresponding day and night time variations in temperatures and solar radiation.

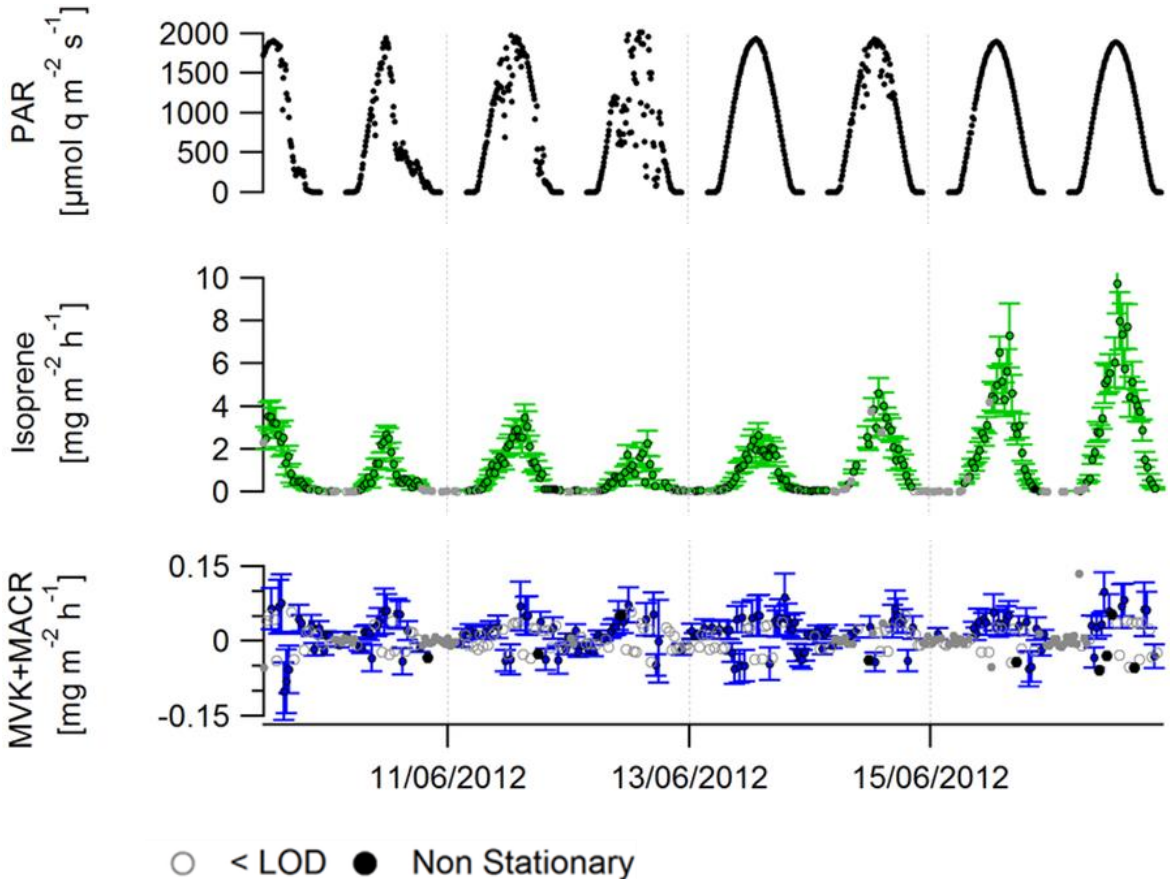

Figure 1.3: Adapted from Kalogridis et al., 2014; A time series plot of isoprene and MVK/MACR fluxes along with PAR measured above the canopy; showing the typical daily minimum and maximum values from the fluctuations usually observed for isoprene, associated with its diurnal pattern of response to the combination of daytime light and temperature changes, and night time variations. The flux error bars show ± standard deviation of the covariance for t lag far away from the true lag (+150, −180 s).

1.2.2. HO radical reactions serve as a major chemical sink

Although, the primary focus here would appear to be the oxidation of VOCs, especially isoprene, by HO radicals and its removal from the forest; three other important oxidation reactions involving the HO radical, have been included, in considering the extent to which reactions with HO radicals serve as a source of the biggest chemical sink. Some key reactions involving HO radicals include:

i. Oxidation of carbon monoxide (CO)

ii. Oxidation of a wide range of VOCs (especially isoprene due to its abundance in forests)

iii. Oxidation of nitrogen dioxide ($NO_{2)}$ and sulphur dioxide (SO_2)

iv Oxidation of methane (CH_4)

I. Oxidation of CO

The oxidation of carbon monoxide (CO) is initiated solely by the reaction with OH (equation E1.1), the H radical released, then combines with oxygen (O_2), to form hydroxy peroxide (HO_2), with the release of energy to a neutral molecule (M) (E1.2). Hydroxyl radical (HO) is eventually regenerated by a reaction of HO_2 with nitrogen oxide (NO) to produce NO_2 (E1.3).

$HO + CO \rightarrow H + CO_2$ E1.1

propagated by HO_2

$H + O_2 + M \rightarrow HO_2 + M$; $M = N_2 / O_2$ E1.2

HO_2 reacts with NO to produce NO_2 and regenerates HO

$HO_2 + NO \rightarrow HO + NO_2$ $\lambda < 420$ nm E1.3

NO_2 from (E1.3) can also proceed to form ozone (O_3) from reaction (E1.5), through the process that starts with the photodissociation of NO_2 into NO and a high energy oxygen radical (O^3P) in reaction (E1.4), which then collides with O_2, in the presence of a neutral molecule M; usually N_2 (Ehhalt 1999, Carslaw et al 2001, Clemitshaw 2003).

$NO_2 + h\nu \rightarrow NO + (O^3P)$ E1.4

$(O^3P) + O_2 + M \rightarrow O_3 + M$ E1.5

Reaction E1.6 below, gives the net overall reaction for the CO oxidation process (from E1.1 to E1.5) as;

$CO + 2O_2 + h\nu \rightarrow CO_2 + O_3$ E1.6

The chemical equations between E1.1 and E1.5 represent a net process that rapidly interconverts HOx (HO and HO_2), within seconds and NOx (NO and NO_2), within minutes, yet keeps HOx and NOx recycled in the process (Clemitshaw 2003, Pugh et al 2010).

2. Oxidation of VOCs

Isoprene like other VOCs in the forest react with hydroxyl radicals (OH) to form intermediate peroxy radicals and other oxidation products. Isoprene is particularly reactive due to its pair of ethylene unsaturated bonds; combined with the rapid reaction rate of the HO radical, results in a fast rate of removal of isoprene from the air by conversion to oxidation products. HO, radicals easily abstract Hydrogen atom (H), from these organic compounds like isoprene (RH) to form a reactive organic radical (R) and water vapour (equation E1.7). Organic peroxides (RO_2) then result from the reaction between R and oxygen (O_2) (E1.8) (Carslaw et al 2001, Clemitshaw 2003).

$RH + HO \rightarrow R + H_2O$ …… E1.7

$R + O_2 \rightarrow RO_2$ ……E1.8

($HO_2 + NO \rightarrow HO + NO_2$ $\lambda < 420$ nm ……..E1.3)

The cycling of NO to NO_2 and HO_2 to HO is basically controlled by the interaction between peroxy radicals and NO (Atkinson 2000, Pugh et al 2010), as already shown in E1.3 above and applies for the conversion of RO_2 to HO_2, (see E1.9 and E1.10)

$RO_2 + HO \rightarrow RO + HO_2$ ……..E1.9

$RO_2 + NO \rightarrow RO + NO_2$ ……E1.10

E1.9 and E1.10 and how they have been applied specifically to isoprene can be seen in Hasson et al. (2004), Jenkin et al. (2007), Butler et al., (2008), Kubistin et al., (2008), Pugh et al (2010) and Taraborrelli et al. (2009, 2012), among others. Figure (E1.1), below also illustrates E1.8; using structural formulae to show the formation of alkyl peroxy radicals from both alkanes and alkenes. The alkene bond in figure (E1.1B), is like the diene bonds in isoprene.

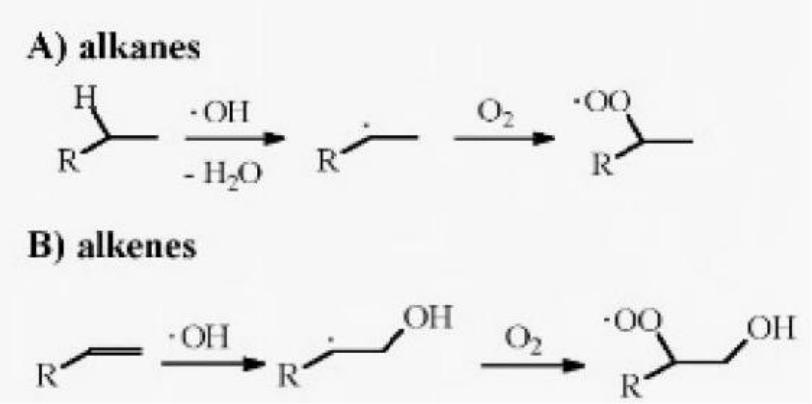

Figure (E1.1): Adapted from ESPERE Climate Encyclopaedia (www.espere.net); Equations; using structural formulae to illustrate OH radical reactions with alkyl groups

3. Oxidation of NO_2 and SO_2

HO also initiates the oxidation of inorganic compounds like NO_2 and SO_2 through the reactions represented in equations E1.11 to E1.14. HOx and NOx in polluted environments are lost through the formation of nitric acid in E1.11. On the other hand,E1.12 to E1.14, not only produce sulfuric acid but interconverts HO to HO_2 (Clemitshaw 2003).

$HO + NO_2 + M \rightarrow HONO_2 + M$ ……..E1.11

$HO + SO_2 + M \rightarrow HSO_3 + M$ ……E1.12

$HSO_3 + O_2 \rightarrow HO_2 + SO_3$ ……E1.13

$SO_3 + H_2 + HO_2 + M \rightarrow H_2SO_4 + OH + M$ ……E1.14

4. Oxidation of methane (CH_4)

OH-initiated oxidation of CH_4 takes place, in an atmosphere with NO, methylperoxy radicals (CH_3O_2) and methoxy radicals (CH_3O) (Clemitshaw 2003). The methylperoxy radicals ($CH_3O_2 \approx RO_2$) functions in a similar way as HO_2 (Jenkin and Clemitshaw 2000)

$OH + CH_4 \rightarrow H_2O + CH_3$ ……..E1.15

That is, an environment that supports equations E1.16 and E1.17, below enables OH to initiate reaction E1.15

$CH_3 + O_2 + M \rightarrow CH_3O_2 + M$ ……E1.16

$CH_3O_2 + NO \rightarrow CH_3O + NO_2$ ……E1.17

Here the RO radical is regenerated by reaction E1.10 in a similar way to the HO radical in E1.3

($RO_2 + NO \rightarrow RO + NO_2$ $\lambda < 420$ nm …… E1.10}

($HO_2 + NO \rightarrow HO + NO_2$ $\lambda < 420$ nm ……..E1.3)

The global scale of HO reactions is put at 40% with CO, about 30% with organic compounds, 15% with methane (CH4) and the balance 15% taken up in reactions with ozone (O_3) and hydrogen gas (H2) (Lelieveld et al., 2016, Zheng et al 2019).

1.2.3. Shawbury air temperature data used in place of missing Flux tower temperatures (19 - 21 August 2015)

The Shawbury air temperature data was used in place of the missing flux tower data in chapter 3, for the period; 19 – 21 August 2015. Figure 1.5; shows a perfect correlation between the regenerated flux tower air temperature and the Shawbury air temperature used; while Figure 1.4; shows the plot of both temperatures in the period; 1- 12 June 2015. The flux tower air temperatures plotted in Figure 1.5 were obtained from (Figure 1.4) using the relationship; X = (y + 1.05)/1.04; where y is the Shawbury temperature values and x the regenerated flux tower temperatures (Figure 1.5). The Shawbury air temperature is from the main weather station for Shropshire (Met office 2019), located at the Royal Air Force (RAF) base in Shawbury village; in the neighbourhood of the BIFoR Mill Haft Forest.

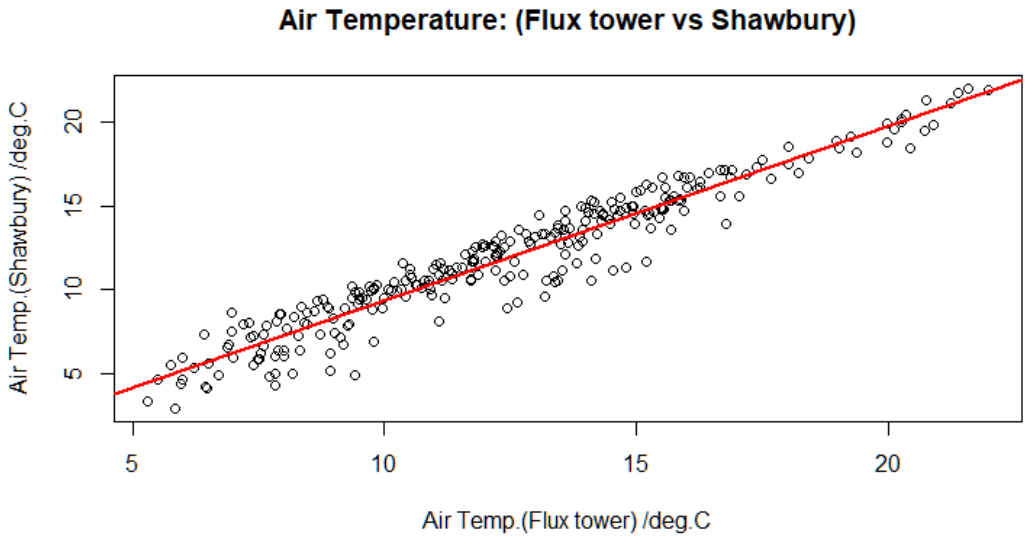

Figure 1.4: Air temperature plot; Shawbury vs Flux tower, 1-12 June 2015; *Y = 1.04x – 1.05; R^2 = 0.92; X = (y + 1.05)/1.04; intercept on y axis = -1.04860, estimated standard error = 0.24027; slope on x axis = 1.04150, estimated standard error = 0.01851*

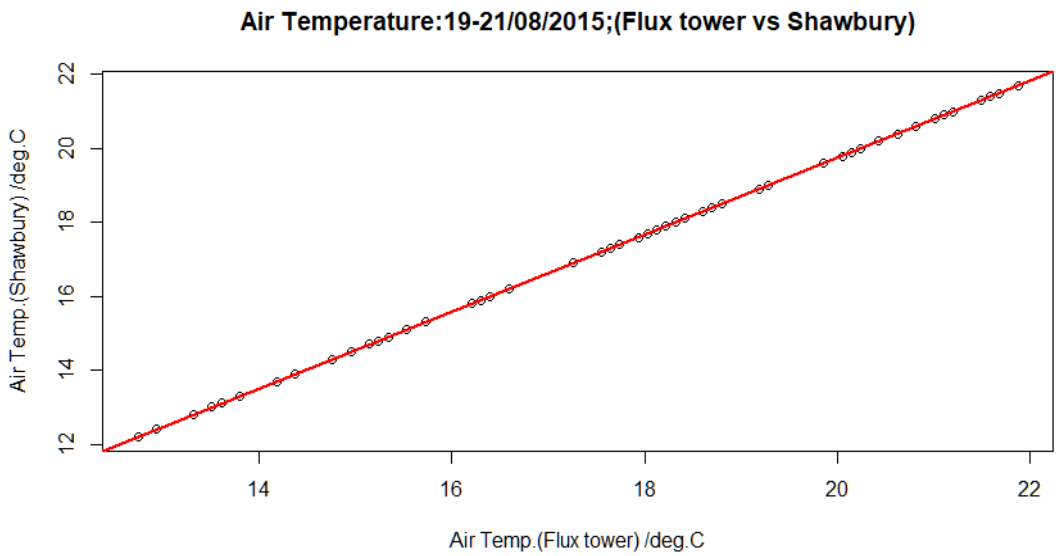

Figure 2.5***: Air temperature; Shawbury vs Flux tower, 19-21 August 2015;*** Equation of the line: y = 1.04x – 1.05. R^2 = 1; intercept on y (Shawbury temperature) = -1.050; *slope on x (flux tower temperature) = 1.040*

1.3. Brief description of the BIFoR FACE Oak Forest

The BIFoR FACE Oak Forest is located at Mill Haft, Staffordshire, a 26 hectare woodland known to be part of the Earl of Lichfield, a former hunting ground. The Mill Haft forest with the English Oak (Quercus robur) or pedunculate Oak as the dominant species dates to about 160 – 180 years, a deciduous forest with trees that have large wide spreading crown of rugged branches. The area also has other, sub - dominant, trees like the hazel (Corylus avellana) coppice, and is believed to have been under continuous tree cover for over 300 years. The coppice is now heavily overstood at a height of approximately 15m. Mill Haft is the site of a Free Air Carbon dioxide Enhancement (FACE) facility, hosted by the Birmingham Institute of forest research (BIFoR); one of three forest-FACE facilities in the world currently commissioned to investigate insitu, the impact of rising CO2 on global ecosystems and biodiversity (Mackenzie et al 2016, BIFoR FACE 2017).

Chapter 2

Description of Method

2.0. Overview: guide to Chapter 2

This chapter deals with data collection, processing tools and procedures; and is written in five sections; with their subsections as follows: Section 2.1; Introduction of method, Section 2.2; The Proton Transfer Reactor (PTR); with sub section 2.2.1; Starting the PTR. Section 2.3; Field Deployment, Section 2.4; 2016 Data: Periods 1 to 5; with a sub section 2.4.1; Explaining mass resolution, data normalisation and calibration Procedures ; divided further into 7 subtopics:

2.4.1.1 Mass resolution using m/z at centre of peak (m) and the width (Δm)

2.4.1.2 Mass resolution showing how the peak width is worked out; An example from

2.4.1.3 Normalisation procedure; An example from (m/z 59), likely acetone peak (figure 2.3).

2.4.1.4 Applying mass resolution and data normalisation on the 2016 data sheet

2.4.1.5 Mass resolution for Protonated (isotope) water, (m/z 21); period 1, 2016 data

2.4.1.6 Normalisation for $(MH+)^{69}$; i.e., Isoprene

2.4.1.7 Normalisation for $(MH+)^{71}$; i.e., MVK/MACR, and finally,

Section 2.5; Statistical guide used for interpreting the box plots in chapters 3 and 4 (see Figures 2.7a and b, below).

2.1 Introduction of method

A brief description of the site is as above in section 1.3, more details can be found at https://www.birmingham.ac.uk/research/activity/bifor/face/index.aspx. The equipment used was the KORE PTR-TOF-MS series 1 (with a mass resolution ≥ 1,500 FWHM; (Full Width Half Maximum (resolution)) and sensitivity for Benzene >200 cps/ppbv; (counts per seconds/parts per billion) (KORE 2014), deployed to carry out the Measurements for both periods 1 and 2 in 2015 and periods 1 to 5, in 2016; as will be noticed in chapters 3 and 4 respectively; where the results of the processed data is reported. Measurements for period 2 of 2015, were taken at heights of 30 and 15 meters respectively, by connecting dual membrane tubes with automated switchable valves, to the PTR inlet while raising the inlet tubes to the respective heights by attaching them to meteorological towers (McKinney et al 2011). Data for both Periods in 2015, and all the 5 periods of 2016 are initial baseline measurements; period 1 (2015); was done without any specific reference to height; but could be estimated within the forest to be about 2 meters, or the height of a normal carrier van, but period 2 (2015) had measurements taken at both 30 and 15 meters height. The 2016 data; was also measured at about 30 meters; at canopy level. Discussion of period 1 (19 - 21 August 2015) is in section 3.1 (subsections 3.1.1 to 3.1.5); measurement period 2 (23 August – 03 September 2015) is presented in section3.2 (3.2.1 to 3.2.6). All five periods in 2016, are presented in chapter 4; period 1 (05 - 09 August 2016) in section 4.1; period 2 (11 - 17 August 2016) in section 4.2; period 3 (17 - 23 August 2016) in section 4.3; period 4 (23 - 25 August 2016) in section 4.4; and finally, period 5 (25 August - 07 September 2016) is discussed in section 4.5 . The data collected were stored using the windows-based GRAMS software adapted by KORE UK into the system, from Thermo Galactic Corporation (KORE 2014). Further processing for normalization, calibration and plotting of data was carried out using RStudio (2017). The steps required to start the PTR, before use are briefly outlined below in (2.2.1), but the normalization of the data, the calibration process and factors, are discussed in more details in section (2.4); under the 2016 data.

Additional material on data normalization and calibration procedure can also be found, in Ellis and Mayhew (2013).

2.2. The Proton Transfer Reactor (PTR)

The Proton Transfer Reactor Mass Spectrometer (PTR-MS) has done away with the need for initial preparation and pre-treatment of atmospheric samples before analysis. The VOCs coming into the drift tube (DT) go through the inlet valve, mixed with sample air, take up H+ (due to stronger proton affinity) from H3O+ generated from the Hollow cathode tube (HC) (Ennis et. al., 2005) and travel through the drift tube as VOCH+ aided by both the electric field generated and the air current of the sample (Hansel et al 1999), to the Mass spectrometer (MS); in this case a Time of Flight (TOF) based unit. The VOCs get differentiated and finger printed at varied count rates based on their mass to charge (m/z) ratios as they travel through the TOFMS unit at different velocities; with m/z effectively reading as the molecular mass of the VOCH+ (i.e., molecular mass of VOC plus proton mass). Since the proton charge (z) and the mass are each equal to 1, and, the mass of the proton (H+) ion is the same on all VOCs, then, molecular mass becomes the determinant, as to how fast each VOC moves towards the MS for resolution (Blake 2004). The system is relatively portable and can be set up onsite, it has a highly sensitive detection range of up to 10 pptv and enables the continuous monitoring of air samples online, in real time. It is fast and reliable and can quickly capture the wide spectrum of primary and secondary reactions capable of taking place within a short time, in the atmosphere. It is adaptable for field deployment and relatively easy to set up compared to alternative systems. It can take readings at different heights in the forest with good repeatability; i.e. easy to reset and repeat processes with negligible compromise to accuracy (Tanimoto, 2007, Jordan et al 2009, Ellis and Mayhew 2013).

2.2.1 Starting the PTR

This involves five basic areas;

1. Setting the Pressure: in two areas;

i) The **Drift Tube** (DT), for the air sample,

ii) The **Hollow cathode** (HC) Tube for the water vapor.

The software for this is on the PTR monitor. The 1st section is for setting the reactor pressure which can be done by using the select option to set the **Glow Tube** and the **PTR reactor** pressure.

1.1. On the **PTR monitor,** select the PTR reactor; while the selector light is green' on the PTR reactor button, set the pressure at 1mb (about 35 mb when off)

1.2. –The **Glow discharge** (set at 1.4 mb): This can be done in two ways;

i). **T**hrough **the PTR monitor or** ii). Through **the handling control unit**

The Glow discharge pressure is set by opening the '**H2O on** valve" and then turning the 'H2O adjust valve" till it shows 1.4mb on the handling control unit or on the PTR monitor.

2. Set the **temperature** for the **PTR oven** at 100°c; (i.e. reactor / drift tube / oven temp.): On the PTR monitor, at the section labelled **'Reactor Temperature'**, click on the sign, **'Change Temperature setpoint'**. Set the temperature to 100°c on the dialogue box that shows up and **click ok**. Then switch on the '**Analyte button'** to heat up the oven. If the temperature reading is less than 100°c (as shown under the '**reactor Temperature'** sign) then the oven will heat up until it gets to that temperature, and then the '**OK' light** will come on at the '**inlet Temperature ok'** sign.

3. Switch on the **power supply** in three areas; i.) on the **PTR controller**, ii) on the **H. V. supply**, and iii) on the **PTR supply unit** (box behind the controller). All three power supply need to be on, for equipment to

work effectively. A "**Warning note";** not to touch any internal part from this point on, as high voltages are now switched on.

4. Set **Glow discharge** source by putting on **"GD source on"** switch and see that the light is on. Otherwise open the H2O valve to get the higher pressure until the light on it comes on.

5. The **reactor E/N** is set at about 323 by setting the entry voltage at about 250 volts, using the "**TTL high"** dialogue box on the **"E/N collision Energy"** software, on the PTR monitor.

6. Switch on the **Detecto**r- The detector is only switched on when ready to use; it is either on "standby" or "operate" position.

2.3. Field deployment

Field deployment, involves moving the equipment for the measurement to site; in this case it means the setting up of the PTR at the BIFoR Mill Haft forest location. This was carried out by Daniel Blenkhorn, under the supervision of Dr Francis Pope.

i**) inlet**, there are two inlets on the PTR; water vapor into the ion source (or hallow cathode tube - HC) and VOC/air inlet into the reactor or drift tube (DT). The inlet system into the reactor can be of capillary or membrane, single or dual. The dual inlet is switchable and can be either of both. There is also a 16-port multiport valve. The membrane inlet is for increased VOC sensitivity down to concentrations as low as 50 ppb (KORE 2014)

ii) **position field**, there is an E/N value or Townsend Number that is most effective for ionizing the VOC molecules in the reactor, with the most minimal fragmentation as well as reducing' clustering of H20 molecules' to a minimum in the ion source. The appropriate input voltage generates an electric field E

from the parallel electrodes in the drift tube, that influences the number of molecules N, going through to the end of the PTR, towards the mass analyzer.

iii) **measurement cycle**: In the TOFMS, the signals generated when VOCH+ ions arrive at the ion detector, are timed to an accuracy of 0.25 nanoseconds, and converted with a software to a mass unit, using the mass to charge ratio (m/z). For a system in which the process is repeated at a frequency of 20KHz, or a cycle of 50 micro seconds, the result would be 200,000 cycles of data accumulation into the mass spectrum for a measurement of 10 seconds duration.

The deployment for period 1 of 2015 and all of 2016, was set up at the temporary met tower (at the start of the met tower ride), while period 2 was stationed at the main met tower, approximately 10 metres away from the temporary met tower. The set up for period 2, 2015, had the inlet of the PTR attached to a teflon T piece, with one end of the T piece going to a pump and the other end to a valco vici switching valve. The valve then had 2 teflon tubes which went up the main met tower at BIFoR, to approximate heights of 15m and 30m. The pump was used to draw air down the inlet lines, allowing for a short residence time. The PTR (and other instruments) just sampled the air from this flow of air. A total of 6 measurements each were made per hour, for both heights 15m and 30m as the valve switched every 5 minutes, to take 1-minute measurements; with reading one, for 30m and two, for 15m samples, respectively. Period 1, 2015 and all of 2016, had a similar set up except, that, there was no need to switch valves between two heights, since it was a single flow into the inlet; with period 1; set at about 2 meters and that for 2016 set at the canopy level; of about 30 meters, as explained earlier, in section 2.1. There is also the radio frequency (RF) ion funnel that was switched on for period 2 of 2015, only. It is simply a tool that guides the ions into the instrument optics (and mass spectrometer). With the RF ion funnel on, the instrument was operated broadly in the same way, with no major changes needed. It cannot be tuned, but just turned off or on.

2.4. 2016 Data: Periods 1 to 5

This 2016 data, like that of 2015, was collected using the KORE PTR-TOFMS series 1, during a field deployment campaign in 2016, at the BIFoR Mill Haft forest, Staffordshire, by Daniel Blenkhorn, and supervised by Dr Francis Pope; between the 5th of August and the 7th September 2016. The data was collected at about 30 meters high; at the canopy level, within the forest. The calibration factors provided with the data (2015 & 2016) were 0.302809 cps/ppb for isoprene and 2.999 cps/ppb for MVK / MACR (see table 2.1, below). These calibration factors (sensitivities) were used to divide the normalised values from the PTR, to obtain the ppb values, used in the analysis; (see figures: 2.2 – 2.6 & Tables 2.2 – 2.6 below, along with sample explanations to illustrate, what was done to normalise and calibrate the data). It was not possible, to reverify these calibration factors, as at the time of this work; so, they had to be used as given, by those who verified them, at the time of data collection. However, calibration factors can vary widely as shown in table 2.1, below; depending on the instrument type/model, purpose/ range of m/z targeted, and even the type/ procedure used for the calibration process.

Table 2.1: Calibration factors (instrument sensitivities) from PTR-MS compared; they vary for each compound depending on equipment and purpose

	Isoprene (cps/ppb)	MVK/MACR (cps/ppb)	Normalisation Value	Manufacturer/ model	Location/equipment	Source
1	0.302809	2.999	4×10^6	KORE / 1	BIFOR/PTRMS 1	Mill Haft data(2015/2016)
2	6.4	13.1	10^6	Ionicon	ECHO/PTRMS 1	(table 2; pg. 4), Spirig et al., 2003
3	4.9	10.3	10^6	Ionicon (similar properties, larger drift tube)	ECHO/PTRMS 2	(table 2; pg. 4), Spirig et al., 2003

ECHO (Emission and Chemical transformation of biogenic volatile Organic compounds), AFO2000 project, Germany

The example used in table 2.1, from (Spirig et al 2003), shows that even though the two instruments were by the same manufacturer, and the same gas standards / procedures used for calibration, the factors (sensitivities) were different for each equipment, as they were different models. The other important factor that needs mentioning here, is the normalisation of ion counts generated per second. The minimum standard is to normalise the counts to 1 million counts of primary ions. This is done by multiplying the normalised counts per unit time by 10^6 (see section 2.4.1.3); below for worked out examples). This minimum requirement to standardise PTR-MS readings across board to 1 million ion counts per second, can also be more instrument specific, depending on the equipment manufacturer and/or model, to reflect the most realistic and relevant output of ions for each equipment type; hence the value of 4×10^6 for normalising this data from BIFoR (see table 2.1). More details about the normalisation and calibration procedures, as well as worked examples are in section 2.4.1. below, (see also; Ellis et al., 2013; de Gouw et al., 2000; Lindinger et al., 1998, for more detail).

2.4.1 Explaining mass resolution, data normalisation and calibration Procedures

The mass resolution procedures as explained and demonstrated below using the first row on the data sheet helps to give very useful clues about the reliability of the entire data analysis process; as it relates to the entire worksheet. Similar conclusions are obtainable for the normalisation and calibration procedures, hence the need for sections 2.4.1.1 and 2.4.1.2. below.

2.4.1.1 Mass resolution using m/z at centre of peak (m) and the width (Δm)

The resultant values from mass resolution enable the differentiation of one ion from the other, through the intensity of the signals they generate in the mass analyser. The higher the value of the resolution (for species with the same m/z), the better the analyser; and, the easier it is, to separate between ions with m/z at very high proximity to each other; where m/z, is the protonated mass of the compound or ion (which, simply put, is the atomic mass plus the mass of the proton; of value = 1 amu; atomic mass unit.), (Biasioli et al., 2011, Loreto et al., 2011, Jordan et al. 2009).

The resolution is; R = m/Δm ……. E2.1

M; gives the m/z value or Protonated mass at peak canter (see figures; 2.1, 2.2 & 2.3)

The width (Δm), = $(m_n - m_1)$**/n** ……E2.2

Where, m_n = m; (which is; m/z value), at the end point of peak base,

While, m_1 = m; (or m/z value), at starting point of peak base

The processes involved in the mass analyser for these calculations are a lot more complex than the simple illustrations presented below, but the examples give a reasonably clear representation of the Gaussian normal distribution pattern from which they were derived. This pattern of mass distribution requires the sum or integration of intensities (ion yield) from the contributing masses, in the process for working out the intensity of the molecular ion of interest. A more detailed explanation of the Gaussian distribution is outside the scope of this write up, (but more detailed write up is available for further reading, from page 144, Ellis et al., 2013). In figure 1; a and b are samples of plots showing intensities/

mass peaks for methyl ketene and butene respectively, used to illustrate mass resolution (image was adapted from Hartungen et al., 2012).

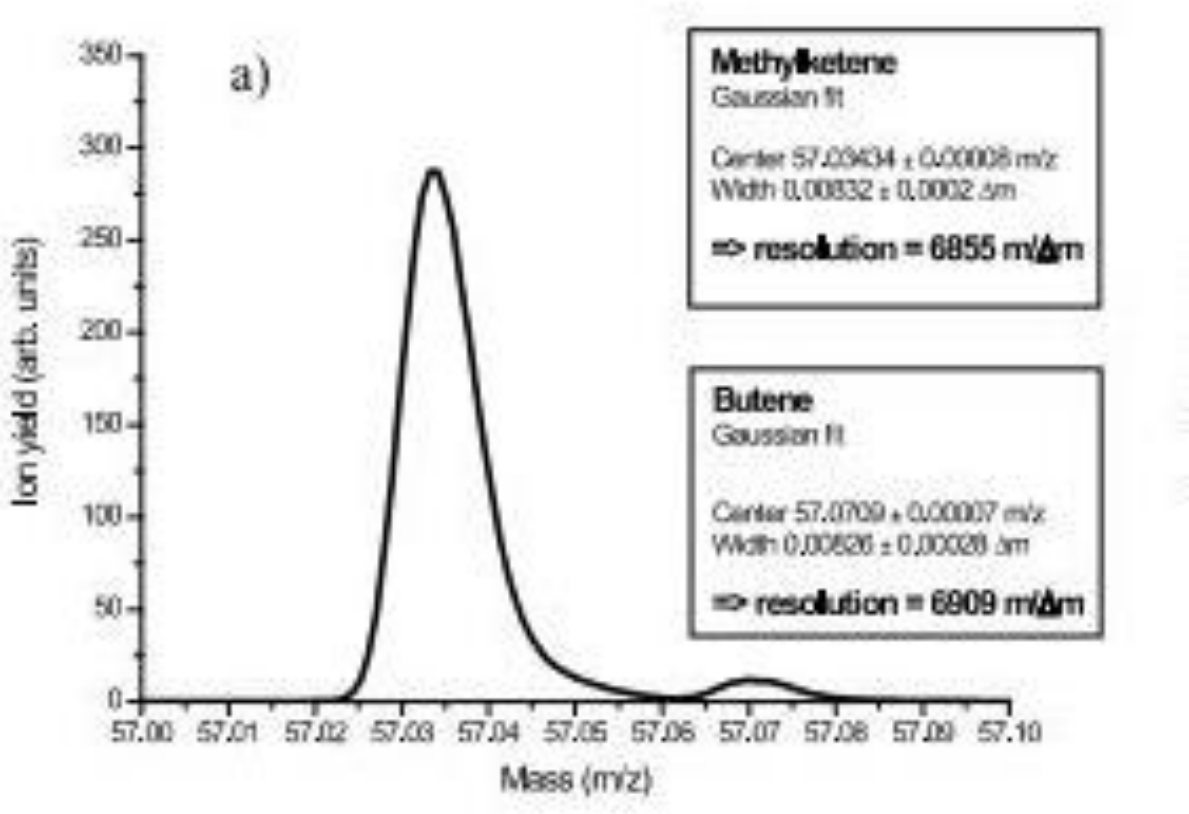

Figure 2.1: An Illustration of mass resolution using m/z in the centre and the width of the peak (Adapted from Hartungen et al 2012)

a) Methyl ketene

Centre of peak = 57.03434 ± 0.00008 m/z

Width of peak = 0.00832 ±0.0002 Δm

The mass resolution, R = 6855 m/Δm (see worked example using figure 2.2 & table 2.2, below)

b) Butene

Centre of peak (m) = 57.0709 ± 0.00007 m/z

Width of peak ($\Delta m = m_n - m_1)/n$ = 0.00826 ± 0.00028 Δm

The mass resolution = 6909 m/Δm (see worked example using figure 2.2 and table 2.3, below)

2.4.1.2 Mass resolution showing how the peak width is worked out; An example from (m/z 59), likely acetone peak.

Using the peak in (figures 2.2 & 2.3) and (tables 2.1 & 2.2), below to illustrate the calculations for $(H3O^+)^{21}$; (m/z 21) and for (acetone + propanol)^{59}; (m/z 59),

2.4.1.2 a) Protonated water (isotope) m/z = 21

Protonated mass (m) at peak centre for $(H3O^+)^{21}$ = 21.03g

The width (Δm) = (21.05 – 21.01)/5 = 0.04/5 = 0.008g

Then, the mass resolution for $(H3O^+)^{21}$ = m/Δm = 21.03/0.008 = 2628.75

2.4.1.2 b) Protonated acetone (m/z = 59)

Protonated mass (m) at peak centre, for (acetone)^{59}, = 59.07g

The width (Δm) = (59.10 – 59.03)/8 = 0.07/8 = 0.00875g

The mass resolution for (acetone)^{59} = m/Δm = 59.07/0.00875 = 7893.714

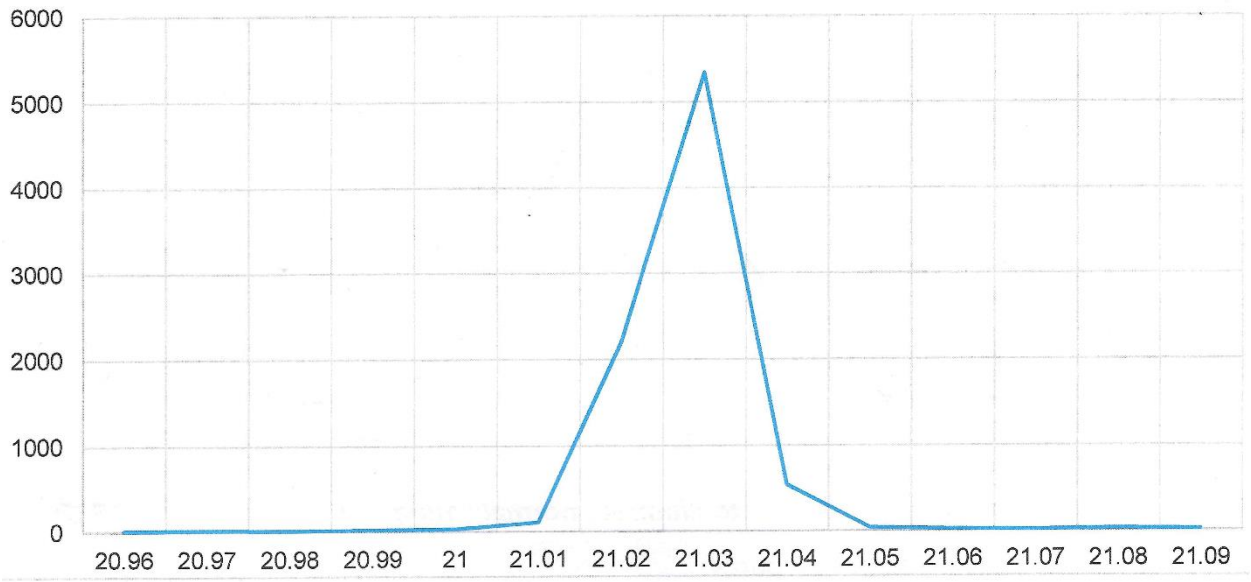

Figure 2.2: Plot of Intensity (i) on Y- axis against m/z 21, for $(H30^{+})^{21}$ on X- axis; Peak area for $(H30^{+})^{21}$ to illustrate mass resolution and data normalization of PTR data; from row 1 of Ms Excel spreadsheet replicated in table 2.2.

Table 2.2: $(H30^{+})^{21}$ Data from row 1 of Ms Excel spreadsheet; to illustrate mass resolution and data normalization.

m/z (21)	20.97	20.98	20.99	21	21.01	21.02	21.03	21.04	21.05	21.06	21.07	∑(I)↓
Intensity (I) cpm	16	12	20	31	106	2203	5338	539	36	19	10	8330

2.4.1.3 Normalisation procedure; An example from (m/z 59), likely acetone peak (figure 2.3).

a) Sum of (I) in counts per minute (cpm) for (H30+) for (m/z = 21) gives the intensity i(MH+) = 8330 (table 2.2) ……E2.3

(i) for $(H30+)^{19}$ at (m/z = 19) = (i) for $(H30+)^{21}$ at (m/z = 21) * 500 ……E2.4

i.e. $i(H30+)^{19} = i(H30+)^{21}$ x 500 = 8330 x 500 = **4,165,000**

Why calculate i[H30+] from m/z 21 (see Tables 2.2 & 2.4)

Notice that the intensity or molecular ion count for hydronium ion; $i[H30+]^{19}$, is done from $[H30+]^{21}$; m/z 21, the value obtained is then multiplied by 500 to get the actual ion count for hydronium ion; m/z 19 as in E2.3 and E2.4. The reason for this indirect method of measurement, is to overcome the difficulties associated with getting an accurate direct measurement for the total hydronium ion count. The approximated ratio, of naturally occurring isotope of oxygen (^{18}O) is 1: 500, when compared to ^{16}O (normal oxygen); it is therefore possible to measure accurately, the count rate of hydronium ions formed, from the isotope directly, without encountering the same type of problems in the ion detectors; usually associated with high ion count rate. The total hydronium ion count rate; i(H30+) is usually very high and can go up to 10^7 counts per second for some models of PTRs; it is practically impossible so far, to measure accurately by direct measurements (Ellis et al 2013).

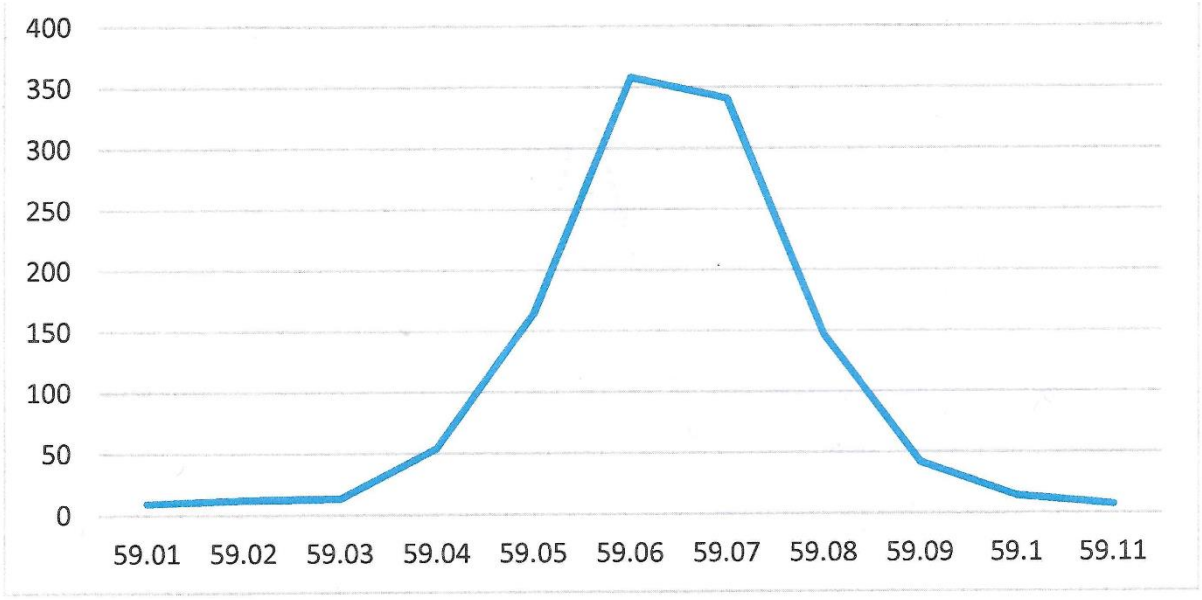

Figure 2.3: Plot of Intensity (i) on Y - axis against m/z 59 for $(MH+)^{59}$ on X – axis; Data from row 1 of Ms Excel spreadsheet replicated in table 2.3; to illustrate mass resolution and data normalization.

Table 2.3: $(MH+)^{59}$ Data from row 1 of Ms Excel spreadsheet; to illustrate mass resolution and data normalization (m/z =59, likely acetone + propanol).

m/z (59)	59.01	59.02	59.03	59.04	59.05	59.06	59.07	59.08	59.09	59.10	59.11	∑(i)↓
Intensity (I) cpm	9	12	13	54	164	358	341	147	42	14	7	1161

b) Sum of (i) in counts per minute (cpm) for $(MH+)^{59}$; at (m/z = 59),

gives the intensity $i(MH+)^{59}$ = **1161** (see ∑(i) in table 2.3 above)

Normalized counts per minute (ncpm) –

(ncpm) = [$i(MH+)^{59}$ / $i(H3O+)^{19}$] x 10^6 = (1161 /41,65000) x 10^6 = **278.75 ncpm** …… E5

Normalized counts per seconds (ncps) = 278.75 / 60 = **4.64 ncps**

The normalised count rate as expressed in E5, gives the ion count rate of the organic molecular ion [MH+] as a relative value to that of [H3O+] instead of the absolute value of the ion. This approach gives a relative value for each ion that stays at the same value, no matter the frequent fluctuations that are usually observed, with the absolute values of [H3O+], due to seasonal or instrumental conditions. Then multiplying by 10^6, reports the ion count rate based on a comparative [H3O+] ion count rate of 1 million counts per second. This assumed count rate is within the magnitude that is representative of most PTRMS equipment and enable a more uniform platform for comparing the same relative ion count rates, rather than absolute values that can be very different, for the different instruments (Ellis etal 2013).

2.4.1.4 Applying mass resolution and data normalisation on the 2016 data sheet

The resolution and normalisation procedures illustrated in(figures 1- 3) and (Tables 2.2 & 2.3) will now be applied on the first row of the 2016 data sheet for period 1; along with the calibration procedure. Figures (2.4 to 2.6) have been used to clearly capture the isoprene and MVK/MACR counts per minute values on the first line of the excel sheet.

Protonated water (isotope) (m/z 21: Ms Excel worksheet; cells 93 to 112

20.885	20.895	20.905	20.915	20.925	20.935	20.945	20.955	20.965	20.975	20.985	20.995	21.005	21.015	21.025	21.035	21.045	21.055	21.065	21.075
45	58	55	52	43	45	31	57	59	55	99	158	794	8107	40081	4277	336	95	59	33
48	60	35	45	43	44	48	59	89	73	100	138	651	7048	40306	5436	408	116	62	41
50	49	42	41	29	46	51	46	70	65	104	150	583	6153	40397	6008	392	120	64	32
41	59	54	63	49	42	49	41	59	63	93	109	530	5206	38405	6753	434	99	66	55

Figure 2.4: Sample of worksheet showing counts for water (m/z 21) or i(H30+)^{21} for period 1 2016; cells 93 – 112 (Figure 1.1c)

Table 2.4: (H30+)^{21} Data from row no. 1; to illustrate mass resolution & data normalization from period 1, 2016 data. Cells 99 to 112.

	99	100	101	102	103	104	105	106	107	108	109	110	111	112	←cells nos.
m/z (21)	20.945	20.955	20.965	20.975	20.985	20.995	21.005	21.015	21.025	21.035	21.045	21.055	21.065	21.075	∑i ↓
Intensity (i)	31	57	59	55	99	158	794	8107	40081	4277	336	95	59	33	54,241

m/z – mass per charge (proton)

2.4.1.5 Mass resolution for protonated (isotope) water, (m/z 21); period 1, 2016 data

a) Protonated mass (m) at peak centre for $(H3O+)^{21}$ = 21.025g

Using (m/z) 20.975 to 21.075 as base width of peak (11 data points)

The width (Δm) = (21.075 – 20.975)/11 = 0.100/11 = 0.00909g

Then, the mass resolution for $(H3O+)^{21}$ = m/Δm = 21.025/0.00909 = **2312.981**

b) The Sum of (i) in counts per minute (cpm) for $(H30^{+})^{21}$ for (m/z = 21) gives the intensity $i(MH^{+})$ =

54,241 cpm

c) Calculating the intensity (i) of hydronium $(H30^{+})^{19}$ from the isotope $(H30^{+})^{21}$

But, (i) for $(H30^{+})^{19}$; (m/z 19) = (i) for $(H30^{+})^{21}$; [(m/z 21) x 500]

i.e. $i(H30^{+})^{19}$ = $[i(H30^{+})^{21}$ x 500] = 54,214 X 500 = 27, 107,000 = **2.7107×10^{7} cpm**

.

Protonated isoprene (m/z 69.12): Ms Excel spreadsheet; **cells 4901 to 4920**

68.965	68.975	68.985	68.995	69.005	69.015	69.025	69.035	69.045	69.055	69.065	69.075	69.085	69.095	69.105	69.115	69.125	69.135	69.145	69.155
7	6	29	58	76	137	177	221	414	474	416	742	912	460	197	50	23	10	7	0
7	9	26	48	79	128	162	183	345	406	383	819	996	554	234	50	20	16	14	4
4	9	15	47	84	109	120	145	334	386	337	692	938	586	245	76	20	12	2	5
8	4	18	42	71	121	127	127	270	323	240	531	636	421	199	59	17	11	4	0

Figure 2.5: Sample of worksheet showing counts for isoprene (m/z 69.12) or i(isoprene+)^{69} for period 1, 2016; cells 4901 - 4920 (Figure 1.1d)

Table 2.5: (MH+)^{69} Data from row 1, for protonated isoprene (m/z =69.12); to illustrate mass resolution & data normalization from period 1, 2016 data. Cells 4903 to 4916 .

	4903	4904	4905	4906	4907	4908	4909	4910	4911	4912	4913	4914	4915	4916	←cells nos.
m/z (69.12)	68.985	68.995	69.005	69.015	69.025	69.035	69.045	69.055	69.065	69.075	69.085	69.095	69.105	69.115	∑i ↓
Intensity (i)	29	58	76	137	177	221	414	474	416	742	912	460	197	50	4363

m/z – mass per charge (proton)

d) Mass resolution for isoprene (protonated mass 69.12)

Using 68.995 to 69.115 as base width of peak (13 data points)

The centre of peak; m = 69.055 g

Δm = (69.115 – 68.995)/13 = 0.120/13 = 0.00923g

Mass resolution for (Isoprene)^{69} = m/Δm = 69.055/0.00923= 7,481.582

e) Mass resolution for MVK/MACR (protonated mass 71.09)

Using 71.005 to 71.115 as base width of peak (12 data points)

The centre of peak; m = 71.055 g

$\Delta m = (71.115 - 71.005)/12 = 0.110/12 = 0.00917$

Mass resolution for $(MVK/MACR)^{71}$ = $m/\Delta m$ = 71.055/0.00917 = **7,748.637**

2.4.1.6 Normalisation for $(MH^+)^{69}$; i.e., Isoprene:

a) Sum of (**i**) in counts per minute (cpm) for $(MH+)^{69}$ at (m/z = 69);

gives the intensity $i(MH^+)$ = 4363 (see table 2.5)

b) Normalized counts per minute (ncpm)-

(ncpm) = [$i(MH^+) / i(H_2O^+)^{19}$] x (4×10^6) = ($4363 / 27.107 \times 10^6$) x ($4 \times 10^6$)= 643.819 cpm

Normalized counts per seconds (**ncps**) = 643.819 / 60 = 1**0.730** cps

c) **Calibrated data (ppbv)** = ncps/cf = 10.730 cs^{-1} / 0.302809 $cs^{-1}ppb^{-1}$ = 35.436 ppb for isoprene

cf is the calibration factor (or instrument sensitivity) for isoprene (see table 2.1)

Simply put; Sensitivity = ncps/ppbv;

Hence, calibrated data in; ppb = ncps/sensitivity (cf)

<u>Protonated MVK/MACR (m/z 71.09)</u>: Ms Excel spreadsheet; Cells- 5101 to 5120

70.965	70.975	70.985	70.995	71.005	71.015	71.025	71.035	71.045	71.055	71.065	71.075	71.085	71.095	71.105	71.115	71.125	71.135	71.145	71.155
4	8	12	54	89	144	337	372	961	1622	1589	1308	512	298	207	88	40	9	11	5
6	12	11	25	74	127	278	343	849	1576	1558	1336	520	301	189	96	35	12	7	7
2	12	9	26	61	114	248	351	765	1331	1473	1294	505	290	183	84	40	16	16	4
3	11	9	24	47	109	235	286	651	1162	1216	1290	526	286	185	92	54	12	7	3

***Figure 2.6**: Sample of worksheet showing counts for MVK/MACR (m/z 71.09) or $(MH+)^{71}$; cells 5101 – 5120*

Table 2.6: $(MH+)^{71}$ Data from row 1, for protonated MVK/MACR (m/z =71.09); to illustrate mass resolution & data normalization from period 1, 2016 data. Cells 5103 to 5116 (see figure 2.6) .

	5103	5104	5105	5106	5107	5108	5109	5110	5111	5112	5113	5114	5115	5116	← cell nos.
m/z (71.09)	70.985	70.995	71.005	71.015	71.025	71.035	71.045	71.055	71.065	71.075	71.085	71.095	71.105	71.115	∑i ↓
Intensity (i)	12	54	89	144	337	372	961	1622	1589	1308	512	298	207	88	7593

m/z – mass per charge (proton)

2.4.1.7 Normalisation for $(MH+)^{71}$; i.e., MVK/MACR:

a) Sum of (**i**) in counts per minute (cpm) for (MH+) at (m/z = 71) gives the intensity i(MH+) = 7593

b) Normalized counts per minute-

(ncpm) = [i(MH+) / $i(H_2O+)^{19}$] x (4 x 10^6) = (7593 /27.107 x 10^6) x (4 x 10^6)= 1120.449cpm

Normalized counts per seconds (ncps) = 1,120.449/ 60 = **18.674 cps**

c) **Calibrated data** = ncps/cf = 18.674 cs^{-1} / 2.999 $cs^{-1}ppb^{-1}$ = **6.227 ppb**

2.5. Statistical guide used for interpreting box plots in Chapters 3 and 4 (see Figures 2.7a and b, below)

Figures 2.7; a and b below give a brief guide to the statistical interpretation for the two basic types of distributions noticed in our box plots. Figure 2.6a; outlines the simplest possible boxplot outlay, with the ideal range of variations from minimum (min.) to maximum (max.) and the box area IQR (or interquartile

region), having the median (med.) line in the middle between the first quartile (1Q) and the third quartile (3Q). For an evenly distributed data, 1Q represents the point for 25% of the data distribution, while the median and the 3Q represent 50 and 75 % respectively. Which means 25% will be between the min. and 1Q, and another 25% between 3Q and max., and 0nly 50 % in the IQR box. The data is said to be **skewed downwards** when the area below the med. Line is smaller than the area above it, in the IQR box; meaning that the values below the median have more compact distribution or are closer together in range to the central value (the number considered to be a more representative member for the entire group in the IQR box i.e., 50% of the data.). The larger area above then reveals a more sparse distribution for values larger than the med; meaning that 25% of the data in the IQR box vary widely from the central value. The reverse situation with a smaller section above the med. Line represents a data set that is **skewed upwards**. The explanation is similar to the compact and the sparse distribution patterns that would follow respectively above and below the median line.

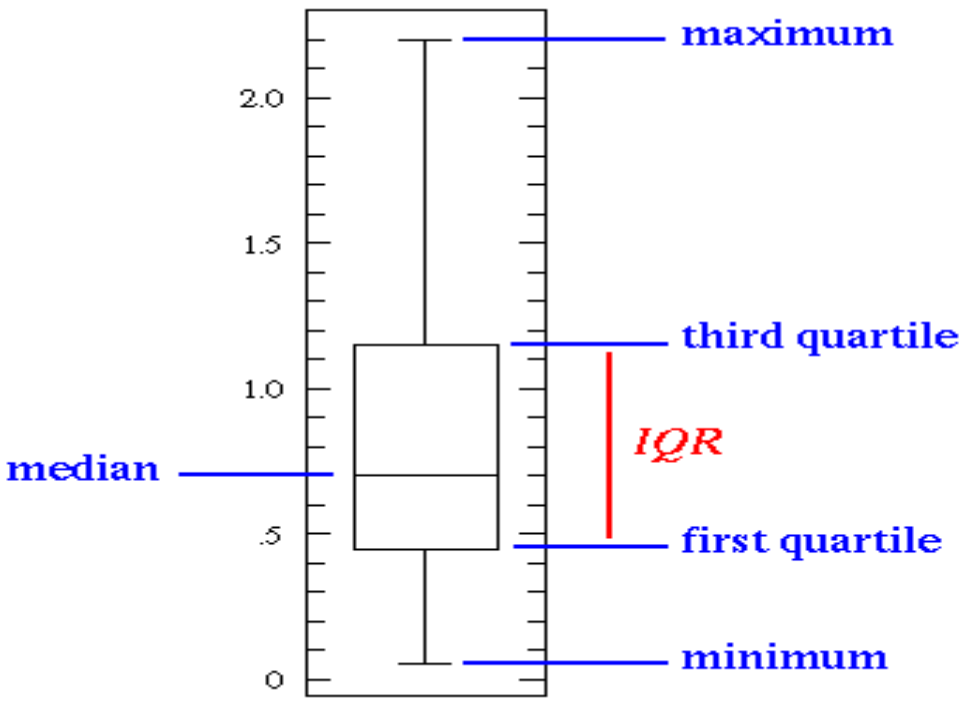

Figure 2.7a: An example of a typical boxplot with all data points ideally distributed between the minimum point (whiskers below) and maximum point (whiskers above). The median (med.) point is in the (interquartile range) IQR box, in between the 1st and 3rd quartiles (no outliers). Adapted from statistics education online (http://www.dummies.com/education/math/statistics/what-a-boxplot-can-tell-you-about-a-statistical-data-set/)

Figure 2.7b; on the other hand show the non-ideal situation that is often more representative of real data sets. Where a small number of data points (sometimes insignificant %age compared to most of the data points) show values that are higher than the max or lower than the min. due sometimes to human error or other factors related to the data (not within the scope of this write up). Depending on how far apart from the min or max, they can be grouped **as suspected or real outliers**. For a case with suspected outliers (not far from min or max but more central), the whiskers (min or max point) is extended (downward or upward from 1Q or 3Q respectively) by 1.5 x IQR. For confirmed outliers (far from min or max) this value is 3 x IQR. The Isoprene30m and 15m data in section 4 (period 2) fall within an almost ideal data set with an insignificant %age of data points in some of the hours, showing up as suspected outliers.

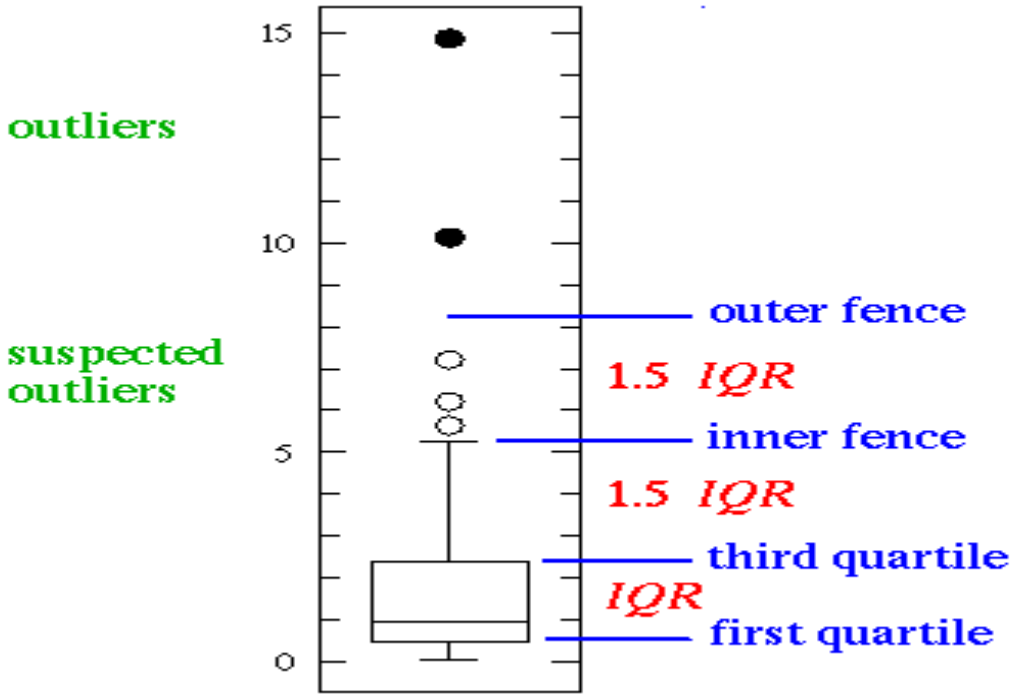

Figure 2.7b: An example of a non-ideal boxplot (but a typical representative of real data sets in some cases). Where all data points appear to be well distributed between the minimum (min.) point (whiskers below) and maximum (max.) point (whiskers above), with a small %age of points (sometimes insignificant), below and above the min. and max. They are either called suspected outliers (when not far from whisker) or outliers (when far removed from whiskers) The median (med.) point is still in the (interquartile range) IQR box, in between the 1st and 3rd quartiles. Adapted from statistics education online (http://www.dummies.com/education/math/statistics/what-a-boxplot-can-tell-you-about-a-statistical-data-set/)

Chapter 3

Isoprene and its reaction products in a deciduous temperate forest: August – September 2015

3.0 Overview: guide to the chapter

The results for the 2015 measurement campaigns are presented in two periods. Discussion of period 1 (19 - 21 August 2015) is in section 3.1 (subsections 3.1.1 to 3.1.5); measurement period 2 (23 August – 03 September 2015) is presented in section 3.2 (3.2.1 to 3.2.6). Within each section, the periods are described under the same five topics;

i. Air temperature versus date, The volatile organic compound (VOC) versus date

ii. Isoprene time series plot, Methyl vinyl ketone and Methacrolein (MVK/MACR) time series plot

iii. Basic statistics

iv. Isoprene versus temperature

v. MVK/MACR versus Isoprene

That is, the environmental context and basic time series data are presented as time series analysis, in sub-sections (I and ii). The last two sub-sections (iv and v) are to investigate co-variations; that is, how isoprene concentrations depend on air temperature and how the change in the concentration of the oxidation products is dependent on isoprene concentration. Sub-section (iii) summarises the data in terms of basic statistics: minimum; 25th percentile (25 %ile; 1st quartile); 50 %ile (median); 75 %ile (3rd quartile); and maximum. In addition, period 2 investigates the above parameters at both 15 meters and 30 metres height in the forest, denoted below by Isoprene30, Isoprene15, MVK/MACR30 and

MVK/MACR15, in the plots and reports in period 2 (3.2.1 to 3.2.6). It is important to note at this point, that all times are based on the Greenish mean time (GMT). Finally, in Section 3.2 is the Summary and conclusion.

3.1. Period 1: (19 - 21 August 2015)

This data was collected between 19/08/2015, 15:10 GMT and 21/08/2015, 13:00 GMT. It consists of 551 entries, at five - minute intervals using the proton transfer reactor (PTR), as described in Chapter 2. The data, produced from the time of flight mass spectrometer (ToF- MS) detector, was converted to a coma separated value (.csv) file format and imported into RStudio (2017), through Microsoft excel (2016). The results from the data processed in RStudio (2017) are presented below.

3.1.1. Environmental context (Period 1)

The air temperature (Figure 3.1) over the three diurnal cycles, show consistent early morning minima and afternoon maxima. Wednesday, and Thursday have minimum values that are closer together at 12.20 ^{o}C. and 13.10 ^{o}C, while the maximum temperatures on Thursday and Friday are even much closer at 21.4 ^{o}C. and 21.5 ^{o}C respectively; they also occur much later in the afternoon at 16.00 GMT, rather than close to noon, as is the case for Wednesday, which occurred at 11.00 GMT. The maximum temperature of 18.1 ^{o}C, on Wednesday, was 0.9 degrees, more than the minimum value of 17.2 ^{o}C, on Friday; (notice this, also in Table 3.1). The diurnal temperature range (DTR); (that is, the difference between the daily maxima and minima temperatures), was highest on Thursday at 8.3 ^{o}C, followed by Wednesday at 5.9 ^{o}C, before Friday at 4.3 ^{o}C.

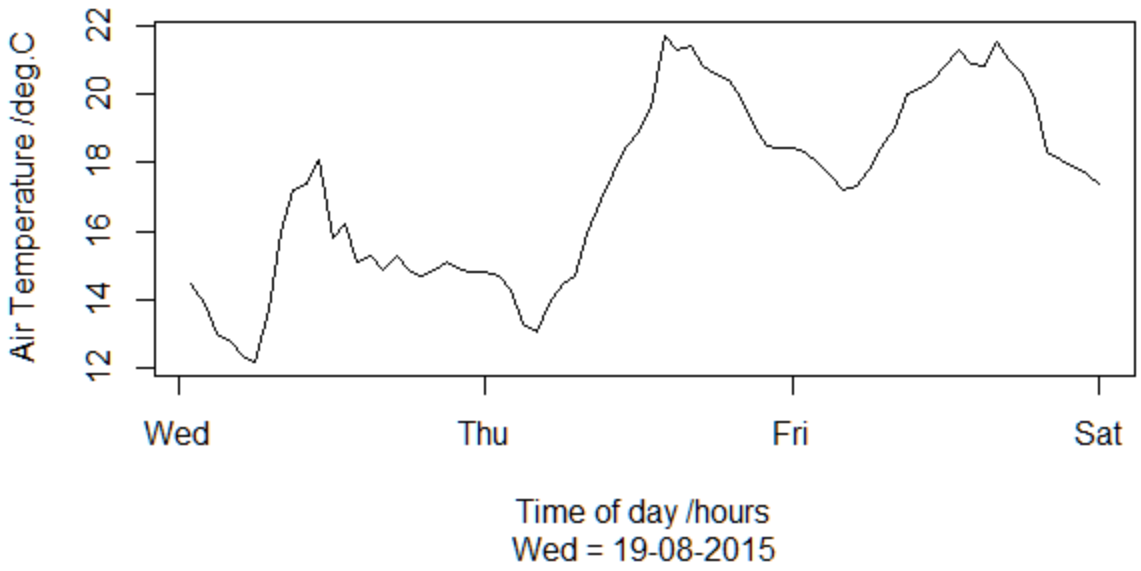

Figure 3.1: Air Temperature against date for Mill Haft data; collected between 00:00 hours on Wednesday, 19 and 00:00 hours (GMT) on Friday/Saturday, 21 August 2015.

The highest and lowest daily temperatures are summarized in table 3.1. The temperature profile for the three days shows increasing minima and maxima resulting in Friday being the hottest day, followed by Thursday, although the maximum temperatures for both days were similar by 16:00 hours.

Table 3.1: Summary of the highest and lowest daily temperature points in Figure 3.1

DAYS	Minimum Temp. (°C) / Time (hrs.) GMT	Maximum Temp. (°C) / Time (hrs.) GMT	Comment
Weds.	12.2 °C at 06.00	18.1 at 11.00	
Thurs.	13.1 at 04.00	21.4 at 16.00	
Fri.	17.2 at 04:00	21.5 at 16.00	

Comparing Figure 3.1 with UK 2015 and long term; summer average temperatures.

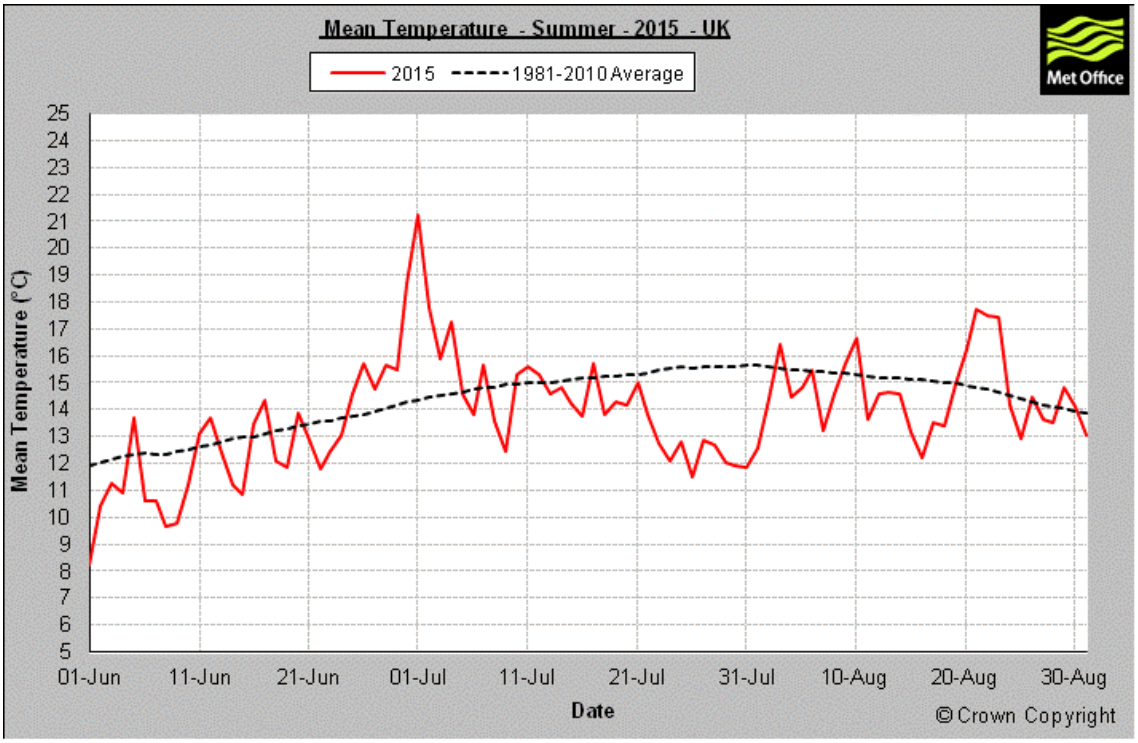

Figure 3.1a: Adapted from Met Office (2015b); Showing the daily mean temperature for summer 2015 in the United Kingdom, as compared to the 1981-2010 average. The 2015 mean temperature was 13.9 °C, it was 0.4 °C, below the 1981-2010 average, which was 14.3 °C.

The 1981 to 2010, average temperature (Figure 3.1a), for the UK, was 14.3 °C (Met Office 2015a). The normal summer temperatures can be as high as 32°C, but only gets up to 26°C, most of the time. The average temperatures in London for high and low respectively, are about 21°C and 12°C., (Barrow M. 2013). In summer 2015, all the three months (June, July, and August) shewed lower mean temperatures, than the UK average, for those month, by; (-0.3) °C in June, (-0.7) °C in July and (-0.2) °C in August. Comparing the UK mean temperature value of 13.9 °C, for 2015 summer, with the UK average 1981 to 2010 (Figure 3.1a), show a decrease of 0.4 °C in 2015, and reflects a cooler overall summer and a slightly cooler August. Although August was generally classified as 'unsettled' due to the temperature

fluctuations which stayed largely close to the normal levels, around eastern England; with warmer days that went as high as 25 °C, but up to 30°C, on the 22nd for the London area (Met Office 2015b). The minima and maxima values noted for the three days, of 19th to 21st August (Figure 3.1 and Table 3.1), are, in agreement with the Met Office observations for 2015 summer, as compared to the UK norm; (Met Office 2015a and b). These days (Table 3.1 and Figure 3.1) were progressively hotter from Wednesday, the 19th; and by Friday the 21st, was beginning to show the range of temperatures, that naturally climaxed into the higher values as observed in London, for the 22nd of August 2015.

3.1.2. Isoprene and MVK/MACR time series (Period 1)

Note that the isoprene dataset (Figure 3.2), started at about 15.00 hrs on Wednesday 19/08/2015, whereas the temperature plot started at 00:00 hrs on the same day. Figure 3.2 shows a decrease in concentration of isoprene, from 1 ppb (parts per billion volume), to a concentration of about 0.4 ppb by 00:00 hrs, on Wednesday/Thursday, 20/08. Comparing this to the temperature profile in Figure 3.1, above we notice that the temperature was fluctuating and steadily decreasing throughout the afternoon, even though, there appears to be only a slight drop between 15:00 hrs and 00:00 hrs, on Wednesday/Thursday, 20/08, when the temperature became 14.8 ^{o}C by 00.00 hrs. Overlaid on this overall decrease in concentration is what appears to be a diurnal cycle on Wednesday and Thursday, although a diurnal pattern is not present on Friday.

So, isoprene concentration dropped (Figures 3.2) with temperature (Figure 3.1) all the way to 06:00 hrs on Thursday (Figure 3.4), and continued to drop below 0.4 ppb, all the way down to about 0.25 ppb, by late afternoon (about 16:00 hrs); (Figure 3.4, actually shows the concentration of isoprene fluctuating between 0.4 ppb and 0.3 ppb until about 10.00 hrs before it began to gradually slide down). This is

despite the observable rise in temperature in figure 3.1, between 04:00 and 16:00 hrs on Thursday, when it reached a peak of 21.4 °C at 16:00 hrs.

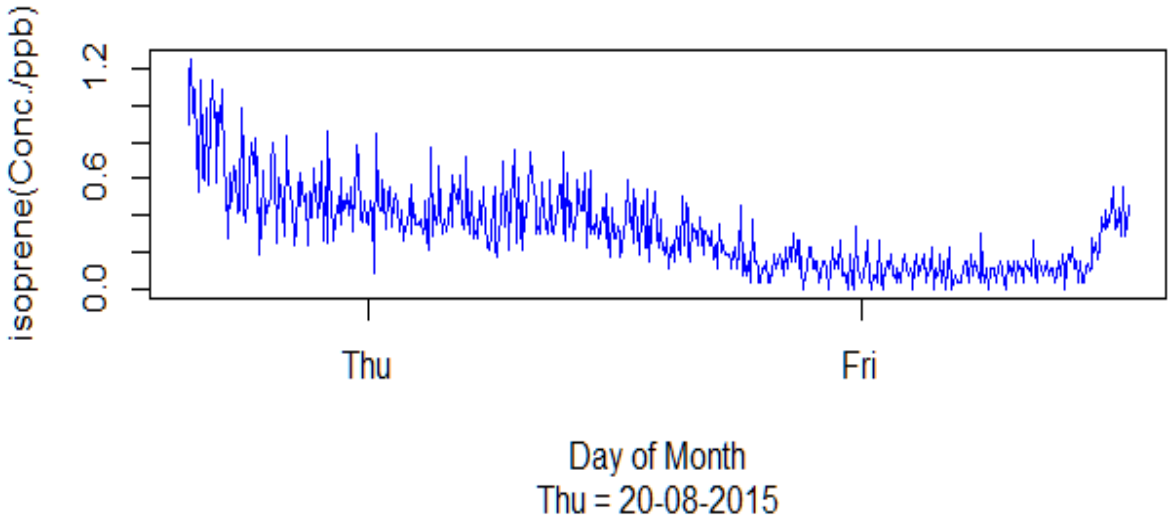

Figure 3.2: Isoprene concentration against date, for Mill Haft data; from between 15.00 hours, on Tuesday, 19 to 13.00 hours (GMT), on Friday, 21 of August 2015. See also Figure 3.4 below, for the plot of the hourly mean concentrations against time for each day.

The isoprene concentration continued to decrease (Figure 3.2), until it got to about 0.1 ppb at 00.00 hours on Thursday/Friday, 21/08 (Figure 3.4). It remained at this level of about 0.1 ppbv, from 00:00 hours, until late morning about 10:00 hours, before rising again from that point (of 0.1 ppbv), back up to 0.4 ppbv, at about 13:00 hours; where this data terminates Figure 3.4).

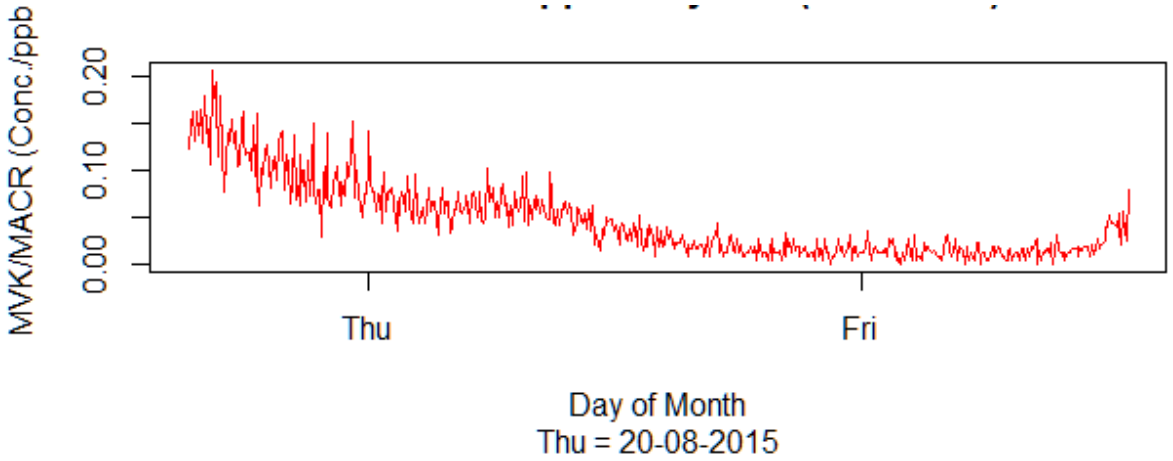

Figure 3.3: Methyl Vinyl Ketone (MVK) / Methacrolein (MACR) concentration against date, for Mill Haft data; from between 15.00 hours. on 19, to 13.00 hours. on 21 of August 2015. See also figure 3.5 below, for the plot of the hourly mean concentrations against time for each day.

The pattern for MVK / MACR (Figure 3.3) is similar to that for isoprene (Figure 3.2) but note that the y - axis scale is a factor of 5 magnified compared to Figure 3.2.

Figure 3.4 shows hour-average isoprene concentrations plotted as a function of time of day, to emphasise diurnal patterns. The two horizontal lines from the end of one day to the beginning of the next (that is; from the right-hand side to the left), indicates a single continuous dataset, and connects the progression with time (see also Figure 3.2, to compare). The concentration pattern shown on day 19 (which is; decreasing from a higher level of, above 0.90 ppb, at 15.00 hours) was consistent, with what is expected, even though at very low concentrations (<0.1 ppb), as is the case here, other types of reactions in the environment, different from the current focus, can more easily influence the expected pattern of concentrations. This might be the case for day 20, where it is expected to rise during the day (especially between noon and about 3pm), but was dropping, due possibly to lower light and radiation, and other reactions, at that height in the forest. The concentration was at its highest point around 15.00 hours on day 19, began to drop rapidly down to about 0.44 ppbv by 0.00 hours on the 20th of August.

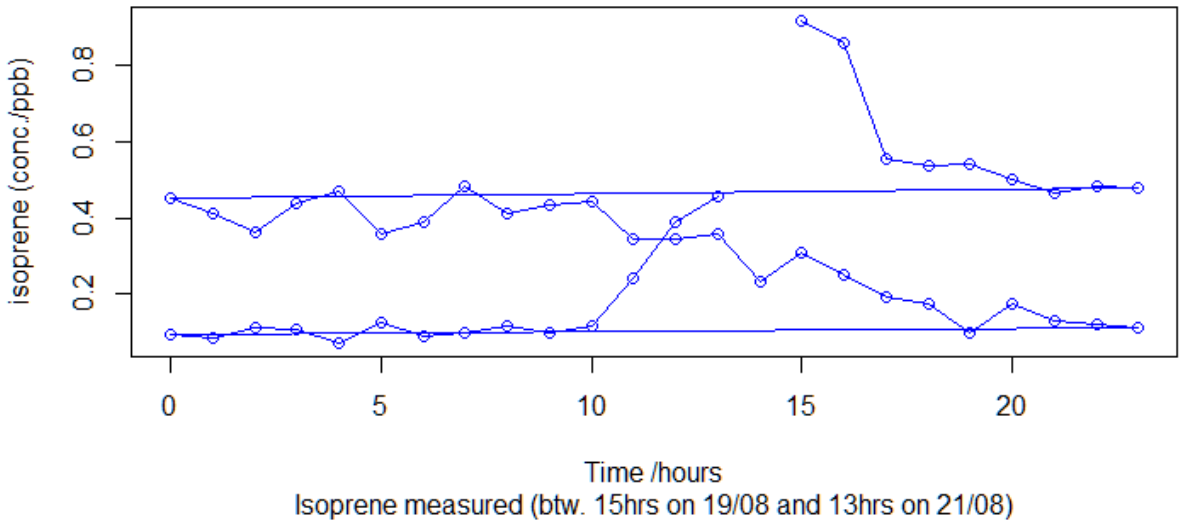

Figure 3.4: Isoprene concentration against time-of-day, for Mill Haft data; from between 15.00 hours. on 19, to 13.00 hours. on 21 August 2015.

The concentration continued to fluctuate (Figure 3.4) around 0.30 ppb, until about noon, on the 20th, before it began to drop rapidly down to less than 0.10 ppb by 0.00 hours on the 21st. This can be due possibly to other reactions including NOx from the neighboring air movements coming from polluted air around the city. The concentration began to rise from that lowest point of about 0.10 ppbv back up to 0.44 ppb, between 10.00 and 14.00 hours. This is also consistent with expected rise in concentration for daytime as temperatures begin to rise and / or light intensity increases (example; Sharkey et al 2008). In this case, there was an actual rise in temperature corresponding to this time frame, on Friday 21/08, as can be seen in Figure (3.1) and Table (3.1), in which temperature was shown to rise from 17.2 °C at 04:00 hours and rose to a peak of 21.5 °C by 16:00 hours. So that, even when a direct linear relationship with temperature, cannot be established throughout the entire period in view; by looking at the concentration/temperature pattern, over the 3 days, it is possible to say, that there appears to be a combination of temperature level and light intensity, that influences the isoprene concentration. The

diurnal patterns for MVK/MACR (Figure 3.5) follows the same general pattern as for isoprene (Figure 3.4), except, that the scale for the concentration axis for MVK/MACR compared to isoprene shows a ratio of about 10 to 1.

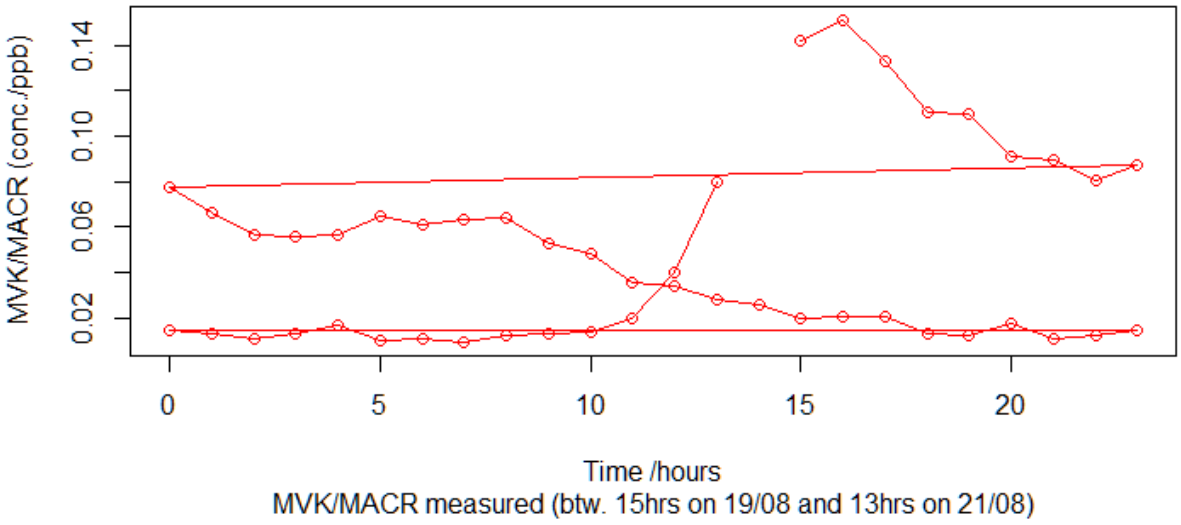

Figure 3.5: Methyl Vinyl Ketone (MVK) / Methacrolein (MACR) concentration against time-of-day for Mill Haft from 15hrs. on 19 to 13 hrs. on 21 of August 2015.

3.1.3. Basic statistics (period 1)

Table 3.2: Summary statistics for Mill Haft Data (Period 1) 19 -21/08 /2015

No. / Type	Minimum	Ist Quartile	Median	Mean	Standard deviation	3rd Quartile	Maximum
1. Temperature	12.2	14.9	17.7	17.3	3.4	19.7	21.7
2. Isoprene	<LoD	0.1	0.3	0.3	0.3	0.5	1.3*
3. MVK/ MACR	<LoD	0.02	0.03	0.05	0.04	0.07	0.2

4. Isoprene (hourly)	0.07	0.1	0.3	0.3	0.3	0.5	0.9 *
5. MVK/MACR (hourly)	0.01	0.01	0.03	0.05	0.05	0.07	0.2
6. Ratios (2./3.)	<LoD	7.7	8.9	6.9	3.1	6.7	6.1

Note- Data used for 1 & 2 were taken at 5-minute intervals while those used for 4 & 5 were from the hourly average of these values. LoD - limit of detection. * - asterisk to make isoprene data more visible. Units for isoprene and MVK/MACR = ppbv

The mean temperature for the three days was 17.3 ± 3.4°C with a maximum temperature of 21.7 °C (see; (Figure 3.1), above, for the air temperature plot against the time of day; for the three days; and (see also; (Table 3.1), for the summary of minimum and maximum temperature points).

3.1.4 Isoprene vs temperature (Period 1)

The isoprene temperature relationship is most often explained in an exponential relationship that also involves light intensity as can be seen in (Guenther et al., 1993; Niinemets et al., 2004; Sharkey et al., 1995; Fehsenfeld et al., 1992). The relationship of temperature on the isoprene concentration can also be determined by how direct or indirect the radiation is, for the height of forest (Greenberg, 2003). Increase in Isoprene emission was directly linked to leaf temperature rise in an exponential relation by (Fehsenfeld et al., 1992); so that, at a given light intensity, there was an increase in emission with temperature rise, that goes through an optimum point, before a decline.

Figure 3.6 shows the relationship between mean hourly isoprene concentration and temperature values, which is obviously not a linear one. Further analysis of this short dataset in this regard is of limited value; further discussion of the isoprene: temperature relationship is deferred to Section 3.2.4.

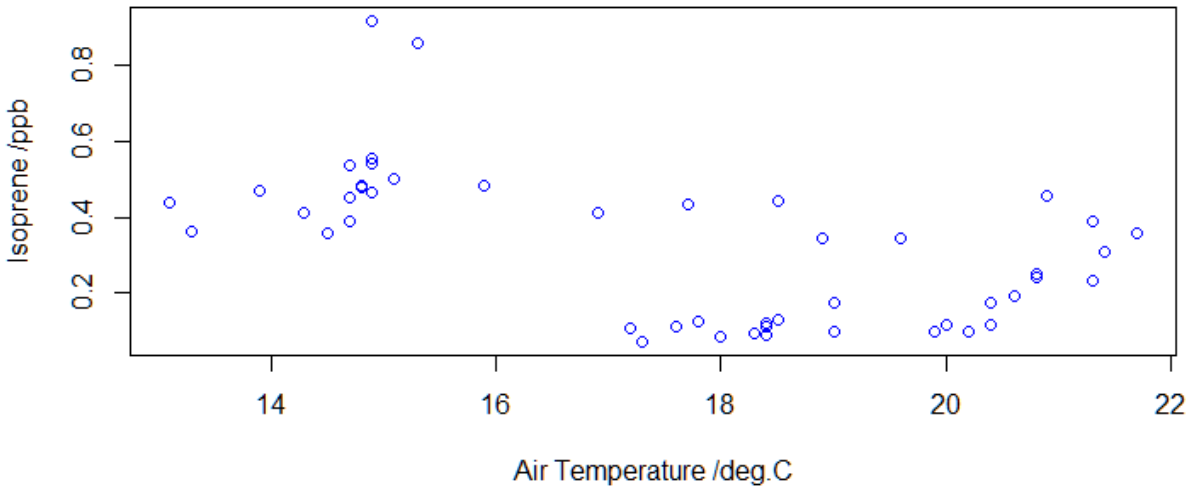

Figure 3.6: Air Temperature plot against Isoprene concentration for Mill Haft data; from between 15hrs. on 19 to 13 hrs. on 21 of August 2015.

3.1.5. MVK/MACR versus Isoprene (period 1)

The equation of the line (Figure 3.7), would result in 0.135 ppb of MVK/MACR, per ppb of isoprene, based on a linear relationship. However, since the coefficient of determination (R^2) shows a 0.57 linear correlation, between the two concentrations, then it means as much as 43% of the process is not predictable, based on the linear relationship in Figure 3.7.

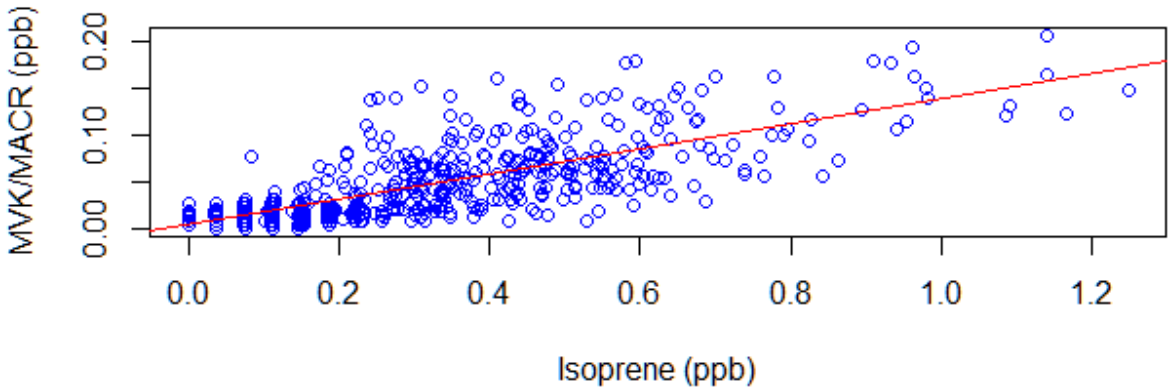

Figure 3.7: Isoprene against MVK / MACR (concentrations, at 5 minute intervals; with a linear trend line) for Mill Haft data; from between 15hrs. on 19 to 13 hrs. on 21 of August 2015. The Coefficients for

the linear trend line are: Intercept (MVK) = 0.003 ppb (MVK) and slope (isoprene) = 0.14 (ppbv (MVK) / ppbv (Isoprene)) hence the equation of the line is; y = 0.003 + 0.14x, and R^2 = 0.57

Then, using just the linear relationship would suggest a 13.5 % rate of change for the oxidation products, when compared to that of isoprene, and a residual 0.34% of MVK/MACR in the absence of any isoprene. Suggesting that only 0. 34% of the oxidation products are, as a result, of other processes, besides the oxidation of Isoprene as represented in Figure 3.7; most of the MVK/MACR (> 99%) at 2 meters height of the forest on those days (19-21/08/2015), could then be attributed to isoprene oxidation. Given the R^2 value, all predictions here are limited to the 56% linear correlation as reflected in the R^2 value.

3.2 Period 2: (23 August – 03 September 2015)

The data to be discussed here are summarised in Table 3.3.

Type of data	Period of data collection	Number of entries	Time interval between entries in minutes	Missing data (rows and dates they represent)*
Isoprene30m	23/08/2015, 19:20 to 03/09/2015, 11:01	1726	10	1562 - 1579; 02/09/2015, 03:31 to 02/09/2015, 06:41
Isoprene15m	25/08/2015, 14:46) to 03/09/2015, 10:56	1272	10	1086 to 1107; 02/09/2015, 03:56 to 02/09/2015, 07:26 and 1226 to 1248; 03/09/2015, 03:16 to 03/09/2015, 06:56.

MVK/MACR30m	25/08/2015, 14:41 to 03/09/2015, 11:01	1251	10	1204 and 1229; 03/09/2015, 03:11 to 03/09/2015, 07:21
MVK/MACR15m	25/08/2015, 14:46 to 03/09/2015, 10:56	1251	10	1204 1229; 03/09/2015, 03:16 to 03/09/2015, 07:26

Table 3.3. Summary of data and data gaps for period 2. * All missing data were removed before data processing.

3.2.1. Environmental context (period 2)

The mean value for the air temperature over the twelve days from August 23 to September 03 was 13.5°C. The linear regression line shows the temperature trend over this time, which was of decreasing temperature as would be expected for the northern middle latitudes. This is further enhanced by (Table 3.4), which captures the times (hours), with the minimum and maximum temperatures for each day. The twelve diurnal cycles represented in (Figure 3.8; Table 3.4), clearly show a consistent early morning minima and afternoon maxima in their air temperatures; except Monday 23, Wednesday 26 and Saturday 29, with minima at 23.00 hours and a maximum, at 11.00 hours on Tuesday 25. The lowest and the highest minima values, were 7.7 °C at 04.00 GMT and 12.9 °C at 23.00 GMT on Wednesdays; 2 and 26 respectively; although 12.8 °C at 23.00 hours on Monday 23 was only lower than the highest minimum temperature by 0.1° C. The temperature of 21.6 °C at 12.00 GMT on Monday 23, was clearly the highest of the maxima, making it (Monday 23), the hottest of the twelve days between 23 August

and 03 September 2015. The lowest of the maxima temperatures was 13.9 at 13.00 GMT on Thursday 03, with the lowest and highest diurnal range (DTR) (that is; the difference, between the highest and lowest daily temperatures); being 3.3 and 9.5; on Monday 31 and (Monday 24 / Friday 28), respectively.

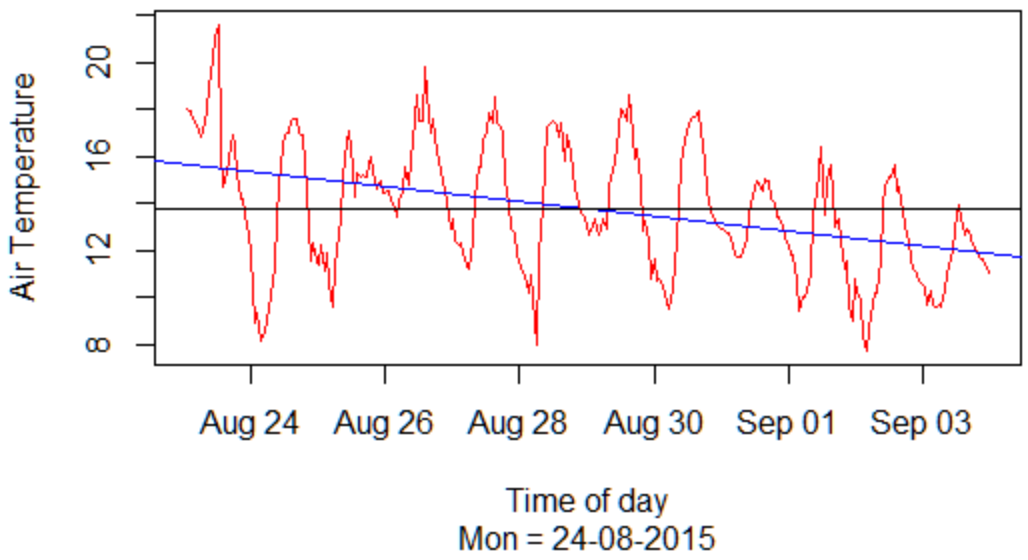

Figure 3.8: Air Temperature against date, for Mill Haft data; plots from 00.00 hours (GMT), on 23 August to 23.00 hours (GMT), on 03 September 2015. The horizontal line shows the mean temperature at 13.51°C, with the linear line fit, to show the trend around the mean temperature.

Table 3.4: Summary of the highest and lowest daily temperature points in Figure 4.1

August 24 – September 03, 2015

DAYS	**Minimum Temp. (° C) / Time (hours) GMT**	**Maximum Temp. (°C) / Time (hours.) GMT**	**Comment;** (DTR (° C) - daily temperature range; highest minus lowest daily temperature)
Sunday 23	12.8 at 23.00	21.6 at 12.00	(DTR; 8.8)
Monday 24	8.1 at 03.00	17.6 at 16.00	(DTR; 9.5), 17.6 **° C** occurred twice, at 15 & 16 hours,
Tuesday 25	9.6 at 05.00	17.1 at 11.00	(DTR; 7.5)
Wednesday 26	12.9 at 23.00	19.8 at 14.00	(DTR; 6.9)
Thursday 27	11.2 at 06.00	18.5 at 15.00	(DTR; 7.3)
Friday 28	8.0 at 06.00	17.5 at 12.00	(DTR; 9.5)

Saturday 29	10.8 at 23.00	18.6 at 15.00	(DTR; 7.8)
Sunday 30	9.5 at 05.00	17.9 at 16.00	(DTR; 8.4)
Monday 31	11.7 at 07.00	15.00 at 16.00	(DTR; 3.3), 11.7 **°C** occurs at two points 06 & 07 hours
Tuesday, 01	9.4 at 04.00	16.4 at 12.00	(DTR; 7.0)
Wednesday 02	7.7 at 04.00	15.6 at 14.00	(DTR; 7.9)
Thursday 03	9.6 at 05.00	13.9 at 13.00	(DTR; 4.3), 9.6 **°C** occurred twice; at 05 & 07 hours

A Summary of UK Climate Between 23 August and 03 September 2015

Sunday the 23rd of August, being the starting date in Figure (3.8), showed up on the satellite image (Figure 3.8a), as a very interesting day, with a contrasting weather across the UK. A dull, wet and cloudy one, over the southwest, but a brilliant summer day over northern England and Scotland; it started out, as a dry and bright day, in many areas, and remained warm, with temperatures up to 25 °C, but the cloudiness observed in the morning, at the southwest, eventually spread towards the northeast, over the day. There was rain and intermittent thunderstorms in the areas around the south, on the 24th morning, but spread towards the north in the afternoon; even though the north was mostly dry and bright, throughout the day. A bit of rain spread into the south on the 26th, but quickly began to move north east. On the 26th, many areas in the south, including Heathrow (Greater London), were affected by thunder and heavy showers, that spread eastwards, even though it started out in the north, as isolated patches of showers; 52 mm of rain was recorded in Heathrow. Days 27 and 28 came out looking similar with bright sunlight and scattered patches of showers, with the heaviest showers recorded respectively for the two days around the west country / Thames valley and the north. The 29th started off with bright sunshine which by afternoon, turned into showers in the north and rain in the areas around the south. The southwest saw rain in the morning, on the 30th, which also spread to the east by

afternoon, but the areas around the north remained mostly dry. Most of the morning on the 31st, brought rain to many areas, which, moving towards the east, gradually reduced to scanty patches of rain; with intermittent thunder in the distant areas of the south (Met office 2015b).

Early September; up to the 11th, was generally cool with showers, by winds from the northwest. Days 1 and 2; were similar with sunshine and a lot of showers, that were more serious in some places than others. Accompanied by thunder in some areas, and a record of 32 mm of rain in Crosby, Merseyside. The only exception to the extensive and intense showers, was the southwest., on day 2. Day 3; weather, was still with a north westerly breeze, but cooler, holding the most cloud in the east, and a less extensive and lighter rain showers (Met Office 2015c). The UK mean temperature at 11.9 °C, was below the long term 1981 – 2010 average by 0.8 °C, while the September mean temperature was also below the long-term average by 1.1 °C, and became the coolest September since 1994 (Met Office 2015c).

Figure 3.8a: Adapted from Met Office (2015b); A satellite image of the UK (Sunday 23 August 2015); showing a contrasting picture of cloudy and bright summer day across the UK. A bright summer day for Scotland and the north of England but a dull, cloudy and wet day for the south and west. (Image copyright Met Office / NASA)

3.2.2. Isoprene time plot, MVK/MACR time plot (period 2)

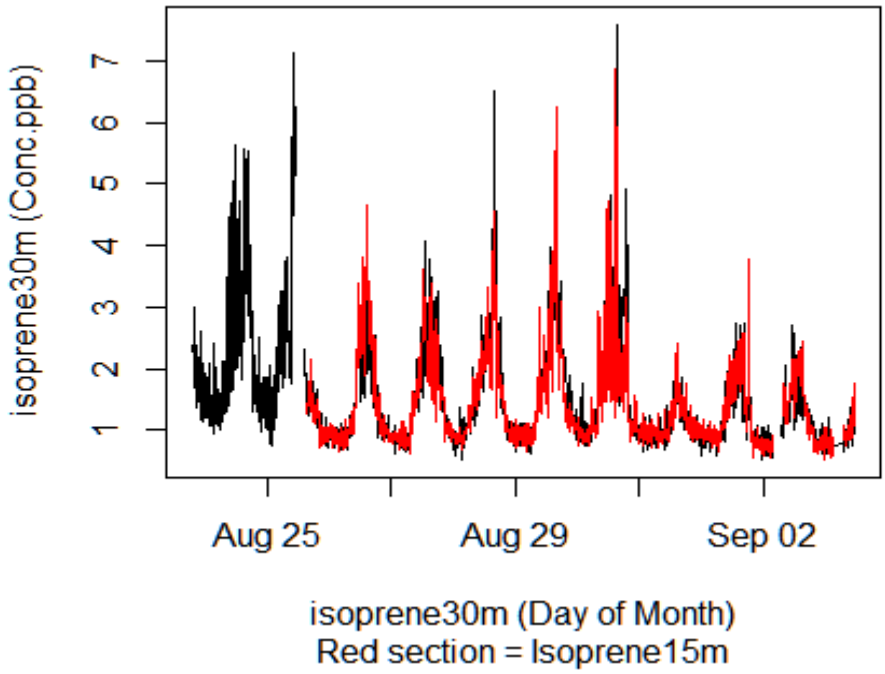

Figure 3.9: Isoprene30m (black) and isoprene15m superimposed (red) against time, for Mill Haft data; from between 19.00 hours on 23 August to 11 hours on 03 of September 2015. There is no data for Isoprene15m before 25 August 2015, while Isoprene30m started on the 23rd of August.

Isoprene concentrations measured at both heights of 15 and 30 meters show that the isoprene concentrations follow a diurnal pattern irrespective of the height (for measurements around 15 and 30 metres respectively) or date, as can be observed in Figures (3.9 to 3.21). A similar pattern is observed in

its oxidative products MVK/MACR (Figure 3.10).

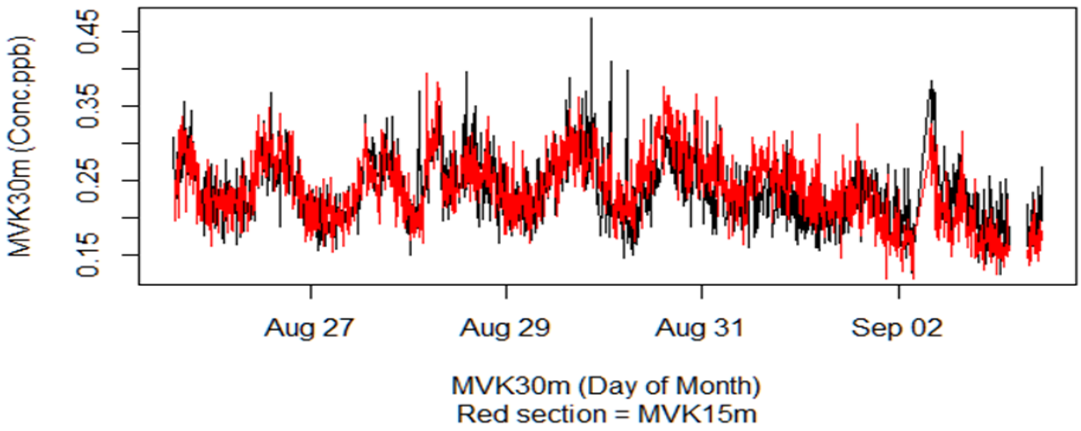

Figure 3.10: MVK/MACR30m plot against date, for Mill Haft data; from between 14hrs. on 23 August to 11 hrs. on 03 of September 2015; (with MVK/MACR15m placed over it for comparison).

The oxidation products of Isoprene; MVK/MACR30m and MVK/MACR15m (measured at about 30 and 15 metres respectively), also show a diurnal pattern of concentration with about 3 hours variation; occurring behind Isoprene see Figures (3.10 to 3.21)

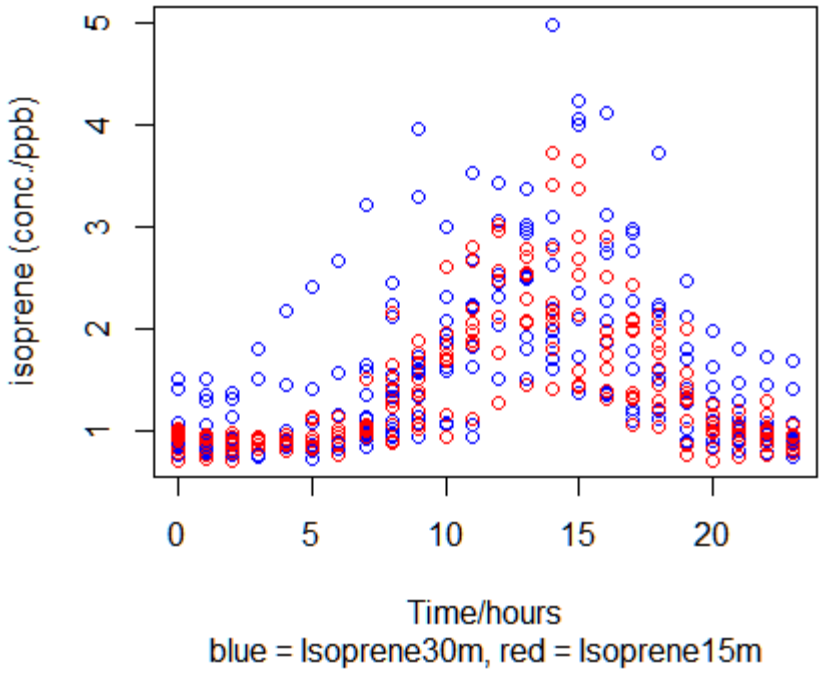

Figure 3.11: Comparing Isoprene hourly concentrations at both heights.

The diurnal patterns at both heights are shown in Figure 3.11. There is some indication that isoprene concentrations are higher at 30 m.

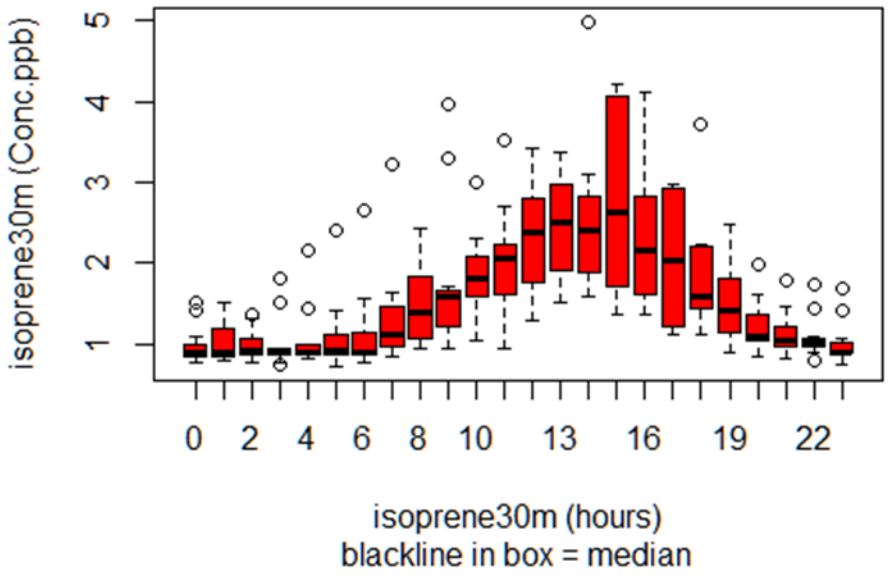

Figure 3.12: A Boxplot for Isoprene hourly concentrations at 30 meters height. *(See Figures 2.7; a and b, for the statistical guide used in interpreting this box plot).*

Figure 3.12 shows the variability of the diurnal pattern at the canopy level of 30 metres. The hours that have no suspected outliers on top or below the whiskers (which are; 1, 2, 8, 12, 13, 15, 16, 17 & 19), have 100% of the data distributed within the lowest whisker, (minimum, **m1**) and the highest (maximum, **m2**). All the other hours (except 0, 3, 22 & 23), have only one suspected outlier above or below the whiskers (m1 or m2), representing 10% or more but less than 20%, outside. Those with two outliers may represent between 10 to 20 % outside the area between m1 and m2. All the hours have at least 75% of the data well represented; that is, the 50% in the shaded area (IQR), is combined with the 25% from either (m1 to 1Q) or (3Q to m2). At 00.00 hours, the 3rd quartile or 75% of the concentration was about 1ppbv and below, while the median values from 00.00 hours to 06.00 hours were about the same level; a range, with the lower margin being the same as 1Q (1st quartile), but the top being (75 % ≤ 1ppbv) at 03.00 hours. The minimum at 00.00 to 02.00 hours is about 0.5 ppbv, with the 3rd quartile

(3Q or 75 percentile) at 00.00 and 02.00 hours at a level below 3Q for 01.00 hours. The maximum (m2) at 01.00 hours is about 1.5 ppbv. The median at 07.00hrs is at the same level as 3Q or 75 percentile for 06.00 hours, with the 75 percentile of 07.00 hours at about 1.5 ppb, and slightly above the median level of 08.00 hours, but the data is skewed downwards towards m1 as are all the other hours before it and 1Q or 25 percentile at 07.00 hour is about 1ppbv. The minimum level started rising from 0.5 ppbv by 07.00 hours and got to the same level as the median for the first 6 hours by 08.00 hours. The 25 percentile at 08.00 was already above 1ppbv, at the same level as the 75 percentile for 02.00 hours, 05.00 hours and just slightly below 75 percentile for the 06.00 hours. The maximum is just below 2.5 ppb at 08.00 hours, the median is the same as the maximum at 02.00 hours and 05.00 hours, 25 percentile at 18.00 hours, median at 19.00 hours and maximum at 21.00 hours. The 09.00 hours has a minimum that is about the same as 08.00 hours but its data is the first to be skewed completely upwards towards m2, so that the top of the median is merged with its 75 percentile. The 25 percentile for 10.00 hours, 11.00 hours and 16.00 hours are about the same level (≤ 1.6 ppb), while the 25 percentile for 12.00 hours, the median at 10.00 hours and the 75 percentile at 19.00 hours are about the same level (i.e. ≤ 1.8 ppb). 11.00 hours is skewed upwards and has the same median as 17.00 hours (i.e. ≈ 2.0 ppbv). The 75 percentile of 11.00 hours equals the median of 16.00 hours and the 75 percentile of 17.00 hours (≤ 2.2 ppbv). The median at 12.00 hours, and 14.00 hours is ≈ 2.45 ppbv but the median at 13.00 hours and the maximum at 19.00 hours are ≈ 2.50 ppbv. The 75 percentile at 12.00 hours, 14.00 hours and 16.00 hours are at the same level of about 2.8 ppbv while the 75 percentile at 13.00 hours is about 3.0 ppbv, the same as the maximum at 17.00 hours. The distribution at !5.00 hours appear, to be the major mirror point between the five hours before and after it, with a reasonably consistent rise from 10.00 hours to 12.00 hours and a similar fairly symmetric drop from 16.00 hours to 20 hours 16.00 hours has the largest spread of the IQR region, has the same minimum point as 12.00 and 17.00 hours of about 1.4 ppbv and cuts across the maximum, at 02.00 hours, median at 08.00 hours,

median at 19.00 hours and 75 percentile at 20.00 hours. Its 25 percentile is > = 1.6 and above the maximum for 00.00 hours to 07.00 hours, 20.00 hours to 23.oo hours and the 75 percentile for 09.00 hours, but same level as the 25 percentile at 12.00 hours. The 75 percentile at 15.00 hours is ≥ 4 ppb and about the same as the maximum at 16.00 hours and is very close to its own maximum at ≈ 4.2 ppbv. The diurnal pattern observed here for isoprene concentrations is consistent with the literature (e.g., Apex et al 2002, Stroud et al 2001)

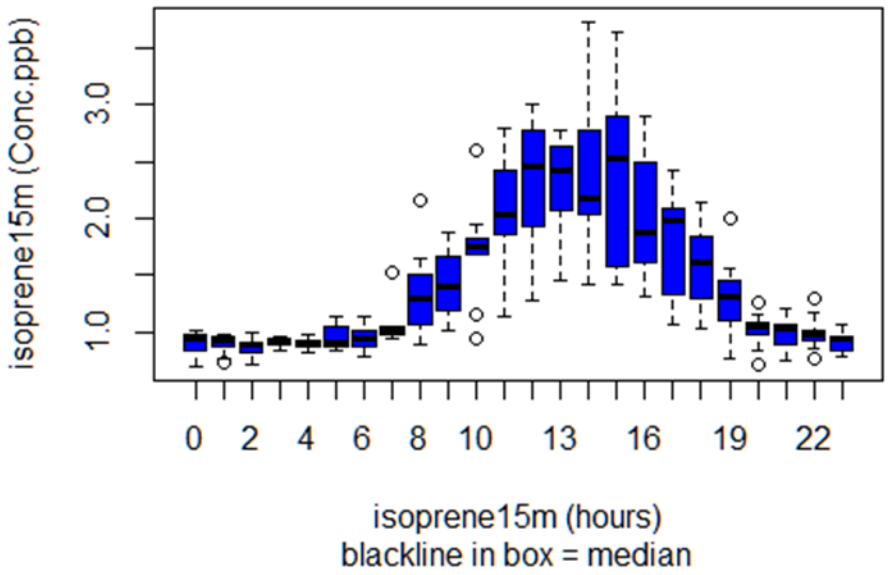

Figure 3.13: A Boxplot for Isoprene hourly concentrations at 15 meters height. ***(See Figures 2.7; a and b, for the statistical guide used in interpreting this box plot)***

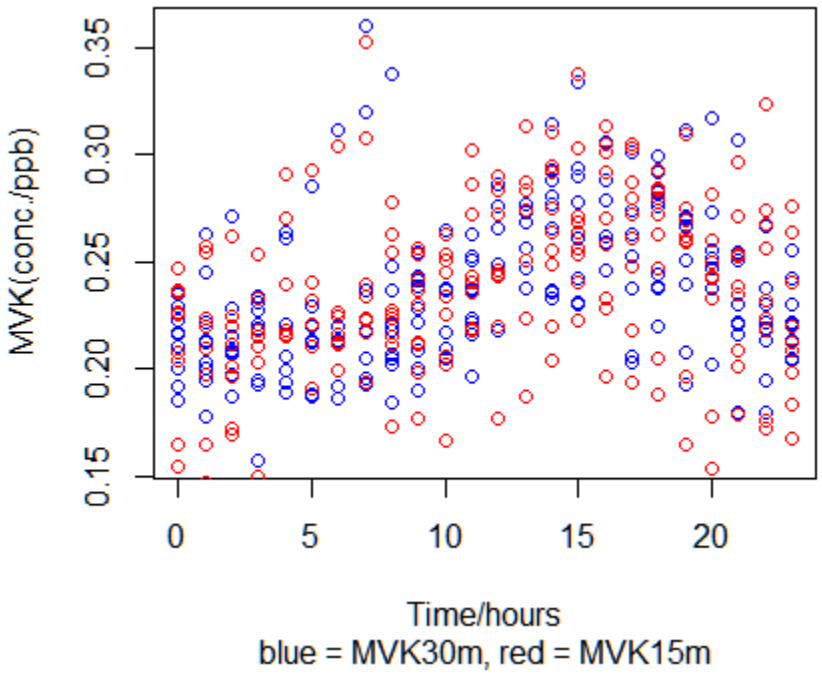

Figure 3.14: Comparing MVK/MACR hourly average concentrations at both heights.

Figure 3.14 compares hourly-average MVK/MACR diurnal patterns at 15 m and 30 m. There is no obvious difference in the two data samples. The box plots for hourly averages at 30 m and 15 m are similar (Figures 3.15 and 3.16). Data from both heights show an indistinct nocturnal minimum and a late afternoon maximum, with amplitude of ~ 0.03-0.05 ppbv in the medians. Data for particular hours are often highly skewed (i.e., medians approach 25th or 75th percentile values) but the direction of skew does not seem to follow any pattern.

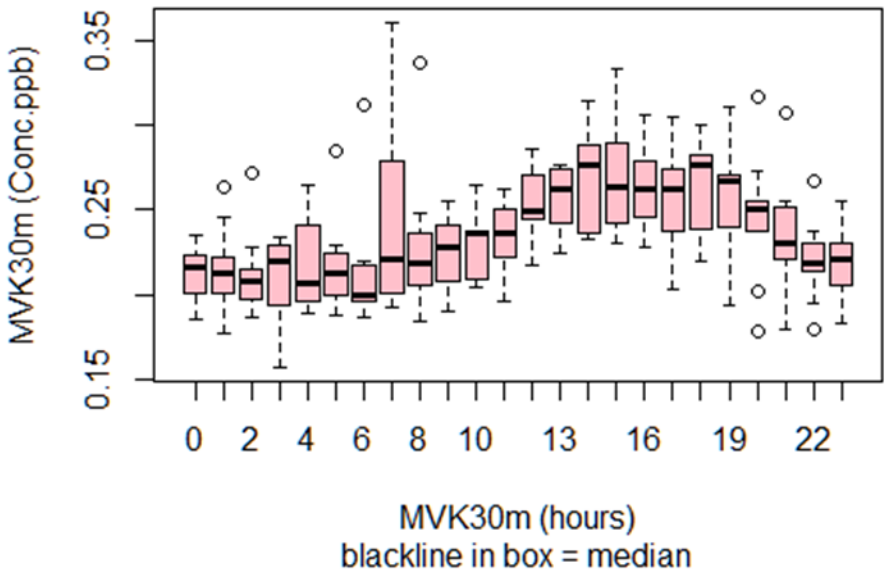

Figure 3.15: A Boxplot for MVK/MACR hourly concentrations at 30 meters height (notice how the concentration points in Figure 3.16 fit into the distribution here). ***(See Figures 2.7; a and b, for the statistical guide used in interpreting this box plot)***

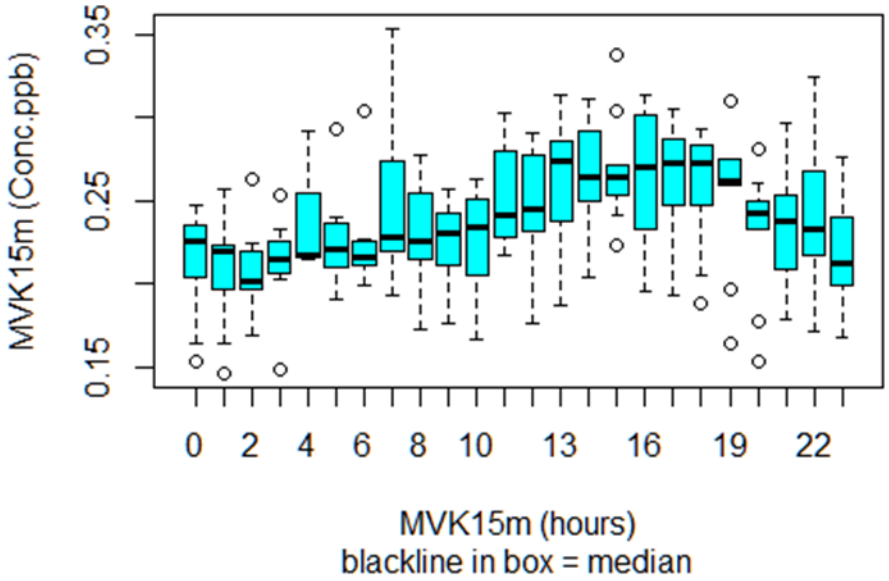

Figure 3.16: A Boxplot for MVK/MACR hourly concentrations at 15 meters height (notice how the concentration points in Figure 4.11 fit into the distribution here). ***(See Figures 2.7; a and b, for the statistical guide used in interpreting this box plot)***

3.2.3. Basic statistics (period 2)

Table 3.5: Summary statistics for Mill Haft data for period 2; 24/08 to 03/09/2015. Notes: all missing data were removed and usually insignificant compared to the rest of the data.

Type	Minimum	Ist Quartile	Median	Mean	Standard deviation (SD)	3rd Quartile	maximum	Number of missing records
1. Air Temp.	7.7	11.5	13.4	13.5	4.0	15.5	19.8	
2. Isoprene30m	0.5	1.0	1.4	1.7	1.7	2.1	7.6	22 *
3. MVK30m	0.1	0.2	0.2	0.2	0.1	0.3	0.5	1277
4. Isoprene15m	0.5	0.9	1.1	1.4	1.3	1.7	6.9	1318 *
5. MVK15m	0.17	0.2	0.2	0.2	0.09	0.3	0.4	1275
6. Isoprene30m (hourly)	0.7	0.9	1.1	1.5	1.1	1.8	5.0	6 *
7. MVK30m (hourly)	0.2	0.2	0.2	0.2	0.06	0.3	0.4	6
8. Isoprene15m (hourly)	0.7	0.9	1.1	1.4	1.0	1.8	3.8	10 *
9. MVK15m (hourly)	0.2	0.2	0.2	0.2	0.06	0.3	0.4	5

* - Asterisk; to make isoprene data more visible

3.2.4. Relationship between Isoprene and Temperature

Figures 3.17 and 3.18, show that isoprene concentration tends to increase monotonically with air temperature over the observed temperature range. The variability in the data suggests that other factors apart from temperature are also making contributions that influence the observed concentration patterns. The bulk of the isoprene30m concentrations between 9 and 16 degrees Celsius in (Figure 3.17) is less than or equal to 1 ppbv.

The rest of the concentrations that rose above 1 ppbv did not show a completely linear rise with temperature. The r^2 (coefficient of determination) value of 0.26 in (Figure 3.18) confirms that the isoprene concentration pattern with air temperature is not completely predictable by a log-linear relationship.

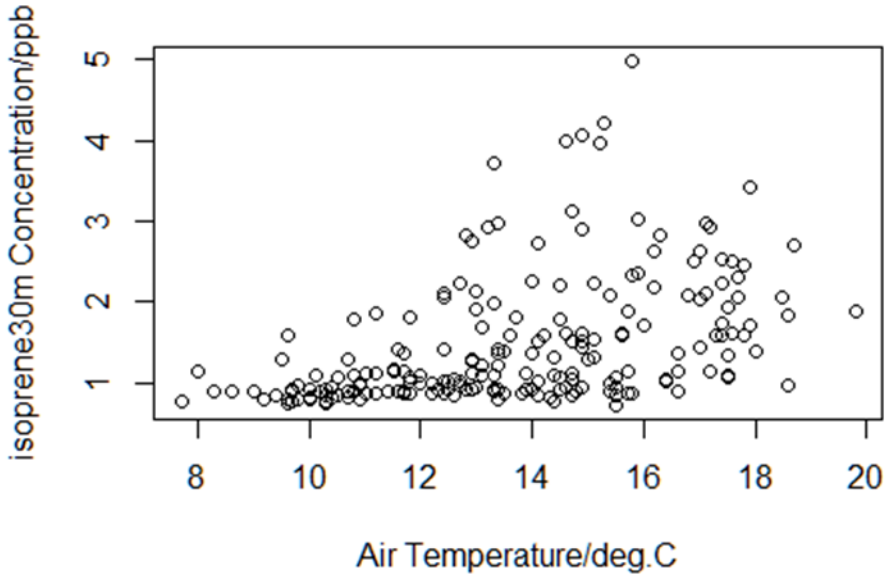

Figure 3.17: Air Temperature against Isoprene at 30 meters height.

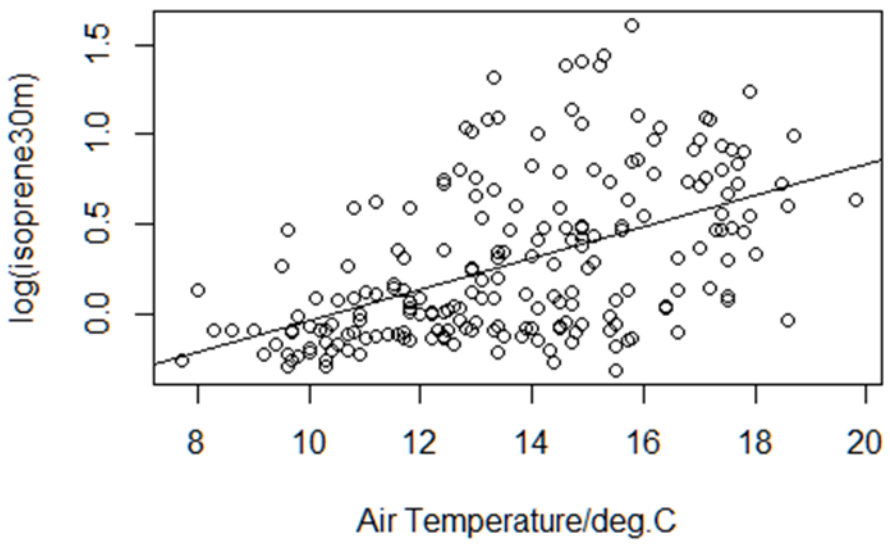

Figure 3.18: Air Temperature against log of Isoprene at 30 meters (with trend line fit). Intercept on log of isoprene30m (y axis) = - 0.9 ppbv and the slope = 0.087 ppbv °C^{-1}. The equation of the line is y = 0.087x- 0.91 and R^2 = 0.26

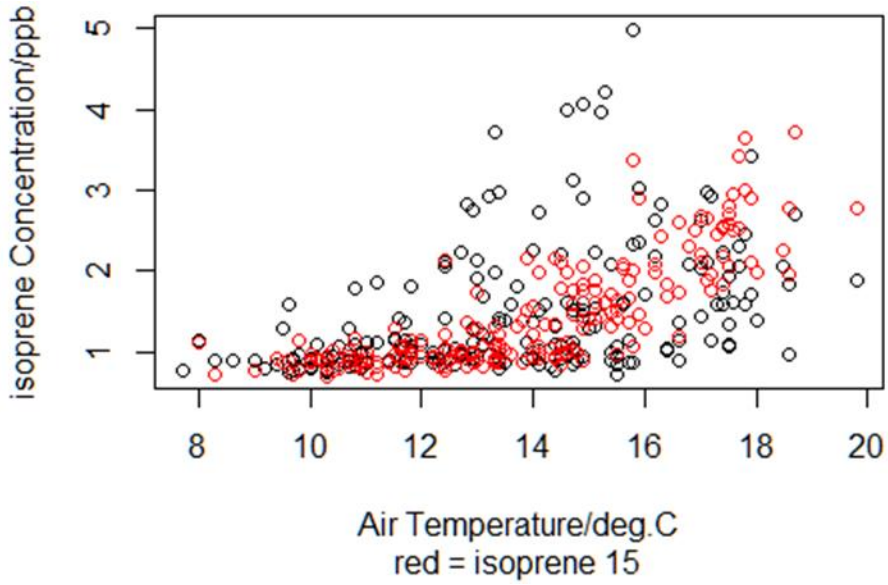

Figure 3.19: Air Temperature plot against Isoprene at both 30 and 15 meters height for comparison.

Figure 3.19, shows that the relationship of isoprene at both heights with air temperature is broadly similar. The isoprene concentration at 30 metres (shown in black) appears to be greater between 9 and after 16 degrees Celsius. They are also more dominant at the dispersed concentrations beyond 1 ppb. Some of these differences can easily be due to the better exposure to light and radiation at the 30 metres height as has been observed in other literature (e.g., Rasmussen and Jones 1973, Tingey et al. 1979, Monson and Fall 1989, Loreto and Sharkey 1990)

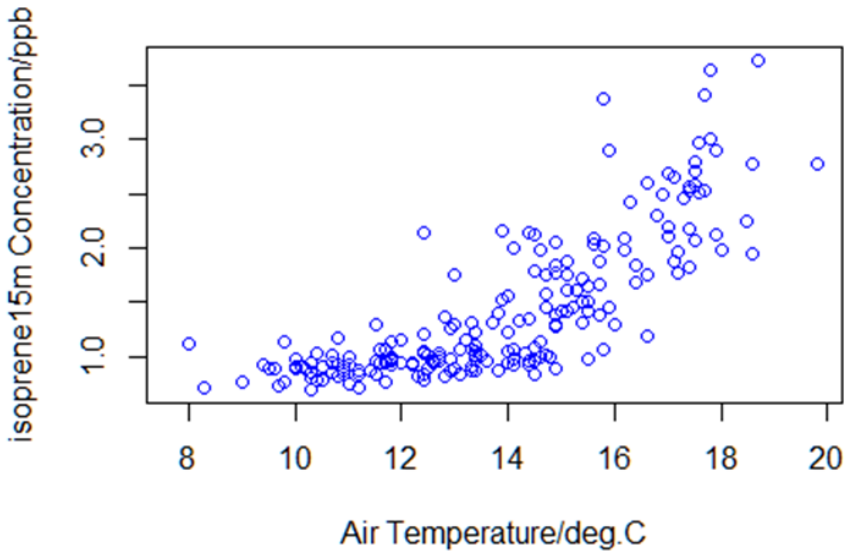

Figure 3.20: Air Temperature plot against Isoprene at 15 meters height.

Figures 3.20 and 3.21 (like 3.17 and 3.18, for isoprene30m), capture the relationship between isoprene at 15 metres height with air temperature. Figure 3.20 show concentrations response to air temperature that is similar in many ways to that of 3.17, but also differ in some crucial aspects, from 3.17, in ways that have been explained using Figure 3.19 above. Isoprene15m relationship with air temperature is also not completely linear, but seems to have a better linear correlation, based on the r^2 value of 0.68 in

Figure 3.21, as compared to that of isoprene30m, which was 0.26, in Figure 3.18; for their respective log-linear relationships with temperature.

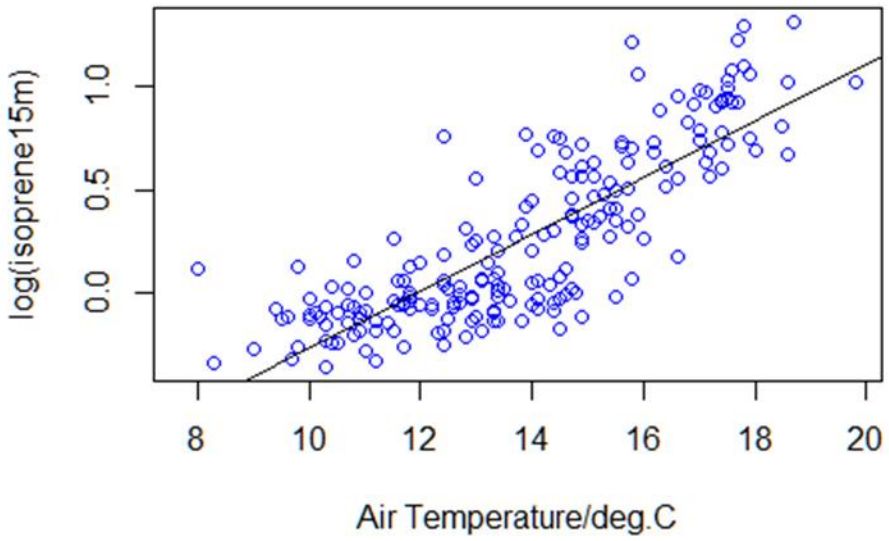

Figure 3.21: Air Temperature plot against log of Isoprene at 15 meters height. ***Intercept on log of isoprene15m (y axis) = -1.6 ppbv and the slope = 0.14 ppbv °C^{-1} The equation of the line is y = 0.14x - 1.6 and R^2 = 0.68***

Based on the r^2 value (Figure 3.21), the relationship with temperature appears to be better at 15 metres height than at 30 metres (compare with Figure 3.18). There is a possibility that the Shawbury data used for the temperature of those days, are more representative of data in the shady mid canopy rather than the top of the canopy, where leaves could be much warmer due to the direct sunlight on them.

3.2.5. Relationship between the oxidation products MVK/MACR and Isoprene (period 2)

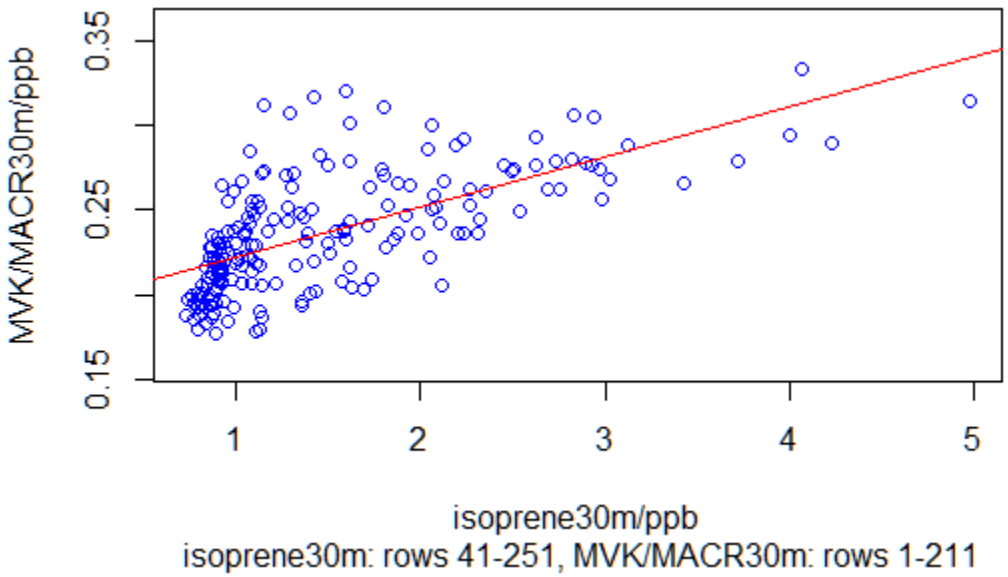

Figure 3.22: Isoprene plot against MVK/MACR; concentrations (at 10 minute intervals); at 30 meters height (with trend line fit). ***Rows 41 – 251 for Isoprene30m and rows 1 to 211 for MVK/MACR30m represent data for the same days and hours; 14 hrs. on 25/08/2015 to 11 hrs. on 03/09/2015.*** **Intercept on MVK/MACR*30m (y axis)* = 0.19 ppbv *and the slope = 0.*030 ppbv (MVK30m) ppbv (isoprene30m)$^{-1}$. *The equation of the line is y =* 0.19 *+ 0.*030*x and* R^2 *= 0.44***

The r^2 value of 0.44 (Figure 3.22), suggests a linear correlation of about 40%, between isoprene and MVK/MACR (its primary oxidation product); at 30 metres height. Based, on this linear equation alone, the MVK/MACR concentration at 1.0 ppbv of isoprene would be 0.2 ppbv, at 30 metres height. The highest density of concentration values is within; 1.2 ppbv on isoprene (x-axis) and 0.27 ppb on MVK/MACR (y-axis). Compare with (Figure 3.23); for isoprene and MVK/MACR (its oxidation product), at 15 metres; and notice that the r2 is 0.31. The linear equation predicts; 0.2 ppbv of MVK/MACR for 1.0 ppbv of Isoprene; and a linear correlation of about 30% at 15 metres. Even though, the relative MVK/MACR concentrations predicted at both heights are similar; the linear correlation at 30 metres is about 10% higher than at 15 metres height, between isoprene and its oxidation products. The

concentration density for 15 metres (Figure 3.23) is also, within 1.2 ppbv, on isoprene (x-axis) and 0.27 ppbv on MVK/MACR (y-axis); similar to 30 metres (Figure 3.22).

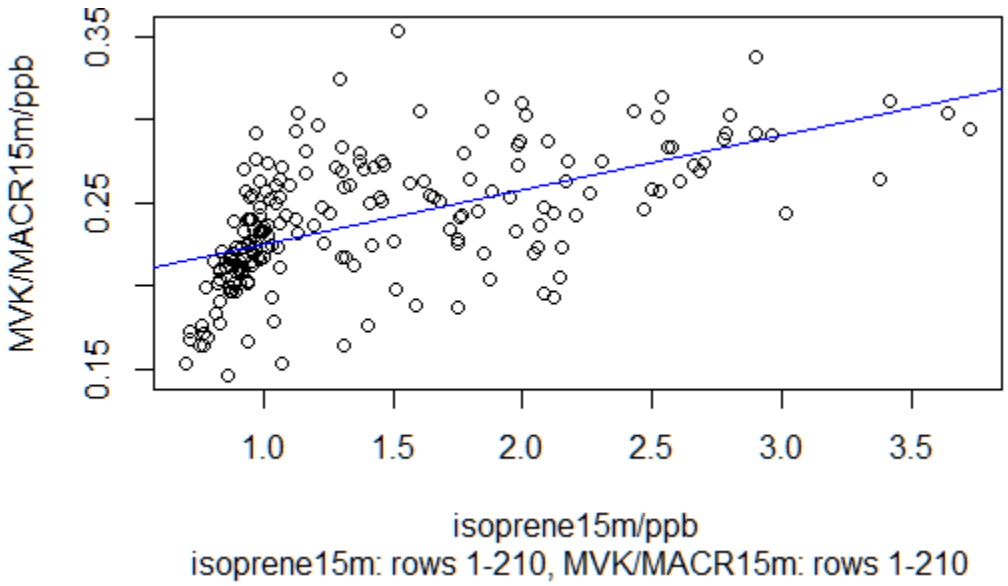

Figure 3.23: Isoprene plot against MVK/MACR; concentrations (at 10 minute intervals); at 15 meters height (with straight line fit). ***Rows 1 – 210 for Isoprene15m and rows 1 to 210 for MVK/MACR15m represent data for the same days and hours; 14 hours on 25/08/2015 to 07 hours on 03/09/2015. The data for MVK/MACR15m does not go beyond 07hours on 03/09/2015. Intercept on MVK/MACR15m (y axis) = 0.19 ppbv and the slope = 0.03 ppbv (MVK15m) ppbv (Isoprene15m)$^{-1}$. The equation of the line is y = 0.19 + 0.03x and R^2 = 0.31***

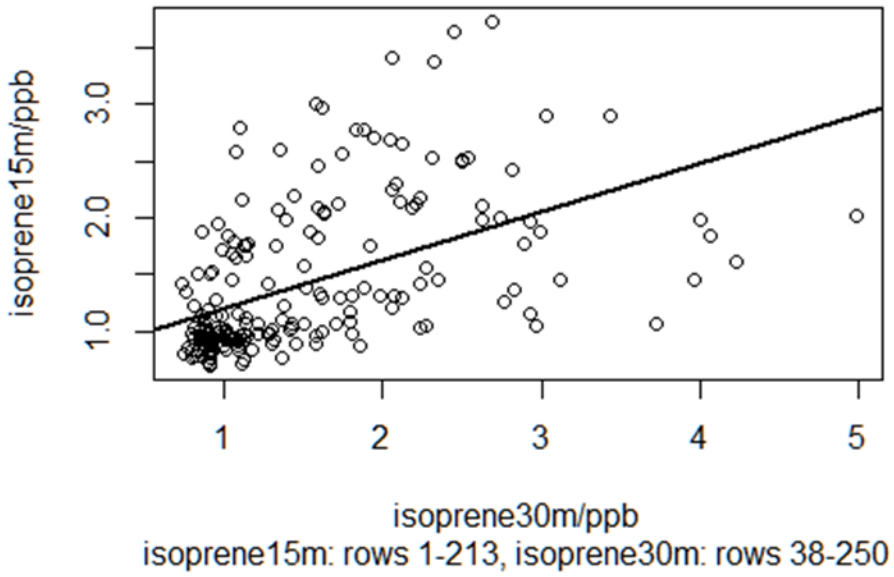

Figure 3.24: Isoprene30m plot against Isoprene15m; concentrations at 10 minute intervals; (with trend line fit). ***Rows 38 – 250 for Isoprene30m and rows 1 to 213 for Isoprene15m represent data for the same days, but 8hrs for 30m and 14hours for 15m; on 25/08/2015 to 10 hours on 03/09/2015. Isoprene15m has no data earlier than 14 hours on the 25/08, and the hourly data points only match up to give equal number of points using 08 hours from Isoprene30m data. Intercept on isoprene15m (y axis) = 0.77 ppbv and the slope = 0.42792 ppb (Isoprene15m) ppb (Isoprene30m$^{)-1}$. The equation of the line is y = 0.77406 + 0.42792x and R^2 = 0.2534***

The concentration pattern (Figure 3.24), only go to confirm an observation in Figure 3.19; that the concentrations at both 30 and 15 metres appear to be broadly similar. The highest density of concentration values appear to fall within 1.2 ppbv on both axis, followed by a less dense region between 1.2 and 2.0 ppbv, on either axis; then a more dispersed region beyond 2.0 ppbv on either axis. The *r^2 value at 0.25, suggests a poor linear correlation of about 25%, based on the above linear equation that gives 1.2 ppbv of isoprene at 15 metres, for 1.0 ppbv of isoprene at 30 metres.*

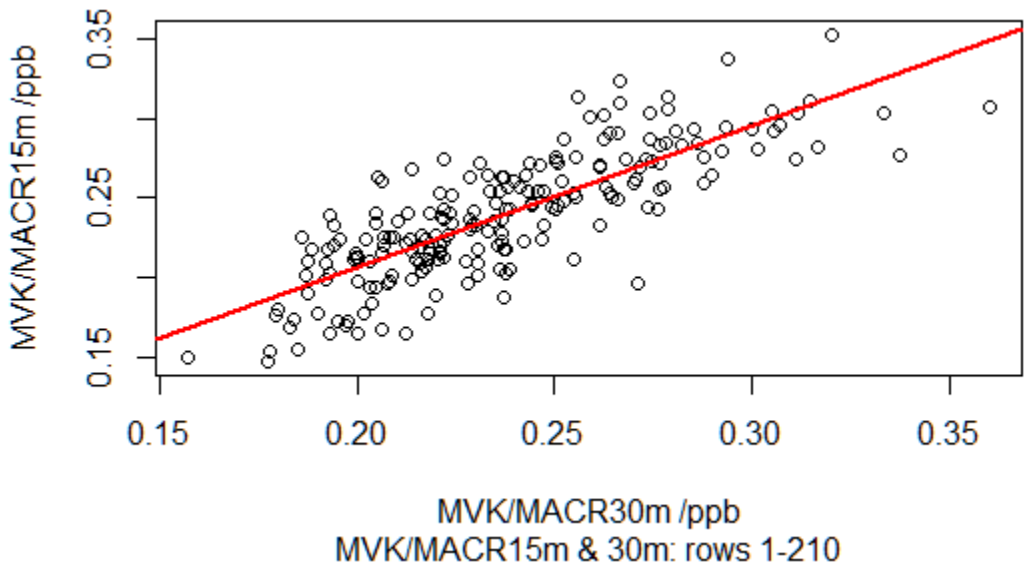

Figure 3.25: MVK/MACR 30m plot against MVK/MCRN 15m; concentrations at 10 minute intervals; (with linear trend line fit). Rows 1 – 210 for MVK/MACR 30m and 15m represent data for the same days, and times; i.e. 14 hours on 25/08/2015 to 10 hours on 03/09/2015. The data for MVK/MACR stops at row 210 for 15m and 211 for 30m; representing 10hrs. and 11hrs respectively on 03/09/2015. Intercept on MVK/MACR15m (y axis) = 0.03 ppbv and the slope = 0.9 ppbv (MVK15m) ppbv (MVK30m)$^{-1}$. The equation of the line is y = 0.03 + 0. 9x and R^2 = 0.65

The r^2 value of 0.65 (Figure 3.25), gives a linear correlation of at least 65%, between the concentration values of the primary oxidation products, formed at 30 and 15 metros height. The linear equation predicts 0.9 ppbv of MVK at 15 meters for every 1.0 ppb of MVK formed at 30 meters height. This goes to suggest, that the key factors at play, for both heights, have approximately equal impact on the concentrations of the oxidation products. The most obvious factors, that appear to be common to both heights so far, is the level of exposure to the diurnal light and radiation at 30 and 15 meters above the forest floor.

3.2. Summary and conclusion

The results discussed so far in chapter 3 are from the 2015 measurement campaigns, as already mentioned; earlier in this chapter and chapter 2; they cover two periods: period 1 (19 - 21 August 2015) was in section 3.1 (subsections 3.1.1 to 3.1.5); while measurement period 2 (23 August – 03 September 2015) was in section 3.2 (3.2.1 to 3.2.6). The equipment used was the KORE PTR-TOF-MS series 1 (with a mass resolution ≥ 1,500 FWHM; (Full Width Half Maximum (resolution)) and sensitivity for Benzene >200 cps/ppbv; (counts per seconds/parts per billion) (KORE 2014), deployed to carry out the Measurements for both periods 1 and 2 in 2015; These are all initial baseline measurements; period 1 was at an estimated height of about 2 meters, or the height of a normal carrier van; Period 2 measurements were carried out at heights of 30 and 15 meters by connecting dual membrane tubes with automated switchable valves, to the PTR inlet while raising the inlet tubes to the respective heights by attaching them to the main met tower at BIFoR. A total of 6 measurements each were made per hour, for both heights 15m and 30m, as the valve switched every 5 minutes, to take 1-minute measurements; with reading one, for 30m and two, for 15m samples, respectively.

The data was collected at the BIFoR FACE Oak Forest located at Mill Haft, Staffordshire, a 26 hectare woodland dominated by the English Oak (Quercus robur); a deciduous forest with trees that have large wide spreading crown of rugged branches alongside others like the hazel (Corylus avellana) coppice; currently believed to be over stood at a height of about 15 meters. The area is said to have been under continuous tree cover for up to 300 years and currently hosts the FACE facility (the 3rd in the world) investigating the impact of rising CO2 on natural (forested) ecosystems (Mackenzie et al 2016, BIFoR FACE 2017). The Collected data was stored using the windows-based GRAMS software adapted by KORE UK into the system, from Thermo Galactic Corporation (KORE 2014). Further processing for

normalization, calibration and plotting of data was carried out using RStudio (2017). The results were presented under five topics in each section;

i. Air temperature versus date, The volatile organic compound (VOC) versus date

ii. Isoprene time series plot, Methyl vinyl ketone and Methacrolein (MVK/MACR) time series plot

iii. Basic statistics

iv. Isoprene versus temperature

v. MVK/MACR versus Isoprene

Using time series analysis in (I and ii) to present the environmental context and basic time series data; but (iii) summarised the data in terms of basic statistics: minimum; 25th percentile (25 %ile; 1st quartile); 50 %ile (median); 75 %ile (3rd quartile); and maximum; in addition, Period 2; investigated the above parameters at both 15 meters and 30 metres height in the forest, denoted by Isoprene30, Isoprene15, MVK/MACR30 and MVK/MACR15, in the plots and reports in sub sections (3.2.1 to 3.2.6). In the last two sub-sections (iv and v); co-variations were investigated; to see how isoprene concentrations depend on air temperature and how the change in the concentration of the oxidation products is dependent on isoprene concentration.

The following observations and conclusions can be made: From (Fig 3.7), in period 1; using just the linear relationship would suggest a 13.5 % rate of change for the oxidation products; MVK/MACR, when compared to that of isoprene, and a residual 0.34% of MVK/MACR in the absence of any isoprene. Suggesting that only 0. 34% of the oxidation products monitored by the PTR are, as a result, of other processes, besides the oxidation of Isoprene as represented in Figure 3.7; most of the MVK/MACR (> 99%) at 2 meters height of the forest on those days (19-21/08/2015), could then be attributed to

isoprene oxidation. Given the R^2 value (0.56), all predictions here are limited to the 56% linear correlation as reflected in the R^2 value.

In Period 2; isoprene concentrations measured at both heights of 15 and 30 meters show that the isoprene concentrations follow a diurnal pattern irrespective of the height (for measurements around 15 and 30 metres respectively) or date, as can be observed in Figures (3.9 to 3.21). A similar pattern is observed in its oxidative products MVK/MACR (Figure 3.10). The oxidation products of Isoprene; MVK/MACR30m and MVK/MACR15m (measured at about 30 and 15 metres respectively), also show a diurnal pattern of concentration with about 3 hours variation; occurring behind Isoprene see Figures (3.10 to 3.21).

From Figure 3.12; the variability of the diurnal pattern at the canopy level of 30 metres can be easily noticed. The diurnal pattern observed there for isoprene concentrations is consistent with the literature (e.g., Apex et al 2002, Stroud et al 2001 and Kalogridis et al 2014)

Figure 3.14 compares hourly-average MVK/MACR diurnal patterns at 15 m and 30 m. There is no obvious difference in the two data samples. The box plots for hourly averages at 30 m and 15 m are similar (Figures 3.15 and 3.16). Data from both heights show an indistinct nocturnal minimum and a late afternoon maximum, with amplitude of ~ 0.03-0.05 ppbv in the medians. Data for particular hours are often highly skewed (i.e., medians approach 25th or 75th percentile values) but the direction of skew does not seem to follow any pattern.

The r^2 value of 0.65 (Figure 3.25), gives a linear correlation of 65%, between the concentration values of the primary oxidation products, formed at 30 and 15 metros height. The linear equation predicts 0.9 ppbv of MVK at 15 meters for every 1.0 ppb of MVK formed at 30 meters height. This goes to suggest, that the key factors at play, for both heights, have approximately equal impact on the concentrations of

the oxidation products. The most obvious factors, that appear to be common to both heights so far, is the level of exposure to the diurnal light and radiation at 30 and 15 meters above the forest floor.

The pattern observed in period 1 compared to period 2 suggest that Isoprene and its oxidation products MVK/MACR do no always show a diurnal pattern when their concentrations are below a certain levels as can be observed in (Figures 3.2 – 3.5). In period1, isoprene concentrations were below 1.30 ppbv while MVK / MACR was below 0.25 ppbv. Isoprene in period 2, was below 5.0 and 4.0 at 30 and 15 metres respectively; while, MVK/MACR concentrations at both levels, was about the same; below 0.4 ppb. The Isoprene concentrations around 15m and 30m (in period 2), are more representative of isoprene concentrations in forested landscapes; in temperate regions like Mill Haft, than concentrations in period 1. Some explanations for this may be because, isoprene is emitted more from the leaves and leafy parts (canopy regions) of these huge, tall trees rather than at lower regions like the trunk of trees. So the concentrations at the lower levels, typical of period 1, will likely be from smaller plants with much less concentrations. Flux rates are known to be influenced by light, temperature, sometimes photosynthesis or even stress (e.g., Monson et al 1992, Rosenstiel et al., 2003, Loreto and Schnitzler 2010). Hence measurements closer to the bottom of the trees like period 1, may show a different pattern than the typical expected for isoprene in period 2 (close to the canopy heights). The influence of poor light and vegetation cover down in the forest may have also contributed to the observed pattern in period 1, which was measured at about 2 meters of height in the forest.

Chapter 4

Isoprene and its reaction products in a deciduous temperate forest: August – September 2016

4.0 Overview: guide to the chapter

The results for the 2016 measurement campaigns are presented in five periods: Period 1 (05 - 09 August 2016) in section 4.1; Period 2 (11 - 17 August 2016) in section 4.2; Period 3 (17 - 23 August 2016) in section 4.3; Period 4 (23 - 25 August 2016) in section 4.4; and finally, Period 5 (25 August - 07 September 2016) is discussed in section 4.5. Each period is described in the same way, as follows:

i. time-series plots of the volatile organic compounds (VOCs) isoprene and its primary oxidation products; MVK/MACR;

ii. scatter plots of Isoprene versus MVK/MACR to investigate co variations between isoprene and MVK/MACR; and

iii. basic statistics combined with boxplots to summarise the data in terms of minimum, 1st quartile (25 percentile; 25 %ile), median (50 %ile), mean, 3rd quartile (75 %ile), and maximum.

Section 4.6 describes some of the other volatile organic compounds (VOCs) having the same molecular mass as isoprene or MVK/MACR. These compounds could contribute to the measured results if they were present in the ecosystem. These compounds may be present either as primary / secondary products from other reactions, or intermediate primary / secondary products from isoprene oxidation,

depending on their concentrations and lifetime in the air (i.e., how transient the compounds are in the atmosphere). The Molecular mass of isoprene is 68.12 g/mol, so the m/z (mass to charge ratio) of the protonated parent ion = 69.12, and the molecular mass of MVK/MACR is 70.09 g/mol with its protonated ion m/z = 71.09. Since the PTR-MS detects compounds purely on the basis of its m/z (or fragmentation pattern, see chapter 2), it is possible for isobaric compounds — i.e., compounds having the same m/z at the resolution of the particular PTR-MS — to interfere with the detection and quantification of the compounds of interest in this study.

4.1 Period 1: (05 - 09 August 2016)

This measurement was carried out at the BIFoR FACE facility, located at Mill Haft, Staffordshire, a 26-hectare woodland formerly owned by the Lichfield family, during which time it served as a pheasant nursery. The most recent planting in Mill Haft forest dates to about 160 – 180 years ago and consists of the English Oak (Quercus robur) or pedunculate Oak as the dominant species. The forest also has other, sub - dominant, trees like the hazel (Corylus avellana) coppice, and is believed to have been under continuous tree cover for over 300 years. The coppice is now heavily 'over stood' at a height of approximately 15m, meaning that it has grown beyond its intended harvest date and has produced a dense sub-canopy that strongly reduces light penetration to ground level. Mill Haft is the site of a Free Air Carbon Dioxide Enhancement (FACE) facility, hosted by the Birmingham Institute of Forest Research (BIFoR); one of two forest-FACE facilities in the world currently commissioned to investigate the impact of rising CO_2 on forest ecosystems and biodiversity in situ (Norby et al., 2015; Hart et al., 2019). The KORE PTR-TOFMS series 1 was deployed to carry out the Measurements for periods 1 to 5, in 2016; with the inlet tube raised to the canopy level; a height of about 30 meters (see also Section 1.2, for site description and Section 2.1 for method and field deployment).

4.1.1. Isoprene and MVK/MACR time series (period 1)

The maximum concentration of 5-minute averages of isoprene, 36.2 ppbv (Table 4.1) occurs right at the start of the data series on the afternoon of Friday 5th August (figure 4.1), after 13:00 GMT. The median value in the measurement sample is 11.0 ppbv, while the mean is 13.0 ppbv. The 1st quartile, is 7.4 ppbv while the 3rd quartile for 75% of the data is 15.8 ppbv, giving an interquartile range of just under 8.5 ppbv. Figure 4.1 shows daily minimum and maximum values as expected for isoprene, but the fluctuations do not appear to correspond with the typical diurnal pattern of response to the combination of daytime light and temperature changes and night time variations as shown in Figure 1.3; Section 1.2. Even though we see a single lowest value given for isoprene concentration at 5.3 ppbv in Table 4.1 (the morning of Tuesday 9th August), all the other days except Saturday, have minimum points with concentrations close to this value (Figure 4.1). The diurnal pattern varies from day to day in the data series. Superimposed on the diurnal pattern, rapid variations occur on each day, particularly late afternoon Saturday, Sunday evening, Monday noon, and night-time Monday into Tuesday. Sudden step-changes of several ppb (up to 15 ppbv between Saturday and Sunday) probably correspond to undiagnosed instrumental errors; no atmospheric chemical or physical process can produce changes of this magnitude over this timescale.

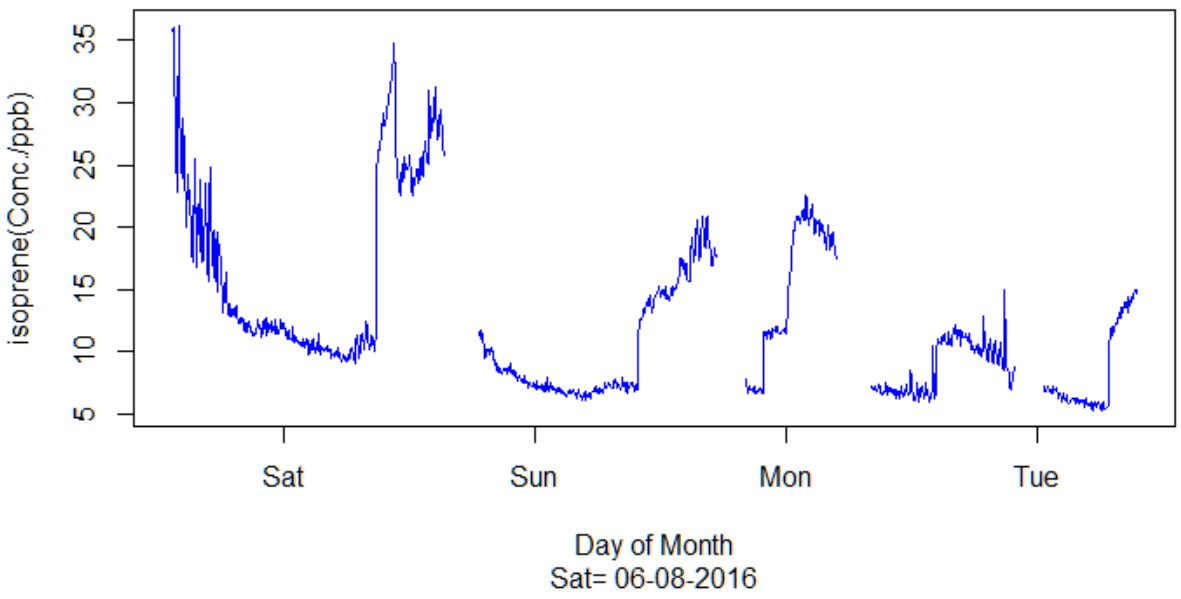

Figure 4.1: Isoprene concentration against date, for Mill Haft data; from between 13:18 hours on 05/08 to 09:28 hours (GMT) on 09/08/2016. Statistics of the time series are reported in Table 4.1; also showing points with missing data; Saturday (06/08); 15:18 -18:28 GMT, Sunday (07/08); 17:18 – 19:58 GMT, Monday (08/08); 04:48 – 07:58 GMT, Tuesday (09/08); 21:48 – 00:28 GMT

Literature indicates that light intensity and temperature are the greatest influences on BVOC emissions (Robinson et al., 2011), including isoprene (Rasmussen and Jones 1973, Tingey et al. 1979, Monson and Fall 1989, Loreto and Sharkey 1990), up to a certain optimal point specific to each VOC. Other climatic factors like soil moisture, prior precipitation, or relative humidity (Sharkey et al. 1995, Holzinger et al. 1999), have also been identified to influence isoprene emissions, under certain conditions. Some more specific contextual factors can also have significant effects on the measured concentration, especially in or just above vegetation or urban canopies: wind speed and direction, height within the forest canopy and the extent of vegetation cover determining radiation penetration through the canopy. Peak isoprene concentrations are known to coincide with maximum canopy temperatures (Tingey et al. 1979, Monson and Fall 1989, Loreto and Sharkey 1990, Fuentes 1996, Sharkey et al. 1996), so for example, days like Friday and Saturday, that show peak concentrations after noon, and a decline in the evening, agree with observations in the literature. The mixing ratios recorded however appear to be much higher

than what is available in the literature for deciduous forests in temperate climates; for example (Fuentes et al. 1996). During the day, at higher temperatures and radiation levels from the sun, a lot more mixing and reaction of species can take place. This mixing may contribute to both the observed concentrations and diurnal variations in Figure 4.1.

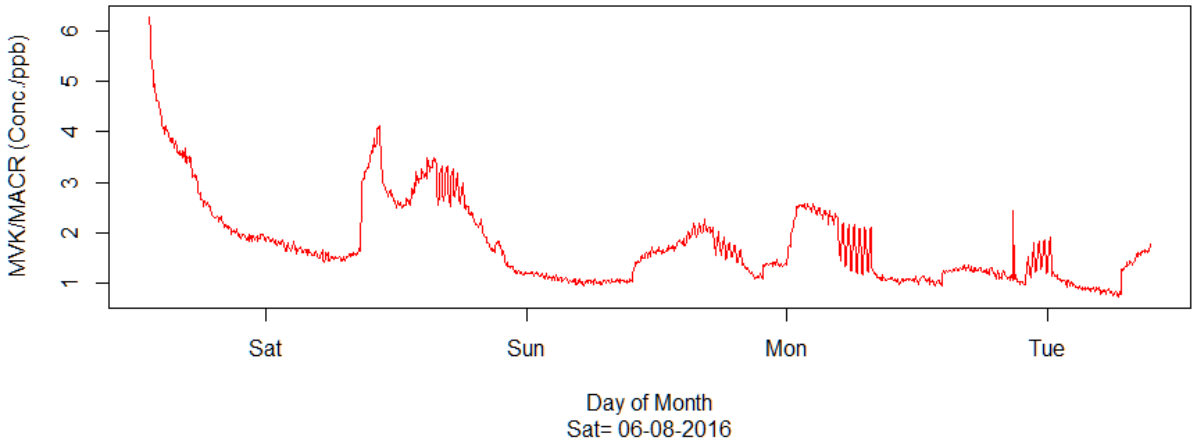

Figure 4.2: Methyl Vinyl Ketone (MVK) / Methacrolein (MACR) concentration against date, for Mill Haft data; from between 13:18 hours on Friday, 05/08 to 09:28 hours (GMT) on Tuesday, 09/08/2016. Statistics of the time series are reported in Table 4.1. **Time periods missing in the equivalent isoprene time series (Figure 4.1, above) are present here, but show suspicious, highly regular, oscillations.**

The maximum concentration for MVK/MACR, principal oxidation products of isoprene, is 6.3 ppbv, the median and mean values respectively are 1.5 and 1.8 (as shown in Table 4.1). Figure 4.2 for MVK/MACR is a close mirror image to Figure 4.1 for isoprene, which shows that a relationship exists between the corresponding sections of both plots in the different days. Relative abundances for MVK/MACR and Isoprene are in an approximate ratio of 1:6 when the maximum and 1st quartile values are compared (see Table 4.1). The medians, means, 3rd quartiles, and minimum values show a ratio of approximately 1:7; so, the ratios are showing between 6 to 7 times more isoprene than its primary oxidation products MVK/MACR over the whole days, when corresponding times within period 1, are compared.

4.1.2. MVK/MACR versus Isoprene (period 1)

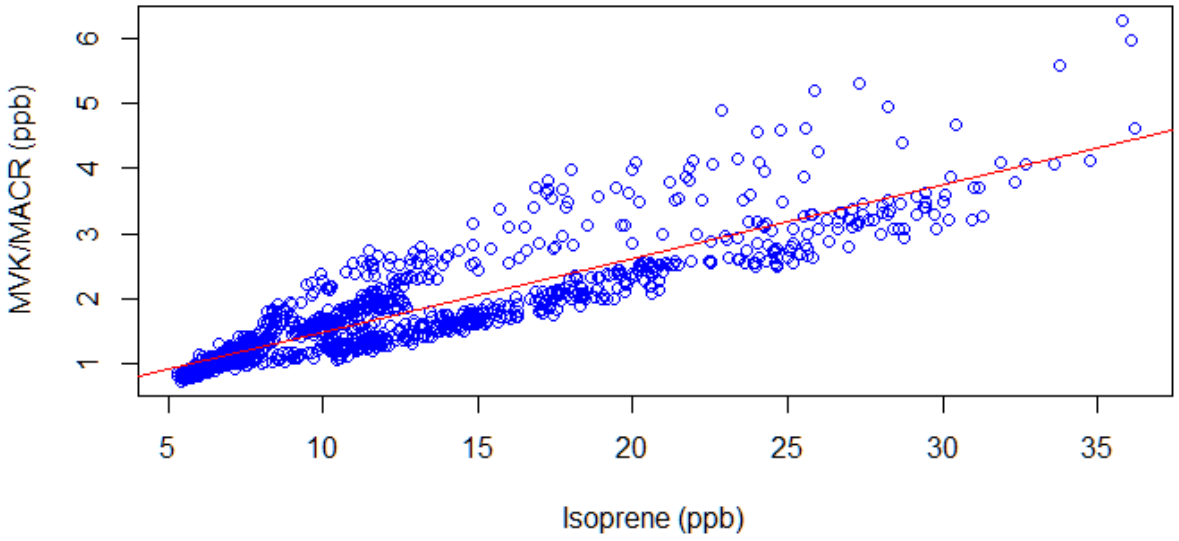

Figure 4.3; Isoprene plot against MVK / MACR (concentrations) for Mill Haft data; from between 13:18 hours on 05/08 to 09:28 hours (GMT) on 09/08/2016. Intercept (MVK) = 0.3 ppbv, Slope ([MVK or MACR]/Isoprene) = 0.1, R^2: 0.775; y = 0.3 + 0.1x. Residual standard error: 0.395 on 1105 degrees of freedom = ±0.036%

In Figures 4.3 and 4.4, a reasonable level of linear correlation has been shown to exist between the concentrations of isoprene and those of its primary oxidation products MVK/MACR, measured during period 1 (05 - 09 August 2016). R^2 is 0.775 and 0.738 respectively for MVK/MACR plotted against isoprene, and against ln(isoprene). The slope in Figure 4.3, which shows the rate of change of MVK/MACR per unit change of isoprene was 0.1, which is a ratio of 8.8 ppb of isoprene to 1 ppbv of MVK/MACR, in broad agreement with the ratios derived from comparison of the quantiles. The r-square value can be interpreted as meaning that approximately 77.5% of the variance of the MVK/MACR data set can be explained by the linear relationship with isoprene.

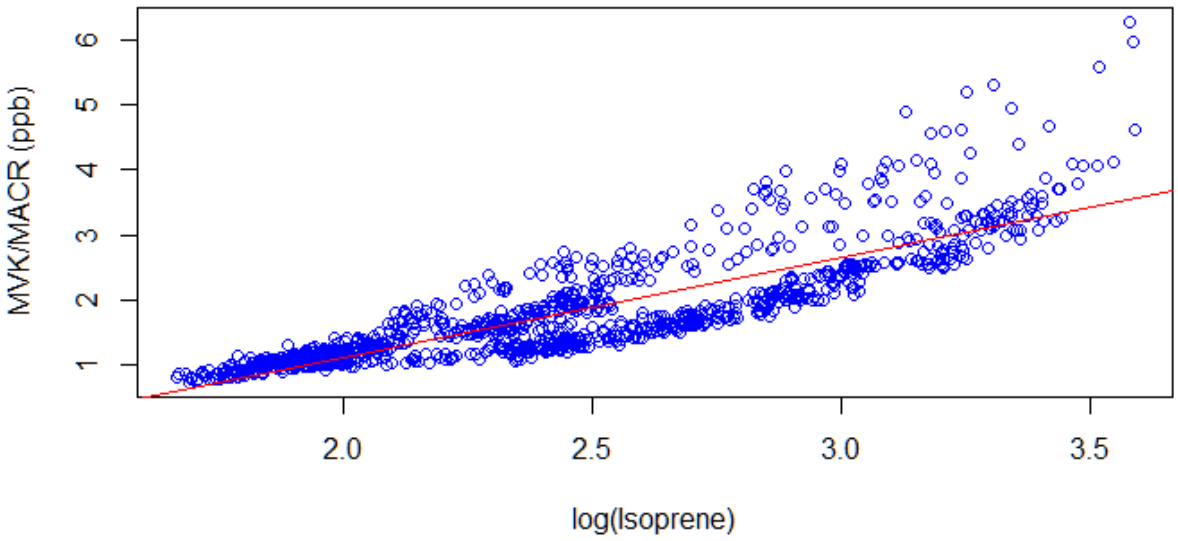

Figure 4.4: Plot of ln(Isoprene) against MVK / MACR (concentrations) for Mill Haft data; from between 13:18 hours on 05/08 to 09:28 hours (GMT) on 09/08/2016. Intercept (MVK) = -2.0, slope (ln(Isoprene)) = 1.6, R^2 : 0.738, Y = 1.6x – 2.0. Residual standard error : 0.4264 on 1105 degrees of freedom = ±0.0386%

4.1.3. Basic statistics (Period 1)

Table 4.1 shows statistics for 5-minute data (rows 1 and 2) and hourly averages (rows 3 and 4) for isoprene and MVK/MACR. The ratio of each statistic for isoprene and MVK/MACR is reported in row 5. The median and mean for isoprene are, 11 and 13, 1st and 3rd quartile are 7.4 and 15.8, then minimum and maximum are 5.3 and 36.2, respectively. The corresponding values for MVK/MACR respectively are, median and mean : 1.5 and 1.8, 1st and 3rd quartiles: 1.1 and 2.1, and finally minimum and maximum: 0.72 and 6.3. The ratios of the distributions; for isoprene to MVK/MACR, going from minimum to maximum values are respectively as follows; minimum = 7.3, 1st quartile = 6.5, median = 7.1, mean = 7.2, 3rd quartile = 7.4 and maximum = 5.8. Apart from the ratios for the 1st quartile and the maximum distribution, that were lower; at approximately 6, all the others were about 7.

Table 4.1: Summary statistics for Mill Haft Data (period 1) 05/08 to 09/08/2016							
No. / Type	**Minimum**	**Ist Quartile**	**Median**	**Mean**	**Standard deviation**	**3rd Quartile**	**Maximum**
1. Isoprene	5.3	7.4	11.0	12.7	8.7	15.8	36.2
2. MVK/ MACR	0.7	1.1	1.5	1.8	1.4	2.1	6.3
3. Isoprene (hourly)	5.7	7.5	11.3	12.8	7.7	14.7	30.7
4. MVK/ MACR (hourly)	0.8	1.2	1.8	1.8	1.2	2.1	5.3
5. Ratios (1./2.)	7.3	6.5	7.1	7.2	1.0	7.4	5.8
Units for isoprene and MVK/MACR = ppbv							

The difference between median and mean, for both isoprene and MVK/MACR, is indicative of skew in the distribution of mixing ratios of both data samples. The skew in data is particularly evident for some hours of the day (Figure 4.5). The diurnal pattern of isoprene for the four days between 13:18 hours on the 5th, and 09:28 hours (GMT), on the 9th of August is shown in the boxplot in figure 4.5. The median value of isoprene concentrations for the first 6 hours from 00.00 to 06.00 hours are all highly skewed downwards, having concentration values equal or less than 10 ppbv but with a long 'tail' of higher concentrations indicative of mixing processes bringing in isoprene-rich air sporadically. The median values rise steadily between 08.00 and 12.00 noon. The median concentrations for 13.00 hours to 16.00 hours are markedly higher than those for 08.00 hours to 12.00 hours and are all equal or greater than 20 ppbv of isoprene; the medians are close to the 75%ile of 09.00 and 10.00 hours. The median values then decrease from 17.00 to 21.00 hours. This pattern of distribution observed in the median of isoprene concentrations is consistent with isoprene diurnal patterns in the literature (e.g., Kalogridis et al 2014). This diurnal pattern for isoprene is explained as due to the combination of solar radiation and temperature changes, the two factors that are consistently observed to be relevant in these types of observed responses (Tingey et al. 1978, Sharkey et al 1996, 2008).

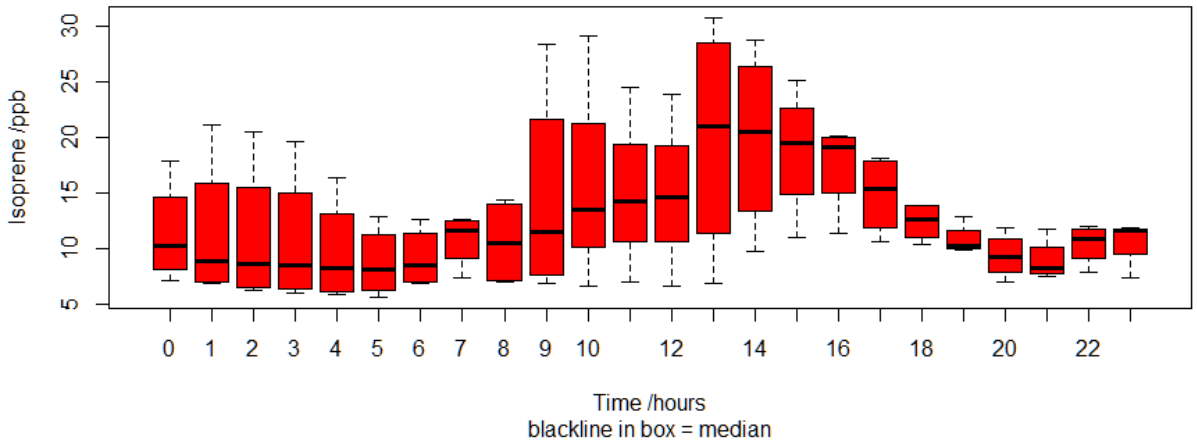

Figure 4.5: Period 1; The distributions of Isoprene hourly concentrations for Mill Haft data; from between 13:18 hours on 05/08 to 09:28 hours (GMT) on 09/08/2016. Maxima and minima are indicated by dotted lines, Interquartile range is indicated by the box, and the median is indicated by the solid black line within the box.

The extremes of the data distribution, below and above the median concentrations, manifest various levels of deviation from the typical isoprene pattern (see figure 1.3; section 1.1) and may be, as a result of other contributors in the environment at the canopy level of measurement. The possibility of compounds other than isoprene contributing to the signal is discussed in section 4.6, below. Since it is a forested area, it is also possible that wind direction and speed could be such that reactions with ground-level ozone may be significant, although in most situations, reaction with HO radicals are expected to be the biggest chemical sink as discussed in section 1.1.2. The variation between the 75%ile and maxima, from the median concentration (that is, the concentration difference between the 75%ile and maxima from the median) show a gradual decline from 01.00 hours to 06.00 hours (GMT), appear more uniform at 08.00 before showing a marked increase between 09.00 and 10.00 hours. The concentration difference drops from that level at 09 and 10 hours to a more uniform distribution at 11.00 and 12.00 hours. The pattern observed for the hours between 01.00 and 06.00 then appear to reverse and show a 75%ile and maxima gradually decline towards the median values, all the way down to 16.00 hours (GMT). These variabilities can be attributed to atmospheric stirring and mixing, resulting from changes in

wind speed and direction at different times of the day (Baldocchi and Meyers 1988, Baldocchi 1989). The higher level of uniformity in the distribution within the hours of 11.00 and 12.00 noon suggest a better mixing of the air due to increased turbulence.

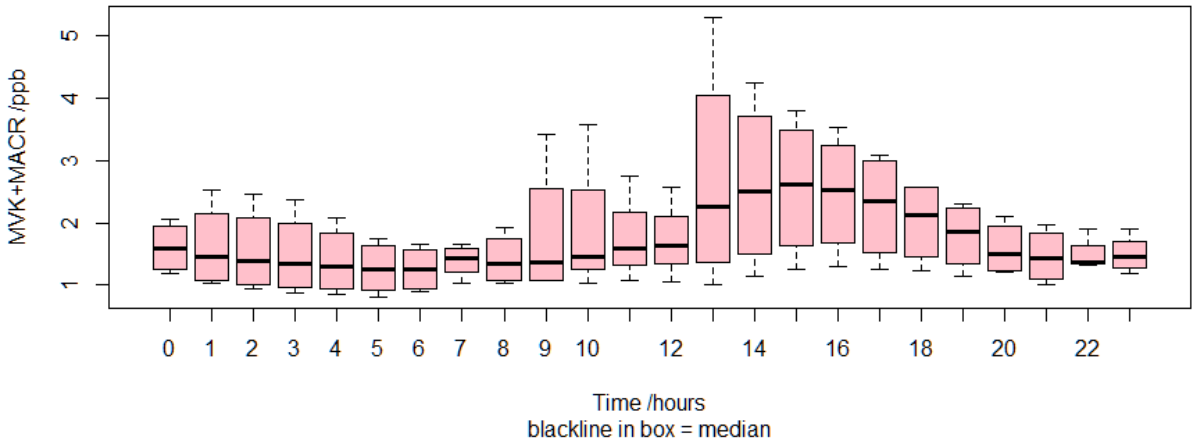

Figure 4.6: Period 1. The distributions of MVK/MACR hourly concentrations for Mill Haft data; from between 13:18 hours on 05/08 to 09:28 hours (GMT) on 09/08/2016

The pattern of hourly concentration distributions for MVK/MACR (Figure 4.6), is broadly similar to that for isoprene in Figure 4.5, although the scale on the concentration axis show an average ratio of about 5 ppbv isoprene to 1 ppbv MVK/MACR. The median concentrations were all around 1.5 ppbv between 00:00 hours and 09:00 hours., except 00:00 and 07:00 hour that were slightly above this concentration. There however, appears to be a very minor, gradual drop in concentration from the hours of 01:00 to 05:00. Then a gradual rise in concentration between 10:00 hrs and 12:00 hours, and then, a very obvious rise, between 13:00 and16:00 hours, before the median concentration levels begin to drop. The median at 15.00 hrs is the highest > 2.5 ppbv. Higher than the maximum concentrations for the hours between 00:00 to 08:00 hours. The peak in the median diurnal pattern occurs 2 hours later for MVK/MACR than

for isoprene (cf. Figures 4.5 and 4.6). This delay in the peak of the diurnal pattern for MVK/MACR reflects the time required for isoprene photochemistry to produce MVK/MACR.

4.2 Period 2: (11 - 17 August 2016)

4.2.1. Isoprene and MVK/MACR time series (period 2)

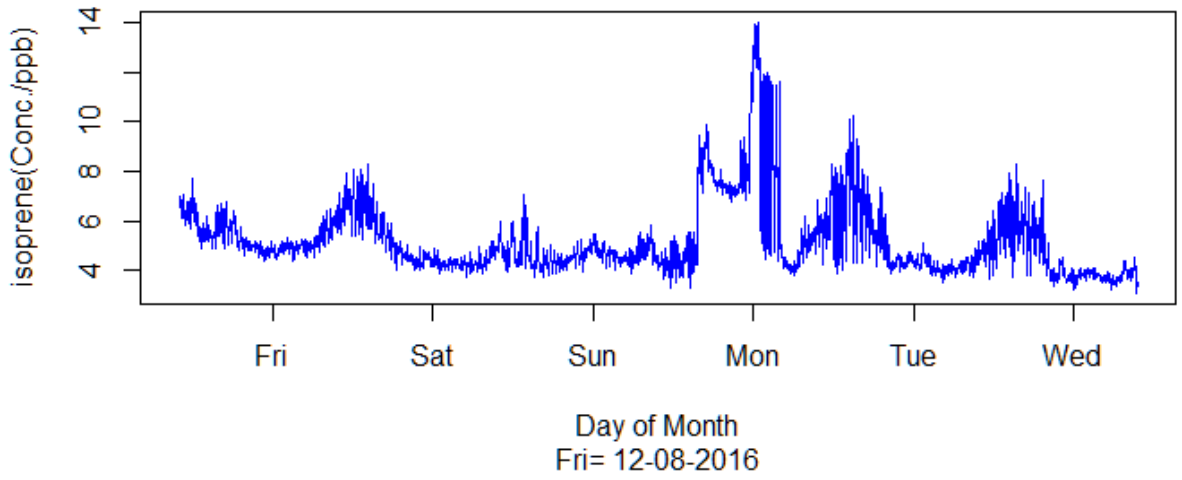

Figure 4.7: Period 2; Isoprene concentration against date, for Mill Haft data; from between 10:03 hours on Thursday, 11/08 to 09:28 hours (GMT) on Wednesday, 17/08/2016. The minimum isoprene concentration (see table 4.2), is 3.105 ppbv which could correspond to more than one point on the plot in figure 4.7; e.g., Sunday evening and Wednesday morning while the maximum point is at 13.980 ppbv on Sunday night / Monday morning; 23:00 / 00:00 hours (GMT). The median and mean concentrations are respectively 4.782 ppbv and 5.235 ppbv.

The shape of figure 4.7 is fairly consistent with the diurnal variation pattern observed for isoprene (see figure 1.3; section 1.2), except for deviations that appear to be specific to each of the days. Its data starts from 10:03 hours (GMT), on Thursday 11th, and ends at 09:28 hours, on Wednesday 17th of August 2016. The plot shows isoprene at less than 8 ppbv from about 10 :03 hours., with an initial drop

towards afternoon, picks up again late afternoon, but did not rise as high as the initial level of concentration (at about 10:00 hours), before returning to a steady drop, towards the late afternoon and into the night hours. The concentration then rises steadily from late morning on Friday (compared to the drop noticed around the same time, on the previous day), then rises consistently to a peak level of about 8 ppbv in the afternoon hours, as expected for the usual diurnal rise (Chang et al 2014, Kalogridis 2014). The concentration then gradually comes down towards the evening, into the night hours all the way down to 00.00 hours on Saturday. The expected diurnal pattern starts off on Saturday and rises to a peak in the afternoon, but most of the concentration levels on Saturday were simply less than the corresponding times for Friday. Monday and Tuesday have similar trends with Friday in their appearance, despite any noticeable differences in the patterns. At first glance, it may appear that the highest level of deviation from the diurnal pattern is observable between late afternoon on Sunday and late morning on Monday, due to a much higher level of isoprene concentration, possibly as a result of other non-isoprene contributors to the signal intensity, as discussed in section 4.6. This spike in concentration, then begins to drop down to an initial minimum of about 8 ppbv, but again, begins to rise throughout the night, until midnight, at 00:00 hours on Monday, before complying with the normal expected drop, all the way down to the normal minimum level (of about 4 ppbv, like most of the other days). The drop from 00:00 hours on Monday all the way down to the normal minimum (about 4 ppbv), before rising again late morning, was consistent with the diurnal behaviour of isoprene (as shown in Figure 1.3; Section 1.2), except that the concentration level declines from a much higher level of about 14 ppbv, compared to Friday and Saturday which were about 8 and 6 ppbv respectively.

The first spike in concentration on Sunday, looks rapid and vertical within the late afternoon, and goes up to a maximum level beyond 9.5 ppb, (but less than 10 ppbv). Other possible reasons apart from non-isoprene contribution mentioned above, could be;

i. a sudden combination of increased brightness and temperature levels, higher than the other days, (for between 1- 3 hours), with higher penetration into the forest (Guenther et al 2006).

ii. a change in relative humidity, as a result, of changes in radiation patterns (Hutchison & Matt 1977), as well as a change in wind direction, bringing in higher concentrations of isoprene, from different locations of the forest.

Iii. There could also be some anthropogenic activity in the forest nearby; Since this is evening / night time and no light / temperature is expected to play any optimal role , then a change in the wind direction can also make some contribution, by bringing higher concentrations of isoprene, from other sources, including sources triggered by anthropogenic activities.

This first part of the peak concentration on Sunday (late afternoon), eventually drops down to about 7 ppbv at night; before another rise around 23:00/ 00:00 hours (GMT) (Sunday/ Monday), all the way up to the second (much higher) peak at a concentration of about 14 ppbv. his second peak however drops down rapidly during the night hours, due possibly to a combination of possible factors (especially rapid cooling at night). It comes all the way down, to the normal low concentration point of about 4 ppbv on Monday morning. The ground level interactions due to daytime radiation from the sun is capable of generating these factors relating to humidity levels, temperature levels, wind direction (as a result of convection currents etc) until they cool down effectively within those early hours of the morning. Considering, that Mill Haft forest is also close to the city centre and a busy high way, the night time processing of isoprene can suddenly become significant if the wind direction changed in a way as to bring in a night time wave of NOx from polluted surroundings into a mix of ozone (O_3) in the neighbourhood. If that happened, and NOx is relatively significant as in (Stan et al 1998b), then the patterns such as is observed for Sunday evening / early Monday morning in figure 2.1, becomes a possibility; as NO_3 also get removed with high relative humidity of the night time.

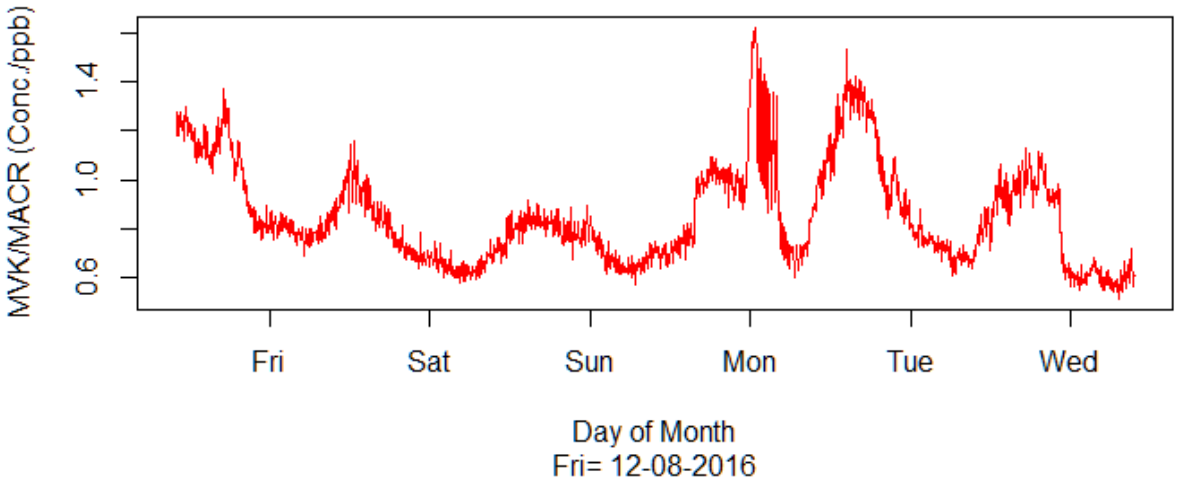

Figure 4.8: Period 2; Methyl Vinyl Ketone (MVK) / Methacrolein (MACR) concentration against date, for Mill Haft data; from between 10:03 hours on 11/08 to 09:28 hours (GMT) on 17/08/2016. The minimum MVK/MACR concentration (see Table 2.1), is 0.516 ppbv; which corresponds to Wednesday morning but closely followed by all other mornings except Thursday and Friday, in Figure 4.8. The maximum point is at 1.6 ppbv on Sunday night / Monday morning; 23:00 / 00:00 hours. The median and mean concentrations are respectively 0.8 ppbv and 0.9 ppbv

The median and mean concentrations respectively for MVK/MACR for period 2; are 0.807 and 0.857 ppb (see table 4.2), but the 1st and 3rd quartiles are respectively; 0.7 and 1.0, while the minimum and maximum are; 0.5 and 1.6 respectively. The ratio of concentrations; MVK/MACR : Isoprene were approximately 1 : 6, across the spectrum of distribution except for the maximum concentration that showed a ratio of 1 : 8.6 (from Table 4.2).

4.2.2. MVK/MACR versus Isoprene (period 2)

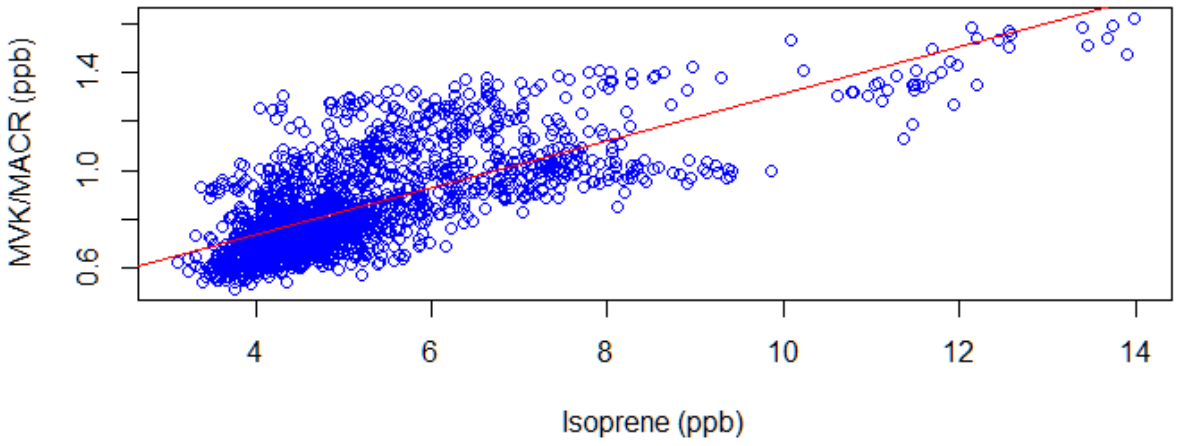

Figure 4.9: Period 2; Isoprene plot against MVK / MACR (concentrations) for Mill Haft data; from between 10:03 hours on 11/08 to 09:28 hours (GMT) on 17/08/2016. Intercept (MVK) = 0.35 ppbv, Slope (Isoprene) = 0.096, R^2 = 0.523; y = 0.35 + 0.096x. Residual standard error: 0.1427 on 1720 degrees of freedom

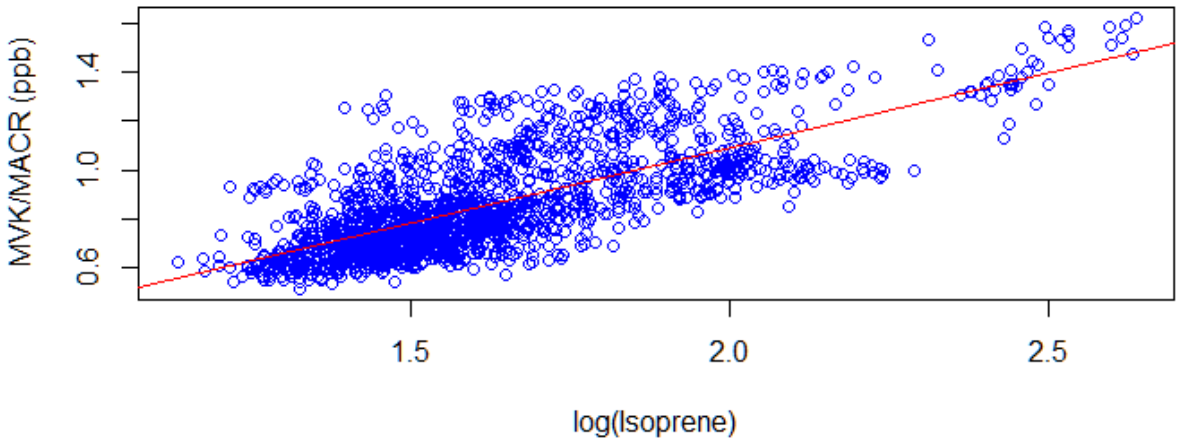

Figure 4.10: Period 2; Plot of ln(Isoprene) against MVK / MACR (concentrations) for Mill Haft data; from between 10:03 hours on 11/08 to 09:28 hours on 17/08/2016. Intercept (MVK) = - 0.14, Slope (ln(Isoprene) = 0.61, R^2 : 0.543; y = 0.61x – 0.14. Residual standard error: 0.1396 on 1720 degrees of freedom.

Figures 4.9 and 4.10 show that the linear relationship between Isoprene and its primary oxidation products MVK/MACR in period 2, is about 50%. R^2 is 0.523 and 0.543 respectively for MVK/MACR plotted against isoprene, and against ln(isoprene). The slope in Figure 4.9, that shows the MVK/MACR

rate of change, to that of Isoprene, is 0.0963 or a 9.6 % rate of change in MVK/MACR concentration compared to that of isoprene for the linear relationship in figure 4.9. The implication is that only about 50% of the data in period 2, fall within this linear relationship of 9.6 % rate of change for the oxidation products. The remaining 50% of the data falls outside this ratio of 9.6 % rate of change for MVK/MACR per unit change of Isoprene. The linear equation suggests that the concentration of MVK/MACR for 1 ppbv of isoprene would be 0.45 ppbv.

4.2.3. Basic statistics (period 2)

Table 4.2 shows statistics for 5-minute data (rows 1 and 2) and hourly averages (rows 3 and 4) for isoprene and MVK/MACR. The ratio of each statistic for isoprene and MVK/MACR is reported in row 5. The median and mean concentrations for isoprene are, 4.8 and 5.3, 1st and 3rd quartile are 4.3 and 5.7, then minimum and maximum are 3.1 and 14.0, respectively. The corresponding values for MVK/MACR respectively are, median and mean : 0.8 and 0.9 , !st and 3rd quartiles: 0.7 and 1.0, and finally minimum and maximum: 0.5 and 1.6.

Table 4.2: Summary statistics for Mill Haft Data (period 2) 11/08 to 17/08/2016.

No. / Type	Minimum	Ist Quartile	Median	Mean	Standard deviation	3rd Quartile	Maximum
1. Isoprene	3.1	4.3	4.8	5.2	2.8	5.7	14.0 *
2. MVK/ MACR	0.5	0.7	0.8	0.9	0.3	1.0	1.6
3. Isoprene (hourly)	3.6	4.3	4.8	5.2	2.4	5.8	13.1 *
4. MVK/ MACR (hourly)	0.6	0.7	0.8	0.9	0.3	1.0	1.6
5. Ratios (1./2.)	6.0	6.1	6.0	6.1	0.7	5.8	8.6

Note - Data used for 1 & 2 were taken at 5 minute intervals while those used for 3 & 4 were from the hourly sum of these values.
*** - asterisk to make isoprene data more visible. Units for isoprene and MVK/MACR = ppbv**

The ratios of the distributions; for isoprene to MVK/MACR, going from minimum to maximum values are respectively as follows; minimum = 6.0, 1st quartile = 6.0, median = 6.0, mean = 6.0, 3rd quartile = 5.8 and maximum = 8.6. Apart from the deviation in the maximum ratio, the rest (from minimum to 3rd quartile), are approximately 6.0; reflecting a more uniform distribution above and below the median value for most of the days in period 2 (as can also be seen in the boxplot; Figure 4.11 below).

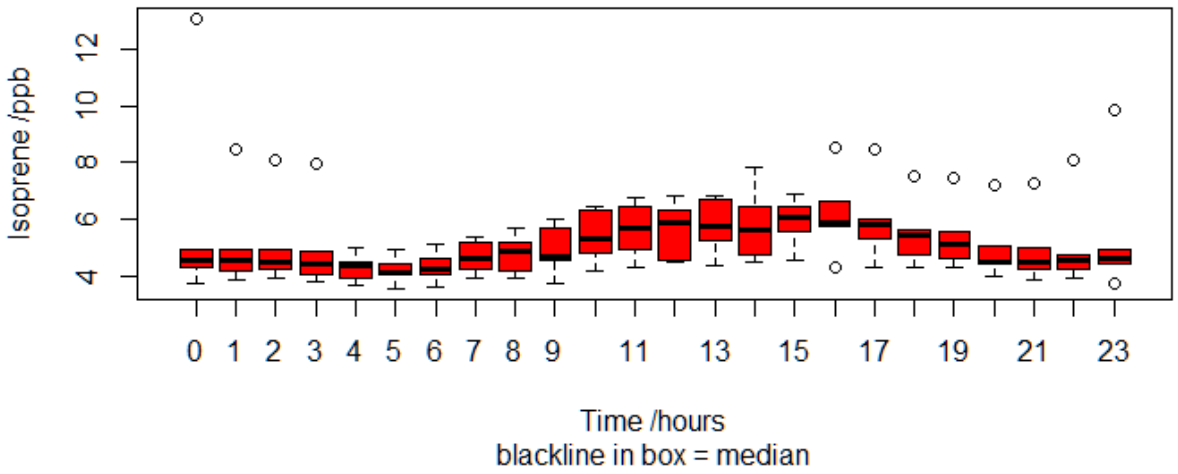

Figure 4.11: Period 2; A Boxplot for Isoprene hourly concentrations for Mill Haft data; from between 10:03 hours on 11/08 to 09:28 hours (GMT) on 17/08/2016.

Figure 4.11 shows that between the hours of 04:00 and 15:00 GMT, this dataset is completely distributed (has 100% distribution) within the minimum and maximum whiskers; all others show, that at least 75% of the dataset is well distributed within the minimum and maximum whiskers except for 16:00 and 23:00 hours, having only about 50%, distributed within the box (between the 1st quartile (25%ile) and 3rd quartile (75%ile). The median is about the same level, for the first five hours, while the 75 %ile concentration values also remained the same for the first four hours. The distribution showed a very distant outlier at 01:00 hours, responsible for the maximum value observed in Table 4.2. Otherwise, most of the data is distributed within 6 ppb concentration; and nine out of the other ten outliers are within 8 ppbv or less. The rise in the median values from 10:00 to 16:00 hours, compared to the earlier

hours is also obvious, but the values remained largely close to each other within those peak hours, remaining between 5 and 6 ppbv.

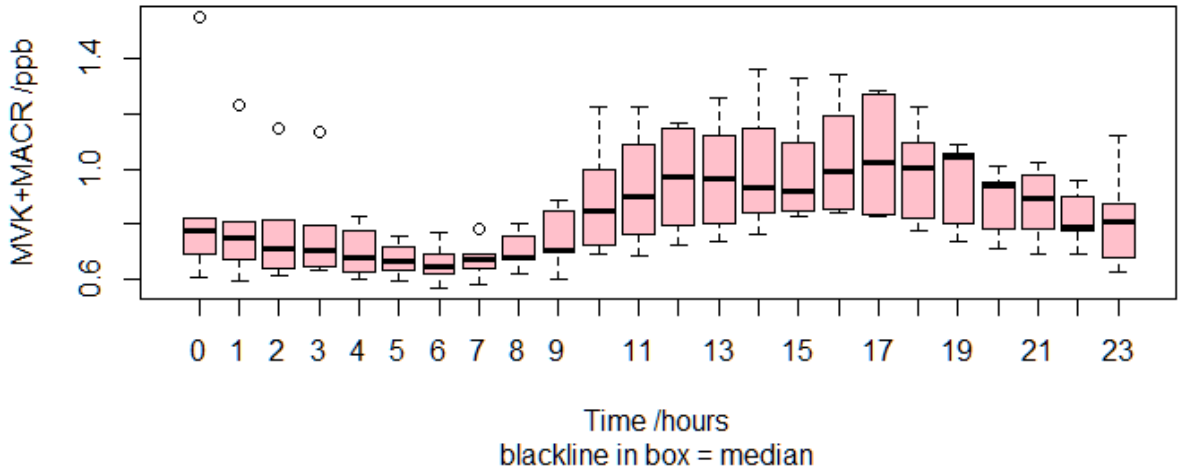

Figure 4.12: Period 2; A Boxplot for MVK/MACR hourly concentrations for Mill Haft data; from between 10:03 hours on 11/08 to 09:28 hours (GMT) on 17/08/2016.

The median values for 23:00 and 00:00 were close to 0.8 ppbv and gradually dropped down until 06:00 hours indicative of a strong contribution from night time reactions as was observed in figures 4.7 & 4.8. There was a gradual rise in the median value between 07:00 and 09:00 hours, although most of the data is skewed upwards for 08 and 09 hours. The rise was more visible from 10:00 hours, going above the 3rd quartile and maximum values for the previous hours, excluding the four outliers from 01:00 to 04:00 hours. The highest midday median values were at 12:00 and 13:00 hours but drops down to the same median concentration as 10:00 and 11:00 hours, by 14:00 and 15:00 hours, before rising again during the evening hours. The highest median value for the evening was at 19:00 hours, but, along with the median values of the two preceding hours, remain at a higher level than the highest midday (12 and 13.00 hours) median values; showing again a strong contribution from evening / night time reactions.

4.3 Period 3: (17 - 23 August 2016)

4.3.1. Isoprene and MVK/MACR time series (period 3)

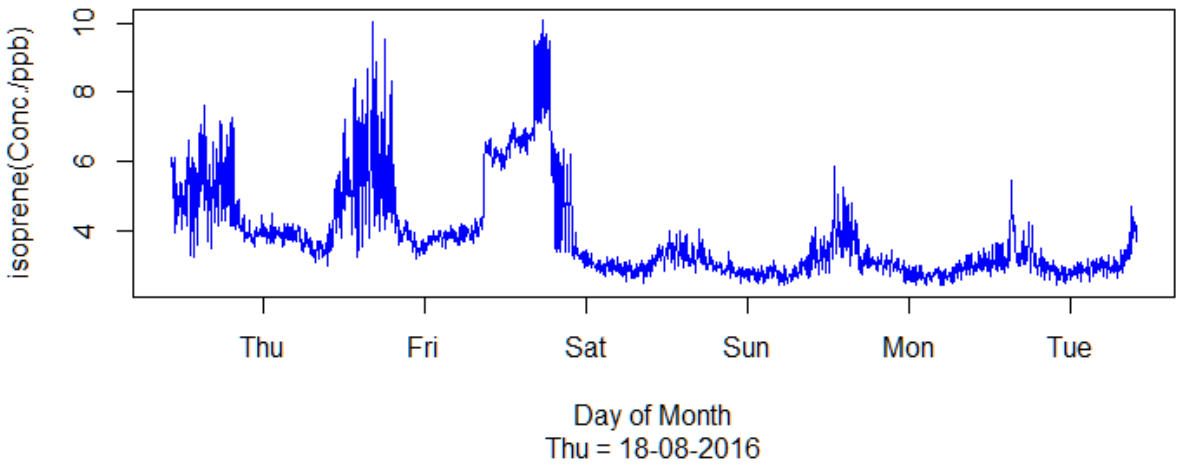

Figure 4.13: Period 3; Isoprene concentration against date, for Mill Haft data; from between 10:18 hours on Wednesday, 17/08 to 09:53 hours (GMT) on Tuesday, 23/08/2016. The minimum isoprene concentration (see Table 4.3), is 2.412 ppbv which could correspond to more than one point on the plot in Figure 4.13; for example, Saturday to Tuesday morning hours, while the maximum concentration is at 10.1 ppbv on Thursday or Friday afternoon / evening hours. The median and mean concentrations are respectively; 3.363 ppbv and 3.851 ppbv.

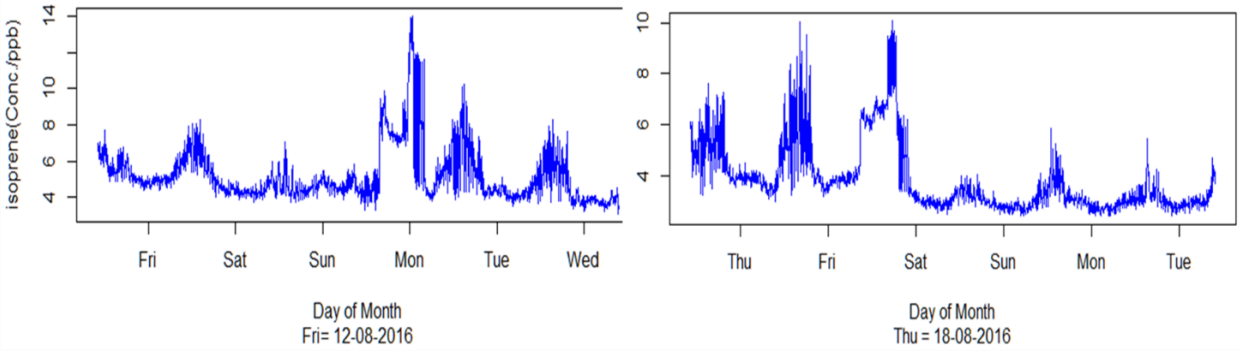

A. Figure 4.7: Isoprene concentration against date, for Mill Haft data; from 10:03 hrs on Thursday, 11/08 to Wednesday, 09:28 hrs on 17/08/2016.

B. Figure 4.13: Isoprene concentration against date, for Mill Haft data; f 10:18 hrs on Wednesday, 17/08 to 09:53 hrs on Tuesday, 23/08/201

Figure 4.13a: Period 3; Showing the continuity of noisy pattern from Figure 4.7 in period 2 into 4.13 in period 3. Notice that item A. in Figure 4.13a, ended at 09:28 hours (GMT). on Wednesday 17/08/2018, while item B, started exactly about 50 minutes later; so, item B is the dataset that immediately follows the dataset collected for A.

The general appearance of Figure 4.13 is consistent with the diurnal behaviour of isoprene. However, the first 3 days, have noisy and higher peaks, that suggest the presence of additional conditions, that were absent, from the last four days; between Saturday morning (20/08) and Tuesday morning (23/08). The noisy isoprene peaks, that showed up in the first three days of Figure 4.13 appear to be a clear continuation from period 2 (see Figure 4.13a), indicative of additional reactions and/or changes in physical conditions that were more dominant in the ecosystem for about five to six days (between 14 and 20 August); judging from the similarity in the patterns. The appearance at the first 'noisy peak', structure on Monday evening, 15th (period 2; fig 4.13a, item A), is similar to the sixth 'noisy peak' structure on Friday evening 19th (in period 3; Figure 4.13a, item B). The two days of 'noisy peaks' following the first; in period 2, and the two before the sixth; in period 3, are also similar in structural appearance, and concentration profiles. Sunday evening to Monday morning (14-15/08), in period 2, and Friday evening to Saturday morning (19-20/08), in period 3, appear to have captured the build-up and diffusing moments for the conditions behind the 'noisy' peaks, that spread across six days, from Sunday/ Monday, (14-15/08) in period 2; (see Figure 4.7), to Friday/Saturday, (19-20/08) in period 3;

(see figure 4.13). For the oxidation products; comparing figures; 4.14 for period 3 below, with 4.8, from period 2, for MVK/MACR reveal a similar pattern. It is important to note that the noisy pattern noticed for isoprene in Figure 4.7 and its continuity in 4.13 were captured for MVK/MACR in Figure 4.8 and continued in 4.14, suggesting a direct relationship of primary conversion by oxidation. This type of pattern (or mirrored image) is generally noticeable between isoprene and MVK/MACR as primary oxidation products (for example Kalogridis et al., 2014).

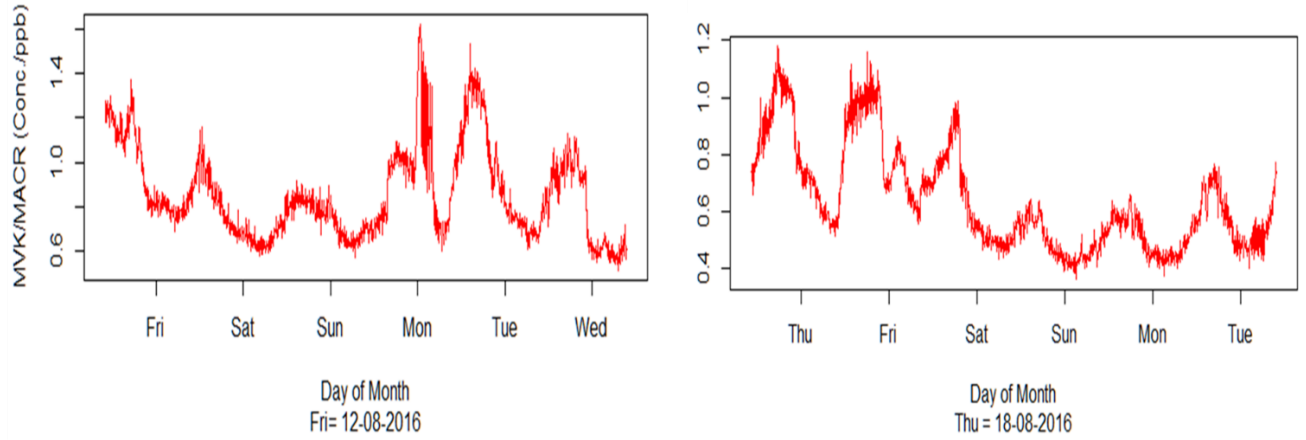

C. Figure 4.8: Methyl Vinyl Ketone (MVK) / Methacrolein (MACR) concentration against date, for Mill Haft data; from between 10:03 hrs on 11/08 to 09:28 hrs on 17/08/2016.

D. Figure 4.14: Methyl Vinyl Ketone (MVK) / Methacrolein (MACR) concentration against date for Mill Haft data; from between 10:18 on 17/08 to 09:53 on 23/08/2016.

Figure 4.13b: Period 3; Showing the continuity of noisy pattern from Figure 4.8 in period 2 into 4.14 in period 3. Notice that item C. in Figure 4.13b, ended at 09:28 hours (GMT). on Wednesday 17/08/2018, while item D, started exactly about 50 minutes later; so, item D, is the dataset that immediately follows the dataset collected for C.

This mirrored pattern between isoprene and MVK/MACR does not always follow for isoprene and MVK/MACR time series, as can be seen in period 4 (Figures 4.19 and 4.20 respectively). In the case of period 4; a sudden spike in isoprene concentration over an 18 hour period, did not register in a corresponding way in the time series of the oxidation products. Suggesting a possible contribution to isoprene intensity (as discussed in section 4.6); by an intermediate compound (possibly contributed partly from anthropogenic actions and wind direction), with alternative reactions that did not primarily yield MVK/MACR under the prevailing physical conditions, at the time.

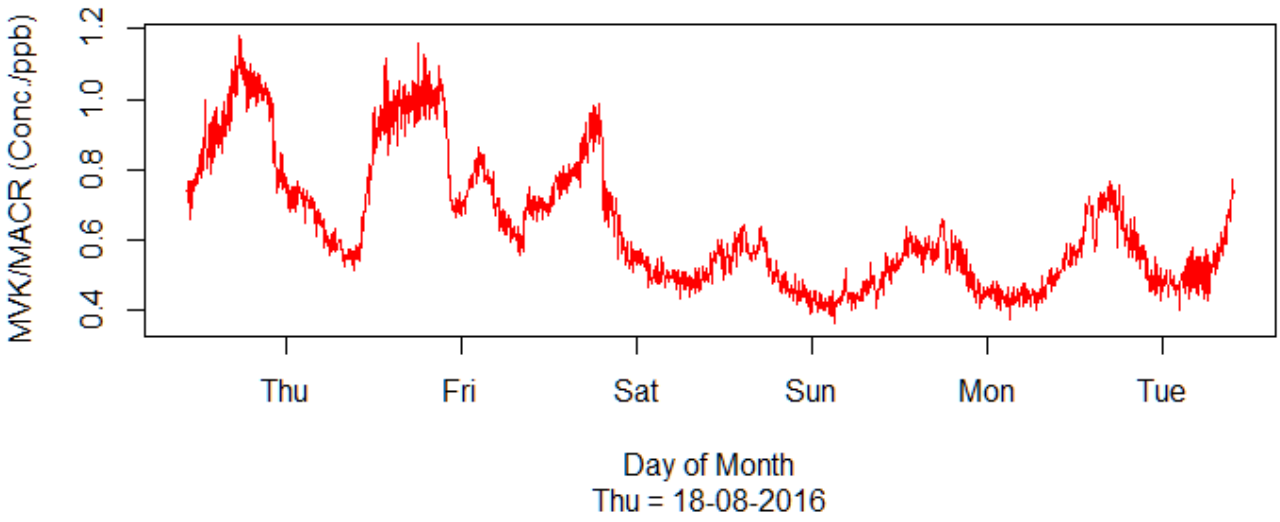

Figure 4.14: Period 3; Methyl Vinyl Ketone (MVK) / Methacrolein (MACR) concentration against date, for Mill Haft data; from between 10:18 hours on 17/08 to 09:53 hours (GMT) on 23/08/2016. The minimum MVK/MACR concentration (see table 3.1), is 0.4 ppbv which could correspond to Sunday and Monday mornings, but closely followed by Saturday and Tuesday mornings, in Figure 4.14, while the maximum concentration is at 1.2 ppbv on Wednesday afternoon, but closely followed by Thursday afternoon/evening. The median and mean concentrations are respectively are 0.6 ppbv and 0.6 ppbv.

The coefficient of determination (R^2) in figures (4.15 & 4.16) respectively are 0.5 and 0.6, showing a linear correlation of at least 50% between isoprene and MVK/MACR, concentrations in period 3. Based on the linear equation in figure 4.15, the MVK/MACR concentration would be 0.4 ppbv for 1 ppbv of isoprene. The rate of change of MVK/MACR compared to that of Isoprene is 9.84 %, as revealed in the slope of the linear regression line. The intercept of 0.3 ppbv for MVK/MACR at 0 ppbv of isoprene; suggests a 26.1 percent residual concentration of MVK/MACR, that is not from the isoprene concentration correlated in figure 4.15.

4.3.2. MVK/MACR versus Isoprene (period 3)

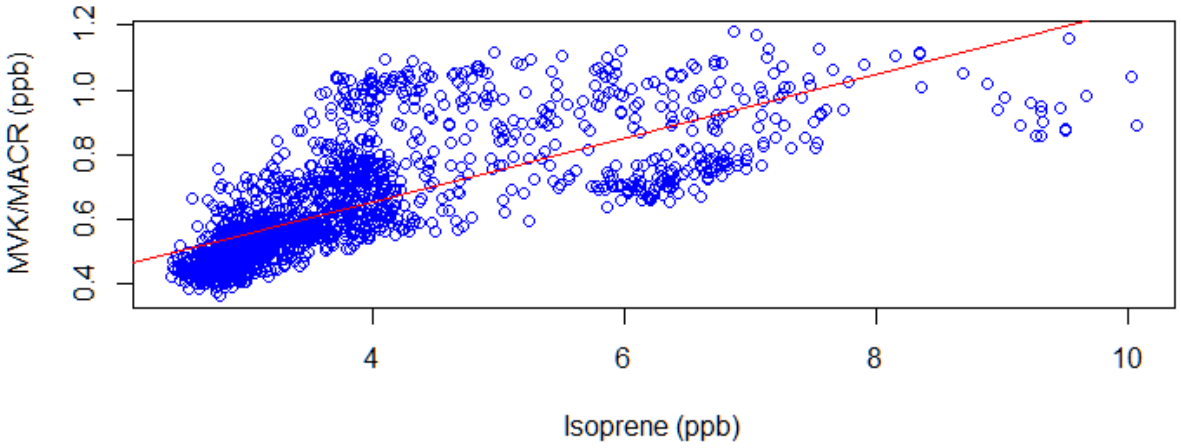

Figure 4.15: Period 3; Plot of Isoprene against MVK / MACR (concentrations) for Mill Haft data; from between 10:18 hours on 17/08 to 09:53 hours (GMT) on 23/08/2016. ***Intercept (MVK) = 0.3, Slope(Isoprene) = 0.1, R^2 : 0.536; y = 0.3 + 0.1x. Residual standard error: 0.12 on 1722 degrees of freedom = 0.007%.***

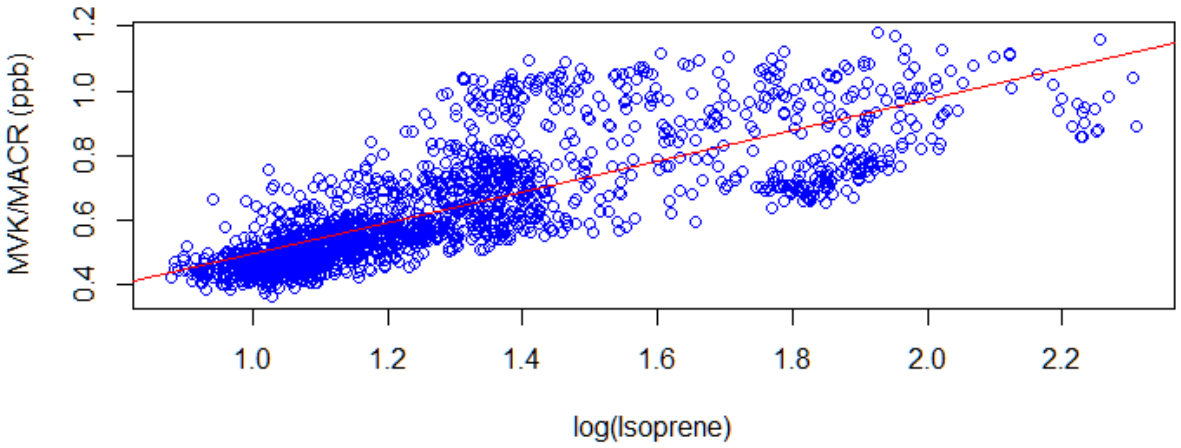

Figure 4.16: Period 3; Plot of ln(Isoprene) against MVK / MACR (concentrations) for Mill Haft data; from between 10:18 hours on 17/08 to 09:53 hours (GMT) on 23/08/2016. ***Intercept (MVK) = 0.02, Slope(ln(Isoprene)) = 0.5, R^2 = 0.604; y = 0.02 + 0.5x. Residual standard error: 0.11 on 1722 degrees of freedom.***

4.3.3. Basic statistics (Period 3)

Table 4.3 shows statistics for 5-minute data (rows 1 and 2) and hourly averages (rows 3 and 4) for isoprene and MVK/MACR. The ratio of each statistic for isoprene and MVK/MACR is reported in row 5.

The median and mean for isoprene are, 3.6 and 3.9, 1st and 3rd quartile are 2.9 and 4.1, while the minimum and maximum are 2.4 and 10.1, respectively. The corresponding values for MVK/MACR respectively are, median and mean : 0.6 and 0.6, !st and 3rd quartiles: 0.5 and 0.7, and finally minimum and maximum: 0.4 and 1.0. The ratios of the distributions in table 4.3; for isoprene to MVK/MACR, going from minimum to maximum values are respectively minimum = 6.7, 1st quartile = 5.927, median = 5.8, mean = 6.0, 3rd quartile = 5.5 and maximum = 8.5. Apart from the deviations in the minimum and maximum values, the rest of the distribution ratios, from the 1st quartile to the 3rd quartile remain at approximately 6.0, between isoprene and MVK/MACR.

Table 4.3: Summary statistics for Mill Haft Data (Period 3) 17/08 to 23/08/2016.

No. / Type	Minimum	Ist Quartile	Median	Mean	Standard deviation	3rd Quartile	Maximum
1. Isoprene	2.4	2.9	3.4	3.9	2.1	4.1	10.1 *
2. MVK/ MACR	0.4	0.5	0.6	0.6	0.3	0.7	1.2
3. Isoprene (hourly)	2.6	3.0	3.4	3.9	1.7	4.1	8.5 *
4. MVK/MACR (hourly)	0.4	0.5	0.6	0.6	0.2	0.7	1.1
5. Ratios (1./2.)	6.7	5.9	5.8	6.0	0.6	5.5	8.5

Note - Data used for 1 & 2 were taken at 5 minute intervals while those used for 3 & 4 were from the hourly sum of these values.
*** - asterisk to make isoprene data more visible. Units for isoprene and MVK/MACR = ppbv**

The overall distribution pattern for isoprene in figure 4.17 is fairly representative of the diurnal variations expected for isoprene. This is easier to see from the changes represented by the median level concentrations. The extremes above and below the median level distribution covey the same information with various degrees of deviation. The early morning hours up to 07:00 hours, all have severely skewed data towards the minima (the median is almost at the minimum position); suggesting that up to 50% of the data for each of those hours, between 00:00 to 07:00 are very close to the minima, while the rest 50% is distributed above the median value. The median concentration starts showing a sign of rising from 08:00 hrs., and progressively rose until it gets to the highest median value at 14:00 hours.

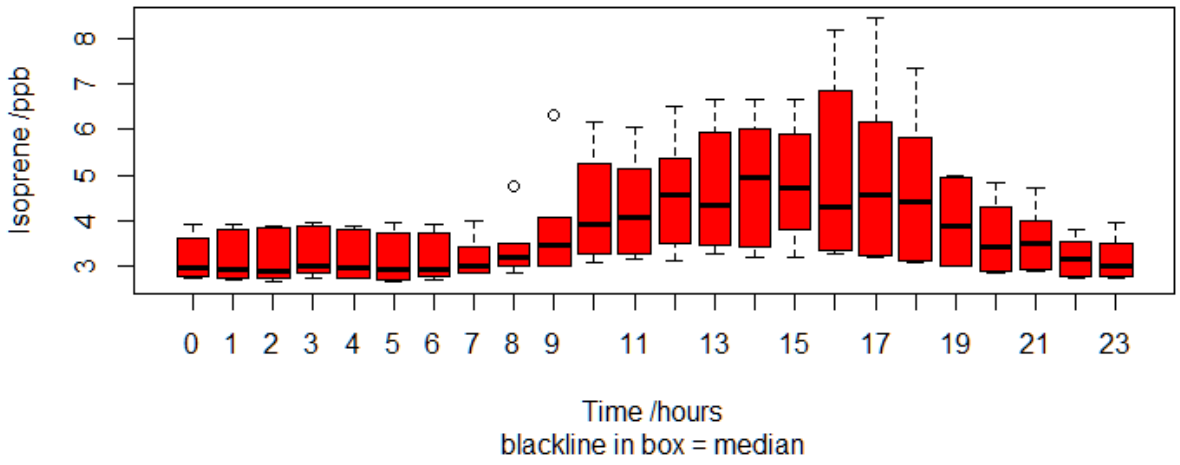

Figure 4.17: Period 3; A Boxplot for Isoprene hourly concentrations for Mill Haft data; from between 10:18 hours on 17/08 to 09:53 hours (GMT) on 23/08/2016.

The median values between 15:00 and 17:00 hours are still high and closely comparable to that of 14:00 hours (being the peak median concentration), but begins to gradually reduce all the way down, until 23:00 hours. The peak median concentration is already close to 5 ppb, (higher than all the maximum concentrations from 00.00 to 09:00 hours, in the morning. This peak median position (at 14.00 hours), when compared to the evening concentrations, is slightly above the median at 15:00 hours, about the same level as the maxima from 19:00 to 21:00 hours and remarkably higher than the maxima for 22:00 and 23:00 hours.

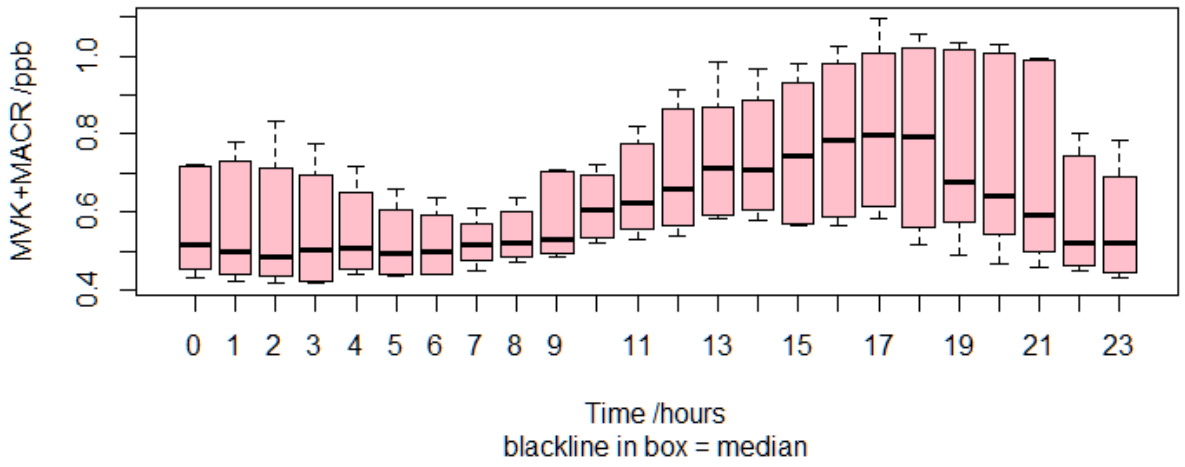

Figure 4.18: Period 3; A Boxplot for MVK/MACR hourly concentrations for Mill Haft data; from 10:18 on 17/08 to 09:53 on 23/08/2016.

The median pattern in figure 4.18 for MVK/MACR concentration, showed a more consistent rise between 10.00 and 16:00 hours, then maintained a stable high at that level around 0.8 ppbv for three hours and then a consistent decrease from 19:00 to 23:00 hours. The concentration went down by about 1 ppbv, between 18.00 and 19:00 hours, before the gradual and consistent decrease all the way down to a median of about 0.5 ppbv at 22:00 and 23:00 hours; which is about the median concentration for the hours between 00:00 and 09:00 GMT (± slight differences; $4.9 \leq y \geq 5.1$). More specifically, having the median concentrations between about 4.9 and 5.2 ppbv; with the median for 00:00 hours at the upper limit and that for 02:00 hours at the lowest. Although these median measurements began from a about 0.52 ppbv at 00:00, it drops down to slightly lower values, all the way to 06:00 hours, before, stabilising between 07:00 and 09:00, then starts on the actual daytime rise as expected; from 10:00 hours.

4.4 Period 4: (23 - 25 August 2016)

4.4.1. Isoprene and MVK/MACR time series (Period 4)

The pattern in figure 4.19 is different from the normal Isoprene diurnal variation pattern. The first 24 hours between late morning on Tuesday and about the same time on Wednesday (24/08), shows a fairly regular range of concentration levels.

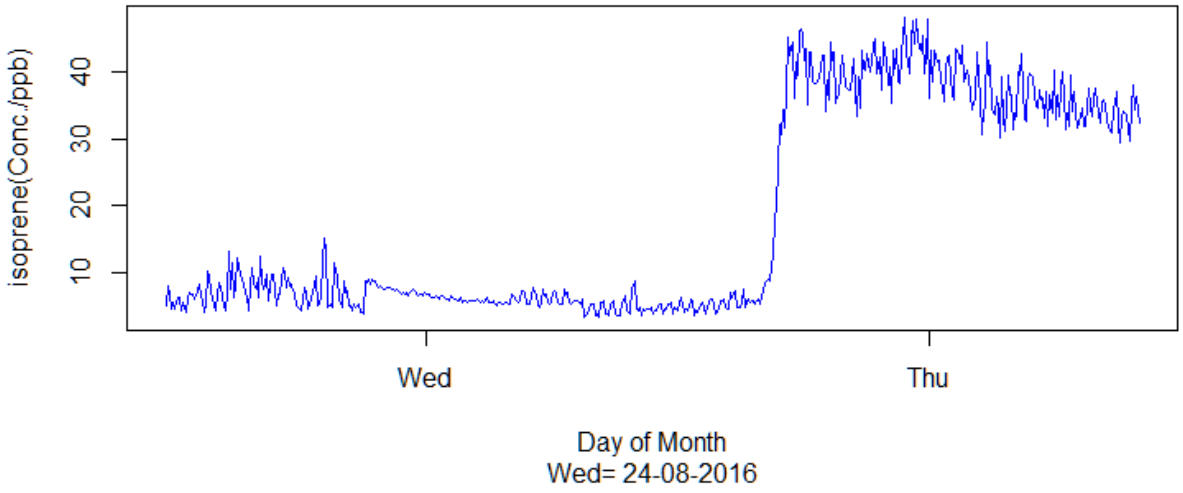

Figure 4.19: Period 4; Isoprene concentration against date, for Mill Haft data; from between 11:33 on* Tuesday, 23/08 to 10:03 hours (GMT) on Thursday, *25/08/2016. The minimum isoprene concentration (see table 4.4), is 3.248 ppbv and could correspond to several points in time on the plot in Figure 4.19, between Tuesday and Wednesday. The maximum concentration is at 48.0 ppbv between Wednesday afternoon and Thursday morning; spreading across several points in time. The median and mean concentrations are respectively 7.5 ppbv and 18.1 ppbv.

The summary of the statistical distribution in Table 4.4, show 5.6 and 7.5 ppbv for the 1st quartile (25%ile) and the median (50%ile) concentrations respectively, with the minima given as 3.25 ppbv, indicative of the lowest points of the fluctuations. There is a very steep rise within a short space of time in the late afternoon of Wednesday, to the values within the range of between 35.6 and 48.0 as revealed for the 3rd quartile (75%ile) and maxima concentrations in table 4.19. The concentration stays around 40 ppb throughout the night of Wednesday and gradually reduces towards the 3rd quartile

concentration, most of the morning hours on Thursday, where this dataset ends. The sharp split in concentration into a more usual (between 3.5 and 18 ppbv) and a very high (between 20 and 50 ppb), after about 24hrs, suggests the possibility of a very strong variation in climatic conditions or anthropogenic activity in the near neighbourhood, resulting in higher concentration of reacting species, including species that are not normally present at higher concentrations; reactions that produce strong contributions to the signal intensity of Isoprene (as discussed in section 4.6 for non- isoprene contributors), hence masking the true contribution of isoprene concentrations that are primary to that part of the forest (see Table 4.6 for a list of some organic compounds within the m/z range of isoprene and MVK/MACR; and likely to make contributions to isoprene signal intensity, if present in the forest at the time of measurement).

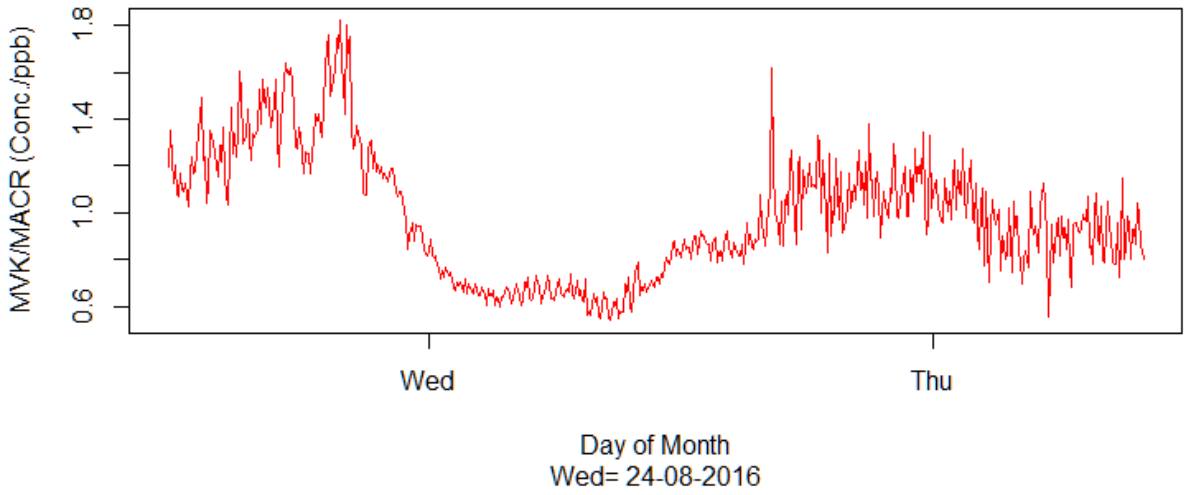

Figure 4.20: Period 4; Methyl Vinyl Ketone (MVK) / Methacrolein (MACR) concentration against date, for Mill Haft data; from between 11:33 hours on Tuesday, 23/08 to 10:03 hours (GMT) on Thursday, 25/08/2016. The minimum MVK/MACR concentration (see Table 4.4), is 0.5 ppb which could correspond to late morning on Wednesday, in Figure 4.20, while the maximum concentration is 1.8 ppbv, (late afternoon) on Tuesday. The median and mean concentrations are respectively 1 ppbv.

The pattern shown here in Figure 4.20 for the primary oxidation products MVK/MACR, is closer to what is expected for the isoprene time series; when compared to the plot in Figure 4.19 (see Figure 1.3;

section 1.1; for the typical diurnal fluctuation pattern for isoprene and MVK/ MACR). The usual structure gives a closer mirror image between isoprene and its oxidation products in the time series plots, if the oxidation products (and ratios) are a true representation of a more uniform conversion of isoprene (source) to MVK/MACR. In which case, the isoprene daily plot in Figure 4.19, would have resulted in a pattern more similar in appearance to that of MVK/MACR in Figure 4.20; if the proportion of isoprene involved in the production of Figure 4.20 has not been masked by the variations that came in from other contributors, not primary to the process that yields the oxidation products.

Figure 4.20 shows a clear rise in concentration from late morning on Tuesday (23/08); rising consistently to the highest peak (about 1.8 ppbv), at night and then decreasing all the way down to about 0.75 ppbv by 00:00 hours. An obvious dip can also be noticed, right between the first peak (about 1.6 ppbv) in the evening and final peak (about 1.6 ppbv) in the night; this corresponding to a similar dip on the isoprene plot in Figure 4.19, showing a representative contribution from isoprene that was not masked by other contributions on the side of the isoprene plot. This type of overall daytime rise, with a peak at around the late afternoon/evening, before decreasing down to a minimum level of concentration, is consistent with diurnal fluctuations expected, for isoprene and its oxidation products; when a source with uniform concentration, contributes the right proportion from the same source into oxidation products. The pattern observed for Wednesday is reasonably in agreement with the same pattern despite the minor deviations, as a result of changes, already noted above for Wednesday, in Figure 4.19. An obvious indication that a contribution was present that affected the normal diurnal variation of isoprene, but did not pass down in to a corresponding pattern in the oxidation products, due possibly to an intermediate process.

4.4.2. MVK/MACR versus isoprene (Period 4)

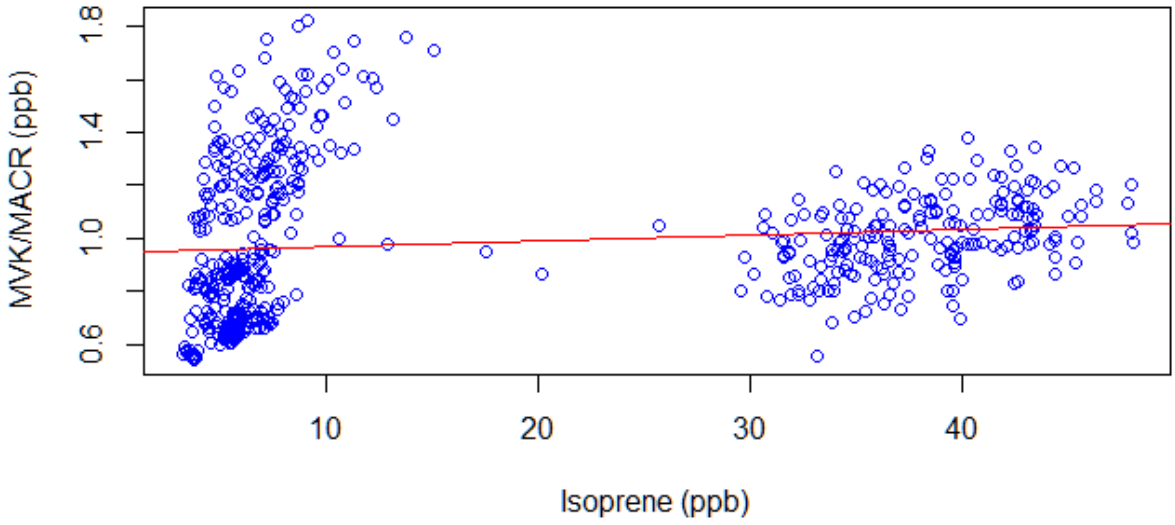

Figure 4.21: Period 4; Plot of Isoprene against MVK / MACR (concentrations) for Mill Haft data; from between 11:33 hours on 23/08 to 10:03 hours (GMT) on 25/08/2016. Intercept (MVK) 0.9, Slope (Isoprene) = 0.0023, R^2 : 0.017; y = 0.9 + 0.0023x. Residual standard error: 0.27 on 557 degrees of freedom.

There is a split in Isoprene concentration into normal or low concentrations (below 10 ppbv) and very high isoprene (above 30 ppbv) with little or nothing in between. Despite this obvious split in Isoprene concentrations, the output or yield profile for MVK/MACR was largely concentrated below 1.4 ppbv for both concentration levels, suggesting that the oxidation products are largely a result of the same range of isoprene concentrations in both groups. There are observable differences in the two sections; for instance, in the first section of Figure 4.21, with up to 99% isoprene concentrations consistently below 10 ppbv, there was still a reasonable percentage of MVK/MACR well above 1.4 ppbv (between 1.4 and 1.7 ppbv); so the large rise in isoprene concentration did not produce higher concentrations of oxidation products, but stayed largely within the same level of MVK/MACR (less than 1.4 ppbv). The bulk of oxidation products under the higher isoprene concentration profile was between 0.8 and 1.4 ppbv of MVK/MACR; with little or nothing above and below. Suggesting the presence of other reaction

processes that result in different products than MVK/MACR. Figure 4.21 presents a peculiar data set in which the mean concentration for isoprene is at least 2.5 times the median. This is much higher than most of the other periods with a difference of more than 11 ppbv as compared to less than 1 ppbv for the other periods. No corresponding difference was observed for the median and mean concentrations for MVK/MACR (see table 4.4). The relationship reflected in Figures (4.21 & 4.22) has no linear correlation, with R^2 at 0.017 and 0.04 respectively for Isoprene and ln(isoprene) against MVK/MACR concentrations.

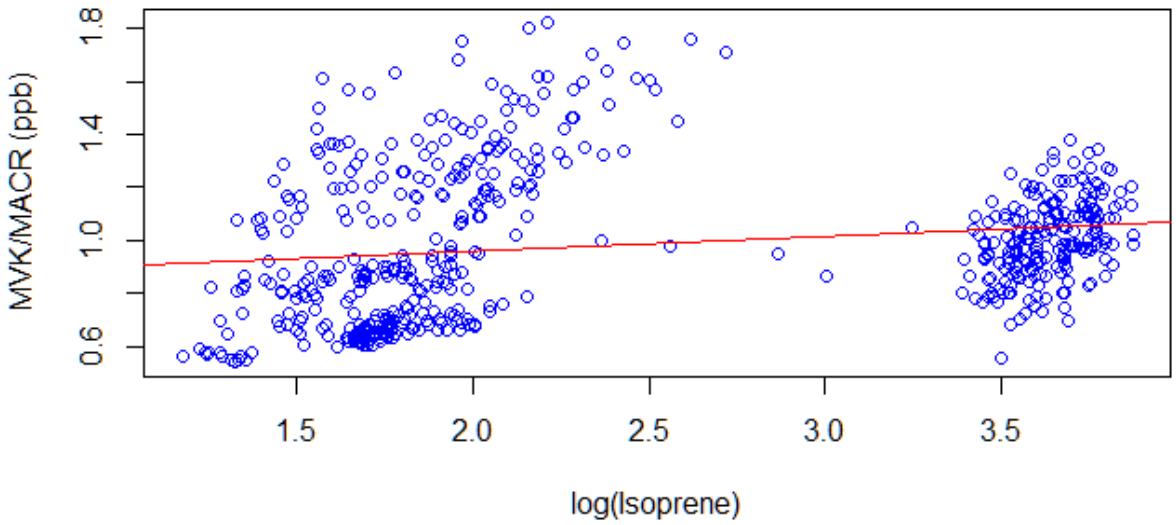

Figure 4.22: Period 4; Plot of log(Isoprene) against MVK / MACR (concentrations) for Mill Haft data; from between 11:33 hours on 23/08 to 10:03 hours (GMT) on 25/08/2016. Intercept(MVK) = 0.9, Slope (ln(Isoprene)) = 0.05645, R^2 : 0.036; y = 0.85 + 0.06x. Residual standard error: 0.27 on 557 degrees of freedom

4.4.3. Basic statistics (Period 4)

Table 4.4 shows statistics for 5-minute data (rows 1 and 2) and hourly averages (rows 3 and 4) for isoprene and MVK/MACR. The ratio of each statistic for isoprene and MVK/MACR is reported in row 5. The median and mean concentrations for isoprene are, 7.5 and 18.1 , 1st and 3rd quartile are 5.6 and 35.6 , then minimum and maximum are 3.3 and 48.0, respectively. The corresponding values for

MVK/MACR respectively are, median and mean: 1.0, !st and 3rd quartiles: 0.78 and 1.2, and finally minimum and maximum: 0.5 and 1.8. The ratios of the distributions; for isoprene to MVK/MACR, going from minimum to maximum values are respectively as follows; minimum = 6.0, 1st quartile = 7.2, median = 8.0, mean = 18.4, 3rd quartile = 30.1 and maximum = 26.4. The values of the statistical ratios are closer together between the minimum, 1st quartile and the median; (that is, between 6.0 and 8.0), than between the median, the 3rd quartile and the maximum, (which are 8.0, 30.1 and 26.4). The standard deviation is much higher as a result of large deviation from the median in the 3rd quartile and maximum distributions.

Table 4.4: Summary statistics for Mill Haft Data (period 4) 23/08 to 25/08/2016

No. / Type	Minimum	Ist Quartile	Median	Mean	Standard deviation	3rd Quartile	Maximum
1. Isoprene	3.2	5.6	7.5	18.1	16.4	35.6	48.0 *
2. MVK/ MACR	0.5	0.8	1.0	1.0	0.4	1.2	1.8
3. Isoprene (hourly)	4.4	5.8	7.8	18.3	15.6	35.5	44.3 *
4. MVK/MACR (hourly)	0.6	0.8	0.9	1.0	0.3	1.1	1.6
5. Ratios (1. /2.)	6.0	7.2	7.9	18.4	13.4	30.5	26.4

Note- Data used for 1 & 2 were taken at 5 - minute intervals while those used for 3 & 4 were from the hourly sum of these values.
*** - asterisk to make isoprene data more visible. Units for isoprene and MVK/MACR = ppbv**

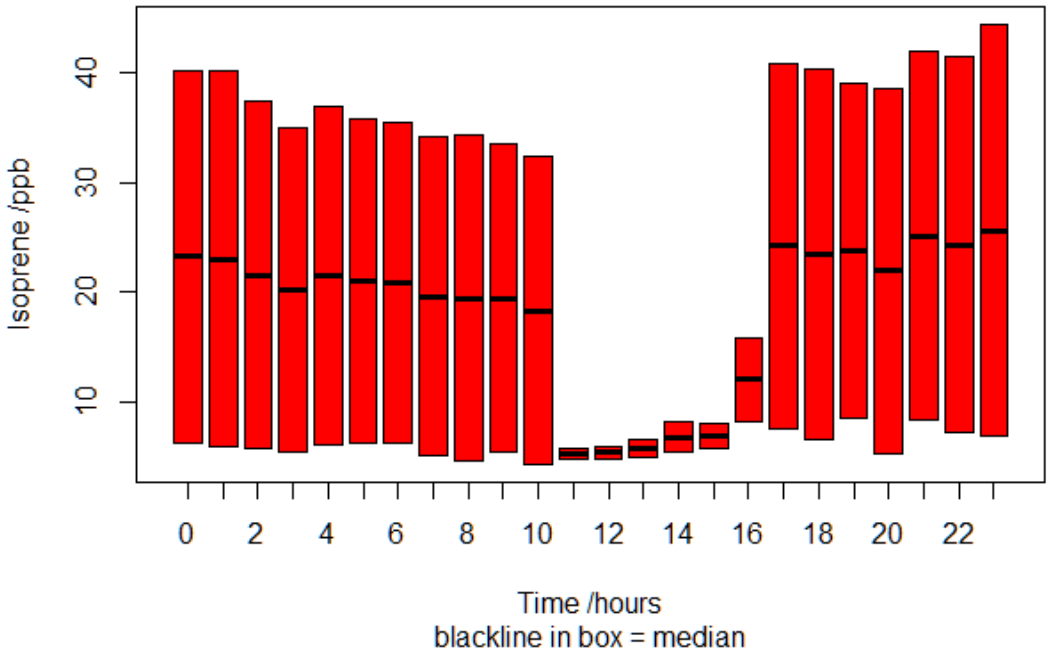

Figure 4.23: Period 4; A Boxplot for Isoprene hourly concentrations for Mill Haft data; from 11:33 hours on Tuesday, 23/08 to 10:03 hours (GMT) on Thursday, 25/08/2016.

The pattern of distribution displayed in figure 4.23 is the reverse to the isoprene normal diurnal variation pattern in its appearance; since the afternoon hours show the least comparative concentrations for the median and the extremes of the distribution above and below the median.

The afternoon concentrations (between 11.00 and 15.00) are at levels comparable to the more normal distributions observed in the other periods (that is ≤ 10 ppbv). while the night time (17.00 – 23.00) and morning hours (00.00 – 10.00) show levels of concentration distribution that are higher than the normal. Suggesting, that the normal level of isoprene generation and conversion to MVK/MACR in the day time is taking place at about the same rate noticed in the earlier periods (see Figures 4.7- 4.11 And 4.13 - 4.17) but overwhelmed or overshadowed by other processes that become more dominant at night/ morning. It is peculiar to note that only the hours expected to produce the highest levels of isoprene were dwarfed in the distribution pattern. The other hours were distributed wide apart from the median,

while those between 11:00 to 16:00 hours (GMT) were more closely distributed. The dataset for each hour fits perfectly within the box (no whiskers to indicate outlying minimum or maximum values) between what used to be 25 and 75%ile marks respectively; so that 100 % of every hour fitted into their distribution boxes. No outliers, the 25%ile becomes the minimum for each hour and the previous 75%ile (see 4.11 and 4.17) at the top of the distribution boxes, becomes 100% of the dataset, for each hour. The data distribution between 11:00 to 16:00 were quite representative of the presence of isoprene, and to note that the median was also increasing proportionately, with the other levels of distribution until 16:00 hours, when the increase became most obvious and has a minimum that is at the same level as the maximum distribution for 15:00 hours. The median levels for the evening hours (from 17:00 to 23:00), were generally higher than the morning hours; and show a slightly decreasing appearance as the time progressed, from 00:00 hrs to 10:00 hours. It is important to note also, that this dataset starts at 11.33 hours on Tuesday and ends at 10.03 hours, on Thursday; part of the implications of this is that the hour ’10:00 to 11:00’ will be short by two contribution points, one on Tuesday as the data collection started after 11:00 hrs the other contribution on Thursday as the data collection stopped at 10:03 hrs. The hour ‘11:00 to 12:00 hrs will also have half contribution on Tuesday as the dataset started at 11.33 hrs. This observation would not need to apply if there is a complete 48 hours of data across all the hours; to give a more uniform number of data points, with which the mean for each hour (from all the days) is worked out for the boxplot. It is obvious that the extremely high concentrations of Wednesday evening and Thursday morning, (see Figure 4.19) has greatly impacted the contributions to those hours (16:00 to 23:00 hours on Wednesday, 24/08 and 00.00 to 10:00 hours on Thursday, 25/08).

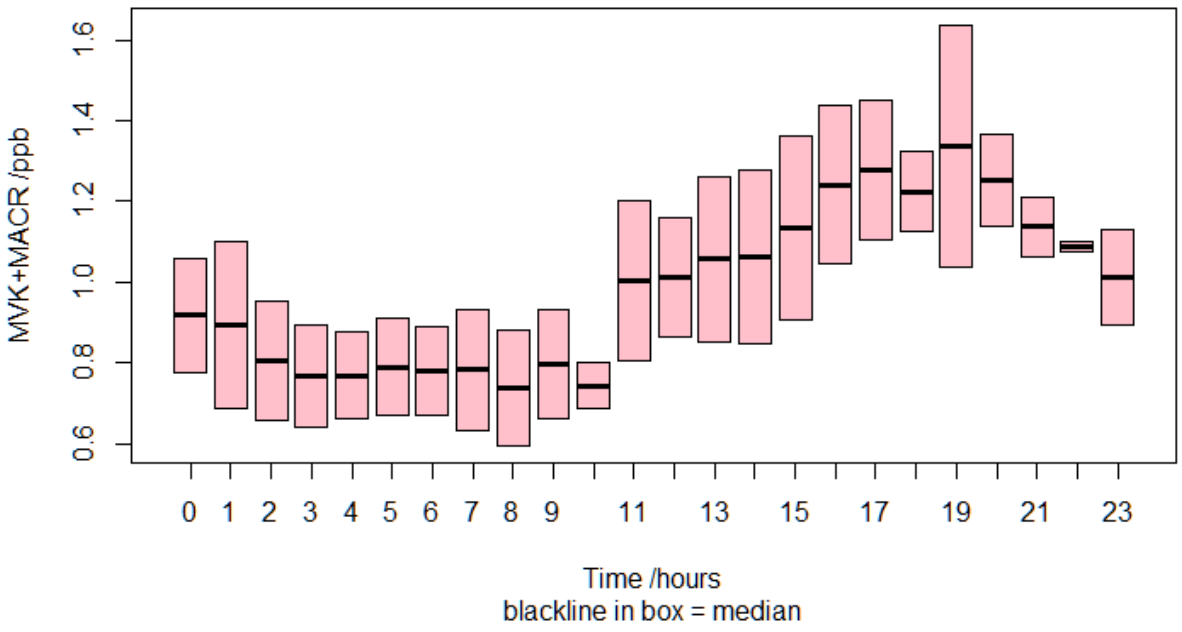

Figure 4.24: Period 4; A Boxplot for MVK/MACR hourly concentrations for Mill Haft data; from 11:33 hours on Tuesday, 23/08 to 10:03 hours (GMT) on Thursday, 25/08/2016.

The median positions displayed in figure 4.24, show a less proportionate conversion of isoprene into the primary oxidation products MVK/MACR for each hour. The hourly distribution of MVK/MACR concentrations in Figure 4.24 is comparable to other periods despite the unusual and sudden spike in isoprene concentrations from less than 15 ppbv to over 35 ppbv in period 4, for about 18 hours between (16:00 hours on Wednesday, 24/08 and 10:00 hours on Thursday, 25/08), as captured in Figure 4.19. This impacted the appearance of the boxplot in Figure 4.23, in such a way as to reverse the normal expected, higher afternoon contributions into an overwhelmingly dominant evening/night and early morning pattern. The same pattern is not reflected in the hourly boxplot for concentration distribution for the oxidation products, as can be seen in Figure 4.24. Thus, suggesting that the very high concentrations in Figure 4.23, for isoprene did not automatically translate into a proportionate level of increase for the oxidation products. The median level of isoprene hourly distribution between 11.00 hours and 16.00 hours appear to be about 4 ppbv at 10:00 and 12.00 ppbv at 16:00, with the other four

hours, showing different median levels, in between them. These levels of isoprene concentration appear to be within normal range when compared to what has so far been observed in the other periods. Even then, they could easily, still appear insignificant, without a careful observation, as they all got completely dwarfed by the dominant contributions, from the nonpeak hours (nonpeak, in terms of heat and light from solar radiation). Using the median as a guide here in Figure 4.24, we see a consistent afternoon rise from 11:00 to 17:00 hours (GMT). The median concentration of those hours are also higher than all the morning hours between 00.00 and 10:00 hours, despite the higher levels of isoprene indicated for those hours. This pattern agrees with generally observed trend for MVK/MACR when they are being produced as primary oxidation products from isoprene and corresponds to a diurnal pattern. There are however noticeable differences that can be attributed possibly to the unusually high night time isoprene concentrations. For instance, those concentration levels continued to remain high between 19:00 and 23:00 hours despite a slight dip at 18:00 hours. The lowest concentration for the night (at 23:00 hours) is at the same level as that of the morning at 00:00 hours, yet, it was the highest of the morning median level concentrations. They then begin to drop gradually until 10:00 hours but were all still above 0.7 ppbv.

4.5 Period 5: (25 August – 07 September 2016)

4.5.1. Isoprene and MVK/MACR time series (period 5)

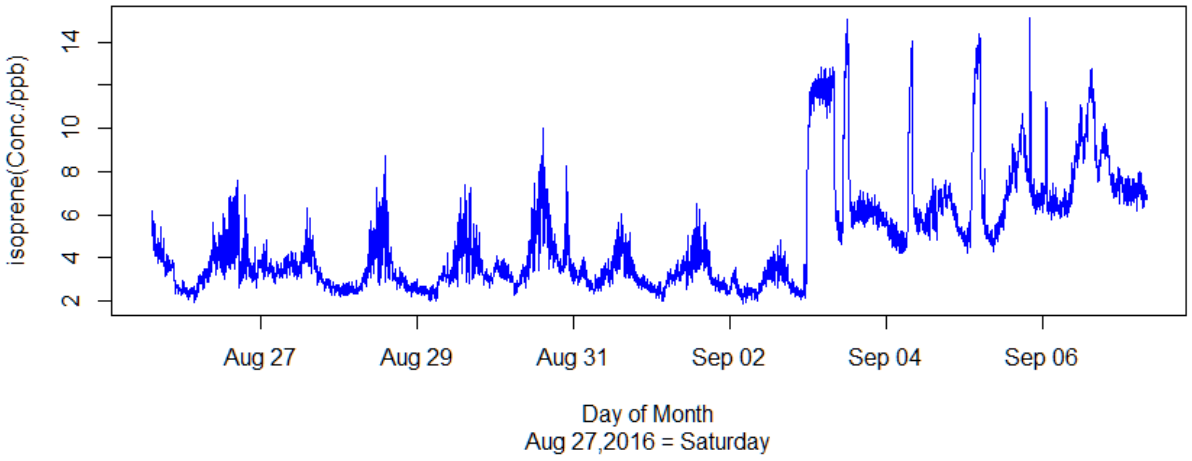

Figure 4.25: ***Period 5;*** **Isoprene concentration against date, for Mill Haft data; from between 14:33 hours on Thursday, 25/08 to 07:53 hours (GMT) on Wednesday, 07/09/2016.** ***The minimum isoprene concentration (see Table 4.5), is 1.883 ppb and could correspond to several points in time across the different days; for example, early hours of the morning on Friday 26, Sunday 28, Monday 29, Tuesday 30, Thursday 01, Friday & Saturday; (02 & 03/09), in Figure 4.25. The maximum concentration is at 15.120 ppbv and could be any of the peaks in the afternoon of Saturday 03 or Monday 05. The median and mean concentrations are respectively 4.0 and 4.8 ppbv.***

The isoprene concentration that was clearly coming down gradually, from concentrations above 45 ppbv, in period 4 (Figure 4.19, 4.25a) and beginning to approach 30 ppbv by late morning on Thursday 25/08, appear to have continued all the way down to somewhere around 6 ppb by afternoon, 14:33 hours on the same day (being Thursday the 25/08/2016,); where the data for Figure 4.25 starts (see Figure 4.25a to compare Figures 4.19 with 4.25, and notice the transition). The downward trend continued till midnight on the 25/08 before starting the next day (Friday 26/08), with an upward trend that is more consistent with the daytime behaviour of isoprene (e.g., Fehsenfeld et al 1992, Kalogridis et al., 2014). The daily diurnal variation of isoprene concentrations stays within a fairly consistent range between 00.00 hours on the 26/08 and 00.00 hours on Sept 03. From this point, the isoprene

concentration rises rapidly (judging by the vertical rise) within the hour, to higher concentration levels than all the previous days (> 12 ppb). The concentration level remains around 12 to 13 ppbv, throughout the morning hours before coming down again to about 5 ppbv (that is, the normal peak concentration of the previous afternoon 02/09), by early afternoon. Then the isoprene concentration suddenly rises again within a short time in the early afternoon to an even higher level beyond 14 ppbv. This time it returns within a short time to the reasonably normal peak of the afternoon and then follows the normal evening decline expected towards the night, yet ends at a low level still higher than the previous days.

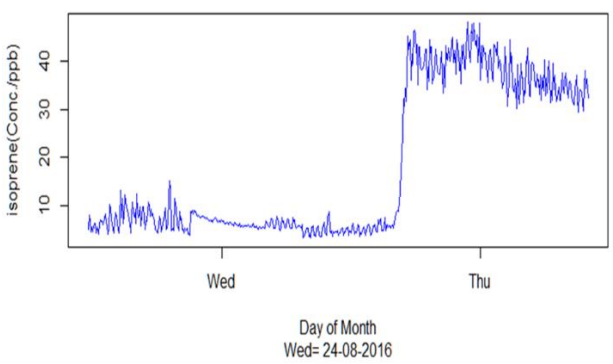

A. Figure 4.19: Isoprene concentration against date, for Mill Haft data; from between 11:33 on Tuesday, 23/08 to 10:03 on Thursday, 25/08/2016.

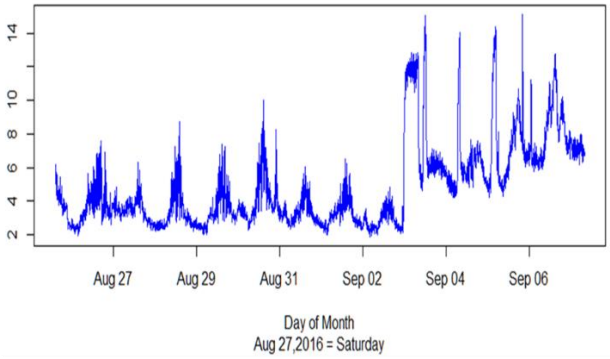

B. Figure 4.25: Isoprene concentration against date, for Mill Haft data; from between 14:33 on Thursday, 25/08 to 07:53 on Wednesday, 07/09/2016.

Figure 4.25a: Period 5; Comparing Figure 4.19 in (period 4) and 4.25 in (period 5). Showing the decrease of isoprene concentration from a very high concentration (above 45 ppb) in the morning (00:00 hours) on Thursday, 25/08/2016, to reasonably low concentration of 6 ppbv by about 14.33 hours on the same day, when the data for Figure 4.25 starts in B. above. The normal pattern of diurnal variation for isoprene becomes more consistent after this.

This pattern that has just been described for Saturday September 03, continues throughout the remaining days up till Wednesday September 07, then declines during the early hours of the morning as expected for isoprene diurnal pattern of concentration levels (see section 1.1; Figure 1.3). The noisy appearance in the afternoon of 26/08 and 28 – 30/08, was mild, and may suggest the presence of other compounds, possibly due to anthropogenic activity around the forest. These compounds in the background, however appeared to have changed, in how they registered in the system, during the last 4

days (that is, between September 03 and 04), possibly due to added changes in the meteorology/ weather conditions; with resultant reactions that registered as increase in isoprene but are actually contributors to the signal intensity of isoprene as discussed in Section 4.6. These are intermittent and occurred at reasonably similar times of the day on each of those days and remained at levels higher than the consistent peak concentration levels, established for the previous days (that is August 27 to September 02), within the period.

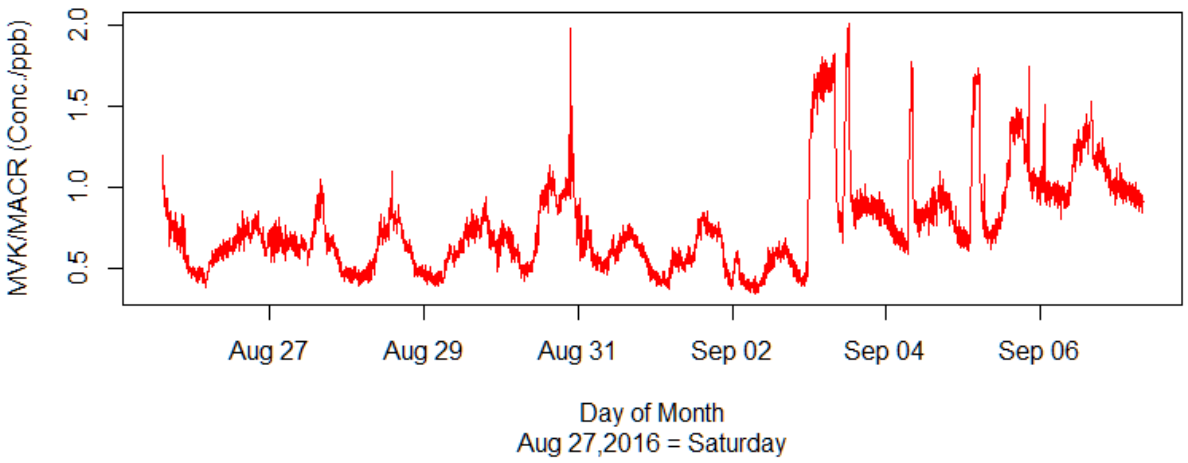

Figure 4.26: Period 5; Methyl Vinyl Ketone (MVK) / Methacrolein (MACR) concentration against date, for Mill Haft data; from between 14:33 hours on Thursday, 25/08 to 07:53 hours (GMT) 0n Wednesday, 07/09/2016. The minimum MVK/MACR concentration (see table 4.5), is 0.3398 ppb which most likely could correspond to mid-morning on Friday 02, but closely representative of the range of concentrations for early morning on Friday 26, Sunday 28, Monday 29, Tuesday 30, Thursday 01 and Saturday 03/09, in Figure 4.26, while the maximum concentration is 2.011 ppbv, most likely Saturday afternoon 03/09. The median and mean concentrations are respectively 0.6987 ppbv and 0.7631 ppbv

However, considering the close mirror image of Figure 4.26 (for MVK/MACR) to 4.25 (for isoprene), it is easier to conclude that the intermediate compounds that may have made contributions to the signal intensity of isoprene, also resulted in the oxidation products, suggesting that they are possibly isoprene and related compounds from both the forest and anthropogenic sources that have similar reaction products to isoprene; depending on what the initial precursors were. The median concentration ratio between isoprene and MVK/MACR is 5.5 : 1. Despite the possible influence of intermediate background compounds, the appearance and concentration profile manifested in Figures 4.25 and 4.26, seem to be

reasonably representative of the isoprene diurnal pattern for the first 9 days (compare section 1.1; Figure 1.3).

4.5.2. MVK/MACR versus Isoprene (period 5)

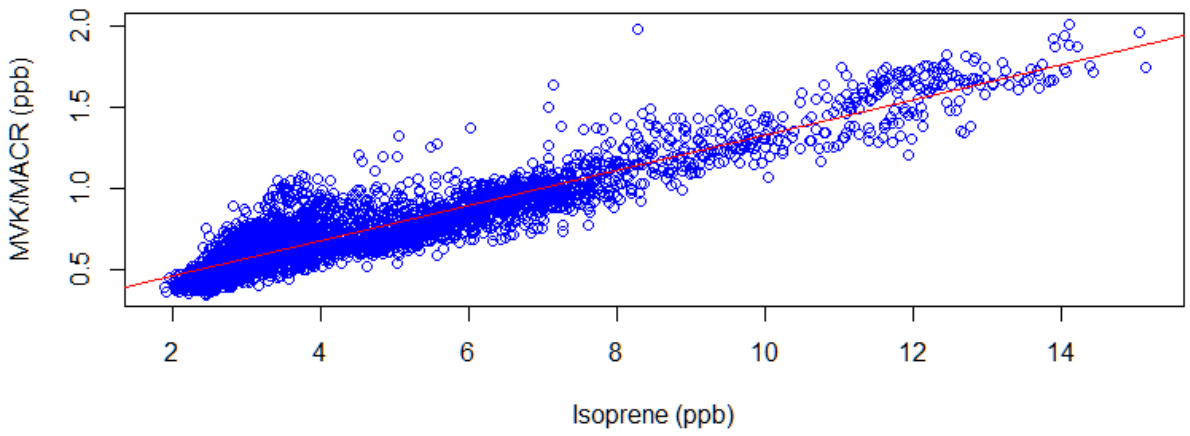

Figure 4.27: Period 5; Plot of Isoprene against MVK / MACR (concentrations) for Mill Haft data; from between 14:33 hours on 25/08 to 07:53 hours (GMT) 0n 07/09/2016. Intercept(MVK) = 0.24, Slope (Isoprene) = 0.11, R^2 : 0.87; y = 0.11x + 0.24. Residual standard error: 0.106 on 3663 degrees of freedom

The coefficient of linear correlation (***R^2***) in figures (4.27 and 4.28) are respectively; 0.87 and 0.81, showing a stronger linear correlation here between the concentrations of isoprene and its primary oxidation products MVK/MACR, than was observed in the previous periods. The rate of change of MVK/MACR to that of isoprene can be worked out from the slope as 10.9 % and the MVK/MACR concentration value from the linear equation based on 1 ppbv of isoprene would be 0.4 ppb, with a residual MVK/MACR concentration of 0.2 ppb when isoprene is 0 ppbv as observable from the intercept value on the y axis. The 0.2 ppb of MVK/MACR (at zero isoprene), will most likely be accounted for, within the 13% of the dataset in Figure 4.27, that fell outside the current linear correlation of 87% (obtained from R^2 : 0.87) .

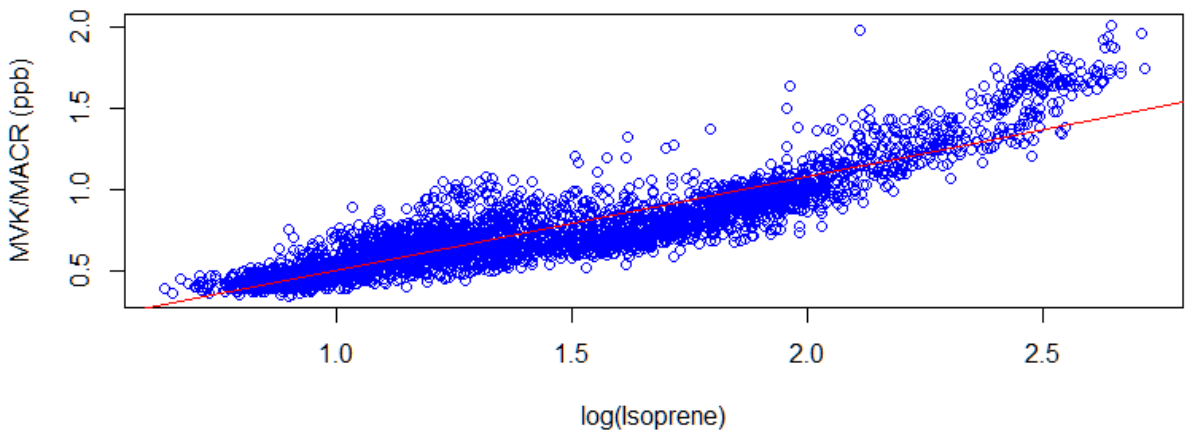

Figure 4.28: Period 5; Plot of ln(Isoprene) against MVK / MACR (concentrations) for Mill Haft data; from between 14:33 hours on 25/08 to 07:53 hours (GMT) on 07/09/2016. Intercept(MVK) = - 0.08 ppbv, Slope (ln(Isoprene)) = 0.58, R^2 : 0.81; y = 0.58x + 0.08. Residual standard error: 0.126 on 3663 degrees of freedom

4.5.3. Basic statistics (Period 5)

Table 4.5 shows statistics for 5-minute data (rows 1 and 2) and hourly averages (rows 3 and 4) for isoprene and MVK/MACR. The ratio of each statistic for isoprene and MVK/MACR is reported in row 5. The median and mean concentrations for isoprene are, 3.9 and 4.8 ppbv, the 1st and 3rd quartile are 3.0 and 6.1 ppb, while the minimum and maximum showed up as 1.9 and 15.1 ppbv respectively. Similarly, the corresponding median and mean for MVK/MACR are 0.7 and 0.8, !st and 3rd quartile came out as 0.6 and 0.9, while the minimum and maximum values are 0.3 and 2.0. The isoprene to MVK/MACR ratios for the median and mean values are 5.5 and 6.3 respectively.

Table 4.5: Summary statistics for Mill Haft Data (period 5) 25/08 to 07/09/2016							
No. / Type	**Minimum**	**Ist Quartile**	**Median**	**Mean**	**Standard deviation**	**3rd Quartile**	**Maximum**
1. Isoprene	1.9	3.0	3.9	4.9	3.6	6.1	15.1 *
2. MVK/ MACR	0.3	0.6	0.7	0.8	0.5	0.9	2.0
3. Isoprene (hourly)	2.3	3.1	4.0	4.9	3.1	6.1	13.3 *
4. MVK (hourly)	0.4	0.6	0.7	0.8	0.4	0.9	1.7
5. Ratios (1. / 2.)	5.5	5.3	5.5	6.3	1.0	6.8	7.5
Note- Data used for 1 & 2 were taken at 5-minute intervals while those used for 3 & 4 were from the hourly sum of these values. * - asterisk to make isoprene data more visible. Units for isoprene and MVK/MACR = ppbv							

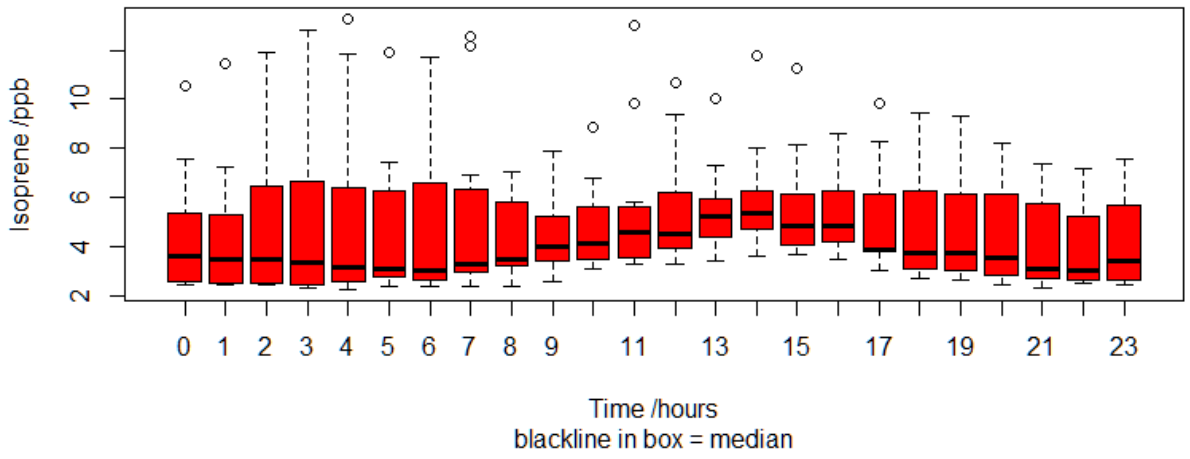

Figure 4.29: Period 5; A Boxplot for Isoprene hourly concentrations for Mill Haft data; from 14:33 hours on Thursday, 25/08 to 07:53 hours (GMT) on Wednesday, 07/09/2016.

One of the first things to notice in Figure 4.29, for isoprene hourly distribution in period 5, is that most of the dataset is skewed downwards, towards the 1st quartile position (the median is closer to the 25 %ile than the centre of the box), except for, 11:00, 13:00, and 14:00 hours. The hours of 05:00 to 08:00 and 21:00 to 22:00 are most skewed followed by the evening hours of 18:00 to 20:00, before the morning hours of 00:00 to 04:00. The morning hours got more skewed as you go from 00:00 hrs to 08:00 hrs. The box at 17:00 hours has its median completely merged with the 25th percentile.

The usual statistical distribution (see Figure 3.20a; chapter 3), has 50 % of the dataset for each hour distributed within the box, while the rest of the 50% is meant to be represented as 25% between the minima (whiskers below) and the lower end of box (1st quartile), while the balance 25 %, is to be between the top of the box (3rd quartile) and the maxima (whisker above); if there are no outliers. But when, there is an outlier above or below the whiskers, then the 25 % is adjusted to accommodate the outlier (see figure 3.20b, in chapter 3, for how this is worked out). The outliers in figure 4.29, are only above the maxima (whiskers) and are mostly single outliers, except for 07:00 and 11:00 hours. Twelve out of the 24 hours are distributed with outliers. The remaining 12 hours without outliers are (2, 3, 6, 8, 9, 16,18 to 23 hours), and have 100 % of their datasets represented between the minima and maxima (whiskers). A single outlier may represent up to 10%, but about 8%; if the dataset is about 12 readings per hour, while two outliers could be between 16 and 20%. The overall distribution pattern suggests some level of night time contribution, the median pattern of rise between 09:00 and 16:00 hours was gradual and minimal but fairly representative of an afternoon or diurnal rise.

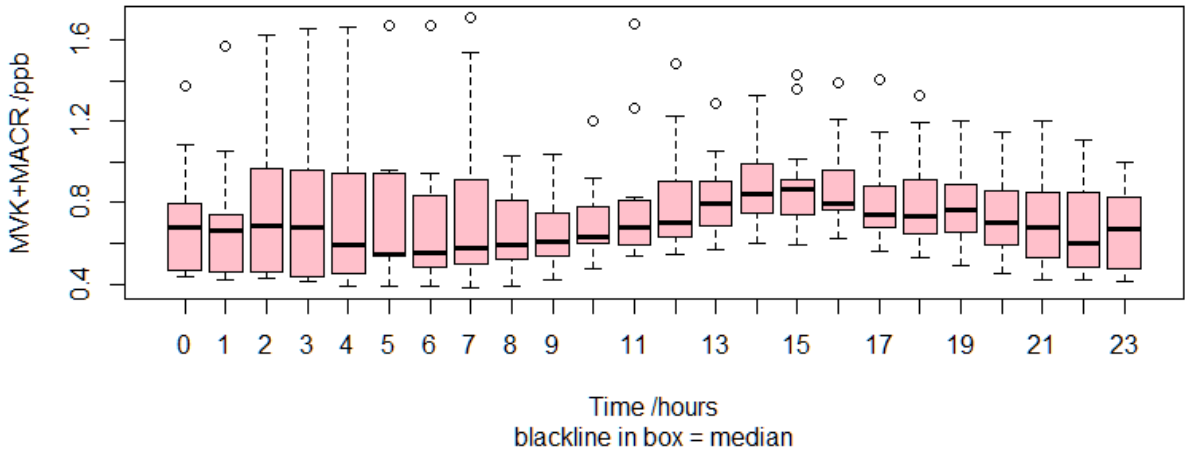

Figure 4.30: Period 5; A Boxplot for MVK/MACR hourly concentrations for Mill Haft data; from 14:33 hours on Thursday, 25/08 to 07:53 hours (GMT) on Wednesday, 07/09/2016.

The median level concentrations for 17:00 to 23:00 hours at night and 00:00 to 03:00 hours of the morning in figure 4.30, suggest some level of night time reactions, partially influencing the MVK/MACR median distributions to stay relatively high during those night hours. There are some similarities in the distribution pattern of MVK/MACR in figure 4.30, and that for isoprene in figure 4.29, except, that they are three to four hours behind those of isoprene; reflecting the time taken for the oxidation process. The data is skewed downwards from 04:00 hours in the morning, all the way to 12:00 hours (Figure 4.30). This also is similar, to (Figure 4.29; for isoprene), but there (that is, for isoprene), the boxplots begin to show signs of being skewed downwards, right from 00.00 hours (about 4 hours earlier) and gradually progress to become more pronounced at 04:00 hours. The pattern of the daytime median peak rise is also similar, but while it begins to be consistent from 11:00 up to 15:00 hours, in Figure 4.30 for MVK/MACR, the consistent rise for isoprene in Figure 4.29, becomes obvious between 09:00 and 14:00 hours (that is, starting about two hours earlier for isoprene). The highest median concentrations in the afternoon are for 14:00 and 15:00 hours. Although the median values are not much higher than the late evening/night time values (carried over to the 1st four hours of the early morning), the general afternoon distribution pattern for 11:00 to 15:00 hours, show the diurnal rise for MVK/MACR in figure 4.30, to be similar to isoprene in Figure 4.29. The outliers in Figure 4.30 are also all above the maxima (whiskers above) but are now 13 out of 24 as compared to 12 in Figure 4.29.

4.6. Other VOCs with possibilities of contributing to the signal intensity (at m/z) of Isoprene and MVK/MACR

Molecular mass of isoprene is 68.12 g/mol, so m/z = 69.12

Molecular mass of MVK/MACR is 70.09 g/mol, so m/z = 71.09

The general patterns observed, in some of the periods (for example most days of periods 1 and 4, and some of the days of 2 and 3), may suggest the possibility of other organic compounds, contributing to the signal intensity of isoprene, because of having their m/z within the same range as isoprene. This type of contribution is one of the possibilities when the consistent diurnal pattern, normally expected; when isoprene is dominant, is not observed, in these periods (compare Figures 4.1; period 1, 4.7; period 2, 4.13; period 3 and 4.19; period 4, with Figure 1.3; section 1.1; notice the typical isoprene diurnal pattern in Figure 1.3). A similar situation may also be applicable for the oxidation products. The list of compounds in table 4.6, have the same m/z as isoprene or its oxidation products and could contribute (in principle) to the intensity of the mass spectrometer signals, from the PTR, if they were found in the immediate environment surrounding the measurement site, at the BIFoR forest location.

Table 4.6: Some VOCs with m/z between 69 to 69.12 and 71 t0 71.09; possible contributors to MS reading

	Compound name	Formula	Molecular mass g/mol	Density g/mL	Boiling point (760)	Melting point	4 Biggest peaks in mass specs (m/e)	Functional Groups	Refraction Index nD(20)
1	2-methyl-1,3-butadiene (isoprene)	C5 H8	68	0.681	34	-146	67,68,53,39	both sat. & unsat. CH	1.4219
2	1,cis-3-pentadiene	C5 H8	68	0.691	45	- 141	67,39,68,53	both sat. & unsat. CH	1.4363
3	1,trans-3-pentadiene	C5 H8	68	0.678	42	- 87	67,39,68,53	Both sat. & unsat' CH	1.4301

4	1,4-pentadiene	C5 H8	68	0.661	26	- 148	39,68,67,53	Both sat. & unsat CH	1.3888
5	3-methyl -1-butyne	C5 H8	68	0.666	26	-90	53,67,27,39	Both sat. & unsat CH	1.3723
6	Cyclopentene	C5 H8	68	0.772	44	-135	67,68,39,53	Both sat & unsat CH	1.4225
7	2-pentyne	C5 H8	68	0.771	56	-109	68,53,39,41	Both sat & unsat CH	1.4039
8	1-pentyne	C5 H8	68	0.690	40	-106	67,39,40,27	Both	1.3852
9	Methyl vinyl ketone (MVK)	C4 H6 O	70	0.842	37	-	55,43,27,70	Carbonyl both	1.4115
10	Methacrolein (MACR)	C4 H6 O	70	0.847	69	-81			
12	cyclopentane	C5 H10	70	0.745	49	-94	42,70,55,41	Saturated CH	1.4065
13	Methyl cyclo butane	C5 H10	70	0.693	36		42,41,55,39	Saturated CH	1.3836
14	Trans1,3dimethylcycloproane	C5 H10	70	0.670	28	-150	55,70,42,41	Saturated CH	1.3713
15	cis-1,2di methyl cyclo propane	C5 H10	70	0.694	37 C	-141 C	55,70,42,39	saturated CH	1.3829
16	**Compound name**	**Formula**	**Molecular mass (g/mol)**	**Density (g/mL)**	**Boiling point (760)**	**Melting point**	**Biggest peaks in mass specs (m/e)**	**Functional Group**	**Refraction Index nD(20**

Adapted from "Organic compounds database" online; http://www.colby.edu/chemistry/cmp/mole.cgi

The list is not exhaustive, but, gives a general ideal of what compounds could make direct contributions if present. These compounds may not appear to be directly relevant in the practical and strict sense of a remote rural forest location but are among factors to be considered when measurement is in a semi urban location like BIFoR. Some of these compounds, within the molecular mass range of 68 to 68.12 g/mol for isoprene and 70 to 70.09 g/mol, for MVK/MACR, are listed as follows ; 1,cis-3-pentadiene, 1,trans-3-pentadiene, 1,4-pentadiene, 2-methyl-1,3-butadiene (isoprene), cyclopentane, 3-methyl-1-butyne, 2-pentyne, methylvinylketone (MVK), cyclopentane, methylcyclobutane, trans-1,2-dimethylcyclopropane, cis-1,2-dimethylcyclopropane (see table 4.6). Their atomic masses and some key

characteristics have also been listed in table 4.6. Those with boiling points around the same range, or lower than isoprene, MVK and MACR are more likely to contribute to the signal intensity than others, at the m/z readings.

Tables 4.7 and 4.8: respectively show summaries from the scatter plots and from the basic statistics from all the five periods and cited with explanations in the conclusions made in section 4.7, below. Table 4.7; shows a summary from the scatter plots for isoprene against MVK/MACR for periods 1 to 5 (P1 – P5). The intercept at y axis (which represents the concentration of the oxidation products at zero isoprene), the slope (which shows the relationship with isoprene), the coefficient of determination (R^2); (which shows the extent of correlation in the linear relationship), the equation for each period (which gives the expected MVK/MACR per unit of isoprene) and a brief conclusion for each period are shown in the different columns.

Table 4.7: Summary from Scatter plots of Isoprene versus MVK/MACR (comparing Periods 1 – 5)

Period	Intercept at y (MVK/MACR)	Slope (Isoprene)	R^2	Linear equation	Conclusion
P1	0.3	0.1	0.8	y = 0.3 + 0.1x	77.5 % linear correlation between both concentrations in P1 (based on R^2), residual MVK/MACR at zero isoprene = 0.3 ppbv (based on intercept at y). change in VK/MACR compared to isoprene is 0.1. 1 ppbv of isoprene results in 0.5 ppbv MVK/MACR
P2	0.4	0.1	0.5	y = 0.4 + 0.1x	52.3 % linear correlation between both concentrations in P2 (based on R^2) and residual MVK/MACR at zero isoprene = 0.4 ppbv (based on intercept at y). Change in MVK/MACR compared to isoprene is 0.1. 1 ppbv of isoprene results in 0.5 ppbv MVK/MACR
P3	0.3	0.1	0.5	y = 0.3 + 0.1x	53.6 % linear correlation between both concentrations in P3 (based on R^2) and residual MVK/MACR at

					zero isoprene = 0.3 ppb (based on intercept at y). Change in MVK/MACR compared to isoprene is 0.1. 1 ppbv of isoprene results in 0.4 ppbv MVK/MACR
P4	0.9	0.002	0.017	y = 0.9 + 0.002x	1.7 % linear correlation between both concentrations in P4 (based on R^2) and residual MVK/MACR at zero isoprene = 0.9 ppb (based on intercept at y). Change in MVK/MACR compared to isoprene is 0.002. 1 ppbv of isoprene results in 0.9 ppbv MVK/MACR
P5	0.2	0.1	0.9	y = 0.2 + 0.1x	86.7 % linear correlation between both concentrations in P5 (based on R^2) and residual MVK/MACR at zero isoprene = 0.2 ppbv (based on intercept at y). Change in MVK/MACR compared to isoprene is 0.1. 1 ppb of isoprene results in 0.4 ppbv MVK/MACR
The periods are left as P1 – P4 for consistency. R^2= Coefficient of determination, y and x in the equations represent MVK/MACR and isoprene respectively. Units for isoprene and MVK/MACR = ppbv					

Table 4.8 is a summary of the basic statistics from the five periods and is cited with explanations in the conclusions made in section 4.7. Table 4.8; compares the statistics for the 5-minute data (rows 1 and 2 in each period), for isoprene and MVK/MACR. The ratios of each statistic for isoprene and MVK/MACR are also compared in the 3rd row of each period but retains the number '5' on the row; (written as '5. Ratios (1/2)'), to maintain consistency with the original tables in the chapter.

Table 4.8: Summary of basic statistics comparing periods 1 to 5 for 2016 Mill Haft Data

Period	No. / Type	Minimum	Ist Quartile	Median	Mean	Standard deviation	3rd Quartile	Maximum
P1 05 - 09 August 2016	1. Isoprene	5.3	7.4	11.0	12.7	8.7	15.8	36.2 *
	2. MVK/ MACR	0.7	1.1	1.5	1.8	1.4	2.1	6.3
	5. Ratios (1./2.)	*7.3*	*6.5*	*7.1*	*7.2*	*1.0*	*7.4*	*5.8*
P2	1. Isoprene	3.1	4.3	4.8	5.2	2.8	5.7	14.0 *
	2. MVK/ MACR	0.5	0.7	0.8	0.9	0.3	1.0	1.6

11 - 17 August 2016	*5. Ratios (1./2.)*	*6.0*	*6.1*	*5.9*	*6.1*	*0.7*	*5.8*	*8.6*
P3 17 - 23 August 2016	1. Isoprene	2.4	2.9	3.4	3.9	2.1	4.1	10.1 *
	2. MVK/ MACR	0.4	0.5	0.6	0.6	0.3	0.7	1.2
	5. Ratios (1./2.)	*6.7*	*5.9*	*5.8*	*6.0*	*0.6*	*5.5*	*8.5*
P4 23 – 25 August 2016	1. Isoprene	3.3	5.6	7.5	18.1	16.4	35.6	48.0 *
	2. MVK/ MACR	0.539	0.8	1.0	1.0	0.4	1.2	1.8
	5. Ratios (1. /2.)	*6.0*	*7.2*	*7.9*	*18.4*	*13.4*	*30.5*	*26.4*
P5 25 August - 07 Sept. 2016	1. Isoprene	1.9	3.0	3.9	4.8	3.6	6.1	15.1 *
	2. MVK/ MACR	0.3	0.6	0.7	0.8	0.5	0.9	2.0
	5. Ratios (1. / 2.)	*5.5*	*5.3*	*5.5*	*6.3*	*1.0*	*6.8*	*7.5*
Note- Data used for 1 & 2 were taken at 5-minute intervals while those used for 3 & 4 (in tables 4.1 – 4.5) were from the hourly sum of these values. (5. Ratios (1./2.); is left as it is in (table 4.1 – 4.5), for uniformity and ease of identification * - asterisk to make isoprene data more visible. Units for isoprene and MVK/MACR = ppbv								

4.7. Summary

The results discussed in this chapter are from the 2016 measurement campaign carried out at the BIFoR FACE Oak Forest, Mill Haft, Staffordshire; where the Free Air Carbon Dioxide Enhancement (FACE) facility is being hosted, by the Birmingham Institute of forest research (BIFoR). It is a deciduous temperate forest, dominated by the English Oak (Quercus robur) and dates to at least 160 years. The FACE facility, is one of the three forest-FACE facilities in the world currently investigating; under natural conditions, the impact of rising carbon dioxide (CO_2), on global ecosystems and biodiversity (Mackenzie et al 2016, BIFoR FACE 2017). The KORE PTR-TOFMS series 1 was deployed for the 2016 Measurements; with the inlet tube raised to the canopy height of about 30 meters. The process is part of the baseline sampling of air, in this deciduous Oak forest made up mostly of trees, that have large wide spreading crown of rugged branches alongside other, sub - dominant, trees like the hazel (Corylus avellana)

coppice; currently overstood at a height of about 15m, in a 25-hectare area of woodland, believed to have been over 300 years under continuous tree cover(Mackenzie et al 2016, BIFoR FACE 2017). The data from the PTR-MS was processed using RStudio (2017) and the results were presented in five period-

i. Period 1 (05 - 09 August 2016) in Section 4.1;
ii. Period 2 (11 - 17 August 2016) in Section 4.2;
iii. Period 3 (17 - 23 August 2016) in Section 4.3;
iv. Period 4 (23 - 25 August 2016) in Section 4.4; and finally
v. Period 5 (25 August - 07 September 2016) was discussed in Section 4.5.

Section 4.6; described some of the other volatile organic compounds (VOCs) having the same molecular mass as isoprene or MVK/MACR and could contribute to the measured results from the PTR-MS; if present in the ecosystem. These compounds may be present either as intermediate (primary or secondary) oxidation products from isoprene or products of other (primary or secondary) reactions in the forest; depending on their concentrations and lifetime in the air. The five periods above were each described in the same way under the following topics-

i. time-series plots of the volatile organic compounds (VOCs) isoprene and its primary oxidation products; MVK/MACR;
ii. scatter plots of Isoprene versus MVK/MACR to investigate co variations between isoprene and MVK/MACR; and
iii. basic statistics combined with boxplots to summarize the data in terms of minimum, 1st quartile (25 percentile; 25 %ile), median (50 %ile), mean, 3rd quartile (75 %ile), and maximum distributions.

The following conclusions can be made from the time series of isoprene and MVK/MACR. The diurnal pattern varies from day to day in the data series, throughout the five periods. Superimposed on the diurnal pattern are rapid variations that occur on each day, but more pronounced in some of the days; and show up with different patterns in the periods, depending on the chemical composition of the ambient air and prevailing physical and weather conditions. Literature indicates that light intensity and temperature are the greatest influences on BVOC emissions (Robinson et al., 2011), including isoprene (Rasmussen and Jones 1973, Tingey et al. 1979, Monson and Fall 1989, Loreto and Sharkey 1990), up to a certain optimal point specific to each VOC. The physical and weather conditions alongside specific contextual factors can also have significant effects on the measured concentration: including wetness or the relative humidity (Sharkey et al. 1995, Holzinger et al. 1999), wind speed and direction, height within the forest canopy and the extent of vegetation cover that determines how much radiation penetrates.

The maximum mixing ratios recorded for some of the periods (Table 4.8) appear to be much higher than what is available in the literature for deciduous forests in temperate climates(Fuentes et al. 1996); (period 1; (P1) and period 4; (P4) are typical examples), although the median distributions are in generally agreement with both the diurnal patterns and concentration profiles for similar forests. Peak isoprene concentrations are known to coincide with maximum canopy temperatures (Tingey et al. 1979, Monson and Fall 1989, Loreto and Sharkey 1990, Fuentes 1996, Sharkey et al. 1996); this can also be inferred from the consistent midday peaks noticeable in nearly all of the periods (for example most of the days in P2; (Figure 4.7), P3; (Figure 4.13) and P5; Figure 4.25).

The mixing ratios of MVK/MACR and Isoprene show an approximate ratio of 1:6, across the statistic ratios (Table 4.8) for almost all the periods despite the extreme deviations in the maxima of periods 1 and 4; (P1 and P4). The mean stayed quite close to the median values in most of the periods despite the

observed extremes in the maxima of (P1 and P4), implying a reasonably consistent distribution pattern, in agreement with the isoprene diurnal variations. Overall, the ratios (in Table 4.8) are showing between 6 to 7 times more isoprene than its primary oxidation products MVK/MACR, across the distribution categories (minima, 1st quartile, median, mean, 3rd quartile and maxima). The largest values for some of the categories (table 4.8) are as follow; maxima; isoprene (P4; 48.0 ppbv), MVK/MACR (P4;6.8 ppbv), minima: (P4: isoprene; 5.3, MVK/MACR0; 0.7), median: (P4: isoprene; 11.0 ppbv, MVK/MACR; 1.5 ppbv), mean: (P4: isoprene; 12.7 ppbv, MVK/MACR; 1.8 ppbv). The lowest values are as follows; maxima; isoprene (P3; 10.1 ppbv), MVK/MACR (P4;1.2 ppbv), minima: (P3: isoprene; 2.4, MVK/MACR0; 0.4 ppbv), median: (P3: isoprene; 3.4 ppbv, MVK/MACR; 0.6 ppbv), mean: (P3: isoprene; 3.9 ppbv, MVK/MACR; 0.6 ppbv).

Table 4.7; shows a summary from the scatter plots for isoprene against MVK/MACR for periods 1 to 5 (P1 – P5). The intercept at y axis (which represents the concentration of the oxidation products at zero isoprene), the slope (which shows the relationship with isoprene), the coefficient of determination (R^2); (which shows the extent of correlation in the linear relationship), the equation for each period (which gives the expected MVK/MACR per unit of isoprene) and finally a brief conclusion for each period are shown in the different columns. The following conclusions can be drawn from the scatter plots-

That approximately 77.5 % linear correlation exists between the oxidation products (MVK/MACR) and isoprene concentrations in Periods 1; (based on the R^2 value of 0.78). There is a residual MVK/MACR concentration of 0.3 ppbv even when there is zero isoprene; suggesting oxidation products unaccounted for by this linear relationship with isoprene (up to 0.3 ppbv, based on the intercept at y axis). The change in the concentration of MVK/MACR, compared to isoprene is 0.1 (related to the slope), and 1 ppbv of isoprene results in 0.4 ppbv of MVK/MACR (obtained from the equation).

In Period 2; there was approximately 52.3 % linear correlation between MVK/MACR and isoprene concentrations (based on the R^2), a residual MVK/MACR concentration of 0.4 ppbv at zero isoprene (based on the intercept at y). The change in the concentration of MVK/MACR, compared to isoprene is 0.1 (related to the slope), and 1 ppbv of isoprene results in 0.5 ppbv of MVK/MACR (obtained from the equation).

Then in Period 3; 53.6 % linear correlation was observed between both concentrations (based on R^2), the residual MVK/MACR at zero isoprene was 0.3 ppbv (based on the intercept at y). The change in the concentration of MVK/MACR, compared to isoprene is 0.1 (related to the slope), and 1 ppbv of isoprene results in 0.3 ppbv of MVK/MACR (obtained from the equation).

While Period 4; showed no linear correlation between both concentrations (at R^2 of 0.017 or 1.7 %), a much higher residual MVK/MACR value of 0.94 ppbv at zero isoprene and the change in MVK/MACR concentration compared to isoprene is 0.002; the lowest of the five periods. 1 ppbv of isoprene results in 0.95 ppbv MVK/MACR. Although Period 4 shows no linear correlation and has the lowest rate of change for MVK/MACR, yet shows the highest MVK/MACR concentration due to the high residual value of MVK/MACR at zero isoprene. This suggest an initial output of MVK/MACR (0.94), not directly related to the measured isoprene. Hence 1 ppbv of isoprene produced 0.96 ppbv, yet only related to a very low rate of change of 0.99.

Finally, Period 5; shows the highest linear correlation of 86.7 % between both concentrations with a residual MVK/MACR concentration of 0.2 ppbv at zero isoprene and the Change in MVK/MACR concentration compared to isoprene is 0.1. 1 ppbv of isoprene results in 0.4 ppbv MVK/MACR.

The results conclude that isoprene and its primary oxidation products; MVK/MACR are present in this sample data collected during the 2016 measurement campaign at the canopy height of about 30 metres;

as part of the baseline air sampling procedures, at the BIFoR Mill Haft Forest, Staffordshire. The daily mixing ratios and diurnal patterns vary based on prevailing environmental, physical and climatic conditions but show median and mean values that give an approximate estimate of what to expect.

Additional methods including gas chromatography will be required alongside the PTR-MS, if more precise mixing ratios are required. The other factors that influence the release of isoprene like temperature, radiation and relative humidity will need to be more closely monitored along with the wind speed and direction. Other volatile organic compounds (VOCs), secondary aerosols (SOAs), ozone (O_3) and nitrogen oxides (NOx) will all need to be monitored, since they impact the oxidation of isoprene.

Chapter 5

Fingerprint of possible volatile organic compounds in a temperate deciduous forest: August – September 2016.

5.0 Overview: guide to the chapter

The results for the fingerprint process for the 2016 measurement campaigns are presented under five sections: in section 5.1; Description of the fingerprint process, in Section 5.2; Identifying compounds from the 2016 data, in section 5.3; Fingerprint plots periods 1-5, in section 5.4; Comparing the fingerprint plots from the five periods of the 2016 measurement campaigns, and finally; the Summary/ Conclusion in section 5.5. Section 5.2; is made of one subsection; 5.2.1; Comparing candidate compounds to literature from similar forests, while section 5.3 is discussed in five subsections: 5.3.1; Fingerprint plot period 1: (05 - 09 August 2016), 5.3.2; Fingerprint plot period 2: (11 - 17 August 2016), 5.3.3; Fingerprint plot period 3: (17 - 23 August 2016), 5.3.4; Fingerprint plot period 4: (23 - 25 August 2016) and finally, 5.3.5; Fingerprint plot period 5: (25 August - 07 September 2016).

5.1 The fingerprint process

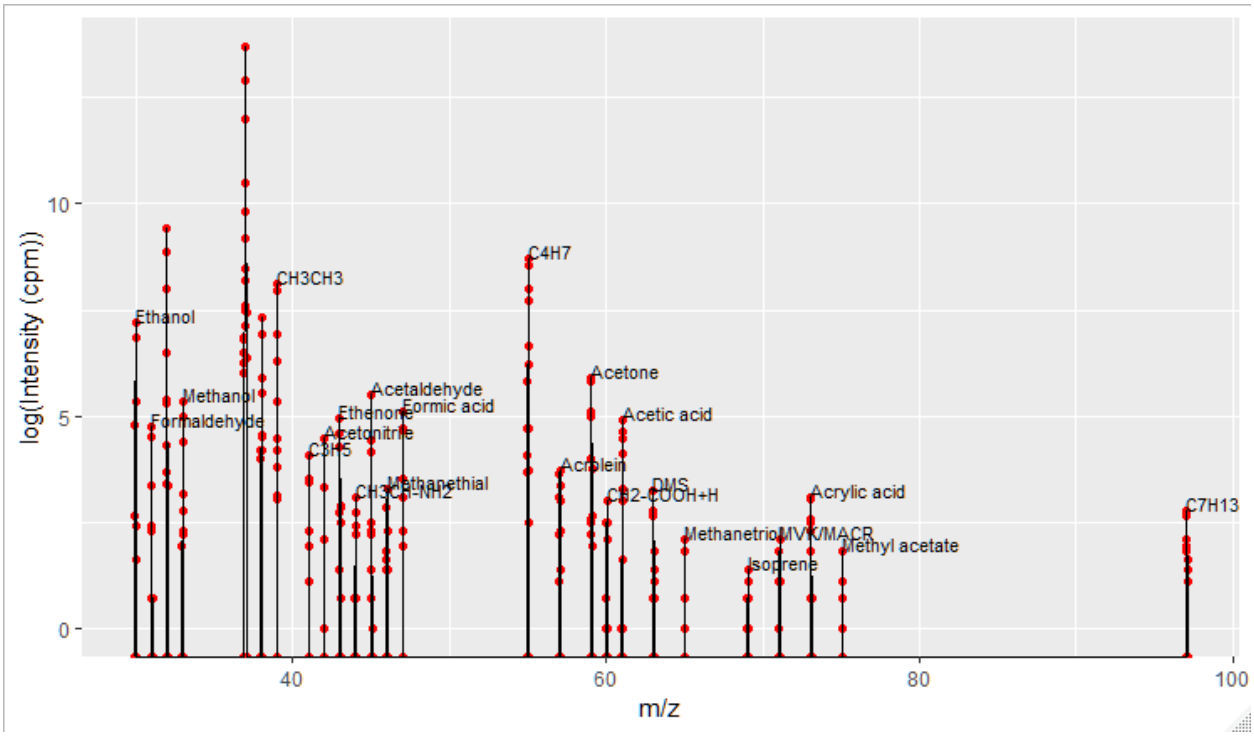

Figure 5.3: An example of a fingerprint plot with labels identifying some of the possible Volatile Organic Compounds in a temperate deciduous forest; (data for this sample plot was from a 2015 measurement campaign at BIFoR; sampling inlet taken from about 2m high in the forest). Red dots show individual intensities from which an individual m/z peak is identified.

The "fingerprint plot" (Figure 5.1), gives a quick overview of the complexity of an environmental sample and the relative intensities of different m/z signals detected by the PTR. The plot provides a 'first look' to assess the need for any additional methods for further compound verification, to confirm and differentiate between closely related compounds in the forest and possible fragments / derivatives that might have resulted from the proton transfer reaction and/or the mass spectrometer system. In a fingerprint plot, the range of signal intensities in counts per minute (cpm), are plotted against the range of associated mass to charge ratios (m/z), at every point, where the characteristic (maximum) peak

intensity is formed; as explained in chapter 2, section 2.4.1. Maximum peak intensity tabulated against m/z is shown in table (5.1). Candidate compound identifications are deduced from the protonated mass (that is; molecular mass of compound or fragment + 1) for those candidate molecules with proton affinity greater than water (that is, the capacity to attract H^+ away from protonated water, also known as the hydronium ion, H_3O^+). The experimental value for the protonated mass is calculable from chemical formulae for unfragmented molecular ions; often it is more reliable to use experimental observations of the most prevalent ions from the literature, to compare with values in table (5.1). The proton affinity values have also been determined experimentally or by theoretical calculations based on thermodynamic and kinetic data, previously well established in peer reviewed literature. The proton affinity for water is about 694 ± 3 kJ mol^{-1}, at 300K (27 °C) (Ellis and Mayhew 2013; Hunter and Lias 1998; Jolly 1991). The proton affinity values for the other candidate compounds are then compared to that of water to determine how strong the capacity is, to take over H^+ from protonated water. The higher values show stronger affinity or attraction to H^+.

Using the combination of Figure 5.1 and Table 5.1, a simple four-step process to pinpoint possible candidate compounds in the mass spectrum from the forest, while excluding others, is used:

1. From the data table, use the m/z value at the peak intensity (that is, Molecular mass + 1); to identify the compound, from the molar mass;

2. Find the proton affinity from literature;

3. Compare the proton affinity to that of water; if sufficiently higher than water (at least a difference of about 22 kJ mol^{-1} or more), then there is a high likelihood that the compound could be detected effectively using the PTR; and

4. Finally compare the outcome with observed pattern of detection in similar forests, from the scientific literature (if available), especially observations using PTR (see table 5.1).

Any compound that successfully appears through this process stands a stronger chance of being present. Additional methods, not used in this study, including gas chromatography (Ellis and Mayhew 2013; Jordan et al 2009), can be applied alongside the PTR method to confirm assignments. The equipment used for these measurements, as stated in section 2.1; is the KORE series 1; PTR-ToF-MS with a mass resolution ≥ 1,500 FWHM; (Full Width Half Maximum) and Sensitivity for Benzene >200 cps/ppbv; (counts per seconds/parts per billion) (KORE 2014).

5.2 Identifying compounds from the 2016 data

This process of identification was applied to the 2016 data and resulted in the large table of candidate species; compounds and fragments in appendix A. Table (5.1), shows the top 15 stable, recurring and identifiable compounds; with verifiable proton affinities that are at least 22 kJ mol-1 units above that of water under the standard gas phase conditions required (Ellis and Mayhew 2013). These compounds have also been identified by PTR in similar forests (Seco et al., 2011 and Federico et al., 2015). Table (5.2), shows the top eight unspecified species (fragments and unidentified compounds); due either to the unavailability of a reliable proton affinity data, and / or uncertainty regarding its chemical structure and components, when compared to available literature. Future studies may profitably use additional methods (eg gas chromatography) to provide more detailed identification for the specific species. However, such subsidiary analysis is beyond the scope of this study.

Table 5.1: The Top 15 stable and identifiable compounds, based on maximum intensity at m/z;
identification based on m/z and proton affinity (pa); as compared to the proton affinity (pa) of H20 (see appendix A; for the table with a more comprehensive list of compounds and fragments). Measurement periods 1 to 5 are shown as 1p, 2p, 3p, 4p and 5p respectively.

No	(m/z) at maximum peak	Maximum (peak) intensity (cpm)	Possible compound / ion detected	Literature Source of fragment identification	Proton affinities of parent species (kJ/mol)	Source of proton affinity data	Comment
1	29.015	1P 21072 2p 28461 3p 39198 4p 21760 5P 22076	C2H5+ Ethanol (alkyl fragment)	2.	776	4	The measured m/z in (2) was 29.039
2	43.025	1p 22183 2p 8062 3p 5317 4p 4862 5p 5494	Ethenone (C_2H_3O+) / propene (C_3H_7+); Alkyl fragments	2	ethenone (779) / propene (752)	4 / 5	measured m/z shown in (2) were: ethenone (43.018)/ propene (43.054). 43.025; here, suggests a mixture of both.
3	59.065	1p 18265 2p 17886 3p 11986 4p 11535 5p 37314	Acetone (2-Propanone) C_3H_7O+	(1, 2)	812	5	Measured at 59.49 in both (1) and (2)
4	45.045	1p 15796 2p 12232 3p 7793 4p 6462 5p 8990	Acetaldehyde (C_2H_5O+)	1, 2	769	5	45.033 was the measured m/z in (1 and 2)
5	61.045	1p 10687 2p 3695 3p 2036 4p 1840 5p 2453	Acetic acid $C_2H_5O_2+$	(1, 2)	784	5	Measured at 61.028 in both (1) and (2)

6	32.995	1p 2p 3p 4p 5p	4754 5920 6431 5362 5368	Methanol (CH_5O+)	1, 2	754	5,7	Measured m/z in (2) was 33.033
7	42.045	1p 2p 3p 4p 5p	2017 1925 2047 1766 3943	Acetonitrile (C_2H_4N+)	2	779	5	
8	73.075	1p 2p 3p 4p 5p	2831 985 664 587 1450	2-Butanone (C_4H_9O+)	(2)	827.2	7	Measured at 73.065 in (2)
9	75.065	1p 2p 3p 4p 5p	1968 365 279 233 428	Methyl acetate ($C_3H_7O_2+$) / Isobutanol (2-Methyl-1-propanol) $C_4H_{11}O+$	(2)	(Acetic acid, methyl ester) 821.7	7	methyl acetate was 75.044 and isobutanol was 75.080 in (2)
10	30.995	1P 2p 3p 4p 5P	1229 1646 1964 1664 1948	Formaldehyde (CH3O+)	2	713		The measured m/z used in (2) was 31.042
11	57.045	1p 2p 3p 4p 5p	1790 1079 539 551 1103	2-Propenal (Acrolein) C_3H_5O+/C_4H_9+ 1-Butene (alkyl fragment)	(2)	Acrolein 797	4	Acrolein was 57.34 and 1-butene was 57.68 in (2)
12	71.055	1p 2p	1622 617	MVK; methyl-vinyl-ketone (3-Buten-2-one) C_4H_7O+ / MACR;	(1, 2, 3a)	834.7 / 808.7	4, 5	MVK/MACR was 71.09 in (1) while MACR was 71.049 and a mix of alkyl

		3p	294	methacrolein (methacroaldehyde)				fragments (C5H11+) was 71.086 in (2). ISOPOOH also reported in this m/z in (3a) (Rivera-Rios, et al. 2014)
		4p	457	C_4H_6O+ /				
		5p	452	ISOPOOH				
13	47.025	1p	1208	Formic acid/ Ethanol (CH_3O_2+/ C_2H_7O+)	1, 2	742 / 776	5	Measured m/z for formic acid was 47.013 and ethanol was 47.049 in (2) and 47.048 in (1)
		2p	711					
		3p	492					
		4p	464					
		5p	788					
14	74.075	1p	1021	Dimethylformamide (C_3H_8NO+)	(2)	884	6	Measured at 74.061 in (2)
		2p	170					
		3p	50					
		4p	61					
		5p	104					
15	69.085	1p	912	Isoprene (2-Methyl-1,3- butadiene) C_5H_9+	(1, 2)	826.4	4, 5	Measured at 69.069 and 69.070 in (1) and (2) respectively
		2p	162					
		3p	158					
		4p	112					
		5p	145					

Species identification source:

1. Seco et al (2011a): online from www.atmos-chem-phys.net/11/13161/2011/doi:10.5194/acp-11-13161-2011

2. Federico et al (2015): Springer 2018; Online from https://www.nature.com/articles/srep12629/tables/1

3. *Hadden Analytical online; references; Hemming and Foster (1992), McLafferty and Turecek (1993), Silverstein et al (1991)*

3a. Rivera-Rios, et al. 2014

Affinity data source*:*

4. Hunter and Lias (1998) / NIST Webbook (2018)

5. Ellis & Mayhew (2013)

6. Jolly (1991), *Modern Inorganic Chemistry*(2nd Edn.). New York: McGraw-Hill. ISBN 0-07-112651-1.

7. KORE technology (2018), online from https://www.kore.co.uk/paffinities.htm

Simply extracting the top 15 species (from the table of all the possible species in Appendix A), would have resulted in a single table dominated mostly by unidentified species (or identified fragments; but not stable recurring VOCs); since most compounds of interest generate parent molecular ions under the

PTR conditions required for isoprene ionisation at E/n of between 80 - 120 Td (Td; Townsend); (see Blenkhorn 2018). An example of the large difference in magnitude (cpm) of peak intensities can be seen from comparing the two top members of tables (5.1 and 5.2); that is, the identified VOC (ethanol), in table (5.1); that is shown in period 3; as (3p 39198), with the top unidentified species in table (5.2); that is, the species in period 2; recorded as (2p 1454289); this same species, is shown in period 3; as, (3p 1161692). The magnitude of the signal intensity (cpm), for both periods 2 and 3, in the unidentified species was much larger than that for ethanol. Hence, this species, in table 5.2, though unidentified / unspecified, at this initial stage of chemical fingerprinting, has been shown to be present and could be considered for further verification using other methods like gas chromatography, alongside the PTR-MS; when the species is known. Then it may be easier to determine, if the large intensity translates to a significant contribution in some ways, based on its chemical, structural and physical properties. The first 15 compounds (Table 5.1), listed in order of the magnitude of their signal intensity at m/z are: ethanol; ethenone / propene; acetone; acetaldehyde; acetic acid; methanol; acetonitrile, 2–butanone; methyl acetate / isobutanol; formaldehyde; 2–propenal / 1-butene; MVK/MACR; formic acid / ethanol; dimethyl formamide; and isoprene (see Figure 5.2; for the chemical structures of these compounds). The rightmost peak in Figure 5.1; at m/z 97.10, identified as $C7H13^{+}$ is also briefly discussed below, with the molecular structures of likely compounds included in Figure 5.3. Table 5.1 was deliberately extended to 15 compounds, to include the primary compound of interest, to this study; that is, isoprene; and its main oxidation products MVK/MACR.

Table 5.2: Top 8 fragments / unidentified species, based on maximum peak intensity at m/z; identification based on m/z and proton affinity (pa); as compared to the proton affinity (pa) of H20 (see Appendix A; for the table with a more comprehensive list of compounds and fragments). Measurement periods 1 to 5 are shown as 1p, 2p, 3p, 4p and 5p respectively.

No	(m/z) at maximum peak	Maximum (peak) intensity (cpm)	Possible compound / fragment	Source of fragment identification	Proton affinities of species (kJ/mol)	Source of proton affinity data	Comment
1	31.985*	1P 117419 2p 1454289 3p 1161692 4p 932558 5P 951691	ui *(alkyl fragment) Possibly related to Methanol or formaldehyde based on the m/z	na	na The pa for formaldehyde (713) and methanol (754.4) are high enough to consider the possibility for this specie	7	* The intensity of this fragment is consistently high and likely associated with methanol / formaldehyde but needs confirmation
2	37.035*	1p 603970 2p 889415 3p 614980 4p 730218 5p 915457	ui	na	na	na	*The pa of HCl (564) is too low to consider HClH+
3	30.005	1p 217210 2p 338052 3p 324616 4p 308087 5P 364602	*CH2NH2+	3.	832.6	7	*Possibly Fragments associated with alkyl amines
4	33.995	1p 16563 2p 25355 3p 26241 4p 19218 5p 24593	ui	na	na	na	

5	55.055	1p 7513 2p 13801 3p 5125 4p 12143 5p 24677	Alkyl fragment (C_4H_7+)	(2)		1,3–butadiene, 2 - methyl- 826	7	m/z 55.054 was measured in (2)
6	39.035	1p 7640 2p 6147 3p 4053 4p 5867 5p 8965	CH_3CH_3		ui	na	na	Likely source; aromatics; suggested in (3)
7	60.055	1p 7524 2p 828 3p 541 4p 513 5p 1404	ui (CH_2-COOH+H) *Acetic Acid	(3)		Acetic acid 783.7	7	* This is listed as a related fragment because, In (2), Acetic acid (C2H5O2+) was at m/z 61.028
8	50.005	1p 1120 3p 1544 4p 1307 5p 1360	ui *C_4H_2	2, 3		Cyclopentane 750	5	

Species identification source:

1. Seco et al (2011a): online from www.atmos-chem-phys.net/11/13161/2011/doi:10.5194/acp-11-13161-2011

2. Federico et al (2015): Springer 2018; Online from https://www.nature.com/articles/srep12629/tables/1

3. *Hadden Analytical online; references; Hemming and Foster (1992), McLafferty and Turecek (1993), Silverstein et al (1991)*

Affinity data source:

4. Hunter and Lias (1998) / NIST Webbook (2018)

5. Ellis & Mayhew (2013)

6. Jolly (1991), *Modern Inorganic Chemistry*(2nd Edn.). New York: McGraw-Hill. ISBN 0-07-112651-1.

7. KORE technology (2018), online from https://www.kore.co.uk/paffinities.htm

Abbreviations used

Pa – proton affinity

ui - unidentified / not conclusive; needs further clarification

na – not available

* - calls attention to areas of more specific explanations

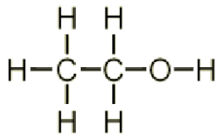

Ethanol (C_2H_6O)

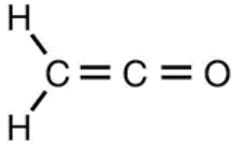

Ethenone (C_2H_2O)

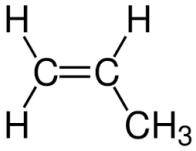

Propene (C_3H_6)

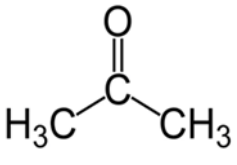

Acetone (C_3H_6O)

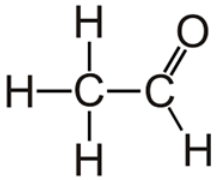

Acetaldehyde(C_2H_4O)

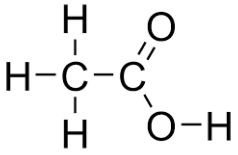

Acetic acid ($C_2H_4O_2$)

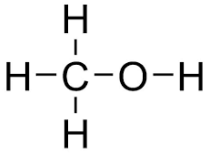

Methanol (CH4O)

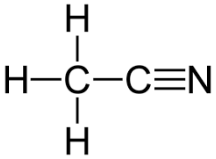

Acetonitrile (C_2H_3N)

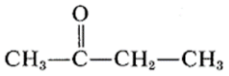

2-Butanone (C_4H_8O)

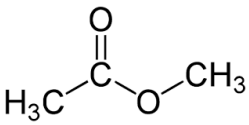

Methyl acetate ($C_3H_6O_2$)

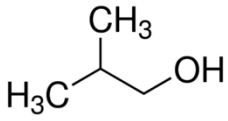

Isobutanol ($C_4H_{10}O$)

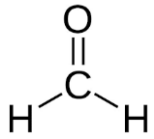

Formaldehyde (CH_2O)

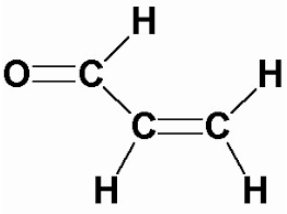

2-propenal (C_3H_4O)

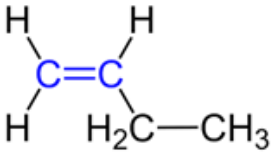

1-Butene (C_4H_8)

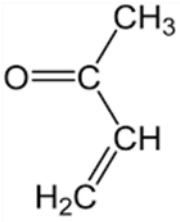

MVK (C_4H_6O)

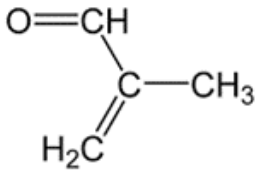

MACR (C_4H_6O)

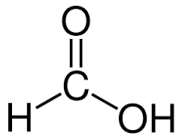

Formic acid (CH_2O_2)

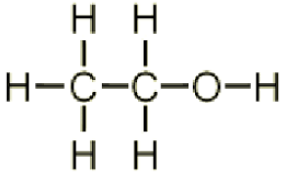

Ethanol (C_2H_6O)

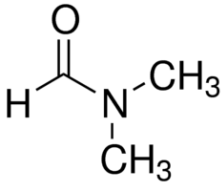

Dimethylformamide (C_3H_7ON)

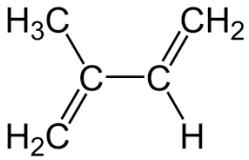

Isoprene (C_5H_8)

Figure 5.4: Chemical structures of compounds in Table 5.1

Cycloheptene; molecular weight: 96.17 g/mol, formula: C_7H_{12}, flash point: −6.7 °C

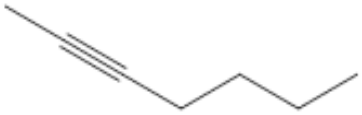

2-Heptyne: Molecular Weight: 96.17 g/mol: formula: C_7H_{12}, boiling point: 112.0°C

Figure 5.3: Example of possible compounds at m/z 97.10;* shown *as C_7H_{13} in Figure 5.1

The product ion $C_7H_{13}^+$; in Figure 5.1 above; from the 2015 data, is at m/z 97.10; it has a molecular mass of 96, which coincides with cycloheptene and 2-heptyne (see the chemical structures in Figure 5.3). Some of the compounds identified in Table 5.1 are isobaric or isomeric mixtures. These compounds and their main differences in terms of separability into the distinct individual constituents, using the PTR-MS, are briefly outlined in Figure 5.4. The isobaric compounds in groups A to D; have the same nominal molecular weight but differ in the decimal units and can be separated with a high enough mass resolution, depending on the compounds involved and the type and combination of the atoms; for example; the presence of oxygen in ethenone that is absent in propene. The isomeric mixtures on the other hand are inseparable using this method since the molecules have exactly the same molecular weight and atoms in combination, which locates them on exactly the same m/z on the mass spectrum; an example is MVK/MACR in group E (Figure 5.4).

Isobaric / Isomeric mixtures among candidate compounds for identification in Figure 5.1

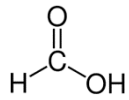

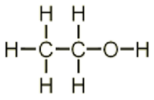

A. Formic acid (HCO_2H); mw: 46.03 / ethanol (CH_3CH_2OH); mw: 46.07 (isobaric = isb)

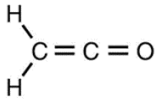

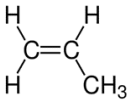

B. Ethenone (CH_2CO); mw: 42.04 / propene(CH_2CHCH_3): mw: 42.08 (isb)

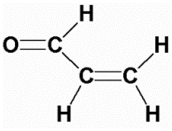

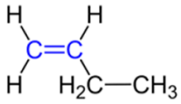

C. 2-propenal (CH_2CHCHO); mw: 56.06 / 1-butene ($CH_2CHCH_2CH_3$); mw: 56.11 (isb)

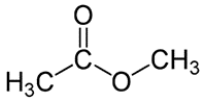

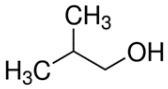

D. Methyl acetate ($CH_3CO_2CH_3$): mw: 74.08 / isobutanol ($CH_3CH(CH_3)CH_2OH$): mw: 74.12 (isb)

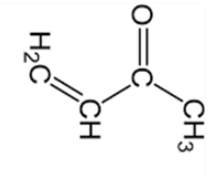

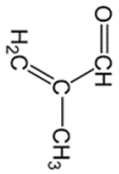

E. MVK ($H_2C=CHCOCH_3$); mw: 70.09 / MACR ($H_2C=C(CH_3)CHO$); mw: 70.09 $gmol^{-1}$ (isomeric = ism)

Mw = molecular weight in $gmol^{-1}$

1. **Isobaric compounds; like those in (A to D), have mw that differ in the decimal part; have different combining atoms in the molecules and are sometimes separable, if the m/z resolution is high enough.**

2. **Isomeric compounds; like those in (E) have exactly the same mw and m/z resolution, because they have the same exact atoms in the molecules. They cannot be separated using only PTR-MS.**

Figure 5.4: Differentiating between isobaric and isomeric mixtures among the identified compounds

5.2.1 **Comparing candidate compounds to literature from similar forests**

Comparing compounds in Table 5.1 to PTR-MS measurements from similar forests in temperate regions show agreement in the results. For example, in (Seco et al 2011a); VOC measurement campaigns were carried out in a holm oak (*Quercus ilex* L.) forest, in the summer of 2009. The site is considered as a very good prototype for the montane holm oak forests, in the Mediterranean regions of eastern Spain, Greece, France and Italy; (Terradas, 1999). These compounds were further confirmed when (Seco et al 2007; 2008; and 2011b), had separate investigations on the release and utility of Short chained oxygenated VOCs, formaldehyde, and methanol, respectively, in similar environments. Table (5.3), shows VOCs identified in Seco et al (2011a); listed in order of mixing ratios (that is, showing the magnitude of intensity for each VOC in units of concentration (ppbv)). Although compounds do have differing sensitivities in the PTR (Chapter 2; Section 2.4; Table 2.1, see also; subsection 2.4.1.5), Table 5.3, would be largely in the same order if listed in (cpm), without converting to (ppbv); (ppb = ncps; normalised counts per second/sensitivity or conversion factor of instrument for each product ion). Compounds in Table 5.3 are similar to those in Table 5.1 and also agree with Table 2, page 9; Kalogridis et al., (2014); confirming the reliability of the fingerprinting process using PTR-MS. All the 15 identified compounds have proton affinities higher than water (with formaldehyde having the least difference, being 22 kJ mol^{-1} above water); in table 5.1). The m/z for the largest peak, methanol, was 32.995 (table 5.1) compared to 33.033 in both Seco et al (2011a); (table 5.3) and Federico et al (2015); the m/z difference of 0.038 is within the combined error of the two instruments. The accuracy of m/z values between instruments is discussed in Chapter 2.

Table 5.3: A typical sample of VOCs identified in Seco et al 2011a;

Using two different PTRMS systems in a holm oak forest in Montseny site, 50 km NNE of Barcelona city, Italy (Adapted from Tables 1 and 2 in pages 3 and 4; Seco et al 2011a)

Assigned VOC identity	Measured exact protonated mass (m/z)	Measured nominal protonated mass	Minimum summer mixing ratios (ppb)	Maximum summer mixing ratios (ppb)
Methanol	33.033	33	1.410	13.400
Ethanol	47.048	na	na	na
Ethanol/formic acid	na	47	0.374	4.480
Acetone	59.049	59	0.967	5.950
Acetaldehyde	45.033	45	<0.036	3.370
Acetic acid	61.028	61	0.270	5.640
Isoprene	69.069	69	<0.021	1.250
MVK/MACR	71.09	71	<0.009	1.040
Monoterpenes	81.070 and 137.132	81 and w37	0.035	2.560
Benzene	79.054	79	0.008	0.194
Toluene	93.069	93	<0.015	1.340
C-8 aromatics	107.085	107	<0.010	0.821
Acetonitrile	42.033	42	0.037	0.588

Ethanol was recorded as m/z 47.048 in Seco et al (2011a) and 47.049 in Federico et al (2015) while formic acid was combined with ethanol at m/z 47, in (Seco et al., 2011a) but given as 47.013 in Federico et al (2015); so that the value of 47.025 in table 5.1; identified as ethanol/formic acid mixture, is in good agreement with the literature (see Figure 5.4; below for further explanations regarding isobaric / isomeric mixtures). A similar pattern can be observed for MVK/MACR at 71.055 in table 5.1, as compared to 71.09 in the respective literature as above. Table 5.4; fully compares the measured m/z in this study (table 5.1), against the measured m/z values for all the identified compounds in Seco et al

(2011a) and Federico et al (2015); in table 5.1. The species at m/z 29.013 (table 5.4); identified as ethanol (alkyl fragment), appears to be a stable recurrent fragment from ethanol and is measured under m/z 29.039 in Federico et al (2015), while the fragments at m/z 43.025; ethenone/ propene were also identified separately as stable, individual and recurrent alkyl fragments at m/z 43.018/ 43.054, in Federico et al (2015); hence 43.025 (in between both figures), being identified as a mixture of both fragments. Ethanol was m/z 47.048 and 47.049 in Seco et al (2011a) and Federico et al (2015) respectively; but m/z 47.025, is in between both figures and therefore, identified as a mixture of formic acid/ ethanol. A similar consideration was applied to m/z 57.045; alkyl fragments from 2-propenal/1-butene; (given as 57.034 / 57.068 in Federico et al (2015)). Acetone (m/z 59.065) and acetaldehyde (m/z 45.045); were, 0.016 and 0.012 more than (m/z 59.049) and (m/z 45.033), respectively; measured by both literature references; (Seco et al., 2011a) and Federico et al (2015), (see table 5.4). Acetic acid (61.045) was 61.028 in both literature, isoprene (69.085) showed up as (69.069 and 69.070) while MVK/MACR (71.055) was (71.09 and 71.086) respectively in Seco et al (2011a) and Federico et al (2015); with MVK separately measured as 71.049 in Federico et al (2015), so that (m/z 71.055 measured in this study), falls within a very good range as identified for MVK/MACR.

Table 5.4: Comparing measured m/z in table 5.1 with measured m/z in the literature references; Seco et al 2011a) and (Federico et al (2015) used in table 5.1

No	Assigned VOC identity	Measured exact protonated mass (m/z); (table 5.1)	Measured exact protonated mass (m/z); (1) Seco et al (2011a); (table 5.3)	Measured exact protonated mass (m/z); (2) Federico et al (2015)
	Ethanol (alkyl fragment) C2H5+	29.015	na	29.039
1	Methanol	32.995	33.033	33.033
2	Ethanol C2H7O +	na	47.048	47.049
3	Formic acid/ ethanol	47.025	na	47.013/47.049
4	Acetone	59.065	59.049	59.049

5	Acetaldehyde	45.045	45.033	45.033
6	Acetic acid	61.045	61.028	61.028
7	Isoprene	69.085	69.069	69.070
8	MVK/MACR	71.055	71.09	71.086 (MVK 71.049)
9	Ethenone/propene (alkyl fragment) (C_2H_3O+)/(C_3H_7+)	43.025	na	43.018 / 43.054
10	2 - Butanone	73.075	na	73.065
11	Methyl acetate/isobutanol	75.065	na	75.044 / 75.080
12	formaldehyde	30.995	na	31.042
13	Acetonitrile	42.045	42.033	42.034
14	2-propenal/1-butene (C_3H_5O+/C_4H_9+) alkyl fragments	57.045	na	57.034 / 57.068
15	Dimethylformamide	74.075	na	74.061

The literature in (Federico et al (2015) also noted that (m/z 71.086) measured in Federico et al (2015) was for a mix of several compounds, not just MVK/MACR; (m/z 71.055), which is slightly more than MVK (71.049), appears to be a better representative of the MVK/MACR mix, rather than (m/z 71.086) in Federico et al (2015), which presents a mix of other compounds along with it. Finally, dimethylformamide (74.074), the last member of table 5.4; was measured as 74.061 in Federico et al (2015). Table 5.4; shows the VOCs in table 5.1; arranged in the same order as table 5.3, to reflect the similarities in the identified compounds, with the literature in Seco et al (2011a); as listed in table 5.3. The only difference in table 5.4, is the replacement of monoterpenes, benzene, toluene and C-8 aromatics with ethenone/propene (alkyl fragment), 2 – butanone, methyl acetate/isobutanol and formaldehyde, before extending the list to include ethanol (alkyl fragment), at the top and 2-propenal/1-butene (alkyl fragments) and dimethylformamide at the bottom of the table. It is however

important to note that, even the replaced compounds are listed in appendix A; for instance, benzene toluene and C8-aromatics are listed in appendix A; at m/z 79.065, 93.065 and 107.075, respectively at positions (53, 66, and 79); and (m/z 107.075) was identified as dimethylbenzene; (in appendix A), rather than with the more inclusive name of C-8 aromatics; shown as (m/z 107.085); (in table 5.3).

5.3 Fingerprint plots Periods 1-5

The top 15 compounds in table 5.1, were listed based on the highest contribution in a group from any of the periods in that group; for instance, ethenone/ propene (alkyl fragment) was number 2, on the list because of (1p 22183); from period 1; but all the other periods listed under number 2, were much lower with; (2p 8062; 3p 5317; 4p 4862 and 5p 5494); respectively, for periods 2 to 5 in group number 2. In this section; periods 1 to 5, are considered separately for their contributions. The plot for each period (Figures 5.5 to 5.9) are combined with (tables 5.5 to 5.9); to explain the contributions and actual positions of the selected compounds in each period. The numbers with the hash tag (#), on each of the tables (5.5 to 5.9), in the periods, show the new relative position of that compound, when compared to the arrangement in table 5.1.

5.3.1 Fingerprint plot Period 1: (05 - 09 August 2016)

=

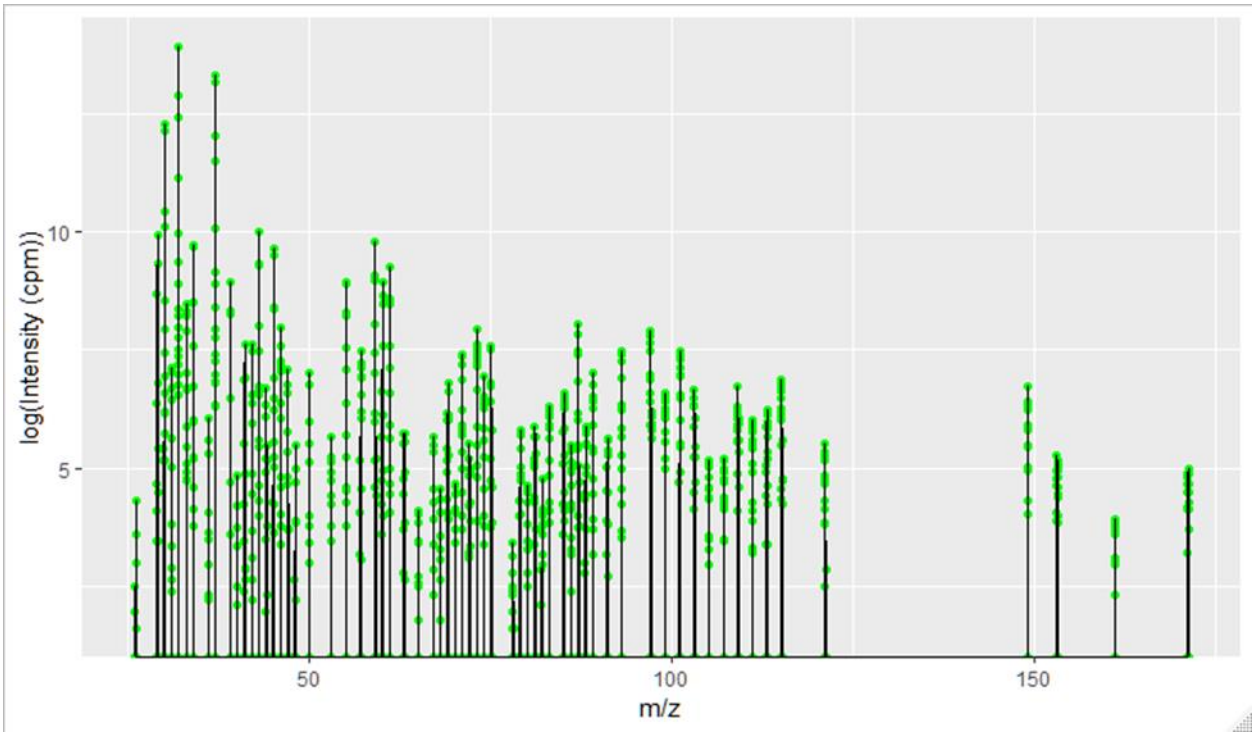

Figure 5.5: Fingerprint plot for period 1 (05 – 09 August 2016)

Table 5.5a: Fingerprint of compounds for Period 1 (05 - 09 August 2016)

The Top 15 stable and identifiable compounds (period 1), based on maximum intensity at m/z (adapted from table 5.1); identification based on m/z and proton affinity (pa); as compared to the proton affinity (pa) of H20 (see appendix A; for the table with a more comprehensive list of compounds and fragments).

No	(m/z) at maximum peak	Maximum (peak) intensity (cpm)	Possible compound / fragment	Source of fragment identification	Proton affinities of species (kJ/mol)	Source of proton affinity data	Comment
1	29.015	1P 21072	C2H5+ Ethanol (alkyl fragment)	2. **Federico et al 2015**	776	4	The measured m/z in (2) was 29.039
#2							
2	43.025	1p 22183	Ethenone (C_2H_3O+) / propene (C_3H_7+); Alkyl fragments	2	Ethanol 779 / 752	4 / 5	43.018 was given for ethenone and 43.054 for propene
#1							

								as measured m/z in (2)
3 #3	59.065	1p	18265	Acetone (2-Propanone) C_3H_7O+	(1, 2)	812	5	Measured at 59.49 in both (1) and (2)
4 #4	45.045	1p	15796	Acetaldehyde (C_2H_5O+)	1, 2	769	5	45.033 was the measured m/z in (1 and 2)
5 #5	61.045	1p	10687	Acetic acid $C_2H_5O_2+$	(1, 2)	784	5	Measured at 61.028 in both (1) and (2)
6 #6	32.995	1p	4754	Methanol (CH_5O+)	1, 2	754	5,7	Measured m/z in (2) was 33.033
7 #8	42.045	1p	2017	Acetonitrile (C_2H_4N+)	2	779	5	
8 #7	73.075	1p	2831	2-Butanone (C_4H_9O+)	(2)	827.2	7	Measured at 73.065 in (2)
9 #9	75.065	1p	1968	Methyl acetate ($C_3H_7O_2+$) / Isobutanol (2-Methyl-1-propanol) $C_4H_{11}O+$	(2)	(Acetic acid, methyl ester) 821.7	7	methyl acetate was 75.044 and isobutanol was 75.080 in (2)
10 #12	30.995	1P	1229	Formaldehyde (CH3O+)	2	713		The measured m/z used in (2) was 31.042
11 #10	57.045	1p	1790	2-Propenal (Acrolein) C_3H_5O+/C_4H_9+ 1-Butene (alkyl fragment)	(2)	Acrolein 797	4	Acrolein was 57.34 and 1-butene was 57.68 in (2)
12 #11	71.055	1p	1622	MVK; methyl-vinyl-ketone (3-Buten-2-one) C_4H_7O+ / MACR; methacrolein (methacroaldehyde) C_4H_6O+	(1, 2)	834.7 / 808.7	4, 5	MVK/MACR was 71.09 in (1) while MACR was 71.049 and a mix of alkyl fragments (C5H11+)

								was 71.086 in (2),
13 #13	47.025	1p	1208	Formic acid/ Ethanol (CH_3O_2+/ C_2H_7O+)	1, 2	742 / 776	5	Measured m/z for formic acid was 47.013 and ethanol was 47.049 in (2) and 47.048 in (1)
14 #14	74.075	1p	1021	Dimethylformamide (C_3H_8NO+)	(2)	884	6	Measured at 74.061 in (2)
15 #15	69.085	1p	912	Isoprene (2-Methyl-1,3- butadiene) C_5H_9+	(1, 2)	826.4	4, 5	Measured at 69.069 and 69.070 in (1) and (2) respectively

Species identification source:

1. Seco et al (2011a): online from www.atmos-chem-phys.net/11/13161/2011/doi:10.5194/acp-11-13161-2011

2. Federico et al (2015): Springer 2018; Online from https://www.nature.com/articles/srep12629/tables/1

3. *Hadden Analytical online; references; Hemming and Foster (1992), McLafferty and Turecek (1993), Silverstein et al (1991)*

Affinity data source:

4. Hunter and Lias (1998) / NIST Webbook (2018)

5. Ellis & Mayhew (2013)

6. Jolly (1991), *Modern Inorganic Chemistry*(2nd Edn.). New York: McGraw-Hill. ISBN 0-07-112651-1.

7. KORE technology (2018), online from https://www.kore.co.uk/paffinities.htm

Symbols

- indicates the new position of compound if rearranged in this period (see table 5.10.)

Combining figure 5.5 and table 5.5a; the new arrangement for the compounds based on their magnitude of contribution (using the # tagged numbers in table 5.5a) would give rise to the listing under period 1 in (table 5.5b); that is, ethenone / propene , ethanol (fragment), acetone , acetaldehyde, acetic acid, methanol, 2-butanone, acetonitrile, methyl acetate / Isobutanol, 2-Propenal / 1-butene, MVK / MACR, formaldehyde, formic acid/ ethanol, dimethylformamide and isoprene.

Table 5.5b: Compounds rearranged to reflect contributions in Period 1

No	Position Table 5.1	Period 1	Intensity (cpm)
1	ethanol	ethenone / propene	22183
2	ethenone / propene	ethanol (fragment)	21072
3	acetone	acetone	18265
4	acet aldehyde	acetaldehyde	15796
5	acetic acid	acetic acid	10687
6	methanol	methanol	4754
7	acetonitrile	2-butanone	2831
8	2- butanone	acetonitrile	2017
9	methyl acetate / isobutanol	methyl acetate / Isobutanol	1968
10	formaldehyde	2-Propenal/ 1-butene	1790
11	2-Propenal / 1-Butene	MVK / MACR	1622
12	MVK /MACR	formaldehyde	1229
13	Formic acid/ Ethanol	formic acid/ ethanol	1208
14	Dimethylformamide	dimethylformamide	1021
15	Isoprene	isoprene	912

In period 1, (table 5.5b); ethenone was on top of the list of contributions at an intensity of 22183 (cpm), followed by ethanol with 21072, then acetone (18265), acetaldehyde (15796), acetic acid (10687), methanol (4750), 2-butanone (2831), acetonitrile (2017), methyl acetate/ isobutanol (1968), 2-propenal/ 1-butene (1790,), MVK/ MACR (1622), formaldehyde (1229), formic acid/ ethanol (1208), dimethylformamide (1021) and isoprene (912). Compared with the initial positions in table 5.1; ethenone swapped positions with ethanol fragment in period 1; while, acetone, acetaldehyde, acetic acid, methanol, methyl acetate/ isobutanol, formic acid/ ethanol, dimethylformamide and isoprene, retained the same positions in period 1, as listed in table 5.1; (hat is, respectively, positions- 3, 4, 5, 6, 9, 13, 14 and 15). For the others, 2-butanone swapped positions with acetonitrile for 7 and 8, and formaldehyde stepped down two places to take position 12, but MVK/MACR, moved one step up to

settle at position 11, above formaldehyde. Isoprene at 912 remained at the bottom of both listings, closely followed by dimethylformamide at 1021 (cpm)

5.3.2 Fingerprint plot Period 2: (11 - 17 August 2016)

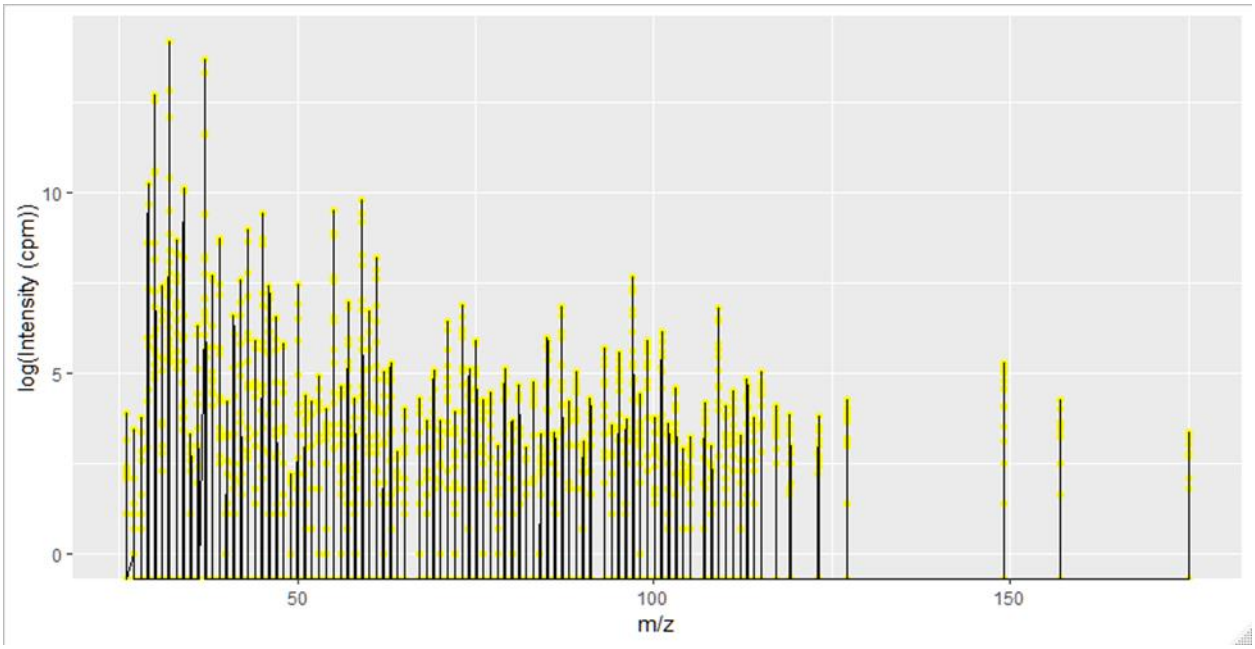

Figure 5.6: Fingerprint plot for period 2 (11 - 17 August 2016)

Table 5.6a: Fingerprint of compounds for Period 2 (11 - 17 August 2016)

The Top 15 stable and identifiable compounds (period 2), based on maximum intensity at m/z (adapted from table 5.1); identification based on m/z and proton affinity (pa); as compared to proton affinity (pa) of H20 (see appendix A; for the table with a more comprehensive list of compounds and fragments).

No	(m/z) at maximum peak	Maximum (peak) intensity (cpm)	Possible compound / fragment	Source of fragment identification	Proton affinities of species (kJ/mol)	Source of proton affinity data	Comment

1 #1	29.015	2p	28461	C2H5+ Ethanol (alkyl fragment)	2. Federico et al 2015	776	4	The measured m/z in (2) was 29.039
2 #4	43.025	2p	8062	Ethenone (C_2H_3O+) / propene (C_3H_7+); Alkyl fragments	2	Ethanol 779 / 752	4 / 5	43.018 was given for ethenone and 43.054 for propene as measured m/z in (2)
3 #2	59.065	2p	17886	Acetone (2-Propanone) C_3H_7O+	(1, 2)	812	5	Measured at 59.49 in both (1) and (2)
4 #3	45.045	2p	12232	Acetaldehyde (C_2H_5O+)	1, 2	769	5	45.033 was the measured m/z in (1 and 2)
5 #6	61.045	2p	3695	Acetic acid $C_2H_5O_2$+	(1, 2)	784	5	Measured at 61.028 in both (1) and (2)
6 #5	32.995	2p	5920	Methanol (CH_5O+)	1, 2	754	5,7	Measured m/z in (2) was 33.033
7 #7	42.045	2p	1925	Acetonitrile (C_2H_4N+)	2	779	5	
8 #10	73.075	2p	985	2-Butanone (C_4H_9O+)	(2)	827.2	7	Measured at 73.065 in (2)
9 #13	75.065	2p	365	Methyl acetate ($C_3H_7O_2$+) / Isobutanol (2-Methyl-1-propanol) $C_4H_{11}O$+	(2)	(Acetic acid, methyl ester) 821.7	7	methyl acetate was 75.044 and isobutanol was 75.080 in (2)
10 #8	30.995	2p	1646	Formaldehyde (CH3O+)	2	713		The measured m/z used in (2) was 31.042
11 #9	57.045	2p	1079	2-Propenal (Acrolein) C_3H_5O+/C_4H_9+ 1-Butene (alkyl fragment)	(2)	Acrolein 797	4	Acrolein was 57.34 and 1-butene was 57.68 in (2)

12 #12	71.055	2p	617	MVK; methyl-vinyl-ketone (3-Buten-2-one) C_4H_7O+ / MACR; methacrolein (methacroaldehyde) C_4H_6O+	(1, 2)	834.7 / 808.7	4, 5	MVK/MACR was 71.09 in (1) while MACR was 71.049 and a mix of alkyl fragments (C5H11+) was 71.086 in (2),
13 #11	47.025	2p	711	Formic acid/ Ethanol (CH_3O_2+/ C_2H_7O+)	1, 2	742 / 776	5	Measured m/z for formic acid was 47.013 and ethanol was 47.049 in (2) and 47.048 in (1)
14 #14	74.075	2p	170	Dimethylformamide (C_3H_8NO+)	(2)	884	6	Measured at 74.061 in (2)
15 #15	69.085	2p	162	Isoprene (2-Methyl-1,3- butadiene) C_5H_9+	(1, 2)	826.4	4, 5	Measured at 69.069 and 69.070 in (1) and (2) respectively

Species identification source:

1. Seco et al (2011a): online from www.atmos-chem-phys.net/11/13161/2011/doi:10.5194/acp-11-13161-2011

2. Federico et al (2015): Springer 2018; Online from https://www.nature.com/articles/srep12629/tables/1

3. *Hadden Analytical online; references; Hemming and Foster (1992), McLafferty and Turecek (1993), Silverstein et al (1991)*

Affinity data source:

4. Hunter and Lias (1998) / NIST Webbook (2018)

5. Ellis & Mayhew (2013)

6. Jolly (1991), *Modern Inorganic Chemistry*(2nd Edn.). New York: McGraw-Hill. ISBN 0-07-112651-1.

7. KORE technology (2018), online from https://www.kore.co.uk/paffinities.htm

Combining the information from Figure 5.6 and Table 5.6a; a rearrangement of the compounds (as listed in Table 5.1) can take place, based on their contributions in Period 2; using the hash tagged numbers in Table 5.6a to indicate the new ranking; (see Table 5.6b for the new ranking based on contributions in period 2). The new arrangement has the following order (Table 5.6a); ethanol (fragment), acetone, acetaldehyde, ethenone / propene, methanol, acetic acid, acetonitrile, formaldehyde, Propenal/ 1-

butene, 2-butanone, formic acid/ ethanol, MVK / MACR, methyl acetate/ Isobutanol, dimethylformamide, isoprene

Table 5.6b: Compounds rearranged to reflect contributions in Period 2

No	Position on Table 5.1	Period 2 (new positions)	Intensity (cpm)
1	ethanol	ethanol (fragment)	28461
2	ethenone / propene	acetone	17886
3	acetone	acetaldehyde	12232
4	acetaldehyde	ethenone/ propene	8062
5	acetic acid	methanol	5920
6	methanol	acetic acid	3695
7	acetonitrile	acetonitrile	1925
8	2- butanone	formaldehyde	1646
9	methyl acetate / isobutanol	2-Propenal/ 1-butene	1079
10	formaldehyde	2-butanone	985
11	2-Propenal / 1-Butene	formic acid/ ethanol	711
12	MVK/ MACR	MVK / MACR	617
13	Formic acid/ Ethanol	methylacetate/ Isobutanol	365
14	Dimethylformamide	dimethylformamide	170
15	Isoprene	isoprene	162

In Period 2; almost all positions changed, when compared to Table 5.1; except for acetonitrile (7), MVK/ MACR (12), dimethyl formamide (14) and isoprene (15), that stayed the same. Ethanol is still on top here, with 28461 (cpm), followed by acetone and acetaldehyde each moving one step up to (2), and (3) at intensities of (17886) and (12232 cpm) respectively. Ethenone/ propene dropped two steps to (4); at (8062 cpm), methanol rose a step up with (5920 cpm) to (5); swapping places with acetic acid at (3695 cpm), which became (6). Formaldehyde was (8); was (1646 cpm), behind acetonitrile (1925 cpm) having

moved up two steps, followed by 2-Propenal/ 1-butene (1079 cpm), which also moved up by two steps. 2-butanone (10) and formic acid/ ethanol (11) sit above MVK/ MACR(12); at intensities of (985) and (711), having each moved two steps; down for the former and up for the latter, with MVK/ MACR at (617 cpm). Methyl acetate/ Isobutanol came down from position (9) to (13; with (365 cpm). Dimethylformamide and isoprene remained still at the bottom of the table with 170 and 167 respectively. The various contributions based on the signal intensities in (cpm) are all listed beside each compound in Table 5.6b.

5.2.3 Fingerprint plot Period 3: (17 - 23 August 2016)

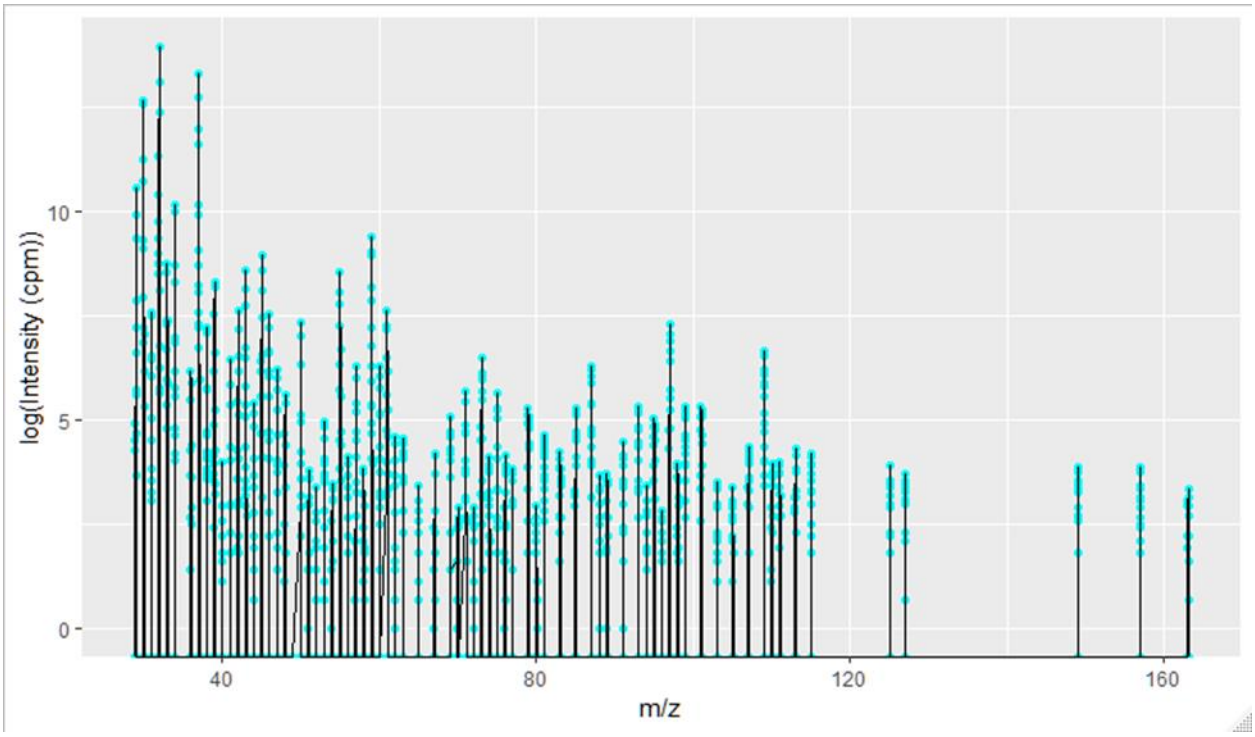

Figure 5.7: Fingerprint plot for period 3 (17 - 23 August 2016)

Table 5.7a: Fingerprint of compounds for Period 3 (17 - 23 August 2016)

The Top 15 stable and identifiable compounds (period 3), based on maximum intensity at m/z (adapted from table 5.1); identification based on m/z and proton affinity (pa); as compared to proton affinity (pa) of H20 (see appendix A; for the table with the more comprehensive list of compounds and fragments).

No	(m/z) at maximum peak	Maximum (peak) intensity (cpm)	Possible compound / fragment	Source of fragment identification	Proton affinities of species (kJ/mol)	Source of proton affinity data	Comment
1 #1	29.015	3p 39198	C2H5+ Ethanol (alkyl fragment)	2. **Federico et al 2015**	776	4	The measured m/z in (2) was 29.039
2 #5	43.025	3p 5317	Ethenone (C_2H_3O+) / propene (C_3H_7+); Alkyl fragments	2	Ethanol 779 / 752	4 / 5	43.018 was given for ethenone and 43.054 for propene as measured m/z in (2)
3 #2	59.065	3p 11986	Acetone (2-Propanone) C_3H_7O+	(1, 2)	812	5	Measured at 59.49 in both (1) and (2)
4 #3	45.045	3p 7793	Acetaldehyde (C_2H_5O+)	1, 2	769	5	45.033 was the measured m/z in (1 and 2)
5 #7	61.045	3p 2036	Acetic acid $C_2H_5O_2$+	(1, 2)	784	5	Measured at 61.028 in both (1) and (2)
6 #4	32.995	3p 6431	Methanol (CH_5O+)	1, 2	754	5,7	Measured m/z in (2) was 33.033
7 #6	42.045	3p 2047	Acetonitrile (C_2H_4N+)	2	779	5	
8 #9	73.075	3p 664	2-Butanone (C_4H_9O+)	(2)	827.2	7	Measured at 73.065 in (2)
9 #13	75.065	3p 279	Methyl acetate ($C_3H_7O_2$+) / Isobutanol (2-Methyl-1-propanol) $C_4H_{11}O$+	(2)	(Acetic acid, methyl ester) 821.7	7	methyl acetate was 75.044 and isobutanol was 75.080 in (2)

10 #8	30.995	3p	1964	Formaldehyde (CH3O+)	2	713		The measured m/z used in (2) was 31.042
11 #10	57.045	3p	539	2-Propenal (Acrolein) C_3H_5O+/C_4H_9+ 1-Butene (alkyl fragment)	(2)	Acrolein 797	4	Acrolein was 57.34 and 1-butene was 57.68 in (2)
12 #12	71.055	3p	294	MVK; methyl-vinyl-ketone (3-Buten-2-one) C_4H_7O+ / MACR; methacrolein (methacroaldehyde) C_4H_6O+	(1, 2)	834.7 / 808.7	4, 5	MVK/MACR was 71.09 in (1) while MACR was 71.049 and a mix of alkyl fragments (C5H11+) was 71.086 in (2),
13 #11	47.025	3p	492	Formic acid/ Ethanol (CH_3O_2+/ C_2H_7O+)	1, 2	742 / 776	5	Measured m/z for formic acid was 47.013 and ethanol was 47.049 in (2) and 47.048 in (1)
14 #15	74.075	3p	50	Dimethylformamide (C_3H_8NO+)	(2)	884	6	Measured at 74.061 in (2)
15 #14	69.085	3p	158	Isoprene (2-Methyl-1,3- butadiene) C_5H_9+	(1, 2)	826.4	4, 5	Measured at 69.069 and 69.070 in (1) and (2) respectively

Species identification source:

1. Seco et al (2011a): online from www.atmos-chem-phys.net/11/13161/2011/doi:10.5194/acp-11-13161-2011

2. Federico et al (2015): Springer 2018; Online from https://www.nature.com/articles/srep12629/tables/1

3. *Hadden Analytical online; references; Hemming and Foster (1992), McLafferty and Turecek (1993), Silverstein et al (1991)*

Affinity data source:

4. Hunter and Lias (1998) / NIST Webbook (2018)

5. Ellis & Mayhew (2013)

6. Jolly (1991), *Modern Inorganic Chemistry*(2nd Edn.). New York: McGraw-Hill. ISBN 0-07-112651-1.

7. KORE technology (2018), online from https://www.kore.co.uk/paffinities.htm

Combining useful information from Figure 5.7 and table 5.7a, a fresh table, (5.7b), was formed showing compounds rearranged based on their intensity contribution in period 3, as compared to table 5.1. Hash tagged numbers in table 5.7a, have been used to initially identify the rearranged order of the compounds. Using table 5.7; the new order and magnitudes are; first ethanol (fragment), (39198 cpm), followed by acetone (11986), acetaldehyde (7793), methanol (6431), ethenone/ propene (5313), acetonitrile (2047), acetic acid(2036), formaldehyde (1964), 2-butanone (664), 2-Propenal/1-butene (539), formic acid/ ethanol (492), MVK / MACR (294), methyl acetate/ Isobutanol (279), isoprene (158), dimethylformamide (50 cpm). Table 5.7b; shows that all the initial positions of the compounds in table 5.1 changed, except for ethanol (fragment) in position (1) and MVK/ MACR in (12), that retained the same positions.

Table 5.7b: Compounds rearranged to reflect contributions in Period 3

No	Position Table 5.1	Period 3	Intensity (cpm)
1	ethanol	ethanol (fragment)	39198
2	ethenone / propene	acetone	11986
3	acetone	acetaldehyde	7793
4	acetaldehyde	methanol	6431
5	acetic acid	ethenone / propene	5313
6	methanol	acetonitrile,	2047
7	acetonitrile	acetic acid	2036
8	2- butanone	formaldehyde	1964
9	methyl acetate / isobutanol	2-butanone	664
10	formaldehyde	2-Propenal/1-butene	539
11	2-Propenal / 1-Butene	formic acid/ ethanol	492
12	MVK /MACR	MVK / MACR	294
13	Formic acid/ Ethanol	methylacetate /Isobutanol	279
14	Dimethylformamide	isoprene	158
15	Isoprene	dimethylformamide	50

5.3.4 Fingerprint plot Period 4: (23 - 25 August 2016)

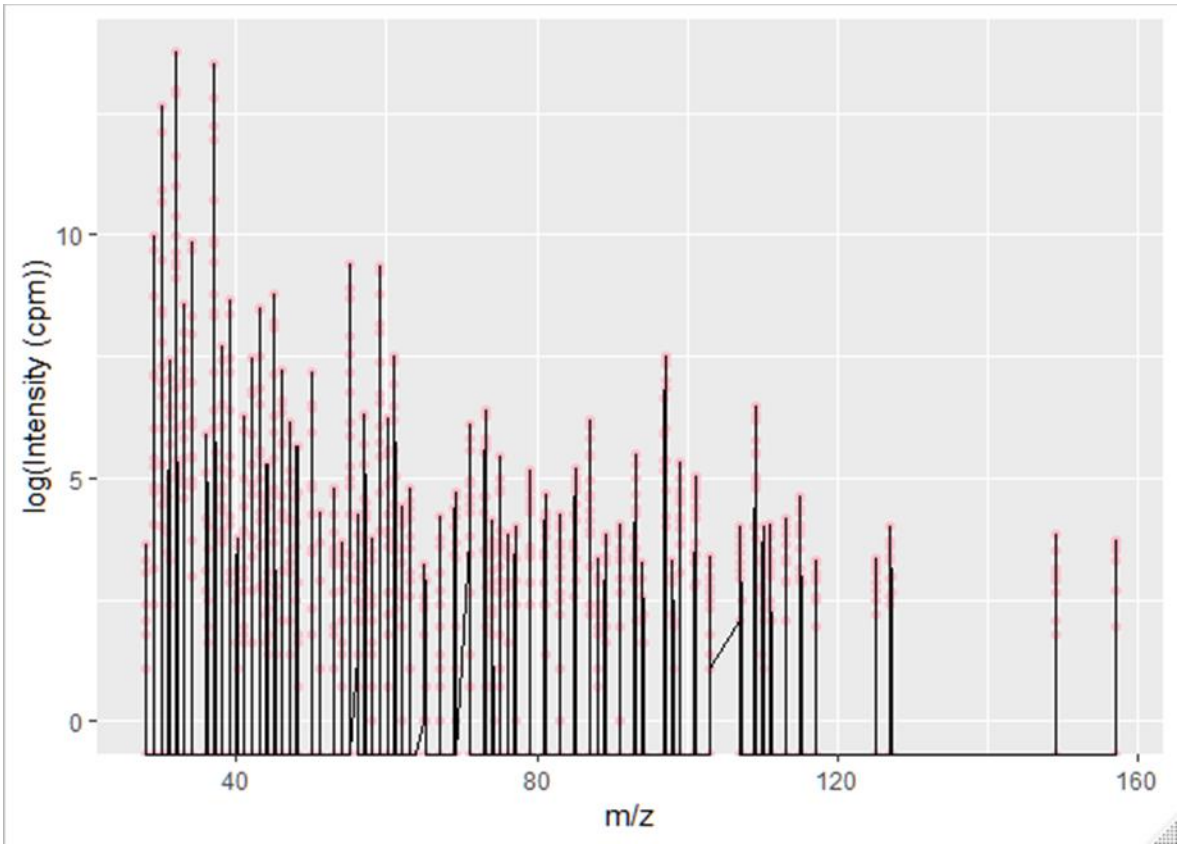

Figure 5.8: Fingerprint plot for period 4 (23 - 25 August 2016)

Table 5.8a: Fingerprint of compounds for Period 4 (23 - 25 August 2016)

The Top 15 stable and identifiable compounds (period 4), based on maximum intensity at m/z (adapted from table 5.1); identification based on m/z and proton affinity (pa); as compared to proton affinity (pa) of H20 (see appendix A; for the table with a more comprehensive list of compounds and fragments).

No	(m/z) at maximum peak	Maximum (peak) intensity (cpm)	Possible compound / fragment	Source of fragment identification	Proton affinities of species (kJ/mol)	Source of proton affinity data	Comment

1 #1	29.015	4p	21760	C2H5+ Ethanol (alkyl fragment)	2. **Federico et al 2015**	776	4	The measured m/z in (2) was 29.039
2 #5	43.025	4p	4862	Ethenone (C_2H_3O+) / propene (C_3H_7+); Alkyl fragments	2	Ethanol 779 / 752	4 / 5	43.018 was given for ethenone and 43.054 for propene as measured m/z in (2)
3 #2	59.065	4p	11535	Acetone (2-Propanone) C_3H_7O+	(1, 2)	812	5	Measured at 59.49 in both (1) and (2)
4 #3	45.045	4p	6462	Acetaldehyde (C_2H_5O+)	1, 2	769	5	45.033 was the measured m/z in (1 and 2)
5 #6	61.045	4p	1840	Acetic acid $C_2H_5O_2$+	(1, 2)	784	5	Measured at 61.028 in both (1) and (2)
6 #4	32.995	4p	5362	Methanol (CH_5O+)	1, 2	754	5,7	Measured m/z in (2) was 33.033
7 #7	42.045	4p	1766	Acetonitrile (C_2H_4N+)	2	779	5	
8 #9	73.075	4p	587	2-Butanone (C_4H_9O+)	(2)	827.2	7	Measured at 73.065 in (2)
9 #13	75.065	4p	233	Methyl acetate ($C_3H_7O_2$+) / Isobutanol (2-Methyl-1-propanol) $C_4H_{11}O$+	(2)	(Acetic acid, methyl ester) 821.7	7	methyl acetate was 75.044 and isobutanol was 75.080 in (2)
10 #8	30.995	4p	1664	Formaldehyde (CH3O+)	2	713		The measured m/z used in (2) was 31.042
11 #10	57.045	4p	551	2-Propenal (Acrolein) C_3H_5O+/C_4H_9+ 1-Butene (alkyl fragment)	(2)	Acrolein 797	4	Acrolein was 57.34 and 1-butene was 57.68 in (2)

12 #12	71.055	4p	457	MVK; methyl-vinyl-ketone (3-Buten-2-one) C_4H_7O+ / MACR; methacrolein (methacroaldehyde) C_4H_6O+	(1, 2)	834.7 / 808.7	4, 5	MVK/MACR was 71.09 in (1) while MACR was 71.049 and a mix of alkyl fragments (C5H11+) was 71.086 in (2),
13 #11	47.025	4p	464	Formic acid/ Ethanol (CH_3O_2+/ C_2H_7O+)	1, 2	742 / 776	5	Measured m/z for formic acid was 47.013 and ethanol was 47.049 in (2) and 47.048 in (1)
14 #15	74.075	4p	61	Dimethylformamide (C_3H_8NO+)	(2)	884	6	Measured at 74.061 in (2)
15 #14	69.085	4p	112	Isoprene (2-Methyl-1,3- butadiene) C_5H_9+	(1, 2)	826.4	4, 5	Measured at 69.069 and 69.070 in (1) and (2) respectively

Species identification source:

1. Seco et al (2011a): online from www.atmos-chem-phys.net/11/13161/2011/doi:10.5194/acp-11-13161-2011

2. Federico et al (2015): Springer 2018; Online from https://www.nature.com/articles/srep12629/tables/1

3. *Hadden Analytical online; references; Hemming and Foster (1992), McLafferty and Turecek (1993), Silverstein et al (1991)*

Affinity data source*:*

4. Hunter and Lias (1998) / NIST Webbook (2018)

5. Ellis & Mayhew (2013)

6. Jolly (1991), *Modern Inorganic Chemistry*(2nd Edn.). New York: McGraw-Hill. ISBN 0-07-112651-1.

7. KORE technology (2018), online from https://www.kore.co.uk/paffinities.htm

Information from Figure 5.8 and table 5.8a; come together to produce the rearrangement of the compounds based on their contributions in Period 4. The hash tagged numbers in Table 5.8a, were used to indicate the new order of arrangements reflected in table 5.8b, under period 4; as compared to the order on table 5.1. The magnitude of the contribution from each compound in the period, in (cpm) is also listed under the intensity column. The new order of arrangements based on intensity of the signal

for period 4; still has ethanol (fragment), at the top of the list with (21760 cpm), others come behind with intensities as follows; acetone (11535), acetaldehyde (5452), methanol (5362), ethenone/ propene (4862), acetic acid (1840), acetonitrile (1766), formaldehyde (1664), 2-butanone (587), 2-Propenal/ 1-butene (551), formic acid/ ethanol (464), MVK / MACR (457), methyl acetate/ Isobutanol (233), isoprene (112) and last of all dimethylformamide (61 cpm). All the other compounds changed positions except

Table 5.8b: Compounds rearranged to reflect contributions in Period 4

No	Position Table 5.1	Period 4	Intensity (cpm)
1	ethanol	ethanol (fragment)	21760
2	ethenone / propene	acetone	11535
3	acetone	acetaldehyde	6462
4	acetaldehyde	methanol	5362
5	acetic acid	ethenone / propene	4862
6	methanol	acetic acid	1840
7	acetonitrile	acetonitrile	1766
8	2- butanone	formaldehyde	1664
9	methyl acetate/ isobutanol	2-butanone	587
10	formaldehyde	2-Propenal)/ 1- butene	551
11	2-Propenal/ 1-Butene	formic acid/ ethanol	464
12	MVK /MACR	MVK / MACR	457
13	Formic acid/ Ethanol	methylacetate /Isobutanol	233
14	Dimethylformamide	isoprene	112
15	Isoprene	dimethylformamide	61

ethanol (fragment) at position (1), acetonitrile at (7) and MVK/ MACR at (12), stayed the same as table 5.1; dimethylformamide became last having been displaced by isoprene, moving one position up the table.

5.3.5 Fingerprint plot Period 5: (25 August - 07 September 2016)

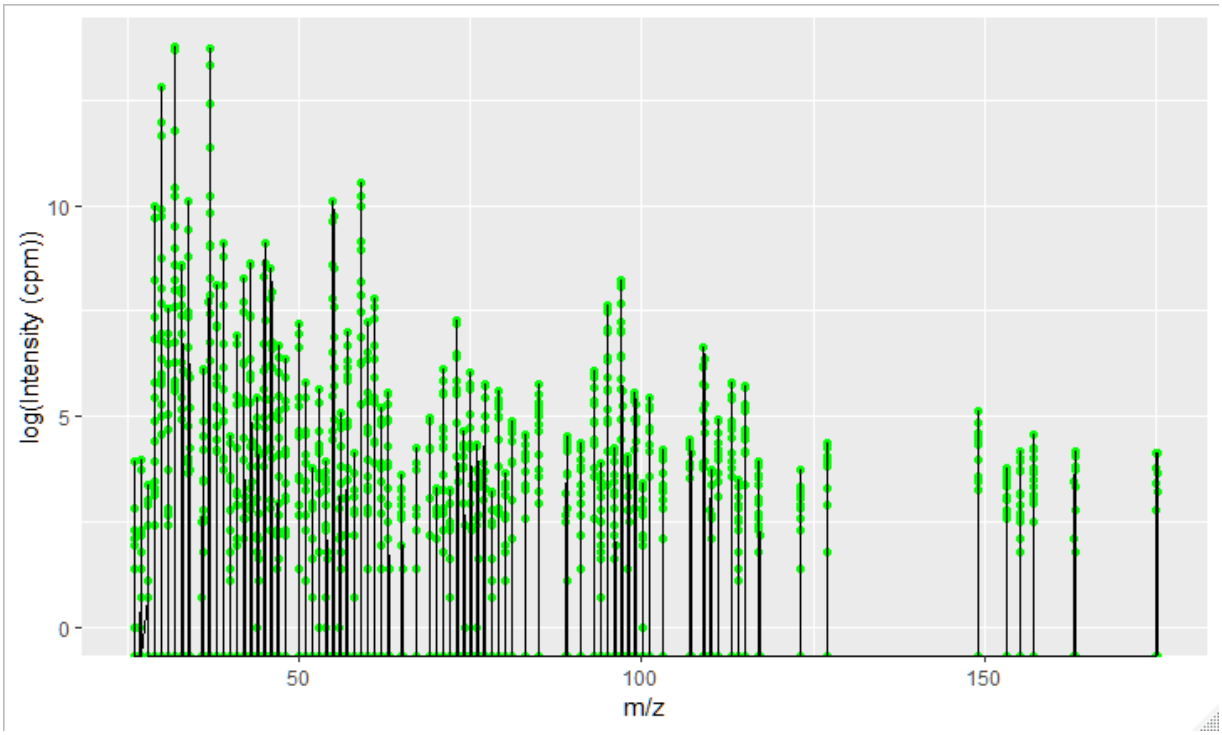

Figure 5.9: Fingerprint plot for period 5 (25 August - 07 September 2016)

Table 5.9a: Fingerprint of compounds for Period 5 (25 August - 07 September 2016)

The Top 15 stable and identifiable compounds (period 5), based on maximum intensity at m/z (adapted from table 5.1); identification based on m/z and proton affinity (pa); as compared to proton affinity (pa) of H20 (see appendix A; for the table with a more comprehensive list of compounds and fragments).

No	(m/z) at maximum peak	Maximum (peak) intensity (cpm)	Possible compound / fragment	Source of fragment identification	Proton affinities of species (kJ/mol)	Source of proton affinity data	Comment
1 #2	29.015	5P 22076	C2H5+ Ethanol (alkyl fragment)	2. **Federico et al 2015**	776	4	The measured m/z in (2) was 29.039
2 #4	43.025	5p 5494	Ethenone (C_2H_3O+) / propene (C_3H_7+); Alkyl fragments	2	Ethanol 779 / 752	4 / 5	43.018 was given for ethenone and 43.054

								for propene as measured m/z in (2)
3 #1	59.065	5p	37314	Acetone (2-Propanone) C_3H_7O+	(1, 2)	812	5	Measured at 59.49 in both (1) and (2)
4 #3	45.045	5p	8990	Acetaldehyde (C_2H_5O+)	1, 2	769	5	45.033 was the measured m/z in (1 and 2)
5 #7	61.045	5p	2453	Acetic acid $C_2H_5O_2+$	(1, 2)	784	5	Measured at 61.028 in both (1) and (2)
6 #5	32.995	5p	5368	Methanol (CH_5O+)	1, 2	754	5,7	Measured m/z in (2) was 33.033
7 #6	42.045	5p	3943	Acetonitrile (C_2H_4N+)	2	779	5	
8 #9	73.075	5p	1450	2-Butanone (C_4H_9O+)	(2)	827.2	7	Measured at 73.065 in (2)
9 #13	75.065	5p	428	Methyl acetate ($C_3H_7O_2+$) / Isobutanol (2-Methyl-1-propanol) $C_4H_{11}O+$	(2)	(Acetic acid, methyl ester) 821.7	7	methyl acetate was 75.044 and isobutanol was 75.080 in (2)
10 #8	30.995	5P	1948	Formaldehyde (CH3O+)	2	713		The measured m/z used in (2) was 31.042
11 #10	57.045	5p	1103	2-Propenal (Acrolein) C_3H_5O+/C_4H_9+ 1-Butene (alkyl fragment)	(2)	Acrolein 797	4	Acrolein was 57.34 and 1-butene was 57.68 in (2)
12 #12	71.055	5p	452	MVK; methyl-vinyl-ketone (3-Buten-2-one) C_4H_7O+ / MACR; methacrolein (methacroaldehyde) C_4H_6O+	(1, 2)	834.7 / 808.7	4, 5	MVK/MACR was 71.09 in (1) while MACR was 71.049 and a mix of alkyl fragments (C5H11+) was 71.086 in (2),

13 #11	47.025	5p	788	Formic acid/ Ethanol (CH_3O_2+/ C_2H_7O+)	1, 2	742 / 776	5	Measured m/z for formic acid was 47.013 and ethanol was 47.049 in (2) and 47.048 in (1)
14 #15	74.075	5p	104	Dimethylformamide (C_3H_8NO+)	(2)	884	6	Measured at 74.061 in (2)
15 #14	69.085	5p	145	Isoprene (2-Methyl-1,3- butadiene) C_5H_9+	(1, 2)	826.4	4, 5	Measured at 69.069 and 69.070 in (1) and (2) respectively

Species identification source:

1. Seco et al (2011a): online from www.atmos-chem-phys.net/11/13161/2011/doi:10.5194/acp-11-13161-2011

2. Federico et al (2015): Springer 2018; Online from https://www.nature.com/articles/srep12629/tables/1

3. *Hadden Analytical online; references; Hemming and Foster (1992), McLafferty and Turecek (1993), Silverstein et al (1991)*

Affinity data source:

4. Hunter and Lias (1998) / NIST Webbook (2018)

5. Ellis & Mayhew (2013)

6. Jolly (1991), *Modern Inorganic Chemistry*(2nd Edn.). New York: McGraw-Hill. ISBN 0-07-112651-1.

7. KORE technology (2018), online from https://www.kore.co.uk/paffinities.htm

Compounds in Period 5 have also been rearranged to reflect their contributions. Information from Figure 5.9 and Table 5.9a; together resulted in the rearrangement of compounds in order of intensity in period 5. The rearrangement is as shown in Table 5.9b, based on the hash tagged numbers in table 5.9a; with their positions in table 5.1 and intensity contributions in period 5. This time, acetone with (37314 cpm) comes first, followed by ethanol (fragment) at (22076), then, acetaldehyde (8990), ethenone / propene (5494), methanol (5368), acetonitrile (3943), acetic acid (2451), formaldehyde (1948), 2-butanone (1450), 2-Propenal/ 1-butene (1103), formic acid/ ethanol (788), MVK / MACR (452), methyl acetate / Isobutanol (428), isoprene (145) and finally dimethylformamide (104 cpm). Only MVK/ MACR retained

Table 5.9b: Compounds rearranged to reflect contributions in Period 5

No	Position Table 5.1	Period 5 (new positions)	Intensity (cpm)
1	ethanol	acetone	37314
2	ethenone / propene	ethanol (fragment),	22076
3	acetone	acetaldehyde	8990
4	acetaldehyde	ethenone / propene	5494
5	acetic acid	methanol	5368
6	methanol	acetonitrile	3943
7	acetonitrile	acetic acid	2453
8	2- butanone	formaldehyde	1948
9	methyl acetate / isobutanol	2-butanone	1450
10	formaldehyde	2-Propenal/ 1-butene	1103
11	2-Propenal / 1-Butene	formic acid/ ethanol	788
12	MVK /MACR	MVK / MACR	452
13	Formic acid/ Ethanol	methyl acetate/ Isobutanol	428
14	Dimethylformamide	isoprene	145
15	Isoprene	dimethylformamide	104

Its position at number (12), on both tables (5.1) and (5.9b); all others changed their positions, with acetone on top and dimethylformamide at the bottom of period 5, isoprene stayed one step off the bottom above it.

5.4 Comparing the fingerprint plots from the five periods of the 2016 measurement campaigns

Figure 5.10 combines with Tables 5.10 and 5.11; to show how the 15 selected VOCs compare; using the magnitude of their intensities across the 5 periods (table 5.11) and their relative positions to their listings in table 5.1, and with each other (table 5.10). The total contribution of each compound over the

entire 5 periods, covered by this study is also shown in table 5.11. The intensity of (39198 cpm) measured for ethanol fragment in period 3, was the basis for putting it on top of the entire listing in table 5.1; it truly has the single highest intensity when compared to all other compounds in all the periods. It also dominated the top position in periods 2 and 4; with (28461) and (21760 cpm) respectively. Although ethanol period 5 (22076); was third largest for the ethanol (fraction) group, it was behind acetone (37314 cpm); in period 5, and ethenone/ propene (22183); in period 1. It also took the place of ethanol (fragment); (21072 cpm) as number 1. So, apart from periods 1 and 5 with ethenone/ propene and acetone respectively at the top ethanol fraction was highest (that is in periods 1 to 3). Ethanol (fraction), was however only moved to the second position in periods 1 and 5; with acetone being the 2nd highest in periods 2, 3 and 4 respectively with (17886), (11986) and (11535 cpm), yet in 3rd position in period 1 with (18265 cpm); but acetaldehyde dominates the 3rd position across periods 2 to 5; with (12232, 7793, 6462 and 8990 cpm), yet ends up in the 4t position in period 1 with a higher intensity if (15796 cpm). Ethenone/ propene (periods 2 and 5) and methanol (periods 2 and 3) then takes over the rest of the 4th positions; respectively with intensities of (8062 and 5494) and (6431 and 5362 cpm).

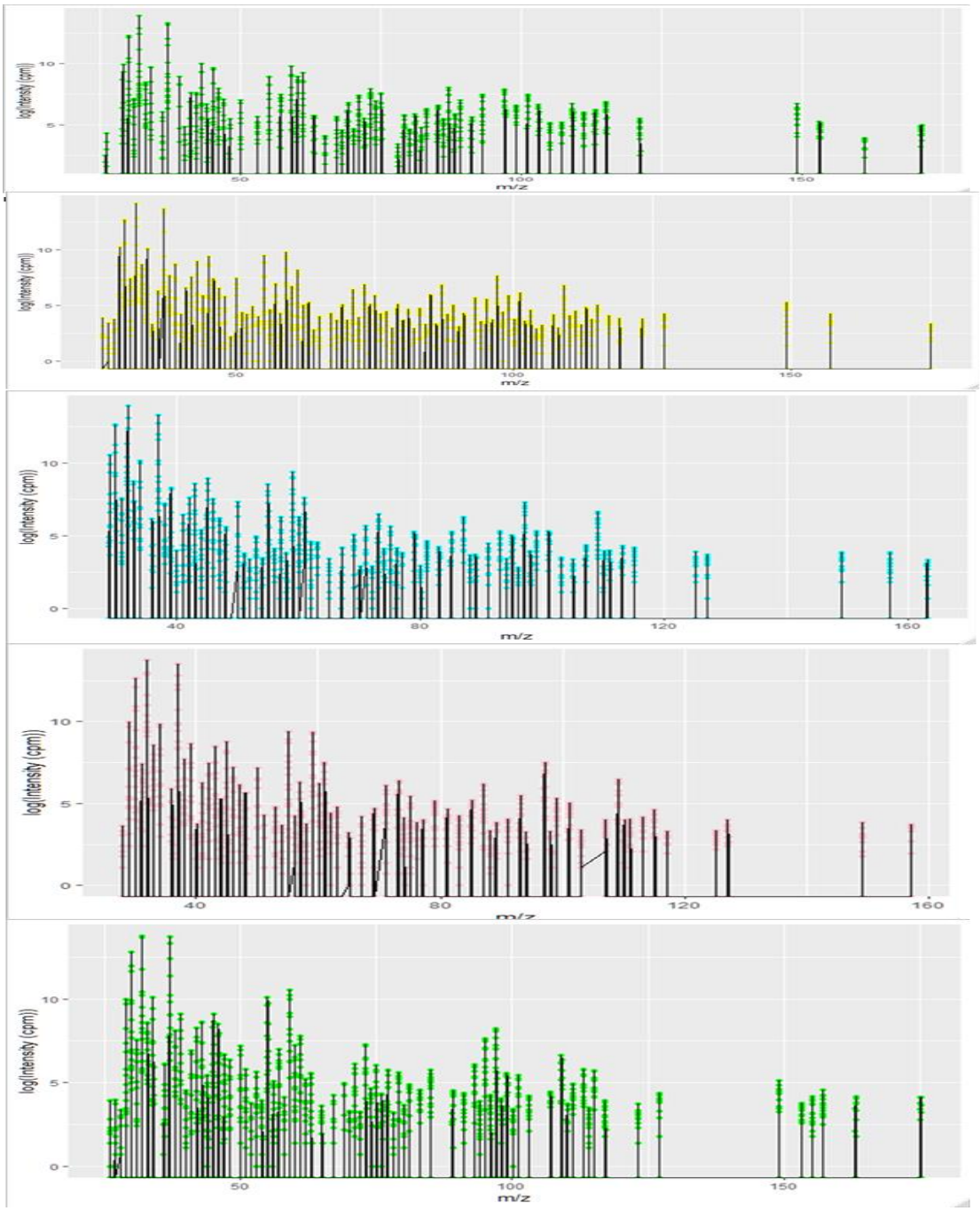

Figure 5.10: Comparing Periods 1 to 5

Table 5.10: Comparing the relative positions of compounds in the five periods with table 5.1 and with each other.

No	Position Table 5.1	Period 1	Period 2	Period 3	Period 4	Period 5
1	ethanol	ethenone / propene	ethanol (fragment)	ethanol (fragment)	ethanol (fragment)	acetone
2	ethenone / propene	ethanol (fragment)	acetone	acetone	acetone	ethanol (fragment),
3	acetone	acetone	acetaldehyde	acetaldehyde	acetaldehyde	acetaldehyde
4	acetaldehyde	acetaldehyde	ethenone / propene	methanol	methanol	ethenone / propene
5	acetic acid	acetic acid	methanol	ethenone / propene	ethenone / propene	methanol
6	methanol	methanol	acetic acid	acetonitrile,	acetic acid	acetonitrile
7	acetonitrile	2-butanone	acetonitrile	acetic acid	acetonitrile	acetic acid
8	2- butanone	acetonitrile	formaldehyde	formaldehyde,	formaldehyde	formaldehyde
9	methyl acetate / isobutanol	methyl acetate / Isobutanol	Propenal/ 1-butene	2-butanone	2-butanone	2-butanone
10	formaldehyde	2-Propenal/ 1-butene	2-butanone	2-Propenal/1-butene	2-Propenal)/ 1-butene	2-Propenal/ 1-butene
11	2-Propenal / 1-Butene	MVK / MACR	formic acid/ ethanol	formic acid/ ethanol	formic acid/ ethanol	formic acid/ ethanol
12	MVK /MACR	formaldehyde	MVK / MACR	MVK / MACR	MVK / MACR	MVK / MACR
13	Formic acid/ Ethanol	formic acid/ ethanol	methylacetate /Isobutanol	methylacetate /Isobutanol	methylacetate /Isobutanol	methylacetate /Isobutanol
14	Dimethylformamide	dimethylformamide	dimethylformamide	isoprene	isoprene	isoprene
15	Isoprene	isoprene	isoprene	dimethylformamide	dimethylformamide	dimethylform amide

Table 5.11: Comparing the intensity of each compound across the 5 periods; using the listing in table 5.1

No	Compound	Period 1	Period 2	Period 3	Period 4	Period 5	Total
1	**ethanol (alkyl fragment)**	21072	28461	**39198**	21760	22076	132567
2	**Ethenone / propene**	**22183**	8062	5317	4862	5494	45918
3	**Acetone**	18265	17886	11986	11535	**37314**	96986
4	**Acetaldehyde**	**15796**	12232	7793	6462	8990	51273
5	**Acetic acid**	**10687**	3695	2036	1840	2453	20713
6	**Methanol**	4754	5920	**6431**	5362	5368	27835
7	**Acetonitrile**	2017	1925	2047	1766	**3943**	11698
8	**2-Butanone**	**2831**	985	664	587	1450	6517

9	**Methyl acetate/ Isobutanol**	**1968**	365	279	233	428	3273
10	**Formaldehyde**	1229	1646	**1964**	1664	1948	8451
11	**2-Propenal/1-Butene**	**1790**	1079	539	551	1103	5062
12	**MVK /MACR**	**1622**	617	294	457	452	3442
13	**Formic acid/ ethanol**	**1208**	711	492	464	788	3663
14	**Dimethylformamide**	**1021**	170	50	61	104	1406
15	**Isoprene**	**912**	162	158	112	145	1489

Generally, Period 1 showed the highest intensities, for most of the compounds, and had the compounds in table 5.1 arranged according to that order except ethanol (fragment) and methanol from Period (3), and acetone and acetonitrile from (5). Isoprene was at the bottom twice in Periods 1 and 2, and one step away from the bottom in the last 3 periods when it came up, above dimethylformamide. MVK/MACR was very consistent at position (12), in all the periods except in period 1 where it went up to (11) to give way to formaldehyde. The total contribution of each compound over the five periods (table 5.11); show ethanol with the highest intensity at (132567 cpm) and the others in their order of magnitude are; acetone (96986), acetaldehyde (51273), ethenone/propene (45918), methanol (27835), acetic acid (20713), acetonitrile (11698), formaldehyde (8451), 2-butanone (6517), 2-propenal/ 1-butene (5062), formic acid/ ethanol (3663), MVK/MACR (3442), methyl acetate/ isobutanol (3273), isoprene (1489) and dimethylformamide (1406 cpm). Along each row in Table 5.11 can be seen the contribution across the periods; for example, ethanol (fragment) was highest in period 3. While isoprene and MVK/MACR were highest in period 1. This pattern can be looked up for each compound across the columns going from left to right along the rows to see the highest period of contribution for each compound (Table 5.11).

5.5 Summary and conclusion

The “fingerprint plot” initially set out in (Figure 5.1); using a plot from the 2015, sample data, gives a quick overview of the complexity of an environmental sample and the relative intensities of different m/z signals detected by the PTR. The need for additional methods for further verification is determined after this first plot is assessed in order to confirm and/or differentiate between closely related compounds/ fragments from the sample. The fingerprint plot uses, the range of signal intensities in counts per minute (cpm), plotted against the range of associated mass to charge ratios (m/z), at every point, where there is a characteristic (maximum) peak intensity; to characterise candidate compounds for identification using the protonated mass (that is; molecular mass of compound or fragment + 1), for compounds or fragments with proton affinity greater than water (that is, the capacity to attract H^+ away from protonated water H_3O^+). The proton affinity for water is about 694 ± 3 kJ mol^{-1}, at 300 K (27 °C) (Ellis and Mayhew 2013; Hunter and Lias 1998; Jolly 1991). The proton affinity values for the other candidate compounds are then compared to that of water to determine how strong the capacity is, to take over H^+ from protonated water. The higher values show stronger affinity or attraction to H^+. The simple four-step process required to pinpoint a possible candidate compound in the mass spectrum from the forest, while excluding others are:

1. From the worksheet, use the m/z value at the peak intensity (that is, Molecular mass + 1); to identify the compound, from the molar mass;

2. Find the proton affinity from literature;

3. Compare the proton affinity to that of water; if reasonably higher than water (at least a difference of about 22 kJ mol^{-1} or more), then there is a high likelihood that the compound has been detected effectively using the PTR; and

4. Finally compare the outcome with observed pattern of detection in similar forests (if available), especially observations using PTR (see Table 5.1).

The equipment used for these measurements, as already stated in section 2.1; is the KORE series 1; PTR-ToF-MS with a mass resolution ≥ 1,500 FWHM; (Full Width Half Maximum) and Sensitivity for Benzene >200 cps/ppbv; (counts per seconds/parts per billion) (KORE 2014). The plot in Figure 5.1 is from the 2015 measurement campaign while the analysis for compound identification was done using the data from the 2016 measurement campaign. Both measurements are part of the initial baseline measurements taken in 2015 and 2016 respectively, at the Mill Haft Forest of the Birmingham Institute of Forest Research (BIFoR). It is a deciduous temperate forest where the FACE facility is being hosted by the University of Birmingham, to investigate the impact of increased CO2 on biodiversity and ecosystem resilience. The list of peak intensities against the protonated mass spectrum results in isolating a number of product ions (see Appendix A) for further consideration; from which the 15 top stable identifiable recurring compounds and fragments of interest were listed, in order of highest peak intensities from any of the five periods (Table 5.1). Table 5.2 was also generated from the selection of the first 8 unidentified or unspecified species due either to a lack of reliable mass spectral information, chemical structure, proton Affinity data or a combination of any of these factors. They were however listed for further attention because of the magnitude of their peak intensities.

The list of 15 identified compounds (Table 5.1), were: ethanol; ethenone / propene; acetone; acetaldehyde; acetic acid; methanol; acetonitrile, 2–butanone; methyl acetate / isobutanol; formaldehyde; 2–propenal / 1-butene; MVK/MACR; formic acid / ethanol; dimethyl formamide; and isoprene. They all have proton affinities above that for water (about 694 ± 3 kJ mol^{-1}) by at least 22 kJ mol^{-1} under the standard gas phase conditions required (Ellis and Mayhew 2013). The results were confirmed by comparing with literature from similar processes using the PTR-MS and the PTR-ToF-MS, in temperate deciduous forests in Europe and the Mediterranean regions of France, Italy and Greece. The

results were consistent with Seco et al (2011a) and Federico (2015) and agreed with Seco et al (2007, 2008, 2011b) and Kalogridis et al (2014). Some of the compounds were identified as mixtures that could be isobaric or isomeric. They were differentiated by definition in Figure 5.4; Isobaric as those with the same nominal molecular weight but differ in the decimal part; and can be separated by the PTR method if a high enough mass resolution can be achieved, depending on the type of atoms and how they combine in the molecules. The isomeric mixtures like MVK/MACR; cannot be separated currently with only the PTR method, since they possess exactly the same molecular weight and have the same exact atoms. Apart from MVK/MACR the other mixture appears to meet the definition for isobaric mixture. Comparing the different periods (Figure 5.11); show ethanol fragment as having the highest total intensity of 132567 cpm, followed by ethenone/ propene mixture with 96986 cpm, before acetone with 45919 while MVK/MACR and isoprene are respectively 3442 and 1489 at positions 12 and 15 based on total cpm across all the periods (Table 5.11). Each of the compounds show highest cpm in different periods with no obvious criteria for immediately predicting the pattern. More compounds however show higher values in period 1, due possibly to the number of days involved in the data collection. The cpm values could change to reveal a different pattern (or order of arrangement); when the specific sensitivities are applied to convert to ppb values using the formula sensitivity = ncps/ppbv.

The conclusion is that fingerprinting of VOCs in a forest environment using the PTR-MS method gives a fast and reliable way of identifying stable and recurring compounds using the protonated mass and the proton affinity table available in literature; although some additional verification may be required for some of the compound mixtures, through the use of other methods like gas chromatography. The results over the five periods basically confirm that the compounds identified are actually present in the forest, although in different quantities depending on the period or season involved.

Chapter 6

Conclusion

6.0 Overview: guide to the chapter

This Chapter contains the following sections: 6.1; The motivation for this study, 6.2; The Method employed in this study, 6.3; Chapter 3, Results; Isoprene and oxidation products; Period 1; (2m) and Period 2; (30m and 15m), 6.4; Chapter 4, Results; isoprene and oxidation products (Periods 1 to 5), 6.5; Chapter 5, Results; Fingerprinting; Identifying secondary plant metabolites (Periods 1 to 5) and 6.6; Final conclusion

6.1 The motivation for this study

In the face of growing evidence that there will be increase in future CO_2 (EPA 2008a, b; OECD 2011; IPCC 2007, 2014, 2018) due to changes in patterns of land use and increases in anthropogenic activities; especially the burning of fossil fuels for energy (NOAA 2016). It is becoming more imperative to monitor accurately the biogenic contributions to the atmospheric hydrocarbon budget; especially the contribution from forested landscapes, which is one of the key reasons BIFoR has been set up. Hence the necessity to follow closely isoprene emissions and ambient concentrations over forests; since it is known to be the most abundant biogenic volatile organic compound (BVOC) in temperate and tropical forest ecosystems (Guenther et al. 1994, 1995, 2012; Geron et al. 1994). Globally, the biogenic hydrocarbon source to the atmosphere is more significant than those from anthropogenic sources (Rasmussen 1970, Lamb et al. 1987, 1993, Guenther et al. 2012). In addition to its strong emission source, Isoprene (2-methyl-1,3-butadiene) is very reactive and has a short life time in the atmosphere

(Pressley et al. 2005), due to its two vinyl unsaturated bonds, which in turn results in several potential degradation pathways producing differing oxidation products (Wennberg et al., 2018). This makes it more useful to adopt a more wholistic approach of monitoring, not only isoprene, but a whole range of associated oxidation products and secondary metabolites.

Chapter 1 clearly highlighted the importance of monitoring these biogenic VOCs that combine to make up sources of significant contribution to the atmospheric hydrocarbon budget; which feeds into updating regional and global atmospheric models of atmospheric composition and chemistry-climate interactions. Understanding the sources of biogenic hydrocarbons is important for predicting ozone episodes in urban and semi urban areas where NOx can build up to a range of concentrations that become significant, in photochemically triggered reactions with these secondary metabolites (hydrocarbons) especially isoprene to form ozone (Trainer et al. 1987, Chameides et al. 1988, Thompson 1992, Baldocchi et al., 1995). Accurate modelling can be effective in designing interventions against low crop and forest outputs as a result of ozone episodes, and to help prevent pollution-induced health crises (Reich and Amundson 1985, Runeckles and Chevone 1992). The present study is therefore expected to contribute positively to the process that is involved in the formulation of mitigation strategies; which requires a proper inventory of major isoprene emitting sources in a region (Sharkey et al. 1996)

6.2. The Method employed in this study

Proton-Transfer-Reaction Mass spectrometry (PTR-MS) is a method that has been used for online measurement of VOCs in various studies; but in this study, the complex process involved when a large data set from a typical PTR is being analyzed, was simplified in order to demonstrate how the PTR works; by giving basic steps that can guide a beginner to start up the PTR. Also demonstrated were:

a. the procedure for establishing mass resolution. That is, showing how mass resolution (m/z) at the centre of a peak and the width (Δm) allow the peak width to be worked out, using m/z = 59 (identified as acetone) as a worked example.

b. the normalisation procedure; using m/z = 59 (acetone) as an example (figure 2.3).

c. A simplified way of illustrating from the top row of each worksheet; how the mass resolution and data normalisation was applied on the 2016 data sheet; with real time examples taken from the 2016 datasheet to further illustrate; mass resolution for Protonated (isotope) water, (m/z = 21); period 1, 2016 data; normalisation for $(MH^+)^{69}$; i.e., Isoprene and normalisation for $(MH^+)^{71}$; i.e., MVK/MACR. The reason for calculating the intensity of protonated water i[$H30^+$] from the Protonated (isotope) i[$H30^+$]^{21} (m/z 21) was also covered in the process (section 2.1.4.3; see also; tables 2.2 & 2.4)

6.3 Chapter 3, Results; isoprene and oxidation products; Period 1; (2m) and Period 2; (30m and 15m)

In period 1; chapter 3; the scatter plot (MVK/MACR plotted against isoprene) (Figure 3.7), showed a linear correlation (R^2) of 0.56; with a residual 0.34% of MVK/MACR in the absence of any isoprene (based on the intercept on y axis). Suggesting that most of the MVK/MACR (> 99%) at 2 meters height of the forest on those days (19-21/08/2015), could be attributed to isoprene oxidation predicted by this linear relationship.

In Period 2; isoprene concentrations measured at 15 and 30 meters both showed, that the isoprene concentrations follow a diurnal pattern irrespective of the height or date (for measurements around 15 and 30 metres respectively), as can be observed in Figures (3.9 to 3.21). A similar pattern was observed for the oxidation products; MVK/MACR (Figure 3.10). MVK/MACR30m and MVK/MACR15m (measured at about 30 and 15 metres respectively), showed a diurnal pattern of concentration with about 3 hours variation; lagged with respect to Isoprene, see Figures (3.10 to 3.21). These diurnal patterns and the

variability observed for isoprene concentrations (see also Figure 3.14) within the canopy (15m) and close to canopy top (30m) are consistent with the literature (example Apex et al 2002, Stroud et al 2001 and Kalogridis et al 2014). The box plots for hourly averages at 30 m and 15 m were similar (Figures 3.15 and 3.16). Data from both heights showed an indistinct nocturnal minimum and a late afternoon maximum, with amplitude of ~ 0.03-0.05 ppbv in the medians. A linear correlation of at least 60%, was established between the concentration values of MVK/MACR30m and MVK/MACR15m, formed at 30m and 15m heights at r^2 value of 0.649 (Figure 3.25). The linear equation predicts 0.919 ppb of MVK/MACR15m for every 1.0 ppb of MVK/MACR30m, due either to loss of MVK/MACR within the canopy or production of MVK/MACR as air moves out of the canopy. The conclusion here is that; the key factors at play, for both heights, have approximately equal impact on the concentrations of the oxidation products. The most obvious factors, that appear to be common to both heights so far, is the level of exposure to the diurnal light and radiation at 30 and 15 meters above the forest floor.

Comparing the pattern observed in Period 1 to Period 2; suggest that Isoprene and its oxidation products MVK/MACR do not always show a diurnal pattern when their concentrations are below certain levels of concentration; as can be observed in (Figures 3.2 – 3.5). In Period 1, isoprene concentrations were below 1.30 ppb while MVK / MACR was below 0.25 ppb. Isoprene in Period 2 was below 5.0 ppb and 4.0 ppb at 30 and 15 metres respectively; while, MVK/MACR concentrations at both levels, was about the same; below 0.4 ppb. The Isoprene concentrations around 15m and 30m (in period 2), are more representative of isoprene concentrations in forested landscapes — i.e., in temperate regions like Mill Haft — than concentrations in period 1. Some explanations for this may be because, isoprene is emitted more at levels closer to the canopy; where flux rates are known to be influenced by higher temperatures and increased exposure to light. The leaves and leafy parts (canopy regions) of these huge, tall trees rather than at lower regions like the trunk of trees (and smaller plants) also show higher concentrations. The lower levels, typical of period 1, will likely be from smaller plants with much less

concentrations; flux rates are known to be influenced by light, temperature, sometimes photosynthesis or even stress (e.g., Monson et al 1992, Rosenstiel et al., 2003, Loreto and Schnitzler 2010). Hence measurements closer to the bottom of the trees like period 1, may show a different pattern than the typical expected for isoprene in period 2 (close to the canopy heights). The influence of poor light and vegetation cover down in the forest may have also contributed to the observed pattern in period 1, which was measured at about 2 meters of height in the forest.

6.4. Chapter 4, Results; isoprene and oxidation products (Periods 1 to 5)

In chapter 4; it was observed throughout the five periods that the diurnal pattern varied from day to day in the data series that resulted from the time series of isoprene and MVK/MACR; that the rapid variations that occur from day to day are superimposed on them; even though they are more pronounced on some days than others; manifesting different patterns in the periods depending on the prevailing environmental conditions. The maximum mixing ratios recorded for some of the periods (see Table 4.8) appear to be much higher than is recorded in the literature for deciduous forests in temperate climates (example; Fuentes et al. 1996); as can be seen in Period 1; (P1) and Period 4; (P4), although the median distributions are in generally agreement with both the diurnal patterns and concentration profiles for these forests. It can be inferred from the consistent midday peaks noticeable in nearly all of the periods, that Peak isoprene concentrations coincide with maximum canopy temperatures as can be seen in Figures 4.7. 4.13 and 4.25; in Periods; 2, 3 and 5, respectively; as examples), this also agree with observations in the literature (example: Tingey et al. 1979, Monson and Fall 1989, Loreto and Sharkey 1990, Fuentes 1996, Sharkey et al. 1996). The statistic ratios in most of the periods (see Table 4.8) show an approximate mixing ratio of 6 to 1

between isoprene and its main oxidation products; MVK/MACR; although extreme deviations were also observed in the maxima of periods 1 and 4.

The summary of the scatter plots (isoprene against MVK/MACR) for Periods 1 to 5 (Table 4.7); show that a linear correlation (R^2) of approximately 77.5 % exist between isoprene and the oxidation products; MVK/MACR in period 1; with a residual MVK/MACR concentration of 0.321 ppbv at zero isoprene (based on the intercept on the y axis). The change in the concentration of MVK/MACR, compared to isoprene was 0.114 and 0.4355 ppbv of MVK/MACR resulted from 1 ppbv of isoprene (based on the linear equation). The linear correlation in period 2 was ≈52.3 % and a residual MVK/MACR concentration of 0.353 ppbv at zero isoprene; the change in the concentration of MVK/MACR, compared to isoprene was 0.096 and 0.449 ppbv of MVK/MACR resulted from 1 ppbv of isoprene. Period 3; showed ≈53.6 % linear correlation (R^2) between both concentrations; the residual MVK/MACR at zero isoprene was 0.261 ppbv; the change in the concentration of MVK/MACR, compared to isoprene was 0.098 and 1 ppbv of isoprene produced 0.359 ppbv of MVK/MACR. Period 4; showed no linear correlation between both concentrations (at R^2 of 0.0172 or 1.72 %), a much higher residual MVK/MACR value of 0.944 ppbv at zero isoprene and the change in MVK/MACR concentrations compared to isoprene was 0.0023; the lowest of the five periods. 1 ppbv of isoprene produced 0.946 ppbv MVK/MACR. Although Period 4 showed no linear correlation and had the lowest rate of change for MVK/MACR yet showed the highest MVK/MACR concentration due to the high residual value of MVK/MACR at zero isoprene, suggesting the presence of an initial output of MVK/MACR (0.944), not directly related to the measured isoprene. 1ppbv of isoprene in this case produced 0.964 ppbv of oxidation products, yet only related to a very low rate of change (MVK/MACR / isoprene); of 0.0023. Finally, Period 5; showed the highest linear correlation (R^2) of 86.7 % between both concentrations with a residual MVK/MACR concentration of

0.237 ppbv at zero isoprene. The Change in MVK/MACR concentrations compared to isoprene (the slope of the correlation graph) was 0.109; and 1 ppbv of isoprene resulted in 0.346 ppbv of MVK/MACR. From the results in chapter 4; it can be concluded that isoprene and its primary oxidation products; MVK/MACR are present in this sample data; collected during the 2016 measurement campaign at the canopy height of about 30 metres; as part of the baseline air sampling procedures, at the BIFoR Mill Haft Forest, Staffordshire. The daily mixing ratios and diurnal patterns vary based on prevailing environmental, physical and climatic conditions but show median and mean values that approximately estimate more representative values that agree with results from similar forests from temperate regions.

6.5. Chapter 5, Results; fingerprinting; identifying secondary plant metabolites (Periods 1 to 5)

In Chapter 5; the fingerprinting process (i.e., using the full mass spectrum as a 'fingerprint' of the overall hydrocarbon composition of the forest air) was shown to be viable. Further identification can then follow based on specific needs or interest; by considering additional methods of separation and/ or quantification specific to the compound of interest; a good example often used alongside PTR-MS for the identification of VOCs being GC-MS (e.g., Riahi and Sellier 1998, Misztal et al., 2010). The simple four-step process required to pinpoint a possible candidate compound in the mass spectrum are:

1. From the worksheet, use the m/z value at the peak intensity for candidate parent molecular ions (that is, Molecular mass + 1); to identify the compound, from the molar mass;

2. Find the proton affinity from literature;

3. Compare the proton affinity to that of water; if reasonably higher than water (at least a difference of about 22 kJ mol^{-1} or more), then there is a high likelihood that the compound has been detected effectively using the PTR; and

4. Finally compare the outcome with observed pattern of detection in similar forests (if available), especially observations using PTR (see table 5.1).

Based on the above process, the first 15 stable, recurring identifiable molecular ions or fragments were selected (Table 5.1) and the top 8 unidentified or unspecified product ions were also selected (Table 5.2), for further consideration; from the long list of protonated product ions in Appendix A. The list of identified molecular ions and fragments were: ethanol; ethenone / propene; acetone; acetaldehyde; acetic acid; methanol; acetonitrile, 2–butanone; methyl acetate / isobutanol; formaldehyde; 2–propenal / butane; MVK/MACR; formic acid / ethanol; dimethyl formamide; and isoprene. They all have proton affinities above that for water (about 694 ± 3 kJ mol^{-1}) by at least 22 kJ mol^{-1} under the standard gas phase conditions required (Ellis and Mayhew 2013). The results were confirmed by comparing with literature from similar processes using the PTR-MS and the PTR-ToF-MS, in temperate deciduous forests in Europe and the Mediterranean regions of France, Italy and Greece. Isomeric and isobaric mixtures among the identified ions were identified and methods for better separation suggested (Figure 5.4).

The conclusion here, is that fingerprinting of VOCs in a forest environment using the PTR-MS method gives a fast and reliable way of identifying stable and recurring compounds using the protonated mass and the proton affinity table available in literature; although some additional verification may be required for some of the compound mixtures, through the use of other methods like gas chromatography (GC-MS). The results over the five periods confirm that the compounds identified are present in the BIFoR Mill Haft forest location; although in different quantities

(intensities) in the different periods; depending on the prevalent environmental factors at play during those day within the period.

6.6. Final conclusion

Overall, the results in Chapters 3, 4 and 5 show that isoprene, its oxidation products and other secondary plant metabolites from biogenic sources; present in the baseline samples collected in the summer of 2015 and 2016; from the BIFoR Mill Haft forest, have been successfully identified; using the PTR-MS method. A more accurate quantification of identified compounds will require additional methods example GC-MS. A better interpretation of observed patterns will result from applying more environmental factors into the investigation like relative humidity, photosynthetic active radiation (PAR), and wind speed and direction, alongside ozone (O_3) and nitrogen oxides (NOx) data for each period, where possible. More in-dept analysis will be required in the directions suggested in chapter 7; to improve on the interpretations made so far.

Chapter 7

Suggestions for Further Work

Lack of time was the major constraining factor in this work and largely determined how much further to go with the investigations, and whether any additional parameters to include as factors in the analysis. More time is required to look closely into the different patterns that emerged in the periods especially in period 1 2015, and all the periods in 2016, to identify specifically the likely environmental or other factors that dominated the prevalent conditions and influenced the observed patterns. Other types of environmental and weather-related data monitored within the specific periods will need to be processed and compared with the results for isoprene and its oxidation products (in Chapters 3 and 4), to identify more likely conditions specific to the patterns observed. Apart from the temperature profile that could have received more investigations; other conditions like the photosynthetic active radiation (PAR), relative humidity, wind speed and direction, could have been considered. These would have been helpful to compare the patterns from their data with each other and with the present results, and possibly with the ozone (O2) and nitrogen oxides (NOx) profiles for those periods. Secondary Organic aerosols (SOAs) are also monitored in relation to isoprene oxidation (e.g., Claeys et al 2004).

For example, it is expected that wind flowing over a forest from a nearby urban area with optimum levels of NOx, will produce a different pattern under a slower wind speed on a warm afternoon than on a day with fast moving wind over the same forest. So that the ozone and NOx; including SOA, levels monitored alongside temperature and the other environmental factors could have given more specific and conclusive explanations to apparent deviations from expected patterns in some aspects involving the environmental factors. The BIFoR Mill Haft Forest can be described as located in a semi urban area; that is; a forest in a semi-rural area surrounded by urban settings and busy motorways including an RAF

base less than 60 km away; in Shawbury. Hence, the likelihood for some of the factors mentioned above, becoming significant at certain seasons especially in the summer when these measurement campaigns where carried out.

There is the need to look more closely at the data processing for any possible errors, that went unnoticed despite the strict scrutiny on the data sets and the processing. The calibration factors used for this work was derived by a colleague (Blenkhorn, 2018), and could have been verified where possible. The limit of detection (LOD) and the Limit of quantification (LOQ) can be worked out at any point for any of the measurements using the definition adopted from Blenkhorn (2018);

Limit of detection (L O D) = Mean + 3 x SD , and

Limit of quantification (LOQ) = Mean + 10 x SD (Blenkhorn 2018); pg. 189.

The depth of this work can be increased by applying the additional environmental factors suggested above to this data, after considering the checks suggested against possible unintended errors.

Additional methods of detection and quantification like gas chromatography (GC-MS) could also be applied alongside the PTR-MS; to help with the separation of isomeric and isobaric VOC mixtures and explore more specific quantification needs for any of the compounds of further interest; in chapter five apart from isoprene and MVK/MACR.

References

1. Ammann, C., Spirig, C., Neftel, A. et al. (2004). Application of PTR-MS for measurements of biogenic VOC in a deciduous forest. Int. J. Mass Spectrum. 239, 87.
2. Atkinson, R., (2000). Atmospheric chemistry of VOCs and NOx. Atmospheric Environment. 34 (2000), 2063–2101.
3. Baldocchi D. Guenther, A., Harley, P., Klinger, L., Zimmerman, P., Lamb, B., Westberg, H. (1995). The fluxes and air chemistry of isoprene above a deciduous hardwood forest. Phil. Trans. R. Soc. Lond. A (1995) 350, 279-296
4. Baldocchi D. D. and Meyers, T. P. (1988). Turbulence structure in a deciduous forest. Boundary-Layer Meteorology 43, 345-364
5. Baldocchi, D. D. and Meyers, T. P. (1989). Turbulent transfer in a deciduous forest. Tree Physiology 5, 357-377.
6. Barrow, M. (2013). Average temperatures in Britain [Online]. Available from: http://projectbritain.com/weather/average.htm
7. Biasioli F., Yeretzian, C., Gasperi, F., Mark, T. D. (2011). PTR-MS monitoring of VOCs and BVOCs in food science and technology, Trends in Analytical Chemistry 30 (7) (2011)
8. BIFoR FACE in situ experiment – modelling the response of a Temperate Woodland to increased levels of Carbon Dioxide. (2017). http://www.naturphilosophie.co.uk/bifor-face-situ-experiment-modelling-response-temperate-woodland-increased-levels-carbon-dioxide/
9. Blake, R. S., Whyte, C., Hughes, C. O. *et al.* (2004). Demonstration of proton-transfer reaction time-of-flight mass spectrometry for real-time analysis of trace volatile organic compounds. Anal. Chem. 76, 3841.
10. Blenkhorn D.L. (2018). Novel approaches to the measurement of complex Atmospheric VOC mixtures using proton transfer reaction Mass spectrometry: Thesis (PhD). University of Birmingham.
11. Butler, T. M., Taraborrelli, D., Bruhl, C., Fischer, H., Harder, H., Martinez, M., Williams, J., Lawrence, M. G., and Lelieveld, J. (2008). Improved simulation of isoprene oxidation chemistry with the ECHAM5/MESSy chemistry-climate model: lessons from the GABRIEL airborne field campaign. Atmos. Chem. Phys., 8, 4529–4546. http://www.atmos-chem-phys.net/8/4529/2008/.
12. Carslaw, N., Creasey, D. J., Harrison, D., Heard, D. E., Hunter, M. C., Jacobs, P. J., Jenkin, M. E., Lee, J. D., Lewis, A. C., Pilling, M. J., Saunders, S. M., and Seakins, P. W. (2001). OH and HO2 radical chemistry in a forested region of north-western Greece, Atmos. Environ., 35, 4725–4737.
13. Chameides, W.L., R.W. Lindsay, J. Richardson and C.S. Kiang (1988). The role of biogenic hydrocarbons in urban photochemical smog: Atlanta as a case study. Science 241:1473--1475.
14. Chang, C-C. Wang J-L., Lung, S-C. C., Chang, C-y., Lee, P-J., Chew, C., Liao, W-C., Chen, W-N., Ou-Yang, C-F. (2014). Seasonal characteristics of biogenic and anthropogenic isoprene in tropical-subtropical urban environments. http://dx.doi.org/10.1016/j.atmosenv.2014.09.019
15. Claeys, M., Graham, B., Vas, G., Wang, w., Vermeylen, R., Pashynska, V., Cafmeyer, J., Guyon, P., Andreae, M. O., Artaxo, P., Maenhaut, W., (2004). Formation of Secondary Organic Aerosols

Through Photooxidation of Isoprene. *Science (*2004). 303, 5661, 1173-1176. DOI: 10.1126/science.1092805
16. Clemitshaw, K. C. (2003). Hydroxyl Radical. Encyclopedia of Atmospheric Sciences: 2nd Edition, Volume 6. http://dx.doi.org/10.1016/B978-0-12-382225-3.00429-1
17. de Gouw, J. A., Howard, C. J., Custer, T. G., Baker, B. M., and Fall, R. (2000). Proton-transfer chemical ionization mass spectrometry allows real-time analysis of volatile organic compounds released from cutting and drying of crops, Environ. Sci. Technol., 34, 2640–2648.
18. Dodge, M. C. (1977). Combined use of modelling techniques and smog chamber data to derive ozone - precursor relationships. Pp. 881—889 in International Conference on Photochemical Oxidant Pollution and its Control: Proceedings, Vol. II., B. Dimitriades, ed. EPA/600/3-77-001b.
19. Ehhalt, D. H. (1999). Photooxidation of trace gases in the troposphere. Physical Chemistry Chemical Physics 1 (24), 5401 –5408.
20. Eisele, F. L., Mount, G.H., Tanner, D., et al. {1997). Understanding the production and interconversion of the hydroxyl radical during the OH Photochemistry Experiment. Journal of Geophysical Research 102 (D5), 6457–6465.
21. Ellis, A. M., Monk, P. A. and Mayhew, C. A. (2013). Proton Transfer Reaction Mass Spectrometry, edited by Andrew M. Ellis, et al., John Wiley & Sons, Incorporated, 2013. ProQuest Ebook Central. [Online]. Available from: http://ebookcentral.proquest.com/lib/bham/detail.action?docID=1582852.
22. Ennis C., J. Reynolds, B. Keely, L. Carpenter (2005). A hollow cathode proton transfer reaction time of flight mass spectrometer, Int. J. Mass Spectrum. 247 (2005)72–80
23. Environmental Protection Agency (US) (2008a). Climate Change - Greenhouse Gas Emissions - Human-Related Sources and Sinks of Carbon Dioxide. [Online]. Available from: http://www.epa.gov/climatechange/emissions/co2_human.html
24. Environmental Protection Agency (2008b) Climate Change: Basic Information. [Online]. Available from: http://epa.gov/climatechange/basicinfo.html
25. Federico et al. (2015). Springer 2018. [Online]. Available from: https://www.nature.com/articles/srep12629/tables/1
26. Fehsenfeld, F., J. Calvert, R. Fall, P. Goldan, A. B. Guenther, C. N. Hewitt, B. Lamb, S. Liu, M. Trainer, H. Westberg et al. (1992). Emissions of volatile organic compounds from vegetation and the implications for atmospheric chemistry. https://doi.org/10.1029/92GB02125
27. Fuentes, J.D., Wang, D., Neumann, H. H., Gillespie, T.J. Den Hartog, G., Dann, T. F. (1996). Ambient biogenic hydrocarbons and isoprene emissions from mixed deciduous forest. Journal of Atmospheric Chemistry. 25. 67-95. 10.1007/BF00053286.
28. Fuentes, J.D., Wang, D., D. R. Bowling, M. Potosnak, R. K. Monson, W. S. Goliff, W. R. Stockwell (2006). Biogenic Hydrocarbon Chemistry within and Above a Mixed Deciduous Forest. Journal of Atmospheric Chemistry. DOI 10.1007/s10874-006-9048-4
29. Geron, C.D., A.B. Guenther and T.E. Pierce. (1994). An improved model for estimating emissions of volatile organic compounds from forests in the eastern United States. J. Geophys. Res. 99:12,773--12,791.
30. Guenther, A.B., P.R. Zimmerman and M. Wildermuth. (1994). Biogenic volatile organic compound emission rate estimates for U.S. woodland landscapes. Atmos. Environ. 28:1197—1210
31. Guenther, A., Hewitt, C., Erickson, D., Fall, R., Geron, C., Graedel, T., Harley, P., Klinger, L., Lerdau, M., McKay, W., Pierce, T., Scholes, B., Steinbrecher, R., Tallamraju, R., Taylor, J., and

Zimmerman, P. (1995). A global model of natural volatile organic compound emissions, J. Geophys. Res., 100, 8873–8892.
32. Guenther, A. B., Jiang, X., Heald, C. L., Sakulyanontvittaya, T., Duhl, T., Emmons, L. K., and Wang, X. (2012). The Model of Emissions of Gases and Aerosols from Nature version 2.1 (MEGAN2.1): an extended and updated framework for modelling biogenic emissions, Geosci. Model Dev., 5, 1471-1492, doi:10.5194/gmd-5-1471-2012.
33. Hamming, M. C. and Foster N. G. (1972). Interpretation of Mass Spectra of Organic Compounds, 1st ed. New York, NY. Academic Press. Online from https://onlinelibrary.wiley.com/doi/abs/10.1002/ange.19740861618
34. Hansel, A.; Jordan, A.; Warneke, C.; Holzinger, R. (1999). Wisthaler, A.; Lindinger, W. Proton-transfer-reaction mass spectrometry (PTR-MS): on-line monitoring of volatile organic compounds at volume mixing ratios of a few pptv. Plasma Sources Sci. Technol. 1999, 8, 332.
35. Hartungen E., P. Sulzer, A. Edtbauer, S. Jurschik, A. Jordan, L. Mark,T.D. Mark (2012). The next generation in high sensitivity and high resolution Proton-Transfer-Reaction Time-of-Flight Mass Spectrometry(PTR-TOFMS); online From www.ionicon.com
36. Hasson, A., Tyndall, G., and Orlando, J. (2004). A product yield study of the reaction of HO2 radicals with ethyl peroxy (C2H5O2), acetyl peroxy (CH3 C*(O)*O2), and acetonyl peroxy (CH3 C*(O)*CH2O2) radicals, J. Phys. Chem. A, 108, 5979–5989, doi: {10.1021/jp048873t}.
37. Holzinger, R., Warneke, C., Hansel, A. et al. (1999). Biomass burning as a source of formaldehyde, acetaldehyde, methanol, acetone, acetonitrile, and hydrogen cyanide. Geophys. Res. Lett. 26, 1161.
38. Hunter, E.P. Lias, S.G. (1998). Evaluated Gas Phase Basicities and Proton Affinities of Molecules: An Update, J. Phys. Chem. Ref. Data. 27, 3, 413-656, https://doi.org/10.1063/1.556018 .
39. Hutchison, B. A and Matt, D. R. (1977). The Distribution of Solar Radiation within a Deciduous Forest. ESA, 47, 2, 185-207. https://doi.org/10.2307/1942616.
40. IPCC (2007). Climate change synthesis Report 2007 (AR4). [Online]. Available from: http://www.ipcc.ch/pdf/assessment-report/ar4/syr/ar4_syr.pdf
41. IPCC (2014). Carbon Dioxide: Projected emissions and concentrations. [Online]. Available from: http://www.ipcc-data.org/observ/ddc_co2.html
42. IPCC, 2018: Global warming of 1.5°C. An IPCC Special Report on the impacts of global warming of 1.5°C above pre-industrial levels and related global greenhouse gas emission pathways, in the context of strengthening the global response to the threat of climate change, sustainable development, and efforts to eradicate poverty [V. Masson-Delmotte, P. Zhai, H. O. Pörtner, D. Roberts, J. Skea, P.R. Shukla, A. Pirani, W. Moufouma-Okia, C. Péan, R. Pidcock, S. Connors, J. B. R. Matthews, Y. Chen, X. Zhou, M. I. Gomis, E. Lonnoy, T. Maycock, M. Tignor, T. Waterfield (eds.)]. In Press.
43. Jenkin, M.E., Clemitshaw, K.C. (2000). Ozone and other secondary photochemical pollutants: Chemical processes governing their formation in the planetary boundary layer. Atmospheric Environment. 34 (16), 2499–2527
44. Jenkin, M. E., Hurley, M. D., and Wallington, T. J. (2007). Investigation of the radical product channel of the CH3 C*(O)*O2+HO2 reaction in the gas phase, Phys. Chem. Chem. Phys., 9, 3149–3162, doi:{10.1039/b702757e }.
45. Jolly, W. L. (1991). Modern Inorganic Chemistry (2nd Edn.). New York: McGraw-Hill. ISBN 0-07-112651-1.

46. Jordan A., S. Haidacher, G. Hanel, E. Hartungen, L. Mark, H. Seehauser, R. Schottkowsky, P. Sulzer, T.D. Mark (2009). A high resolution and high sensitivity time-of-flight proton-transfer-reaction mass spectrometer (PTRTOF-MS), International Journal of Mass Spectrometry. 286 (2009), 122-128.
47. Kaharabata, S.K., Schuepp, P.H., Fuentes, J.D. (1999). Source footprint considerations in the determination of volatile organic compound fluxes from forest canopies. J. Appl. Meteorol. 38, 878–884.
48. Kalogridis, C., Gros, V., Sarda-Esteve, R., Langford B., Loubet B., B. Bonsang B., Bonnaire N., Nemitz, E.,Genard, A. C., Boissard C., Fernandez C., Ormeño, E., Baisnée, D., Reiter I., and J. Lathière (2014). Concentrations and fluxes of isoprene and oxygenated VOC. Atmos. Chem. Phys., 14, 10085–10102. doi:10.5194/acp-14-10085-2014
49. KORE (2014). Kore Technology Limited 2014. (online) http://www.kore.co.uk/sdi.htm
50. Kubistin, D., Harder, H., Martinez, M., Rudolf, M., Sander, R., Bozem, H., Eerdekens, G., Fischer, H., Gurk, C., Klupfel, T., Knigstedt, R., Parchatka, U., Schiller, C. L., Stickler, A. (2008). MEGAN, ECMWF analyses and a detailed canopy environment model, Atmos. Chem. Phys., 8, 1329–1341. http://www.atmos-chem-phys.net/8/1329/2008/
51. Lamb, B., D. Gay, H. Westberg and T.E. Pierce. (1993). A biogenic hydrocarbon emission inventory for the U.S. using a simple forest canopy model. Atmos. Environ. 27A:1673—1690.
52. Lamb, B., A. Guenther, D. Gay and H. Westberg. (1987). A national inventory of biogenic hydrocarbon emissions. Atmos. Environ. 21:1695--1705.
53. Lelieveld, J., Gromov, S., Pozzer, A., and Taraborrelli, D. (2016). Global tropospheric hydroxyl distribution, budget and reactivity, Atmos. Chem. Phys., 16, 12477-12493, doi: 10.5194/acp-16-12477-2016.
54. Lindinger, W.: Eddy covariance measurements of oxygenated volatile organic compound fluxes from crop harvesting using a redesigned proton-transfer-reaction mass spectrometer, J. Geophys. Res., 106, 24 157–24 167, 2001.
55. Liu, Y. J., I. Herdlinger-Blatt1,2, K. A. McKinney3, and S. T. Martin. (2013).Production of methyl vinyl ketone and methacrolein via the hydroperoxyl pathway of isoprene oxidation, Atmos. Chem. Phys., doi:10.5194/acp-13-5715-2013
56. Loreto, F. and T.D. Sharkey. (1990). A gas-exchange study of photosynthesis and isoprene emission in *Quercus rubra* L. Planta 182:523—531
57. Loreto, F., Centritto, M., Barta, C., Calfapietra. C., Fares, S., Monson, R. K. (2007). The relationship between isoprene emission rate and dark respiration rate in white poplar (Populus alba L.) leaves. Plant, Cell & Environment 30: 662–669.
58. Loreto, F., Schnitzler, J-P. (2010). Abiotic stresses and induced BVOCs. Trends in Plant Science 15: 154–166.
59. Loreto, F., Hansel, A. (2011): Detection of Plant Volatiles after Leaf Wounding and Darkening by Proton Transfer Reaction "Time-of-Flight" Mass Spectrometry (PTR-TOF), PLoS ONE, 6(5) (2011), e20419.
60. MacKenzie, R., Thomas, R., Ellsworth, D., Hemming, D., Crous, K., Blaen, P., Poynter, A., Blenkhorn, D., Pope, F. (2016). A Free-Air Carbon Dioxide Enrichment (FACE) facility in old-growth temperate deciduous woodland. http://adsabs.harvard.edu/abs/2016EGUGA..18.4919M

61. McLafferty, F. W., Turecek, F. (1993), Interpretation of Mass Spectra, 4th ed. Mill Valley, CA. University Scientific Books. [Online]. Available from: https://onlinelibrary.wiley.com/doi/abs/10.1002/bms.1200230614
62. Met office (2015a). UK climate summer-2015, updated: 13 April 2016 [Online]. Available from: https://www.metoffice.gov.uk/climate/uk/summaries/2015/summer [Accessed: 10 August 2018].
63. Met office (2015b). UK climate August-2015 updated: 13 April 2016 [Online]. Available from: https://www.metoffice.gov.uk/climate/uk/summaries/2015/august [Accessed: 10 August 2018].
64. Met office (2015c). UK climate September-2015, updated: 13 April 2016 [Online]. Available from: https://www.metoffice.gov.uk/climate/uk/summaries/2015/september [Accessed: 20 August 2018].
65. Met office (2019). Shawbury observations map, updated:30 September 2019 [Online]. Available from https://www.metoffice.gov.uk/weather/observations/gcqh76ug7 [Accessed: 30 September 2019].
66. Misztal, P.K., et al. (2012). Development of PTR-MS selectivity for structural isomers: Monoterpenes as a case study. International Journal of Mass Spectrometry. 310: p. 10-19
67. Monson, R.K. and R. Fall. {1989). Isoprene emission from Aspen leaves. The influence of environment and relation to photosynthesis and photorespiration. Plant Physiol. 90:267--274.
68. Monson, R. K., Jaeger, C. H., Adams, W. W., Driggers, E. M., Silver, G. M. (1992). Relationships among Isoprene Emission Rate, Photosynthesis, and Isoprene Synthase Activity as Influenced by Temperature. Fall R Plant Physiol. 98(3):1175-80
69. Niinemets, U., Loreto, F. and Reichstein M. (2004). Physiological and physicochemical controls on foliar volatile organic compound emissions. www.sciencedirect.com 1360-1385/$, doi:10.1016/j.tplants.2004.02.006
70. NIST webbook (2018). National Institute of Standards and Technology. [Online]. Available from: https://webbook.nist.gov/cgi/cbook.cgi?ID=C78795&Mask=20
71. NOAA (2016). National Oceanic and Atmospheric Administration Earth System Research Laboratory. [Online]. Available from: https://www.esrl.noaa.gov/research/themes/carbon/
72. Norby, R. J., et. al., (2015). Model–data synthesis for the next generation of forest free-air CO2 enrichment (FACE) experiments. https://doi.org/10.1111/nph.13593
73. OECD (2011). OECD Environmental Outlook To 2050, Chapter 3: Climate Change, Pre-Release Version, Nov. 2011. [Online]. Available from: https://www.oecd.org/env/cc/49082173.pdf
74. Pressley, S., B. Lamb, H. Westberg, J. Flaherty, J. Chen, and C. Vogel (2005). Long-term isoprene flux measurements above a northern hardwood forest. J. Geophys. Res., 110, D07301, doi:10.1029/2004JD005523.
75. Pugh, TAM, AR MacKenzie, CN Hewitt, B Langford, PM Edwards, KL Furneaux, DE Heard, JR Hopkins, CE Jones, A Karunaharan, J Lee, G Mills, P Misztal, S Moller, PS Monks, and LK Whalley (2010). Simulating atmospheric composition over a South-East Asian tropical rainforest: Performance of a chemistry box model, Atmos. Chem. Phys., 10, 279-298.
76. Rasmussen, R.A. (1970). Isoprene: identified as a forest-type emission to the atmosphere. Environ. Sci. Technol. 4:667—671
77. Rasmussen, R.A. and C.A. Jones. (1973). Emission isoprene from leaf discs of *Hamamelis*. Phytochemistry 12:15--19.

78. Reich, P.B. and R.G. Amundson. (1985). Ambient levels of ozone reduce net photosynthesis in tree and crop species. Science 230:566--570.
79. Riahi, K. and N. Sellier (1998). Separation of Isomeric Polycyclic Aromatic Hydrocarbons by GC-MS: Differentiation Between Isomers by Positive Chemical Ionization with Ammonia and Dimethyl Ether as Reagent Gases. Chromatographia. 47: 309-312
80. Robinson, N. H., Hamilton, J. F., Allan, J. D. et al. (2011). Evidence for a significant proportion of Secondary Organic Aerosol from isoprene above a maritime tropical forest. Atmos. Chem. Phys. 11, 1039
81. Rosenstiel T. N, Potosnak M. J, Griffin K. L, Fall R, Monson R. K. (2003). Increased CO2 uncouples growth from isoprene emission in an agriforest ecosystem. Nature 421: 256–259.
82. RStudio (2017). RStudio: Integrated development environment for R (Version 1.0.143 for windows vista/7/8/10) [Computer software]. Boston. [Online]. Available from: https://www.rstudio.com/products/rstudio/download/#download
83. Runeckles, V.C. and B.I. Chevone. (1992). Surface level ozone exposures and their effects on vegetation. *In* Crop Responses to Ozone. Ed. A.S. Lefohn. Chelsea, Mich: Lewis Publishers, Inc., pp 189--270.
84. Seco, R., Penuelas, J., and Filella, I.: Short-chain oxygenated VOCs (2007): Emission and uptake by plants and atmospheric sources, sinks, and concentrations, Atmos. Environ., 41, 2477–2499, doi:10.1016/j.atmosenv.2006.11.029.
85. Seco, R., Penuelas, J., and Filella, I. (2008). Formaldehyde emission and uptake by Mediterranean trees *Quercus ilex* and *Pinus halepensis*, Atmos. Environ., 42, 7907–7914, doi:10.1016/j.atmosenv.2008.07.006.
86. Seco R., J. Penuelas, I. Filella, J. Llusia, R. Molowny-Horas, S. Schallhart, A. Metzger, M. Muller, A. Hansel (2011a). Contrasting winter and summer VOC mixing ratios at a forest site in the Western Mediterranean Basin: the effect of local biogenic emissions. **[O**nline]. Available from www.atmos-chem-phys.net/11/13161/2011/doi:10.5194/acp-11-13161-2011
87. Seco, R., Filella, I., Llusia, J., and Pe` nuelas, J. (2011b). Methanol as a signal triggering isoprenoid emissions and photosynthetic performance in *Quercus ilex.* Acta Physiol. Plant., 33, 2413–2422, doi:10.1007/s11738-011-0782-0, 2011.
88. Sharkey T. D., Singsaas P. J., Vanderveer And Geron C. (1996). Field measurements of isoprene emission from trees in response to temperature and light, Tree Physiology 16, 649—654.
89. Sharkey, T.D., Wiberley, A. E., Donohue, A. R. (2008). Isoprene Emission from Plants: Why and How. Annals of botany. 101. 5-18. 10.1093/aob/mcm240.
90. Sillman, S., and D. He (2002). Some theoretical results concerning O3-NOx-VOC chemistry and NOx-VOC indicators. J. Geophys. Res., 107(D22), 4659, doi:10.1029/2001JD001123.
91. Silverstein, R. M., Bassler, G. C. and Morrill, T. C. (1991). Spectrometric Identification of Organic Compounds, 5th ed. New York, NY. Wiley and Sons. Inc. [Online]. Available from: https://onlinelibrary.wiley.com/doi/abs/10.1002/oms.1210260923
92. Tanimoto, H., Aoki, N., Inomata, S. *et al.* (2007). Development of a PTR-TOFMS instrument for real-time measurements of volatile organic compounds in air. Int. J. Mass Spectrum. 263, 1.
93. Taraborrelli, D., Lawrence, M. G., Butler, T. M., Sander, R., and Lelieveld, J. Mainz (2009). Isoprene Mechanism 2 (MIM2): an isoprene oxidation mechanism for regional and global

atmospheric modelling, Atmos. Chem. Phys., 9, 2751–2777. [Online]. Available from: http://www.atmos-chem-phys.net/9/2751/2009/.
94. Taraborrelli, D., Lawrence, M. G., Crowley, J. N., Dillon, T. J., Gromov, S., Groß, C. B. M., Vereecken, L., and Lelieveld, J. (2012). Hydroxyl radical buffered by isoprene oxidation over tropical forests, Nat. Geosci., 5, 190–193.
95. Thompson, A.M. (1992). The oxidizing capacity of the Earth's atmosphere: probable past and future changes. Science 256:1157—1165.
96. Tingey, D.T., M. Manning, L.C. Grothaus and W.F. Burns. (1979). The influence of light and temperature on isoprene emission rates from live oak. Physiol. Plant. 47:112--118.
97. Trainer, M., E.J. Williams, D.D. Parrish, M.P. Buhr, E.J. Allwine, H.H. Westberg, F.C. Fehsenfeld and S.C. Liu. (1987). Models and observations of the impact of natural hydrocarbons on rural ozone. Nature 329:705--707.
98. Wennberg, P.O., et al. (2018). *Gas-Phase Reactions of Isoprene and Its Major Oxidation Products.* Chemical Reviews, 2018. **118**(7): p. 3337-3390.
99. Zheng B., Chevallier, F., Yin, Y., Ciais, P., Fortems-Cheiney, A., Deeter, M. N., Parker, R. J., Wang, Y., Worden, H. M. and Zhao, Y. (2019). Global atmospheric carbon monoxide budget 2000–2017 inferred from multi-species atmospheric inversions Earth Syst. Sci. Data Discuss. https://doi.org/10.5194/essd-2019-61

Appendix A: Possible Compounds identified using their m/z values

(All chemical species are based on protonated mass; even those without the positive sign. Literature sources used for identification are numbered at the bottom of this table)

S/N	(m/z) at maximum peak	Maximum (peak) intensity (cpm)	Possible compound / fragment	Source of fragment identification	Proton affinities of species (kJ/mol)	Source of proton affinity data	Comment
1	21.025	1P 40081	H3O+ (Hydronium ion from ^{18}O)	1. Seco et al 2011 2. **Federico et al 2015**	E.g. H2O 691	4,5,6	
2	26.015	1P 75 2p 49 5P 50	*C2H2+	3 Hadden Analytical online	Not available (na)	na	*Possibly fragments associated with acetylene
3	26.975	2p 31 5P 52	*C2H3+	2	Acetylene-641	4,5,6	The measured m/z in (2) was 27.025
4	28.005	2p 44 4p 38 5P 29	*C2H4+	3	na	na	Possibly fragments associated with acetylene
5	29.015	1P 21072 2p 28461 3p 39198 4p 21760 5P 22076	C2H5+ Ethanol (alkyl fragment)	2. **Federico et al 2015**	776	7	The measured m/z in (2) was 29.039
7	30.005	1p 217210 2p 338052 3p 324616 4p 308087 5P 364602	*CH2NH2+	3. Hadden Analytical online	832.6	7	Possibly Fragments associated with alkyl amines

8	30.995	1P 2p 3p 4p 5P	1229 1646 1964 1664 1948	Formaldehyde (CH_3O^+)	2		713	7	The measured m/z used in (2) was 31.042
9	31.985*	1P 2p 3p 4p 5P	117419 1454289 1161692 932558 951691	ui *(alkyl fragment) Possibly related to Methanol or formaldehyde based on the m/z	na	na The pa for formaldehyde (713) and methanol (754.4) are high enough to consider the possibility for this specie	7		* The intensity of this fragment is consistently high and likely associated with methanol / formaldehyde but needs confirmation
10	32.995	1p 2p 3p 4p 5p	4754 5920 6431 5362 5368	Methanol (CH_5O^+)	1, 2		754	5	Measured m/z in (2) was 33.033
11	33.995*	1p 2p 3p 4p 5p	16563 25355 26241 19218 24593	(alkyl fragment) possibly *SH+	3		712	6	*SH+ was suggested since SH was identified as a common fragment at m/z 33 in (3).; especially as 34.995 was the measured m/z for H2S in (2), at m/z 34,
12	34.995	2p	27	H_2S^+	2		705	7	34.995 was used as the measured m/z for H2S+ in (2) at m/z 34
13	36.025*	1p 2p 3p 4p 5p	423 544 473 367 447	Unidentified (ui)		na	na	na	

14	37.035*	1p	603970	Unidentified (ui)	na	na	na	*The pa of HCl is too low to consider HClH+
		2p	889415					
		3p	614980					
		4p	730218					
		5p	915457					
15	38.035	2p	2226	ui	na	na	na	
		3p	1352					
		4p	2231					
		5p	3275					
16	39.035	1p	7640	CH_3CH_3	3	na	na	Likely source; aromatics; suggested in (3)
		2p	6147					
		3p	4053					
		4p	5867					
		5p	8965					
17	40.035	1p	125	ui	na	na	na	
		2p	68					
		3p	53					
		5p	92					
18	41.045	1p	2027	Alkyl fragment (C_3H_5+)	2, 3	Cyclopentane 750	5	
		2p	734					
		3p	633					
		4p	525					
		5p	1006					
19	42.045	1p	2017	Acetonitrile (C_2H_4N+)	1, 2	779	5	
		2p	1925					
		3p	2047					
		4p	1766					
		5p	3943					
20	43.025	1p	22183	Ethenone (C_2H_3O+) / propene (C_3H_7+); Alkyl fragments	(2)	Ethanol 779 / 752	4 / 5	measured m/z shown in (2) were: ethenone (43.018)/ propene
		2p	8062					
		3p	5317					

		4p	4862						(43.054). 43.025; here, suggests a mixture of both.
		5p	5494						
21	44.025	1p	811	ui	ui		na	na	Alkyl amines have been suggested as possible sources for ions at m/z 44 in (3)
		2p	368						
		3p	226						
		4p	199						
		5p	228						
22	45.045	1p	15796	Acetaldehyde (C_2H_5O+)	(1, 2)		769	5	45.033 was the measured m/z in (1 and 2)
		2p	12232						
		3p	7793						
		4p	6462						
		5p	8990						
23	46.035	1p	2934	ui	na		na	na	
	46.005	2p	1641						
		3p	1867						
	45.995	4p	1355						
		5p	4971						
24	47.025	1p	1208	Formic acid/ Ethanol (CH_3O_2+/ C_2H_7O+)	(1, 2)		742 / 776	5	Measured m/z for formic acid was 47.013 and ethanol was 47.049 in (2) and 47.048 in (1)
		2p	711						
		3p	492						
		4p	464						
		5p	788						
25	48.015	1P	244	CH_3OO+		ui	745	7	Proton affinity for CH3COOCN was given. But CH3S+ H was also suggested in (3) as possible at m/z 48
		2p	343						
		3p	271						
		4p	288						
		5P	576						
26	50.005	1p	1120	ui	na	na		na	
		3p	1544						

		4p	1307					
		5p	1360					
27	51.045	2p	80	ui	na	na	na	
		3p	44					
		4p	74					
		5p	328					
28	52.005	2p	68	ui	na	na	ns	
		3p	30					
		5p	43					
29	53.015	1p	287	Cyclobutadiene (C_4H_5+)	(2)	≥ 750.4 ≤ 839 depending on sources	4	Measured m/z in (2) was 53.038
		2p	137					
		3p	145					
		4p	122					
		5p	282					
30	54.025	2p	55	Alkyl fragment C_4H_6+	(3)	771	7	Fragments at m/z 54; possibly from the fragmentation of protonated alkenes / cyclic alkanes
		3p	32					
		4p	39					
		5p	50					
31	55.055	1p	7513	Alkyl fragment (C_4H_7+)	(2)	955.6	7	m/z 55.054 was measured in (2)
		2p	13801					
		3p	5125					
		4p	12143					
		5p	24677					
32	56.055	2p	103	C4H8+	(3)	746	7	
		3p	61					
		4p	71					
		5p	162					
33	57.045	1p	1790	2-Propenal (Acrolein) C_3H_5O+/C_4H_9+ 1-Butene (alkyl fragment)	(2)	Acrolein 797	4	Acrolein was 57.34 and 1-butene was 57.68 in (2)
		2p	1079					
		3p	539					

		4p	551					
		5p	1103					
34	58.035	2p	74	ui	na	na	na	
		3p	45					
		4p	43					
		5p	62					
35	59.065	1p	18265	Acetone (2-Propanone) C_3H_7O+	(1, 2)	812	5	Measured at 59.49 in both (1) and (2)
		2p	17886					
		3p	11986					
		4p	11535					
		5p	37314					
36	60.055	1p	7524	CH_2-COOH+H	(3)	na	na	Suggested as possible fragment at m/z 60. It must be closely related to m/z 61
		2p	828					
		3p	541					
		4p	513					
		5p	1404					
37	61.045	1p	10687	Acetic acid $C_2H_5O_2+$	(1, 2)	784	5	Measured at 61.028 in both (1) and (2)
		2p	3695					
		3p	2036					
		4p	1840					
		5p	2453					
38	62.035	2p	157	ui	na	na	na	
		3p	99					
		4p	83					
		5p	183					
39	63.045	1p	308	Dimethyl sulphide (C_2H_7S+)	(2)	831	5	Measured at 63.026 in (2)
		2p	199					
		3p	96					
		4p	118					
		5p	260					

40	65.045	1p	59	Methanetriol (CH_5O_3+)	(2)	Not readily available (na)	na	Measured at m/z 65.023 in (2)
		2p	55					
		3p	31					
		4p	25					
		5p	37					
41	67.065	1p	290	3-Penten-1-yne (C_5H_7+)	(2)	na	na	Measured at 67.054 in (2)
		2p	73					
		3p	66					
		4p	68					
		5p	70					
42	68.065	1p	96	Pyrrole (C_4H_6N+)	2	875.4	4	Measured at 68.05 in (2)
		2p	39					
43	69.085	1p	912	Isoprene (2-Methyl-1,3-butadiene) C_5H_9+	(1, 2)	826.4	4, 5	Measured at 69.069 and 69.070 in (1) and (2) respectively
		2p	162					
		3p	158					
		4p	112					
		5p	145					
44	70.045	1p	107	C_5H_{10}				
		2p	40					
		3p	18					
		5p	27					
45	71.055	1p	1622	MVK; methyl-vinyl-ketone (3-Buten-2-one) C_4H_7O+ / MACR; methacrolein (methacro aldehyde) C_4H_6O+	(1, 2)	834.7 / 808.7	4, 5	MVK/MACR was 71.09 in (1), while in (2); MACR was 71.049 and a mix of alkyl fragments (C5H11+) was 71.086 in (2). ISOPOOH also reported in this m/z in (3a) (Rivera-Rios, et al. 2014)
		2p	617					
		3p	294					
		4p	457					
		5p	452					
46	72.065	1p	246	$C_3H_5O_2$ + Acrylic acid	(2)	na	na	Acrylic acid was 73.03 in (2)
		2p	33					
		3p	18					

		4p	587						
		5p	26						
47	73.075	1p	2831	2-Butanone (C_4H_9O+)	(2)	827.2	7	Measured at 73.065 in (2)	
		2p	985						
		3p	664						
		4p	587						
		5p	1450						
48	74.075	1p	1021	Dimethylformamide (C_3H_8NO+)	(2)	884	6	Measured at 74.061 in (2)	
		2p	170						
		3p	50						
		4p	61						
		5p	104						
49	75.065	1p	1968	Methyl acetate ($C_3H_7O_2+$) / Isobutanol (2-Methyl-1-propanol) $C_4H_{11}O+$	(2)	(Acetic acid, methyl ester) 821.7	7	methyl acetate was 75.044 and isobutanol was 75.080 in (2)	
		2p	365						
		3p	279						
		4p	233						
		5p	428						
50	76.045	2p	70	C6H4	(3)	*812	7	* This fragment is shown as a unit in several organic molecules in (7) and has more than one associated proton affinity value depending on source	
		3p	64						
		4p	46						
		5p	75						
51	77.065	2p	87	!- propane thiol C_3H_9S +	(2)	na	na	1- propanethiol Was 77.01 in (2),	5p322
		3p	45						
		4p	56						
		5p	322						
52	78.065	1p	30	Methylsulfinyl)	(2)	na	na	Measured as 78.046 in (2)	

		2p	20	methanide (C_2H_6OS +)				
		5p	25					
53	*79.065	1p	327	Benzene) C_6H_{13}+	(1)	746.4	4	Most likely benzene; m/z in (1) was 79.054 for benzene, but m/z 79.021 in (2) was given as dimethyl sulfoxide (C_2H_7OS +)
		2p	169	or				
		3p	200	dimethyl sulfoxide (C_2H_7OS +)				
	79.035	4p	177		(2)			
		5p	269					
54	80.065	1p	102	Pyridine (C_5H_6 N+)	(2)	*930	7	Pyridine was given as 80.049 in (2). * There are several associated pa values depending on source molecule
		2p	40					
		3p	19					
		5p	38					
55	81.085	1p	356	Alkyl fragment (hexenals /hexenols /terpenoids) (C_6H_9+)	(2)	na	na	The m/z given in (2) was 81.069. Bis (methylthio) methane (CH_5S_2+) was 81.000
		2p	107					
		3p	102					
		4p	106					
	81.045	5p	130					
56	82.085`	1p	116	Cyclopentenyl carbenium (C_6H_{10}+)	(2)	na	na	82.06 was m/z measured in (2)
		2p	19					
57	83.105	1p	484	2-Methylfuran (C_5H_7O+)	(2)	na	na	Any m/z in a group that is different by > 0.020 is recorded separately as shown in 2p. m/z used in (2) was 83.049
	83.065	2p	117					
		3p	68					
		4p	70					
		5p	98					
58	84.065	2p	28	ui	na	na	na	
59	85.035	1p	713	5 h-Furan-2-one ($C_4H_5O_2$+)	(2)	na	na	m/z was 85.029 in (2)
		2p	391					
		3p	193					
	85.065	4p	180					
		5p	315					

60	86.085	1p 2p	239 29	Thiophenium (C_4H_6S+)	(2)	na	Na	m/z measured in (2) was 86.018
61	87.035 87.085	1p 2p 3p 4p	930 933 530 481	Butan-4-olide ($C_4H_7O_2$+) / 2-Methyl butanal ($C_5H_{11}O$+)	(2)	na	na	When the difference in m/z is > 0.020 within the same group, they are recorded separately as shown in 4p. 47.043/ 47.081 were respectively measured in (2) for identified compounds
62	88.065	1p 2p 3p 4p	321 69 39 29	3,4-Dihydro-2H-thiophene (C_4H_8S+)	(2)	na	na	Measured m/z in (2) was 88.030
63	89.085 89.055	1p 2p 3p 4p 5p	1133 155 40 47 94	3-Hydroxy-2-butanone (acetoin) ($C_4H_9O_2$+) / Allyl methyl sulphide C_4H_9S+)	(2)	na	na	Measured m/z for identified species in (2) were 89.56 / 89.41 respectively. Separate m/z is recorded when differences are > 0.020 as shown for 3p in this group.
64	90.065	2p	22	ui	na	na	na	
65	91.065	1p 2p 3p 4p 5p	280 73 87 58 79	2-3-Butanediol ($C_4H_{11}O_2$+)	(2)	915.5	7	m/z measured in (2) was 91.055
66	93.065	1p 2p 3p 4p 5p	1752 303 203 241 446	Methylbenzene (toluene) (C_7H_9+)	(1, 2)	784	4	Measured m/z in (1, 2) were (93.069, 93.068) respectively.

67	94.065	2p	35	ui	na		na	na	
		3p	31						
		4p	26						
		5p	49						
68	95.075	2p	263	Dimethyl sulfone ($C_2H_7O_2S$ +)	(2)		na	na	m/z in (2) was 95.010. The m/z with a difference of more than 0.020 are recorded separately as shown in 5p
		3p	152						
	95.035	5p	2092						
69	96.045	2p	41	ui	na		na	na	
		3p	117						
		5p	70						
70	97.025	1p	2702	Furfural (2-Furancarboxaldehyde) ($C_5H_5O_2$+)	(2)	(Furan) ≥ 875.4 (pyrrol)	812	4	m/z here is the same as in (2). There was also 2,4-dimethylfuran (C6H9O +) measured at 97.065 in (2)
		2p	2122						
		3p	1472						
		4p	1845						
		5p	3717						
71	98.045	2p	83	ui	na	na		na	
		3p	52						
	98.075	4p	27						
		5p	58						
72	99.065	1p	726	4-Methyl-5 h-furan-2-one ($C_5H_7O_2$+)	(2)	na		na	m/z in (2) was 99.044. m/z with a difference > 0.020 in the group was recorded separately as shown in 2p
	99.035	2p	364						
		3p	205						
		4p	205						
		5p	260						
73*	100.075	2p	44	ui	na	na		na	
		5p	27						
74	101.075	1p	1801	2,3-Pentanedione ($C_5H_9O_2$+)	(2)	na		na	m/z measured in (2) was 101.060
		2p	474						
		3p	204						

		4p	151					
		5p	236					
75	102.055	2p	36	ui	na	na	na	
76	103.065	1p	789	Ethynylbenzene (C_8H_7+) / 4-Hydroxy-3-methyl-2-butanone ($C_5H_{11}O_2$+)	(2)	na	na	m/z for identified species in (2) were 103.076 / 103.050 respectively
		2p	98					
		3p	33					
		4p	30					
		5p	67					
77	104.085	2p	18	ui	na	na	na	
78	105.075	1p	175	4-Hydroxybutanoic acid ($C_4H_9O_3$+)	(2)	na	na	m/z in (2) was 105.060 for identified specie, but m/z 105.037 was also given for methional (C_4H_9OS+)
		2p	25					
		3p	29					
79	107.075	1p	180	1,3-Dimethylbenzene terpenes fragment (C_8H_{11}+)	(2)	na	na	m/z 107.086 was measured in (2)
		2p	66					
		3p	79					
		4p	55					
		5p	84					
80	108.085	2p	20	ui	na	na	na	
81	109.045	1p	850	Anisole (C_7H_9O+) / 2-Ethynylthiophene (C_6H_5S+)	(2)	na	na	m/z in (2) were 109.065 / 109.010 respectively for identified species
		2p	890					
		3p	770					
		4p	647					
		5p	751					
82	110.065	2p	60	ui	na	na	na	
		3p	51					
		4p	56					
		5p	42					

83	111.075	1p 2p 3p 4p 5p	411 92 55 57 137	4-Methyl-1,3-heptadiene (C_8H_{15}+) / 2-Acetylfuran ($C_6H_7O_2$+)	(2)	na	na	The m/z in (2) for the identified species were 111.104 / 111.044 respectively.
84	112.085	2p	26	ui	na	na	na	
85	113.065	1p 2p 3p 4p 5p	503 128 75 65 329	2,5-Dimethylthiophene (C6H9S) / 2-Heptenal ($C_7H_{13}O$+)	(2)	na	na	m/z in (2) were 113.040 / 113.100 respectively for the species identified
86	114.045	2p 5p	43 33	ui	na	na	na	
87	115.085 115.055	1p 2p 3p 4p 5p	982 156 67 102 309	3,5-Dimethyldiidro-2(3 h)-furanone ($C_6H_{11}O_2$+)	(2)	na	na	m/z 115.075 was measured in (2) for identified specie. m/z 115.020 was also given for 2-Methyl-3-furanthiol (C_5H_7OS+)
88	117.095 117.055	2p 4p 5p	59 27 51	methylsulfanyl cyclopentane (Cyclopentyl-1-thiaethane) ($C_6H_{13}S$+)	(2)	na	na	Measured m/z used in (2) was 117.078. when the difference in m/z any member of a group > 0.020, the m/z is shown separately; e.g. as in 5p.
89	119.075	2p	47	1-(Methylthio) pentane ($C_6H_{15}S$+)	(2)	na	na	m/z 119.06 was used in (2)
90	121.085	1p	253	1,2,4-Trimethylbenzene (C_9H_{13}+); / 2-Hydroxyethyl propylsulphide ($C_5H_{13}OS$ +)	(2)	na	na	Measured m/z used in (2) respectively were 121.101 / 121.065

91	123.075	2p 5p	45 41	1-Methoxy-3-methylbenzene ($C_8H_{11}O+$)	(2)	na	na	Measured m/z in (2) was 123.080, but then, diethanol sulphide ($C_4H_{11}O_2S+$) was measured as 123.045
92	125.065	3p 4p	49 29	2-Butylfuran ($C_8H_{13}O+$)	(2)	na	na	Measured m/z used for identified specie in (2) was 125.096. m/z 125.010 was given, as (Methylsulfiyl) (methylthio) methane ($C_3H_9OS_2+$)
93	127.065	2p 3p 4p 5p	70 40 54 78	Methyl 2-Furan carboxylate ($C_6H_7O_3+$)	(2)	na	na	Measured m/z for identified specie was 127.035 in (2). m/z 127.112 was given as 1-Octen-3-one ($C_8H_{15}O+$)
94	149.055	1p 2p 3p 4p 5p	852 195 47 47 169	1-Ethylpropyl benzene ($C_{11}H_{17}+$);	(2)	na	na	Measured m/z was 149.130 in (2)
95	153.085 153.115	1p 5p	194 44	Carveol ($C_{10}H_{17}O+$); 2-Methyl-5-(1-methyl ethenyl) -2-cyclohexen-1 - ol	(2)	na	na	Measured m/z for identified specie was 153.130. when the m/z differ by more than 0.020 they are listed separately e.g. as shown in 5p
96	155.125	5p	66	Diethyl trisulfide ($C_4H_{11}S_3+$)	(2)	na	na	155.010 was the measured m/z in (2)
97	157.035	2p 3p 4p	71 47 41	Decanal ($C_{10}H_{21}O+$)	(2)	na	na	Measured m/z used in (2) was 157.159

		5p	98					
98	161.105	1p	51	1,9-Nonanediol ($C_9H_{21}O_2$+)	(2)	na	na	Measured m/z was 161.155 in(2)
99	163.105	1p 3p	66 28	3-Methyl-2-(penta-2,4-dienyl) cyclopent-2-enone $C_{11}H_{15}O$+)	(2)	na	na	Measured m/z was 163.075 in (2)
100	171.155	1p	145	2-Undecanone ($C_{12}H_{11}O$+)	(2)	na	na	171.080 was the measured m/z in (2)
101	175.065 175.035	2p 5p	29 63	4-Hydroxy benzene sulfonic acid ($C_6H_7O_4S$+)	(2)	na	na	175.010 was the measured m/z in (2)

Species identification source:

1. Seco et al 2011: online from www.atmos-chem-phys.net/11/13161/2011/doi:10.5194/acp-11-13161-2011

2. Federico et al 2015: Springer 2018; Online from https://www.nature.com/articles/srep12629/tables/1

3. ***Hadden Analytical online; references; Hemming and Foster (1992), McLafferty and Turecek (1993), Silverstein et al (1991)***

Affinity data source*:*

4. Hunter and Lias (1998) / NIST Webbook (2018)

5. Ellis & Mayhew (2013)

6. Jolly (1991), ***Modern Inorganic Chemistry*****(2nd Edn.). New York: McGraw-Hill. ISBN 0-07-112651-1.**

7. KORE technology (2018), online from https://www.kore.co.uk/paffinities.htm